2-2009

Synthesis and Interfacial Behavior of Functional Amphiphilic Graft Copolymers Prepared by Ring-opening Metathesis Polymerization

Kurt E. Breitenkamp
University of Massachusetts Amherst, kurt.breitenkamp@gmail.com

SYNTHESIS AND INTERFACIAL BEHAVIOR OF FUNCTIONAL AMPHIPHILIC GRAFT COPOLYMERS PREPARED BY RING-OPENING METATHESIS POLYMERIZATION

A Dissertation Presented

by

KURT E. BREITENKAMP II

Submitted to the Graduate School of the
University of Massachusetts Amherst in partial fulfillment
of the requirements for the degree of

DOCTOR OF PHILOSOPHY

February 2009

Polymer Science and Engineering

SYNTHESIS AND INTERFACIAL BEHAVIOR OF FUNCTIONAL AMPHIPHILIC GRAFT COPOLYMERS PREPARED BY RING-OPENING METATHESIS POLYMERIZATION

A Dissertation Presented

by

KURT E. BREITENKAMP II

Approved as to style and content by:

_____
Todd S. Emrick, Chair

_____
E. Bryan Coughlin, Member

_____
Anthony D. Dinsmore, Member

_____
Shaw L. Hsu, Department Head
Polymer Science and Engineering

DEDICATION

In memory of my father, Kurt E. Breitenkamp, and grandmother, Frances Rogers, who made this possible and continue to inspire me everyday.

ACKNOWLEDGMENTS

I would like to thank my thesis advisor, Professor Todd Emrick for inspiring my love of chemistry and allowing me the freedom to test my own creativity in the lab. You have been and continue to be a great mentor and friend without condition. I would also like to thank my committee members, Professors Bryan Coughlin and Tony Dinsmore. The work contained herein would not have been possible without your assistance in many key experiments. I would also like to thank all the other members of the Polymer Science and Engineering faculty and staff for their education and assistance during my time in graduate school.

I would like to thank the agencies who financially supported this research: Center for UMass-Industry Research on Polymers (CUMIRP), National Science Foundation - Materials Research Science & Engineering Center (MRSEC) at UMass-Amherst, National Science Foundation (NSF) – Chemical Transport Systems (CTS), and Office of Naval Research (EUWP).

Thank you to those who contributed directly to the work contained in this thesis: Dr. Bryan Parrish, Rebecca Breitenkamp, Dr. Ravindra Revanur, Bryan McClosky, Professor Benny Freeman, Dr. Grégoire Cardoen, Dan Burke, Matt Kade, Jennifer Simeone, Euhna Jin, and Professor Denise Junge. I would also like to specifically thank members of the Polymer Science and Engineering staff who assisted me throughout the course of graduate school and who contributed to many experiments herein: Dr. Steve Eyles, Lou Raboin, Dr. Sekar Thirunavukkarasu, and Dr. Charlie Dickinson.

I would like to thank all my fellow group members for their help and support. In particular, I would like to thank the early Emrick group members from whom I learned so

much: Dr. Bryan Parrish, Dr. Habib Skaff, Dr. Rui Hong, Dr. Kevin Sill, and Dr. Ken Ellzey. I would also like to thank all the current Emrick group members, especially Katrina Kratz and Brent Hammer. Thanks to my friends, Doug and Meghan Holmes, for making the second round of graduate school much more entertaining.

Many thanks to my family – Mom, James, Pappy, Robin, Michael, Rudy, Becky, Ryan, Lyndi, Sean, and Ally. None of this would be possible without your continued love and moral support. Finally, I would like to thank my wife, Rebecca Breitenkamp, for all of the memories during our journey through graduate school. Words cannot describe how much you mean to me.

ABSTRACT

SYNTHESIS AND INTERFACIAL BEHAVIOR OF FUNCTIONAL AMPHIPHILIC GRAFT COPOLYMERS PREPARED BY RING-OPENING METATHESIS POLYMERIZATION

FEBRUARY 2009

KURT E. BREITENKAMP II, B.S., UNIVERSITY OF SOUTHERN MISSISSIPPI

M.S., UNIVERSITY OF MASSACHUSETTS-AMHERST

Ph.D., UNIVERSITY OF MASSACHUSETTS-AMHERST

Directed by: Professor Todd S. Emrick

This thesis describes the synthesis and application of a new series of amphiphilic graft copolymers with a hydrophobic polyolefin backbone and pendent hydrophilic poly(ethylene glycol) (PEG) grafts. These copolymers are synthesized by ruthenium benzylidene-catalyzed ring-opening metathesis polymerization (ROMP) of PEG-functionalized cyclic olefin macromonomers to afford polycyclooctene-*graft*-PEG (PCOE-*g*-PEG) copolymers with a number of tunable features, such as PEG graft density and length, crystallinity, and amphiphilicity. Macromonomers of this type were prepared first by coupling chemistry using commercially available PEG monomethyl ether derivatives and a carboxylic acid-functionalized cyclooctene. In a second approach, macromonomers possessing a variety of PEG lengths were prepared by anionic polymerization of ethylene oxide initiated by cyclooctene alkoxide. This methodology affords a number of benefits compared to coupling chemistry including an expanded PEG molecular weight range, improved hydrolytic stability of the PEG-polycyclooctene linkage, and a reactive hydroxyl end-group functionality for optional attachment of biomolecules and probes.

The amphiphilic nature of these graft copolymers was exploited in oil-water interfacial assembly, and the unsaturation present in the polycyclooctene backbone was utilized in covalent cross-linking reactions to afford hollow polymer capsules. In one approach, a *bis*-cyclooctene PEG derivative was synthesized and co-assembled with PCOE-*g*-PEG at the oil-water interface. Upon addition of a ruthenium benzylidene catalyst, a cross-linked polymer shell is formed through ring-opening cross-metathesis between the *bis*-cyclooctene cross-linker and the residual olefins in the graft copolymer. By incorporating a fluorescent-labeled cyclooctene into the graft copolymer, both oil-water interfacial segregation and effective cross-linking were confirmed using confocal laser scanning microscopy (CLSM). In a second approach, reactive functionality capable of chemical cross-linking was incorporated directly into the polymer backbone by synthesis and copolymerization of phenyl azide and acyl hydrazine-functional cyclooctene derivatives. Upon assembly, these reactive polymers were cross-linked by photolysis (in the phenyl azide case) or by addition of glutaraldehyde (in the acyl hydrazine case) to form mechanically robust polymer capsules with tunable degradability (*i.e.* non-degradable or pH-dependent degradability). This process permits the preparation of both oil-in-water and water-in-oil capsules, thus enabling the encapsulation of hydrophobic or hydrophilic reagents in the capsule core. Furthermore, the assemblies can be sized from tens of microns to the 150 nm - 1 μm size range by either membrane extrusion or ultrasonication techniques. These novel capsules may be well-suited for a number of controlled release applications, where the transport of encapsulated compounds can be regulated by factors such as cross-link density, hydrolytic stability, and environmental triggers such as changes in pH.

TABLE OF CONTENTS

LIST OF TABLES

Table Page

LIST OF FIGURES

LIST OF SCHEMES

Scheme Page

LIST OF ABBREVIATIONS

Å	angstrom(s)
ADMET	acyclic diene metathesis
AFM	atomic force microscopy
aq	aqueous solution
ATR	attenuated total reflectance
ATRP	atom transfer radical polymerization
BHT	2,6-di-*tert*-butyl-*p*-cresol
BIE	1,2-bis(2-iodoethoxy)ethane
Boc	N-butyloxycarbonyl
br	broad
BSA	bovine serum albumin
But	butyl
C	Celcius
CLSM	confocal laser scanning microscopy
cm	centimeter(s)
CM	cross-metathesis
CMC	critical micelle concentration
COD	1,5-cyclooctadiene
COE	cyclooctene
d	doublet
Da	dalton(s)

DCC	dicyclohexylcarbodiimide
DCM	dichloromethane
DCU	N,N'-dicyclohexylurea
DIAD	diisopropyl azodicarboxylate
DI	deionized
DIC	diisopropylcarbodiimide
DIPEA	diisopropylethylamine
DLS	dynamic light scattering
DMA	2-(dimethylamino)ethyl methacrylate
DMAP	4-dimethylaminopyridine
DMF	dimethylformamide
DMSO	dimethylsulfoxide
DOX	doxorubicin
DP	degree of polymerization
DSC	differential scanning calorimetry
DTT	dithiothreitol
eq	equivalent(s)
E_2	bimolecular elimination
EO	ethylene oxide
EPR	enhanced permeation and retention
ESI	electrospray ionization
EtOAc	ethyl acetate
f	volume fraction

FTIR	Fourier transform infrared
Fmoc	9-fluorenylmethoxycarbonyl
g	gram(s)
Gly	glycine
GPC	gel permeation chromatography
GRGDS	glycine-arginine-glycine-aspartic acid-serine
HBr	hydrobromic acid
HBTU	O-(Benzotriazol-1-yl)-N,N,N',N'-tetramethyluronium hexafluorophosphate
HCl	hydrochloric acid
HOBt	1-hydroxybenzotriazole
HPMA	N-(2-hydroxypropyl)methacrylamide
IR	infrared
KCN	potassium cyanide
kDa	kilodalton
LbL	layer-by-layer
M	mole/liter
m	multiplet
MALDI	matrix-assisted laser desorption/ionization
MALLS	multiple angle laser light scattering
MCPBA	*meta*-chloroperbenzoic acid
MeOH	methanol
MHz	megahertz
min	minute(s)

μL	microliter(s)
mL	milliliter(s)
μm	micrometer(s) or micron(s)
mm	millimeter(s)
mmol	millimole(s)
M_n	number-average molecular weight
mol	mole(s)
M_p	peak molecular weight
MTD	maximum tolerated dose
M_w	weight-average molecular weight
MWCO	molecular weight cutoff
NHC	N-heterocyclic carbene
nm	nanometer(s)
NMR	nuclear magnetic resonance
PAA	poly(acrylic acid)
PAH	poly(allylamine hydrochloride)
Pbf	2,2,4,6,7-pentamethyldihydrobenzofuran-5-sulfonyl
PCOE	polycyclooctene
PCOE-*g*-PEG	polycyclooctene-*graft*-poly(ethylene glycol)
PDI	polydispersity index
PE	polyethylene
PE-*g*-PEG	polyethylene-*graft*-poly(ethylene glycol)
PEG	poly(ethylene glycol)

PEG-*b*-PCL	poly(ethylene glycol)-*block*-poly(ε-caprolactone)
PEG-*b*-PLA	poly(ethylene glycol)-*block*-poly(L-lactic acid)
PEGMA	poly(ethylene glycol) methacrylate
PEO	poly(ethylene oxide)
PES	polyethersulfone
PGA	poly(L-glutamic acid)
PLL	poly(L-lysine)
PMAA	poly(methacrylic acid)
PMMA	poly(methyl methacrylate)
PMMA-*g*-PEG	poly(methacrylic acid)-*graft*-poly(ethylene glycol)
PVP	poly(N-vinyl pyrrolidone)
ppm	parts per million
PS	polystyrene
PSS	poly(styrene sulfonate)
PVDF	poly(vinylidene fluoride)
PVDF-UF	poly(vinylidene fluoride) ultrafiltration
q	quartet
RCM	ring-closing metathesis
RES	reticuloendothelial system
ROMP	ring-opening metathesis polymerization
RGD	arginine-glycine-aspartic acid
RI	refractive index
RNAi	ribonucleic acid interference

ROMP	ring-opening metathesis polymerization
s	singlet
SDGRG	serine-aspartic acid-glycine-arginine-glycine
SEM	scanning electron microscopy
SC/MS	solid core/mesoporous shell
SCN	shell cross-linked nanoparticles
siRNA	short interfering ribonucleic acid
S_N2	bimolecular nucleophilic substitution
SPPS	solid phase peptide synthesis
T	temperature
t	triplet
t-But	*tert*-butyl
TEG	tetraethylene glycol
TFA	trifluoroacetic acid
TFE	trifluoroethanol
THF	tetrahydrofuran
TIPS	triisopropylsilane
TPP	triphenylphosphine
UV	ultraviolet
wt	weight

CHAPTER 1

SYNTHETIC POLYMERS FOR ENCAPSULATION AND DELIVERY

1.1 The Role of Synthetic Polymers in Drug Delivery

Advances in modern medicine for the treatment of human illness continue to improve the length and quality of human life. While new therapeutic agents play a major role in these advances, drug delivery strategies also represent key components of successful treatments. Synthetic polymers are important for implementing delivery strategies and hold significant promise for enhancing the therapeutic benefits of current and future drugs.[1] While polymer-based drug delivery systems provide a means to improve the bioavailability, safety, and efficacy of drug therapy, several important problems are currently under investigation. For example, a number of strategies are being developed to improve the *controlled* nature of therapeutic delivery to include long time periods, predetermined time intervals, and response to physiological changes.[2-4] In addition, functional polymer materials are being designed to provide *targeted* drug delivery mechanisms with a specificity that simultaneously promotes healing and diminishes unwanted side effects.[5]

Since the introduction of polymer-based drug delivery principles by Ringsdorf and coworkers,[6,7] polymer therapeutics have expanded considerably in scope and are now poised to revolutionize medical treatment protocols. Synthetic polymers have been important for implementing delivery strategies currently used in the clinic and will continue to be significant in designing drug delivery systems in the future. Figure 1.1 illustrates several different polymer-based systems that are currently being utilized for therapeutic delivery. In one approach, drugs can be attached directly to a polymer

backbone (*i.e.* polymer-drug conjugation) to improve their solubility and greatly improve their pharmacokinetic profiles.[8] Recent polymer-drug conjugation techniques make use of branched polymer architectures (*e.g.* star, graft and dendritic) which dramatically increase drug payloads and allow for the attachment of bioactive functionality such as cell targeting groups or cell permeation enhancers. Polymers also serve as key building blocks in the production of encapsulating delivery systems such as polymer microparticles, micelles, and capsules which can be tailored, through appropriate chemistries, to control the release of the therapeutic at the site of disease and/or over long time periods (*e.g.* from hours to days) following administration.

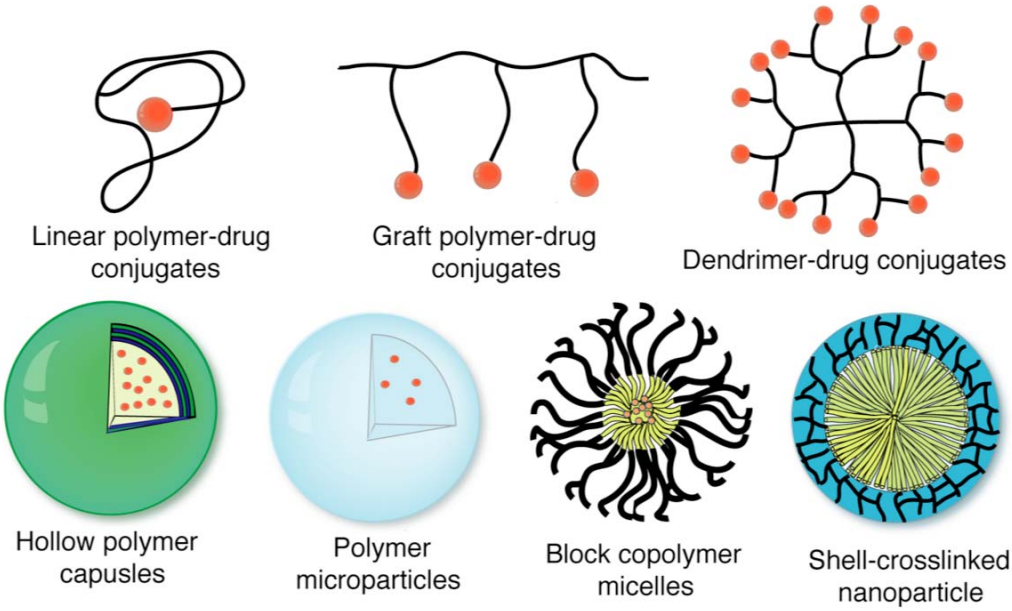

Figure 1.1 Polymer architectures and encapsulation techniques for therapeutic delivery

Polymeric drug delivery systems offer great flexibility with regard to their chemistry and physical properties and have been tailored to suit a number of different therapeutic applications. While polymeric delivery systems possess unique attributes, they also share many common requirements such as biocompatibility (*e.g.* low toxicity

and immunogenicity) and the ability to control the release of therapeutics over time and/or in response to physiological changes. The development of future polymer-based delivery systems will capitalize on many of these existing technologies and focus on 1) expanding the range of drugs that can be formulated and administered, 2) targeting drug release at the diseased site or inside diseased cells using physiological triggers, and 3) developing delivery systems with cell-targeting moieties, such as antibodies, peptides, and aptamers that actively bind to diseased cells and tissue. The objective of such efforts is to concentrate drug delivery at the site of disease, thus improving drug efficacy while reducing toxic side effects. To produce such advanced delivery systems, a shifted interest from conventional, off-the-shelf polymer materials to the rational design and synthesis of new, multi-functional polymers is anticipated.

1.1.1 Conjugation of Polymers to Drugs and Delivery Systems

One of first significant demonstrations of synthetic polymer drug delivery was reported in 1977 when Abuchowski and coworkers described the covalent linking of poly(ethylene glycol) (PEG) to bovine serum albumin (BSA) (shown in Figure 1.2A).[9,10] Following conjugation, a dramatic reduction in immunogenicity was observed in the PEG-conjugated BSA compared to the unmodified protein, and this "PEGylation" strategy was quickly applied to other therapeutic proteins that were previously unusable due to their immunological toxicity.[11,12] Since these early discoveries, many studies have validated PEGylation of small molecule drugs and biomolecules for improving water-solubility of the drug and extending *in vivo* circulation time by slowing the metabolism and renal clearance of the conjugated therapeutic.[13] PEGylation has been particularly successful for protein- and gene-based conjugations as the non-conjugated versions are

highly immunogenic and susceptible to rapid *in vivo* degradation following administration. In fact, several PEGylated protein drugs have been approved in the U.S., with additional PEGylated therapeutics currently undergoing clinical trials.[14]

As in the case of protein therapeutics, the attachment of poly(ethylene glycol) to drug delivery systems has also been shown to improve *in vivo* stability and extend circulation times. For example, liposomes emerged in the 1970's as a potentially revolutionary method of delivering therapeutics, but their clinical implementation was slowed by their poor stability *in vivo* and rapid clearance from the bloodstream by the reticuloendothelial system (RES). The incorporation of PEG into liposomes using PEGylated phospholipids (shown in Figure 1.2B) addressed many of these shortcomings and led to the development of Stealth® liposomal technology which has been utilized in several delivery systems for cancer treatment such as Doxil[15] and Myocet.[16]

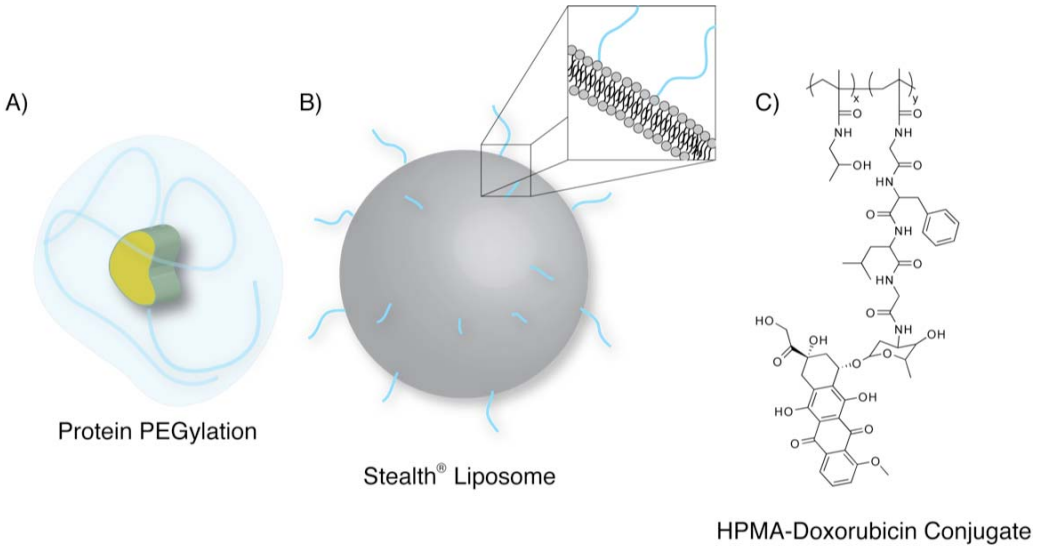

Figure 1.2 Examples of polymer-based drug delivery systems in use today

While PEGylation is typically limited to conjugation reactions involving the PEG chain-ends, a number of new conjugate systems, based on well-defined polymer

architectures, are emerging in which drugs are attached pendent to the polymer backbone or as the chain-ends of branched polymers and dendrimers. These systems offer enhanced drug payload per molecule and also improve the blood solubility, circulation time, and efficacy of small molecule drugs. For example, poly(N-(2-hydroxypropyl)methacrylamide) (HPMA) drug conjugates, illustrated in Figure 1.2C, were reported by Duncan and coworkers and have shown good promise in clinical trials.[17] The covalent coupling of chemotherapy drugs such as doxorubicin (DOX) and paclitaxel to these HPMA copolymers resulted in increased uptake into tumor cells relative to non-conjugated DOX, an observation attributed to the enhanced permeability and retention (EPR) effect.[18,19] The EPR effect results from the disorganized nature of the tumor vasculature which leads to an increased permeability to polymer therapeutics.[20,21] Poor lymphatic drainage in the tissue allows drug retention at the tumor site. The EPR effect is a unique feature of polymer-based therapeutics, which arises from increased blood circulation times of the polymer-drug conjugate relative to their non-conjugated analogues.

The manipulation and control of polymer architecture offers exciting opportunities in drug delivery. Conjugates based on branched polymer architectures are particularly interesting, as these polymers possess 1) multiple chain-ends for drug attachment, and 2) the potential for engineering degradation sites and cell targeting moieties into the structure.[22-25] In this context, dendritic polymers are unique, as their highly branched structure leads to a large number of chain-ends for drug attachment. In addition, the uniform molecular weight distribution of dendrimers, reminiscent of proteins, makes them special relative to conventional linear polymers, providing a well-

characterized molecular platform that is appealing for medical applications. Fréchet and coworkers are among the leaders in designing dendrimers for drug delivery and have reported several examples of water-soluble, polyester-based dendrimer-DOX conjugates.[26,27] These conjugates are modular by design and can be equipped with higher drug payloads than linear polymer-drug conjugates, as well as chain-end solubilizing groups and cell-targeting moieties. The utility of dendrimer-DOX conjugates was demonstrated through *in vitro* models, which showed dramatically increased serum half-life compared to free DOX, as well as anti-proliferation effects in cancer cells. In preliminary *in vivo* studies, dendrimer-drug conjugates were well-tolerated in mice, and showed no accumulation in liver, heart, or lung tissue.[28]

1.1.2 Encapsulation and Release Strategies using Polymeric Delivery Systems

Another therapeutic delivery approach involves the encapsulation and release of drugs within a synthetic polymer matrix or membrane. Delivery methods based on this approach are well-suited for controlled release applications, in which the encapsulating polymer is designed to release the encapsulated drug over some time period or in response to changing pH, ionic strength, or temperature. Precisely regulating drug release following injection aids in producing more effective therapies while also reducing the possibilities of under- and overdosing. An additional feature of controlled-delivery systems is a reduction in dosing frequency which often improves patient compliance with the treatment.

1.1.2.1 Delivery Systems Based on Polymer Microspheres

The use of biodegradable polymers such as aliphatic polyesters (*e.g.* polylactide[29] and poly(lactide-*co*-glycolide)),[30] polyorthoesters,[31] and polyanhydrides[32] for microsphere-based delivery systems has been studied widely. The advantage of such polymers is their degradation into biocompatible molecules that can be metabolized readily and excreted. In addition, microsphere degradation and subsequent release rates can be tuned through appropriate control of polymer synthesis and composition. Drug-loaded microspheres can be prepared by emulsion[33] or spray-drying[34] techniques which permit the encapsulation of a wide range of therapeutics including small molecule drugs and proteins. Drug release from degradable polymer microspheres is controlled by two separate mechanisms. As shown in Figure 1.3A, the drug can be released by simple diffusion (*i.e.* through pores or between polymer chains). Degradation of the polymer matrix over time, shown in Figure 1.3B, also stimulates drug release in a time-dependent manner. Microparticles based on degradable polymers have led to several clinically used therapeutics including injectable formulations such as Lupron Depot for prostate cancer and endometriosis treatment,[35] and inhalable forms of insulin[36] (*e.g.* Exubera) for diabetes treatment.

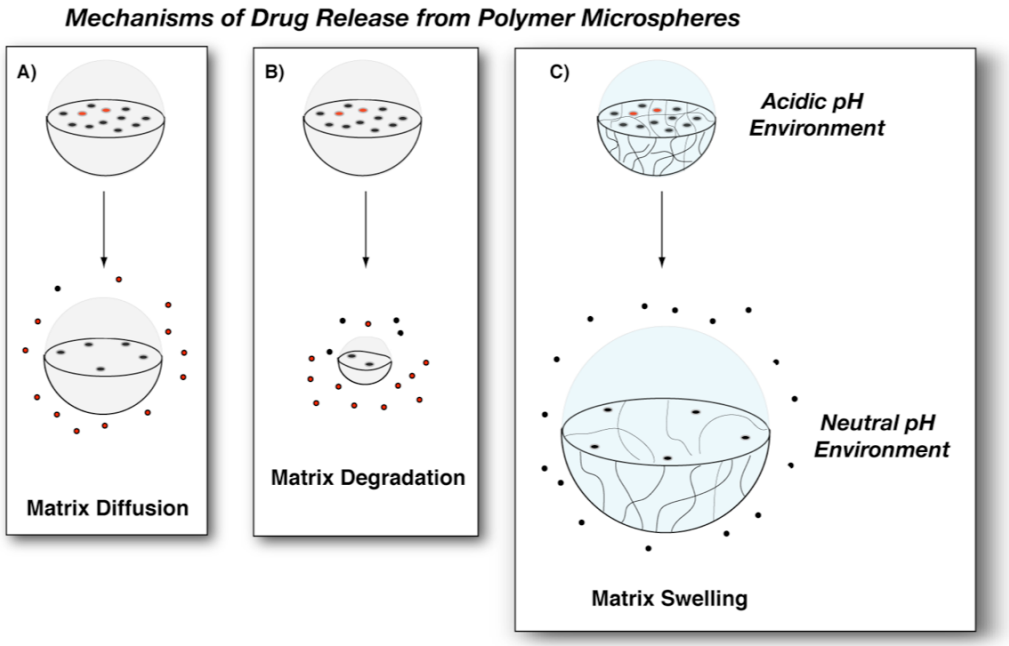

Figure 1.3 Illustration of drug release mechanisms from polymer microspheres

In addition to biodegradable polymer microspheres, other controlled release strategies have been developed which offer many advanced features beyond simply controlling release rates over time. For example, Peppas and coworkers have synthesized polymer micro- and nanospheres using poly(methacrylic acid)-*graft*-poly(ethylene glycol) (PMAA-*g*-PEG) copolymers that control drug release based on changes in the physiological environment.[37,38] These materials have proven suitable for oral delivery systems since the drug is effectively encapsulated at low pH values in the stomach and rapidly released at higher pH values encountered in the gastrointestinal tract. As shown in Figure 1.3C, PMAA and PEG segments complex in strongly acidic environments to form collapsed networks with very small inter-chain distances between polymers. Inter-polymer complexation within the spheres limits therapeutic release until the carrier reaches the gastrointestinal tract, where the pH is elevated to approximately 6 or higher. The increase in pH reverses complexation, which allows the particles to swell and release

their contents.[39,40] Using pH-responsive delivery systems, formulations of proteins and small molecule drugs have been developed, including an oral dosage form of insulin,[41,42] which has proven to be an effective alternative to traditional injectable diabetes therapies.

1.1.2.2 Encapsulation Systems Based on Block Copolymer Assembly

An emerging effort in polymer therapeutics centers on drug encapsulation using polymer assemblies. Both block copolymers and functional polymers of complex architectures can be used as precursors to micro- and nanoscale drug delivery vehicles. For example, amphiphilic triblock copolymers known as Pluronics,® composed of poly(ethylene oxide)-*block*-poly(propylene oxide)-*block*-poly(ethylene oxide), are the polymers of choice for a number of researchers working on polymer therapeutics. In water, these amphiphilic copolymers assemble by multimolecular micellization when present in solution above the critical micelle concentration (CMC). As shown in Figure 1.4 (top), the hydrophobic poly(propylene oxide) block collapses to form the micellar core, while the hydrophilic PEG blocks form a peripheral corona. These core-shell polymer micelles have been used to encapsulate small molecule drugs, polypeptides, and polynucleotides.[43-45]

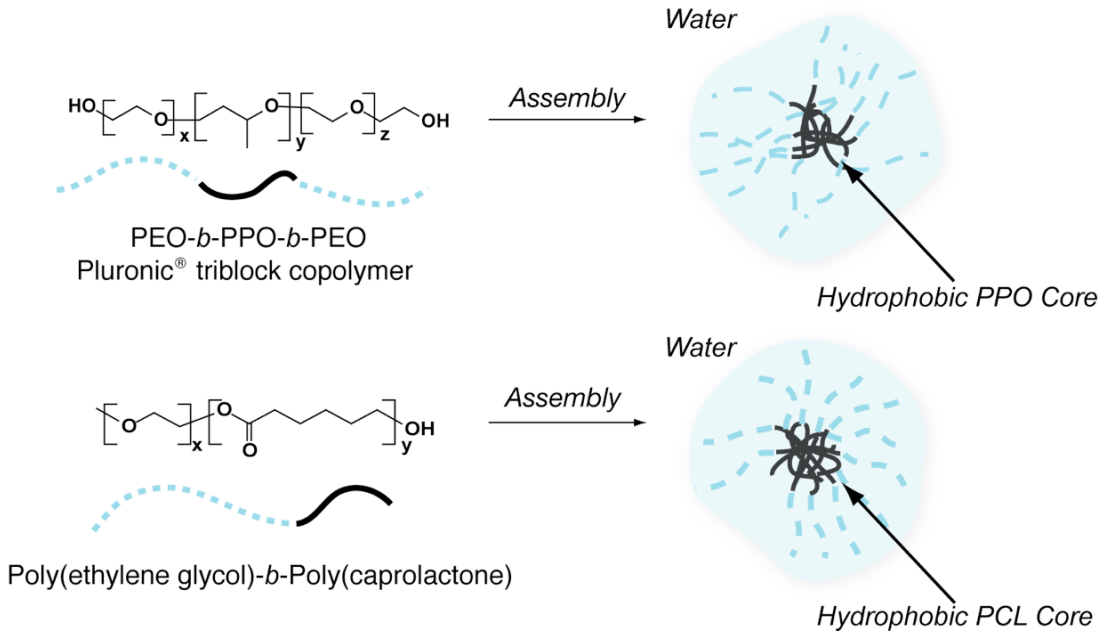

Figure 1.4 Aqueous assembly of amphiphilic triblock and diblock copolymers

A variety of amphiphilic diblock copolymers self-assemble in aqueous solution to form nano- and micron-sized structures, with applications ranging from drug encapsulation to artificial viruses and cells.[46] While PEG is most often used as the hydrophilic segment, a variety of hydrophobic core-forming blocks can be used, providing a means to tune features such as drug loading, stability, and release characteristics.[46-48] Figure 1.4 (bottom) illustrates a PEG-*b*-poly(ε-caprolactone) (PEG-*b*-PCL) diblock copolymer, where the PCL core encapsulates and solubilizes hydrophobic compounds such as indomethacin[49] and DOX.[50] Eisenberg and coworkers used PEG-*b*-PCL copolymers to demonstrate *in vitro* delivery of organic dyes to intracellular compartments.[51] Issues to address for present and future development of block copolymer drug delivery vehicles include 1) improved stability of the assembly upon dilution in the bloodstream, 2) higher drug payload, and 3) improved targeting by integration of cell-seeking functionality into these structures. Wooley and coworkers are

among the research groups addressing these issues through novel synthesis, for example by covalently cross-linking a poly(acrylic acid) (PAA) micellar corona about a poly(ε-caprolactone) core to form shell-cross-linked nanoparticles (SCNs).[52] The cross-linking imparts stability to the nanostructures, and removal of the polyester core by hydrolysis significantly increases the encapsulation volume.

In an effort to produce improved cancer-targeting treatments, several groups have reported the development of stimuli-responsive, drug-loaded polymer micelles that respond to environmental pH changes.[53,54] Acid-sensitive delivery systems designed to target drug release inside cancerous tissues and cells are of clear clinical interest since these carriers limit harmful side effects and can also bypass many of the cellular mechanisms responsible for multi-drug resistance.[55,56] In one example, Kataoka and coworkers synthesized PEG-*b*-poly(aspartic acid) with pendent doxorubicin linked via pH-sensitive hydrazone groups.[57] This polymer micelle-conjugate hybrid retains DOX in the blood (pH 7.4) but rapidly liberates DOX upon hydrazone hydrolysis in the late-early endosome (pH ~ 5.0 - 6.0). Other pH gradients exist within solid tumors due to elevated glycolytic rates and lactic acid production compared to healthy cells. These factors, along with poor lymphatic drainage present in cancerous tissue result in an excess of lactic acid and a subtle pH gradient between the blood and the solid tumor microenvironment (pH 6.0 - 7.0).[58] Fréchet and coworkers have developed PEG-dendrimer micelles which possess acid-sensitive acetal functionality on the dendrimer periphery to exploit such pH gradients.[59] When the dendritic portion is protected with a hydrophobic acetal moiety, the copolymers assemble in water with the dendrimer portion forming the micelle core and the PEG creating the micelle corona. In acidic

environments, such as those encountered in solid tumors, the acetal functionality is hydrolyzed rapidly, exposing the hydroxyl functionality in the micelle core leading to micelle dissociation and drug release. Thus far, pH-responsive micelles based on this acetal protecting scheme have been utilized to encapsulate small-molecule chemotherapeutics such as doxorubicin. It is anticipated that pH sensitive delivery systems, coupled with the EPR effect, could represent an effective method for limiting drug release to solid tumors and may potentially lead to future clinical successes.

1.1.2.3 Polymer Capsules as Drug Delivery Platforms

Capsules and vesicles derived from polymer-based materials are well-suited for many delivery applications because of their mechanical stability and tunable chemistries that can provide control over degradation rates, charge, and cross-linking. Like polymer microspheres, capsules made from polymeric materials can be designed to release active agents over defined time periods, or in response to environmental changes. Capsules are distinguished by a characteristic hollow core with a polymeric membrane that can be utilized for the release of an encapsulated agent.

A number of methods exist to produce hollow polymer capsules.[60] A well-studied method of capsule production employs oil-water emulsion techniques in conjunction with interfacial polymerization reactions on the droplet surface. For example, capsules have been produced by the interfacial condensation polymerization of oil-soluble carboxylic acid chlorides and water-soluble di- and tri-amines to form hollow capsules with nanometer to micron-thick polyamide shells.[61] Free radical polymerization techniques such as emulsion and suspension polymerization can also produce hollow capsules with micron-thick polymer shells when the polymer is immiscible with the dispersed and

continuous phases.[62,63] The production of polymer capsules using these synthetic methodologies requires harsh reaction conditions (*e.g.* high temperature and highly reactive reagents such as acid chlorides and free radical initiators) that can compromise sensitive, encapsulated agents. In most cases, interfacial and emulsion polymerization techniques are also difficult to control with regards to capsule size, wall thickness, and wall uniformity, all of which are critical design parameters in controlled release systems.

To circumvent these problems, there has been growing interest in producing polymer capsules using precisely controlled assembly techniques. Several examples of capsules produced using a self-assembly approach are illustrated in Figure 1.5. These include micron-sized capsules prepared by layer-by-layer (LbL) deposition of polyelectrolytes onto a sacrificial liquid[64] or colloidal core (Figure 1.5A),[65] the interfacial assembly of polymers and/or colloidal particles (Figure 1.5B),[66] and polymersomes produced through aqueous self-assembly of diblock copolymers (Figure 1.5C).[67,68] Many of these polymer capsules can be further functionalized with cell targeting groups or diagnostic agents and then cross-linked to improve overall stability. Such systems can be designed for dual use applications whereby drugs and contrast agents can be incorporated into a single delivery system. For example, Gaponik and coworkers have reported new methods for producing LbL capsules which incorporate fluorescent quantum dots.[69] Preliminary *in vitro* studies using human cancer cells have demonstrated effective cell uptake and fluorescence response of the capsules, and the development of systems such as this may hold future promise for simultaneous diagnosis and treatment of cancer.

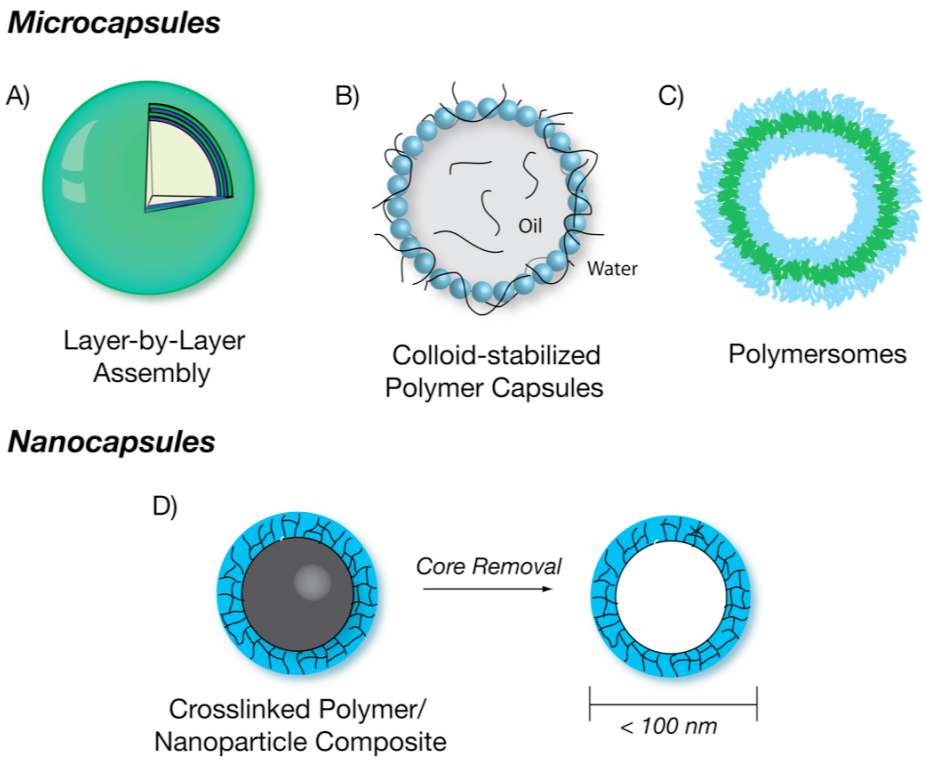

Figure 1.5 Examples of polymer micro- and nanocapsules

To date, most capsules produced using assembly techniques possess diameters of greater than one micron. Future developments in capsule production for *in vivo* applications will likely focus on generating capsules on the nanometer size scale. The advantages of nanoscale delivery systems are numerous and include tumor-selective delivery resulting from the EPR effect and reduced clearance from the bloodstream by the RES and other biological pathways. Polymersomes, for example, can be sized from the multi-micron scale down to 100 nm or less by extrusion through a track-etch membrane, a technique first used with liposomes.[70] In another approach, illustrated in Figure 1.5D, Möhwald and coworkers developed nanometer sized capsules by radial growth and cross-linking of polymers from degradable nanocrystal templates. Following core-removal, hollow nanocapsules with a very well defined diameter and wall thickness

were produced.[71] Many of these approaches to produce hollow polymer capsules will be discussed further in Chapter 3.

1.2 Thesis Outline

This thesis describes the synthesis and application of a new series of amphiphilic graft copolymers with a hydrophobic polyolefin backbone and pendent hydrophilic PEG grafts. As discussed in Chapter 2, these copolymers are synthesized by ruthenium benzylidene-catalyzed ring-opening metathesis polymerization (ROMP) of PEG-functionalized cyclic olefin macromonomers to afford polycyclooctene-*graft*-PEG (PCOE-*g*-PEG) copolymers with a number of tunable features, such as PEG graft density and length, crystallinity, and amphiphilicity. Macromonomers of this type were prepared first by coupling chemistry using commercially available PEG monomethyl ether derivatives and a carboxylic acid-functionalized cyclooctene. In a second approach, macromonomers possessing a variety of PEG lengths were prepared by anionic polymerization of ethylene oxide initiated by cyclooctene alkoxide. This methodology affords a number of benefits compared to coupling chemistry including an expanded PEG molecular weight range, improved hydrolytic stability of the PEG-polycyclooctene linkage, and a reactive hydroxyl end-group functionality for optional attachment of biomolecules and probes. For example, in a few steps, the reactive hydroxyl end-group was converted to carboxylic acid functionality and used in solid-phase chemistry to synthesize a PEG-functional cyclic olefin with a terminal RGD-containing oligopeptide. This unique macromonomer was subsequently copolymerized to produce graft copolymers with both pendent PEG and oligopeptide functionality. The ability to tune PEG molecular weight and density and to incorporate bio-functionality may be

particularly useful when preparing polymer capsules for delivery applications, as well as in implantable biomaterials made from unsaturated PCOE graft copolymers or hydrogenated polyethylene-based graft copolymers.

As described in Chapter 3, the amphiphilic nature of these graft copolymers was exploited in oil-water interfacial assembly, and the unsaturation present in the polycyclooctene backbone was utilized in covalent cross-linking reactions to afford hollow polymer capsules. In one approach, a *bis*-cyclooctene PEG derivative was synthesized and co-assembled with PCOE-*g*-PEG at the oil-water interface. Upon addition of a ruthenium benzylidene catalyst, a cross-linked polymer shell is formed through ring-opening cross-metathesis between the *bis*-cyclooctene cross-linker and the residual olefins in the graft copolymer. By incorporating a fluorescent-labeled cyclooctene into the graft copolymer, both oil-water interfacial segregation and effective cross-linking were confirmed using confocal laser scanning microscopy (CLSM). In a second approach, reactive functionality capable of chemical cross-linking is incorporated directly into the polymer backbone by synthesis and copolymerization of phenyl azide and acyl hydrazine-functional cyclooctene derivatives. Upon assembly, these reactive polymers can be cross-linked by photolysis (in the phenyl azide case) or by addition of glutaraldehyde (in the acyl hydrazine case) to form mechanically robust polymer capsules with tunable degradability (*i.e.* non-degradable or pH-dependent degradability). This simple interfacial assembly and cross-linking approach to produce capsules is particularly attractive when compared to more widely used methods such as LbL assembly which requires a multi-step assembly and removal of the core. This process also permits the preparation of both oil-in-water and water-in-oil capsules, thus enabling the

encapsulation of hydrophobic or hydrophilic reagents in the capsule core. These novel capsules may be well-suited for a number of controlled release applications, where the transport of encapsulated compounds can be regulated by factors such as cross-link density, hydrolytic stability, and environmental triggers such as pH and temperature.

The application of phenyl azide-containing PCOE-*g*-PEG copolymers as coatings for commercially available poly(vinylidene fluoride) ultrafiltration (PVDF-UF) membranes is described in Chapter 4. The structure and tunable nature of these graft copolymers, in terms of PEG graft density and cross-linkable functionality, make it particularly applicable for enhancing the properties of existing polymer membranes with regards to membrane fouling. Photo-cross-linking of the graft copolymer coating makes them resistant to delamination from the underlying membrane, which in turn reduces fouling of the membrane when compared to uncoated PVDF-UF membranes.

Chapter 5 describes the synthesis of a ruthenium benzylidene metathesis catalyst made amphiphilic by ligand exchange of Grubbs' Generation II catalyst with PEG-substituted pyridine ligands. The PEG-substituted catalyst represents a unique combination of the enhanced reactivity given by a N-heterocyclic carbene (NHC) ligand and the amphiphilicity imparted by PEGylation. The catalyst is soluble in both organic and aqueous solvents and effectively polymerizes cyclic olefins in both dichloromethane and water. In dichloromethane, polymers with low PDIs are obtained, suggesting a controlled or ''living'' polymerization similar to the 3-bromopyridine-substituted Grubbs' Generation III catalyst. The polymerization of cyclic olefins in water proceeds rapidly but without the fine molecular weight control observed in the dichloromethane case.

1.3 References

(1) Duncan, R. *Nat. Rev. Drug Discov.* **2003**, *2*, 347-360.
(2) Park, K. *Controlled drug delivery: challenges and strategies*; American Chemical Society: Washington, DC, 1997.
(3) Hoffman, A. *J. Control. Release* **1998**, *132*, 153-163.
(4) Kost, J.; Langer, R. *Adv. Drug Deliver. Rev.* **2001**, *46*, 125-148.
(5) Langer, R. *Nature* **1998**, *392*, 5-10.
(6) Ringsdorf, H. *J. Polym. Sci. Pol. Sym.* **1975**, 135-153.
(7) Gros, L.; Ringsdorf, H.; Schupp, H. *Angew. Chem. Int. Edit.* **1981**, *20*, 305-325.
(8) Brocchini, S. D., R In *Encyclopedia of Controlled Drug Delivery*; Mathiowitz, E., Ed.; Wiley: New York, 1999, 786-816.
(9) Abuchowski, A.; Mccoy, J. R.; Palczuk, N. C.; Vanes, T.; Davis, F. F. *J. Biol. Chem.* **1977**, *252*, 3582-3586.
(10) Abuchowski, A.; Vanes, T.; Palczuk, N. C.; Davis, F. F. *J. Biol. Chem.* **1977**, *252*, 3578-3581.
(11) Abuchowski, A.; Davis, F. F. *Biochim. Biophys. Acta* **1979**, *578*, 41-46.
(12) Abuchowski, A.; Kazo, G. M.; Verhoest, C. R.; Vanes, T.; Kafkewitz, D.; Nucci, M. L.; Viau, A. T.; Davis, F. F. *Cancer Biochem. Bioph.* **1984**, *7*, 175-186.
(13) Greenwald, R. B.; Choe, Y. H.; McGuire, J.; Conover, C. D. *Adv. Drug Deliver. Rev.* **2003**, *55*, 217-250.
(14) Li, C.; Wallace, S. *Adv. Drug Deliver. Rev.* **2008**, *60*, 886-898.
(15) Safra, T.; Muggia, F.; Jeffers, S.; Tsao-Wei, D. D.; Groshen, S.; Lyass, O.; Henderson, R.; Berry, G.; Gabizon, A. *Ann. Oncol.* **2000**, *11*, 1029-1033.
(16) Mross, K.; Niemann, B.; Massing, U.; Drevs, J.; Unger, C.; Bhamra, R.; Swenson, C. *Cancer Chemoth. Pharm.* **2004**, *54*, 514-524.
(17) Vasey, P. A.; Kaye, S. B.; Morrison, R.; Twelves, C.; Wilson, P.; Duncan, R.; Thomson, A. H.; Murray, L. S.; Hilditch, T. E.; Murray, T.; Burtles, S.; Fraier, D.; Frigerio, E.; Cassidy, J. *Clin. Cancer Res.* **1999**, *5*, 83-94.
(18) Kopecek, J.; Kopeckova, P.; Minko, T.; Lu, Z. R. *Eur. J. Pharm. Biopharm.* **2000**, *50*, 61-81.
(19) Sat, Y. N.; Bibby, M.; Duncan, R. *Brit. J. Cancer* **1999**, *81*, 583-583.
(20) Matsumura, Y.; Maeda, H. *Cancer Res.* **1986**, *46*, 6387-6392.
(21) Maeda, H.; Wu, J.; Sawa, T.; Matsumura, Y.; Hori, K. *J. Control. Release* **2000**, *65*, 271-284.
(22) Tomalia, D. A.; Baker, H.; Dewald, J.; Hall, M.; Kallos, G.; Martin, S.; Roeck, J.; Ryder, J.; Smith, P. *Polym. J.* **1985**, *17*, 117-132.
(23) Fréchet, J. M. J.; Hawker, C. J.; Gitsov, I.; Leon, J. W. *J. Macromol. Sci. Pure* **1996**, *A33*, 1399-1425.
(24) Hawker, C. J.; Fréchet, J. M. J. *Step-Growth Polymers for High-Performance Materials - ACS Sym. Ser.* **1996**, *624*, 132-144.
(25) Gillies, E. R.; Fréchet, J. M. J. *Drug Discov. Today* **2005**, *10*, 35-43.
(26) Ihre, H. R.; De Jesus, O. L. P.; Szoka, F. C.; Fréchet, J. M. J. *Bioconjugate Chem.* **2002**, *13*, 443-452.

(27) Ihre, H.; De Jesus, O. L. P.; Fréchet, J. M. J. *J. Am. Chem. Soc.* **2001**, *123*, 5908-5917.
(28) De Jesus, O. L. P.; Ihre, H. R.; Gagne, L.; Fréchet, J. M. J.; Szoka, F. C. *Bioconjugate Chem.* **2002**, *13*, 453-461.
(29) Conti, B.; Pavanetto, F.; Genta, I. *J. Microencapsulation* **1992**, *9*, 153-166.
(30) Bala, I.; Hariharan, S.; Kumar, M. N. V. R. *Crit. Rev. Ther. Drug Carrier Systems* **2004**, *21*, 387-422.
(31) Heller, J.; Barr, J.; Ng, S. Y.; Abdellauoi, K. S.; Gurny, R. *Adv. Drug Deliver. Rev.* **2002**, *54*, 1015-1039.
(32) Thomas, P. A.; Padmaja, T.; Kulkarni, M. G. *J. Control. Release* **1997**, *43*, 273-281.
(33) Couvreur, P.; BlancoPrieto, M. J.; Puisieux, F.; Roques, B.; Fattal, E. *Adv. Drug Deliver. Rev.* **1997**, *28*, 85-96.
(34) Pavanetto, F.; Genta, I.; Giunchedi, P.; Conti, B. *J. Microencapsulation* **1993**, *10*, 487-497.
(35) Badaru, A.; Wilson, D. M.; Bachrach, L. K.; Fechner, P.; Gandrud, L. M.; Durham, E.; Wintergerst, K.; Chi, C.; Klein, K. O.; Neely, E. K. *Journal of Clin. Endocr. Metabo.* **2006**, *91*, 1862-1867.
(36) Quattrin, T. *Curr. Drug. Saf.* **2006**, *1*, 151-158.
(37) Peppas, N. A.; Klier, J. *J. Control. Release* **1991**, *16*, 203-214.
(38) Peppas, N. A. *J. Bioact. Compat. Pol.* **1991**, *6*, 241-246.
(39) Bell, C. L.; Peppas, N. A. *J. Control. Release* **1996**, *39*, 201-207.
(40) Bell, C. L.; Peppas, N. A. *Biomaterials* **1996**, *17*, 1203-1218.
(41) Kim, B.; Peppas, N. A. *Biomed. Microdevices* **2003**, *5*, 333-341.
(42) Kim, B.; Peppas, N. A. *Int. J. Pharm.* **2003**, *266*, 29-37.
(43) Kabanov, A. V.; Batrakova, E. V.; Alakhov, V. Y. *Adv. Drug Deliver. Rev.* **2002**, *54*, 759-779.
(44) Kabanov, A. V.; Batrakova, E. V.; Alakhov, V. Y. *J. Control. Release* **2002**, *82*, 189-212.
(45) Kabanov, A. V.; Batrakova, E. V.; Sriadlbhatla, S.; Yang, Z. H.; Kelly, D. L.; Alakov, V. Y. *J. Control. Release* **2005**, *101*, 259-271.
(46) Adams, M. L.; Lavasanifar, A.; Kwon, G. S. *J. Pharm. Sci.* **2003**, *92*, 1343-1355.
(47) Kataoka, K.; Harada, A.; Nagasaki, Y. *Adv. Drug Deliver. Rev.* **2001**, *47*, 113-131.
(48) Allen, C.; Maysinger, D.; Eisenberg, A. *Colloid. Surface B* **1999**, *16*, 3-27.
(49) Kim, S. Y.; Lee, Y. M.; Shin, H. J.; Kang, J. S. *Biomaterials* **2001**, *22*, 2049-2056.
(50) Shuai, X. T.; Ai, H.; Nasongkla, N.; Kim, S.; Gao, J. M. *J. Control. Release* **2004**, *98*, 415-426.
(51) Savic, R.; Luo, L. B.; Eisenberg, A.; Maysinger, D. *Science* **2003**, *300*, 615-618.
(52) Zhang, Q.; Remsen, E. E.; Wooley, K. L. *J. Am. Chem. Soc.* **2000**, *122*, 3642-3651.
(53) Hoffman, A. S.; Stayton, P. S.; Ei-Sayed, M. E. H.; Murthy, N.; Bulmus, V.; Lackey, C.; Cheung, C. *J. Biomed. Nanotech.* **2007**, *3*, 213-217.

(54) Hoffman, A. S.; Stayton, P. S.; Press, O.; Murthy, N.; Lackey, C. A.; Cheung, C.; Black, F.; Campbell, J.; Fausto, N.; Kyriakides, T. R.; Bornstein, P. *Polym. Advan. Technol.* **2002**, *13*, 992-999.
(55) Tian, Y.; Bromberg, L.; Lin, S. N.; Hatton, T. A.; Tam, K. C. *J. Control. Release* **2007**, *121*, 137-145.
(56) Lee, E. S.; Na, K.; Bae, Y. H. *J. Control. Release* **2005**, *103*, 405-418.
(57) Bae, Y.; Fukushima, S.; Harada, A.; Kataoka, K. *Angew. Chem. Int. Edit.* **2003**, *42*, 4640-4643.
(58) Engin, K.; Leeper, D. B.; Cater, J. R.; Thistlethwaite, A. J.; Tupchong, L.; McFarlane, J. D. *Int. J. Hyperthermia* **1995**, *11*, 211-216.
(59) Gillies, E. R.; Fréchet, J. M. J. *Bioconjugate Chem.* **2005**, *16*, 361-368.
(60) Lensen, D.; Vriezema, D. M.; van Hest, J. C. *Macromol. Biosci.* **2008**, *8*, 991-1005.
(61) Arshady, R. *J. Microencapsulation* **1989**, *6*, 13-28.
(62) Ali, M. M.; Stover, H. D. H. *J. Polym. Sci. Pol. Chem.* **2006**, *44*, 156-171.
(63) Tiarks, F.; Landfester, K.; Antonietti, M. *Langmuir* **2001**, *17*, 908-918.
(64) Grigoriev, D. O.; Bukreeva, T.; Mohwald, H.; Shchukin, D. G. *Langmuir* **2008**, *24*, 999-1004.
(65) Sukhorukov, G. B.; Donath, E.; Davis, S.; Lichtenfeld, H.; Caruso, F.; Popov, V. I.; Mohwald, H. *Polym. Advan. Technol.* **1998**, *9*, 759-767.
(66) Dinsmore, A. D.; Hsu, M. F.; Nikolaides, M. G.; Marquez, M.; Bausch, A. R.; Weitz, D. A. *Science* **2002**, *298*, 1006-1009.
(67) Discher, B. M.; Won, Y. Y.; Ege, D. S.; Lee, J. C. M.; Bates, F. S.; Discher, D. E.; Hammer, D. A. *Science* **1999**, *284*, 1143-1146.
(68) Discher, D. E.; Ortiz, V.; Srinivas, G.; Klein, M. L.; Kim, Y.; David, C. A.; Cai, S. S.; Photos, P.; Ahmed, F. *Prog. Polym. Sci.* **2007**, *32*, 838-857.
(69) Gaponik, N.; Radtchenko, I. L.; Gerstenberger, M. R.; Fedutik, Y. A.; Sukhorukov, G. B.; Rogach, A. L. *Nano Lett.* **2003**, *3*, 369-372.
(70) Ahmed, F.; Discher, D. E. *J. Control. Release* **2004**, *96*, 37-53.
(71) Duan, H. W.; Kuang, M.; Zhang, G.; Wang, D. Y.; Kurth, D. G.; Mohwald, H. *Langmuir* **2005**, *21*, 11495-11499.

CHAPTER 2

SYNTHESIS OF PEG-FUNCTIONALIZED CYCLIC OLEFINS AND PEG-GRAFTED POLYOLEFINS

2.1 Polymer Architectures

Advances in synthetic polymer chemistry have led to a number of diverse polymer architectures that have dramatically expanded the range and scope of polymer properties and their applications. Well-defined polymers possessing two or more chemically-linked polymeric components as well as a number of branched polymer architectures are now accessible using a variety of currently available polymerization techniques. The advent of these chemically sophisticated polymers has thus enabled the development of highly advanced materials with tunable macro-, micro-, and nanoscale features.[1] Through chemical tailoring of composition and architecture, polymeric self-assembly, both in the bulk and solution, can now be controlled with extraordinary levels of precision. Polymer self-assembly has evolved to the level of being a viable tool to prepare materials for a wide array of applications in electronics,[2] alternative energy sources,[3] and biotechnology.[4]

By synthetically tailoring polymer composition, molecular weight, branching, and functionality, polymer architectures, and their resulting material properties, can be tuned to suit an expanding number of applications. Several examples of polymer architectures commonly encountered in modern polymer chemistry are illustrated in Figure 2.1. Unlike linear homopolymers, which are often limited in chemical tunability and functionalization capacity, polymers based on block, star, graft, and dendritic

architectures are appealing since their properties can be varied through the incorporation of numerous polymer segments and functional chain-ends.

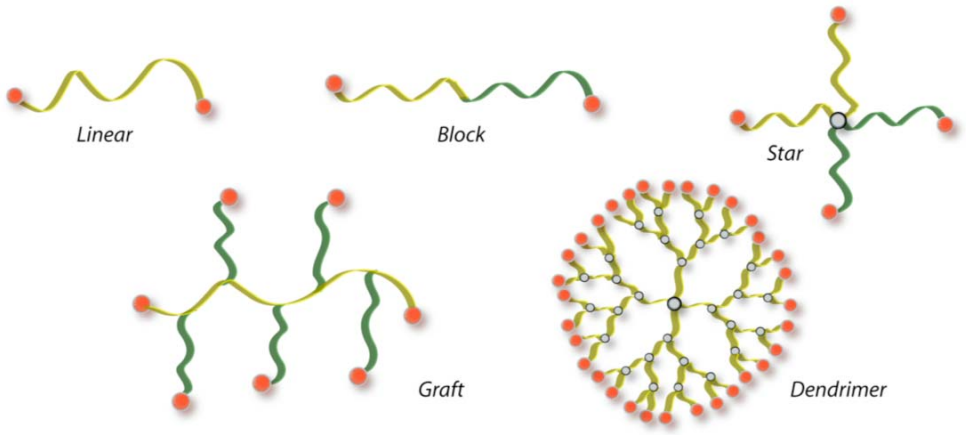

Figure 2.1 Examples of several common polymer architectures

In biotechnology, many of these polymer architectures are well-suited for a number of applications where the synergistic blending of properties imparted by one or more different polymer or biological components can enhance properties such as biocompatibility, mechanical strength, or responsiveness to physiological stimuli. The design of synthetic biomaterials based on block, star, and dendritic copolymers has accelerated tremendously during the past decade with many new materials emerging for applications in drug delivery,[5] implantation,[6] and tissue regeneration.[7] For example, block and graft copolymers that utilize water-soluble polymers such as poly(ethylene glycol) (PEG) in conjunction with biodegradable polymers such as aliphatic polyesters,[8] poly(ortho esters),[9] and polyamino acids[10] have been utilized extensively for the delivery of hydrophobic drugs[11] as well as structural materials for cartilage and muscular repair.[12] Further functionalization of these synthetic polymers with biological ligands (*e.g.* streptavidin/biotin, peptides, polysaccharides) has been shown to greatly improve

biocompatibility and/or illicit desirable interactions between the material and biological components (*e.g.* cells, proteins, antibodies, etc.).[13-15] Many of these advanced biomaterials offer a number of advantages over traditional materials and may potentially lead to future clinical products for disease diagnosis and/or treatment.

Like block and star copolymers, graft copolymers also possess multiple polymer components and in many cases can contain higher quantities of chemical functionality with a wider range of tunable properties through control of the pendent grafts. These features present a number of obvious advantages when designing synthetic biomaterials such as the ability to incorporate numerous pendent grafts that can enhance water solubility or elicit biological functions.

Graft copolymers can be prepared by several synthetic methods such as post-polymerization grafting approaches and direct polymerization of macromonomers as shown in Figure 2.2. Post-polymerization "grafting-to" methods utilize reactive functionality on the polymer backbone for covalent attachment of pendent polymer grafts.[16-18] In the "grafting-from" method, the polymerization of additional monomers is initiated from functionality present on the polymer backbone.[19,20] These synthetic methods are often not ideal since post-polymerization reactions suffer from limitations such as poor grafting efficiency as well as numerous side-reactions that may result in the presence of homopolymer contaminants or cross-linking.

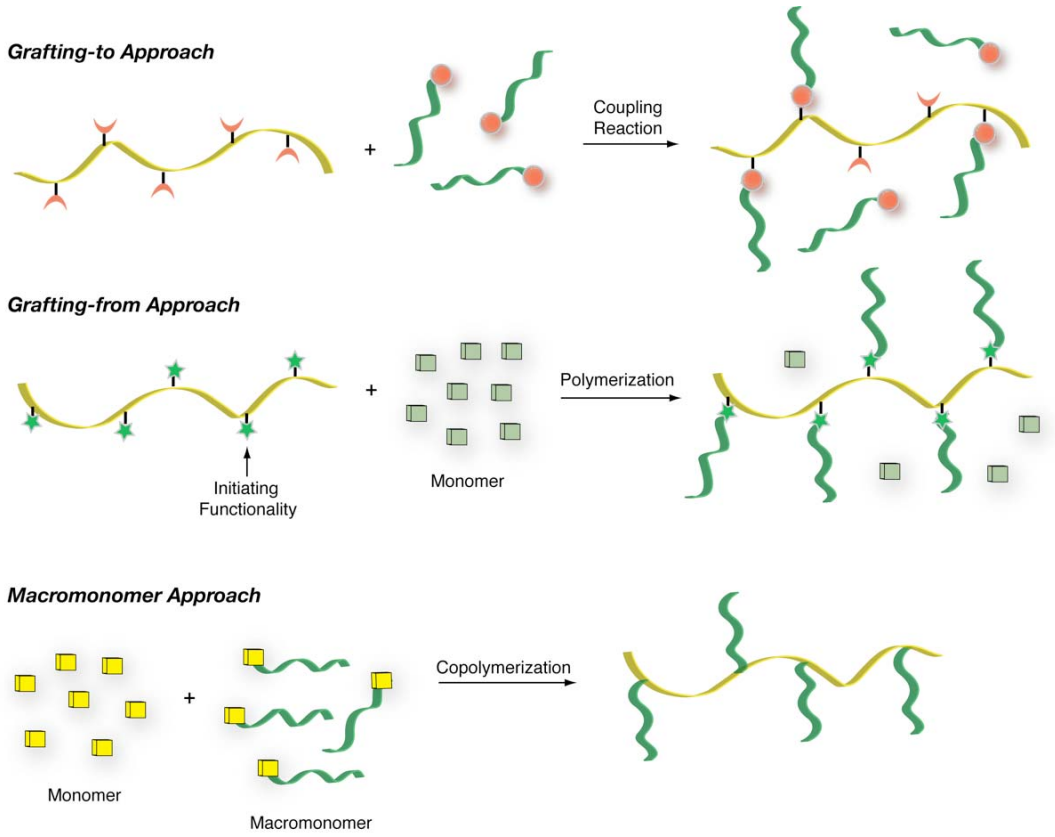

Figure 2.2 Synthetic methodologies commonly used to prepare graft copolymers

In contrast to post-polymerization grafting reactions, the polymerization of macromonomers represents a more convenient and effective method of synthesizing graft copolymers since pendent grafts are incorporated directly through polymerization or copolymerization of the macromonomer itself.[21,22] Thus, better control over graft density is possible, and if complete macromonomer conversion is achieved, the removal of homopolymer contaminants can be avoided. By varying the concentration of macromonomer with respect to other comonomers, physical properties such as crystallinity, mechanical strength, and solubility can be tuned considerably. Graft copolymers have been synthesized by a number of polymerization chemistries. Recent examples include the ring-opening metathesis polymerization (ROMP) of norbornene

macromonomers containing polystyrene (PS) and PEG-*b*-PS grafts prepared by Gnanou and coworkers,[23,24] PEG-grafted polyolefins prepared by acyclic diene metathesis (ADMET) polymerization of PEG-functional a,ω-dienes,[25] and poly(methyl methacrylate) functionalized with integrin-binding RGD (arginine-glycine-aspartic acid) oligopeptides prepared by free radical polymerization.[26]

2.1.1 Olefin Metathesis and the Synthesis of Polyolefin Graft Copolymers by ROMP

In recent years, olefin metathesis reactions (shown in Figure 2.3A) have emerged as powerful tools for C-C bond formation in organic and polymer synthesis. In organic synthesis, ring-closing metathesis (RCM) and cross-metathesis (CM) reactions represent effective methods for the preparation of complex organic molecules that are difficult to prepare by other methods.[27-29] In polymer synthesis, ROMP[30-32] and ADMET[33,34] offer convenient routes to functionalized polyolefins not attainable by conventional olefin polymerization methods (*e.g.* Ziegler-Natta and metallocene-based catalysis).

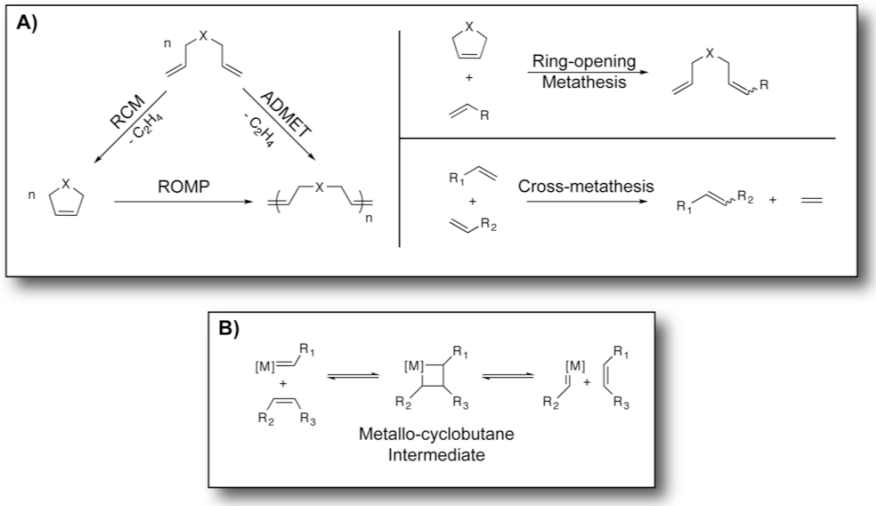

Figure 2.3 A) Examples of olefin metathesis reactions utilized in organic and polymer chemistry, B) mechanism of olefin metathesis

Olefin metathesis is achieved through interconversion of an olefin and a metal alkylidene catalyst as illustrated in Figure 2.3B. This "scrambling" of double bonds is believed to proceed through a metallo-cycloobutane intermediate by alternating cycloadditions and cycloreversions. Early metathesis catalyst systems based on transition metals salts of titanium, tungsten, and ruthenium were only capable of performing a limited scope of metathesis reactions and possessed low catalytic activity.[35,36] These limitations, along with deeper insights into the metathesis reaction mechanism,[37] inspired the development of highly active, structurally well-defined organometallic metathesis catalysts. One of the first such catalysts to gain widespread acceptance was $(NAr)(OR')_2Mo=CHR$ (Ar = 2,6-Pr^i_2-C_6H_3, R = CMe_2-Ph, and R' = $C(CH_3)(CF_3)_2$) developed by Schrock and coworkers.[38] This catalyst displayed unprecedented reactivity towards olefins but was also sensitive to oxygen, water, and many polar functionalities that prevented its widespread use. Subsequent discoveries of well-defined, functional group tolerant ruthenium catalysts[39-41] by Grubbs and coworkers (shown in Figure 2.4) have resulted in the widespread adoption of the metathesis reaction in organic and polymer synthesis. In particular, state-of-the-art ruthenium benzylidene catalysts **II** and **III** possess similar or better olefin reactivity as compared to earlier molybdenum-based catalysts, are relatively stable to air and water, and are compatible with most polar organic functionality. Grubbs, Schrock, and Chauvin were awarded the 2005 Nobel Prize in Chemistry for the development of these well-defined metal alkylidene catalysts and the elucidation of the olefin metathesis mechanism.

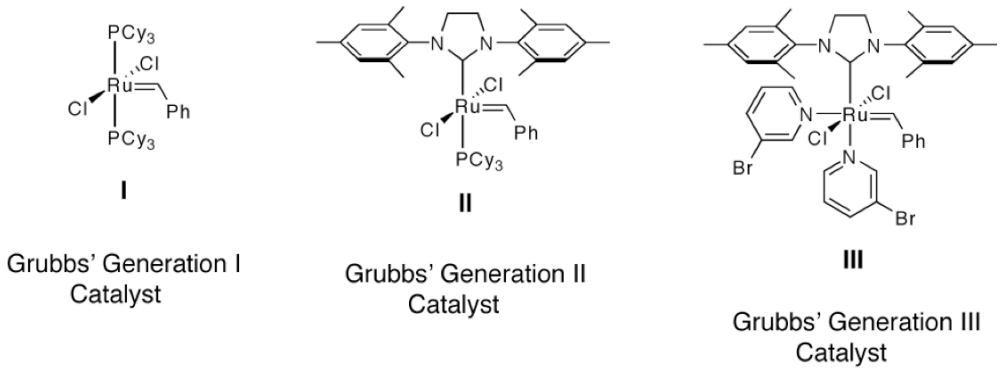

Figure 2.4 Ruthenium benzylidene catalysts commonly used in olefin metathesis

The unprecedented functional group tolerance of new Ru-based catalysts has permitted the ROMP of cyclic olefins containing a multitude of polar functionalities, including many with applications in biology. Prior syntheses of cyclic olefin macromonomers with biologically significant functionality have been performed exclusively on substituted norbornene derivatives. For example, polynorbornene with poly(ethylene glycol) grafts was prepared by Gnanou and coworkers,[42] oligopeptide functional polynorbornene was prepared by Grubbs and coworkers,[43] and saccharide-bearing polynorbornenes were prepared by Kiessling and coworkers.[44] The effectiveness of norbornene polymerization is attributed to its high ring strain (27.2 kcal/mol [45]) which allows for living polymerization with Schrock-type molybdenum catalysts[38,46] and by Grubbs' Generation I and III ruthenium catalysts.[39,41,47]

2.2 Synthesis of Polycyclooctene Graft Copolymers

In contrast to polynorbornene-based copolymers, graft copolymers synthesized from low-strain monocyclic olefin (*e.g.* cyclopentene (6.8 kcal/mol [48]), *cis*-cyclooctene (7.4 kcal/mol [48]), and cyclooctadiene (13.3 kcal/mol [48])) macromonomers have not been exploited due to slower rates of initiation and facile secondary metathesis reactions that

have led to only a few reports of their controlled polymerization.[49,50] Nevertheless, polymers and copolymers synthesized from monocyclic macromonomers are of interest since hydrogenation of the unsaturated backbone gives graft copolymers of polyethylene (PE), a polymer widely utilized due to its inherently robust and tunable mechanical properties. The incorporation of hydrophilic grafts such as PEG and oligopeptides could represent a convenient method to improve the biocompatibility of PE-like polymers, which are used as structural and implantable materials in, for example, joint replacements,[51] and ocular applications.[52]

PEG-grafted polyolefins are also of interest because of their inherent amphiphilic properties, imparted by the combination of a hydrophobic polymer backbone and hydrophilic PEG grafts. These unique copolymers have been shown to segregate to the oil-water interface and can stabilize polymer particles for weeks to months. For example, Gnanou and workers utilized a PEG-grafted norbornene macromonomer as a reactive surfactant in the dispersion and emulsion polymerization of norbornene and cyclooctadiene.[53] They demonstrated that the incorporation of PEG grafts into the copolymer was a key parameter in obtaining stable polymer particles with consistent size and morphology.

This thesis describes the first recorded efforts to synthesize and characterize polycyclooctene-*graft*-poly(ethylene glycol) (PCOE-*g*-PEG) copolymers. Several potential applications for PCOE-*g*-PEG graft copolymers were envisioned at the outset of the project. As previously discussed, the synthesis and hydrogenation of PCOE-*g*-PEG copolymers yields polyethylene-*g*-PEG (PE-*g*-PEG), a semi-crystalline polymer with tunable hydrophilicity based on the number and length of PEG grafts. In addition, the

amphiphilic nature of these graft copolymers provided a potential route for assembly at the oil-water interface. The residual olefins in the polycyclooctene backbone proved useful for post-polymerization cross-linking reactions at the oil-water interface. It was later found that these unsaturated PCOE-*g*-PEG copolymers were excellent candidates for use as anti-fouling coatings for commercial water purification membranes. The low glass transition temperature of the PCOE backbone, which imparts suitable film forming properties, and the hydrophilic PEG grafts, which minimize membrane surface fouling, were key elements in this project.

2.3 Synthesis of PEGylated Cyclooctene Macromonomers

2.3.1 Synthesis of Ester-linked PEG-functional Cyclooctene Macromonomers

The initial strategy to prepare PEG-substituted cyclooctene macromonomers involved a two-step synthetic procedure starting from 5-hydroxy-1-cyclooctene (**1**)[54] as illustrated in Scheme 2.1. Ring-opening of succinic anhydride by **1** in the presence of 4-dimethylaminopyridine (DMAP) gave the corresponding carboxylic acid **2**. This was followed by esterification with PEG-monomethyl ethers under dicyclohexylcarbodiimide (DCC) coupling conditions. While this provided an efficient route to preparing PEGylated cyclooctene macromonomers, initial polymerization chemistry with catalyst **I** led to rapid gelation and intractable materials. The contamination of commercially available mPEGs with appreciable quantities of PEG diol gave a mixture of mono- and *bis*-functionalized cyclooctene macromonomers. The presence of *bis*-cyclooctenes in the polymerization led to cross-linking of the graft copolymers by a ring-opening cross-metathesis mechanism. For mPEG molecular weights less than 1000 g/mol, PEG diol

was removed by column chromatography over silica gel, eluting with chloroform/acetone/methanol mixtures.

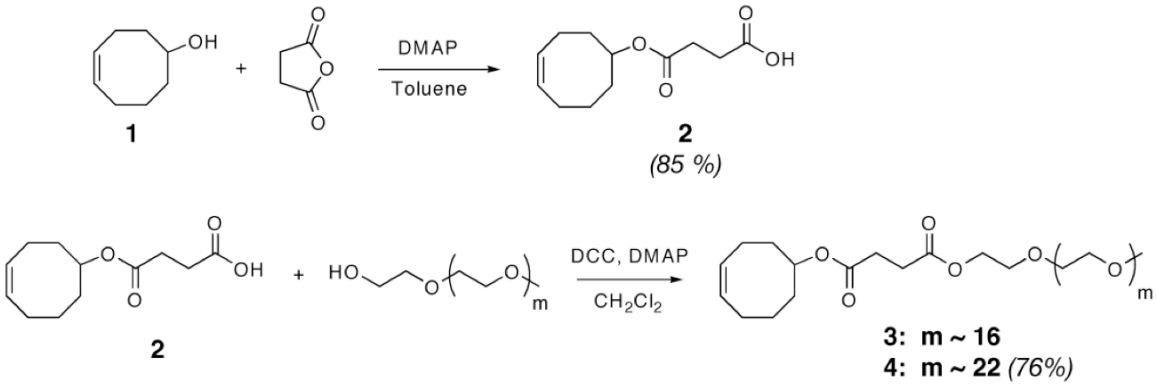

Scheme 2.1 Synthesis of PEGylated cyclooctene macromonomers by carbodiimide coupling of mPEGs to 2

Using carbodiimide coupling, macromonomers **3** and **4** were prepared with column-purified mPEGs possessing molecular weights of approximately 750 and 1000 g/mol, respectively. The coupling strategy proved quite convenient, as it allowed attachment of PEG without the need for anionic polymerization of ethylene oxide. In addition, this synthetic route introduces an ester linkage, which could be potentially exploited in controlled-release applications. The ^{1}H NMR spectrum of macromonomer **4** in $CDCl_3$ consists of olefinic resonances at δ 5.65 ppm and resonances for the protons of the succinic anhydride linker centered at δ 2.65 ppm. A broad signal centered at δ 3.70 ppm reflects interior methylene protons of PEG, while a singlet at δ 3.38 ppm reflects the methoxy end-group. ^{13}C NMR spectroscopy ($CDCl_3$) proved useful to confirm the absence of residual mPEG (removed by extraction in water) and contains a diagnostic methylene signal at δ 61.9 ppm (H_3CO-PEG-$\underline{C}H_2$-OH). Figure 2.5 shows gel permeation chromatography (GPC) overlays of **3**, **4** and mPEG starting materials, where

macromonomers **3** and **4** exhibit low PDI values (shown in Table 2.1) that are in accord with those of the mPEG starting materials.

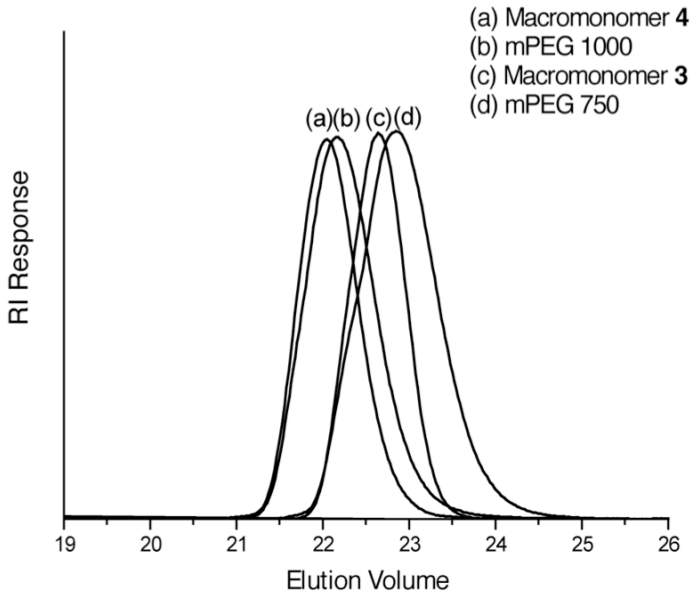

Figure 2.5 Gel permeation chromatograms of macromonomers 3 and 4 and mPEG starting materials

Table 2.1 Molecular weight and PDI estimation for macromonomers 3 and 4 and mPEG starting materials

Entry	M_n (GPC, g/mol)	M_w (GPC, g/mol)	PDI
Macromonomer 4	1290	1350	1.05
mPEG 1000	1180	1250	1.07
Macromonomer 3	970	1000	1.03
mPEG 750	815	870	1.07

2.3.2 Synthesis of Ether-linked PEG-functional Cyclooctene Macromonomers

While carbodiimide coupling of carboxylic acid-functional cyclooctenes and commercially available mPEGs proved suitable for the synthesis of low molecular weight PEGylated cyclooctene macromonomers, a number of limitations motivated us to seek additional synthetic methods to prepare PEG-functional macromonomers. For example, the ester linkage that connects the cyclooctene and PEG moieties is subject to hydrolysis

over time, which would be detrimental for long-term applications in aqueous environments. Applications for polyolefin-*g*-PEG copolymers such as long-term therapeutic encapsulation and release, as well as water purification membrane coatings, require stable PEG linkages to maintain water-solubility, protein resistance, and anti-fouling properties. This motivated the exploration of additional synthetic pathways to produce macromonomers where the cyclooctene is connected to the PEG graft via a hydrolytically-stable ether linkage.

Initial attempts to synthesize ether-linked macromonomers involved the coupling of **1** with mPEG-mesylates (**5**) of low molecular weight to produce macromonomer **6** as shown in Scheme 2.2. Initially, the reaction was performed in THF, but the sodium alkoxide of **1** was only moderately solvent in THF at concentrations greater than 0.1 M, which led to low yields of **6**. In contrast, when dimethylformamide (DMF) was used as the reaction solvent, complete reaction of the mPEG-mesylate was observed after stirring for 16 hours at room temperature. This was confirmed by ^{1}H NMR spectroscopy in $CDCl_3$, which showed an absence of methyl proton resonances at δ 3.01 ppm, attributed to the mPEG-mesylate end-group. New resonances at δ 5.52 ppm and δ 1.32 - 2.30 ppm, corresponding to the olefinic and aliphatic resonances of cyclooctene, respectively, were also observed. However, additional resonances at δ 6.40 ppm and δ 4.10 ppm were observed in the spectrum and attributed to the presence of vinyl ether-functionalized PEG **7**, a by-product of the competing elimination reaction (E_2). By comparing the peak integration of olefinic protons at δ 5.52 ppm to vinyl protons at δ 6.40 ppm, the yield of the E_2 by-product was found to be approximately 10%. Vinyl ethers, such as ethyl vinyl ether, are commonly utilized to terminate the ROMP of cyclic olefins and even small

concentrations of vinyl ether PEG inhibited the polymerization of macromonomer **6**. Unfortunately, column chromatography and other solid phase extraction techniques were ineffective at removing the vinyl ether by-product from the macromonomer.

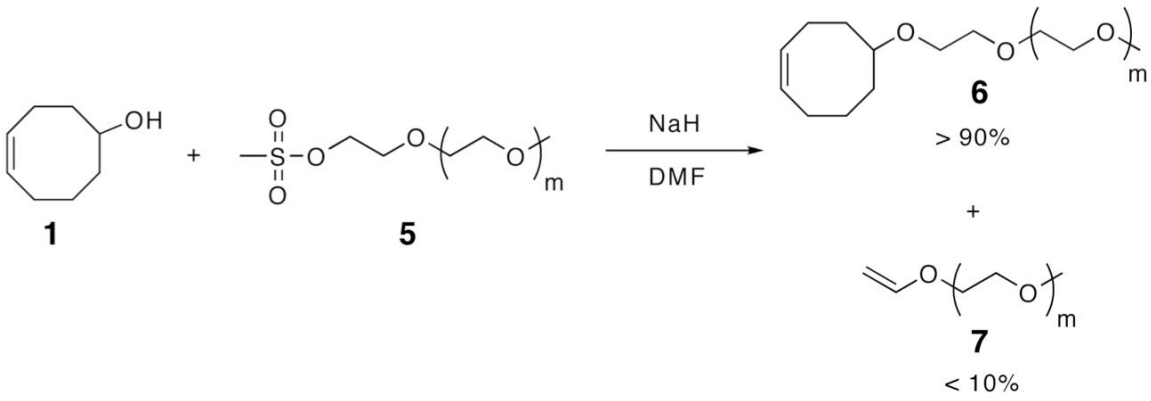

Scheme 2.2 Synthesis of ether-linked PEG macromonomer 6 by coupling of 1 and mPEG mesylate 5

The removal of the vinyl ether by-product **7** from macromonomer **6** proved challenging and several additional factors also limited the use of coupling chemistry to produce ether-linked macromonomers. For example, the removal of diol contaminants from the mPEG starting material by column chromatography becomes progressively more difficult as the mPEG molecular weight exceeds approximately 1000 g/mol (ca. 25 repeat units). Thus, preparing monosubstituted PEG derivatives and macromonomers from higher molecular weight mPEGs proved difficult. Furthermore, the utilization of mPEGs, which possesses an unreactive methyl terminus precludes the preparation of bifunctional PEG derivatives.

For the reasons outlined above, the living, anionic polymerization of ethylene oxide (EO), initiated by cyclooctene alkoxides, offers an attractive synthetic route to the desired macromonomer. The construction of a stainless-steel polymerization manifold,

detailed by Coughlin and coworkers,[55] provided a viable system in which EO, a toxic gaseous monomer, could be transferred safely from the lecture bottle to the reaction flask, thus significantly reducing the risk of exposure. Using this manifold, ether-linked PEG macromonomers were prepared by anionic polymerization of ethylene oxide initiated by **1** (shown as **8**, **9**, and **10** in Scheme 2.3) on the 1 - 30 gram scale. In a typical polymerization, a 1.0 M solution of **1** in THF was introduced to an air-free reaction flask containing anhydrous THF using standard Schlenk techniques and subsequently deprotonated with an organic base such as potassium naphthalenide or triphenylmethyl potassium. The solution containing the potassium alkoxide of **1** was then connected to the manifold, where a measured volume of condensed EO (-78 ^{o}C) was slowly warmed to room temperature and transferred as a gas to the stirring initiator solution at 0 ^{o}C. The polymerization was conducted in a sealed, argon-filled reaction vessel at room temperature for 16 hours, and the macromonomer was purified by repetitive precipitation into diethyl ether or by column chromatography using chloroform/methanol mixtures.

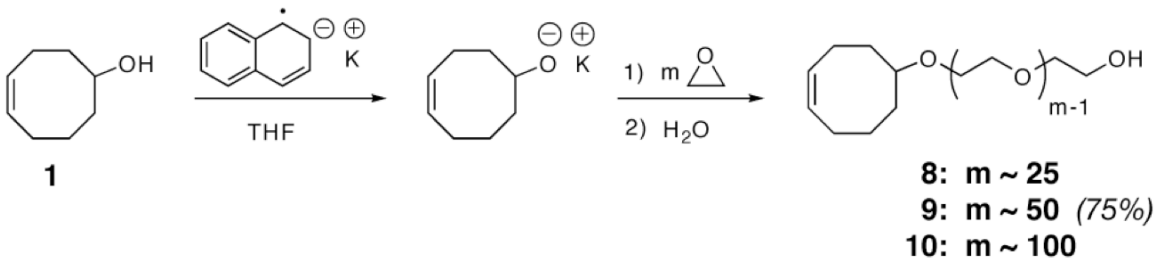

Scheme 2.3 Synthesis of ether-linked PEG macromonomers by anionic ring-opening polymerization of ethylene oxide initiated by the potassium alkoxide of 1

In addition to improved hydrolytic stability, the living polymerization of ethylene oxide permits the synthesis of macromonomers with a wide range of PEG molecular weights by simply varying the monomer-to-initiator ratio. GPC traces of

macromonomers **8** - **10** (25, 50 and 100 EO units, respectively) in THF are shown in Figure 2.6 and molecular weight estimates are detailed in Table 2.2. Using this approach, macromonomers with PEG molecular weights ranging from 1100 g/mol (25 EO units) to 4400 g/mol (100 EO units) and PDI values less than 1.10 were produced with excellent control of PEG molecular weight. ^{1}H NMR analysis of macromonomers **8**, **9**, and **10** in d_6-DMSO showed resonances at δ 5.58 ppm arising from olefinic protons of the cyclooctene initiator as well as a broad peak centered at δ 3.60 ppm corresponding to methylene protons of the PEG backbone. In d_6-DMSO, the hydroxyl proton of the PEG terminus (COE-PEG-O<u>H</u>) is visible as a triplet centered at δ 4.55 ppm.

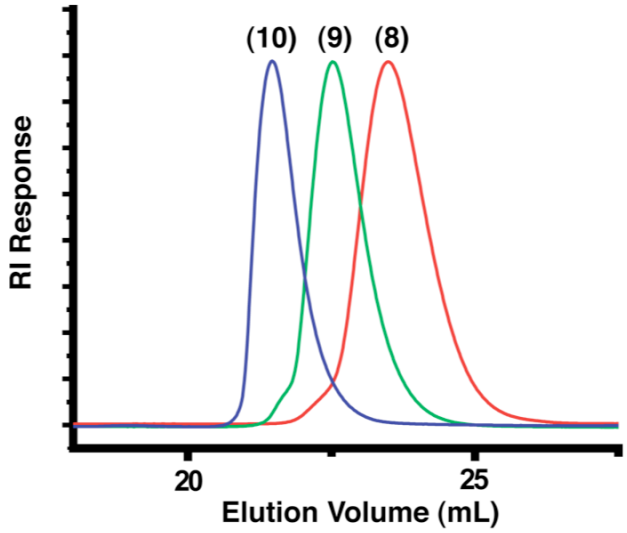

Figure 2.6 GPC chromatograms of ether-linked macromonomers 8, 9, and 10 prepared by anionic polymerization of ethylene oxide

Table 2.2 Molecular weight and PDI estimation for macromonomers 8 - 10

Entry	m (target)	M_n (target, g/mol)	M_n (GPC, g/mol)	PDI
Macromonomer 8	25	1200	1250	1.09
Macromonomer 9	50	2300	2350	1.09
Macromonomer 10	100	4500	4600	1.08

2.3.3 End-functionalization of Ether-linked Macromonomers 9 with an RGD-containing Oligopeptide

The anionic polymerization of EO initiated by **1** provides an ideal synthetic pathway to produce macromonomers with a very broad range of well-defined PEG molecular weights. In addition to these benefits, EO polymerization also provides heterobifunctional PEG macromonomers that possess a terminal hydroxyl group for further attachment of targeting groups, drugs, or fluorescent labels. The attachment of cell targeting groups at the macromonomer terminus is advantageous for drug delivery and biomaterials applications since the peptide should be readily accessible to cellular receptors on targeted cells. By comparison, the copolymerization of a cyclooctene-functionalized oligopeptide would place the targeting group close the polycyclooctene backbone, and thus, the pendent PEG grafts might sterically shield the desired cellular interactions. As an initial proof-of-concept, macromonomer **9** was functionalized with an oligopeptide containing the $\alpha_V\beta_3$-integrin binding motif, RGD. RGD-containing oligopeptides have been widely utilized in a number of biotechnology applications, including, for example, active targeting of drug delivery systems to rapidly proliferating endothelium around cancerous tissue[56] and the promotion of cell attachment to a variety of biomaterial scaffolds.[57]

To accomplish this, a PEG-functional macromonomer possessing terminal carboxylic acid-functionality was prepared and coupled directly to an RGD-containing oligopeptide prepared by solid phase synthesis (SPS) by Ph.D. candidate Rebecca Breitenkamp in the Emrick group. The initial synthetic route to carboxylic-acid functionalized macromonomers involved end-capping the "living" PEG alkoxide of **9** with *t*-butyl bromoacetate as shown in Scheme 2.4A. Using rigorously purified reagents

and Schlenk techniques, macromonomer **11** was prepared in 89% yield and with near quantitative functionalization of the alkoxide end-group. This was confirmed by ^{1}H NMR spectroscopy of **11** in d_6-DMSO which showed the absence of the hydroxyl proton resonance at δ 4.55 ppm and new resonances at δ 3.98 ppm and δ1.47 ppm corresponding to acetate and *t*-butyl protons, respectively. However, GPC analysis of **11** and deprotected macromonomer **12** showed a bimodal molecular weight distribution, indicative of substantial quantities of the dimer of macromonomer **12**, presumably resulting from coupling through both the acetate and ester moieties.

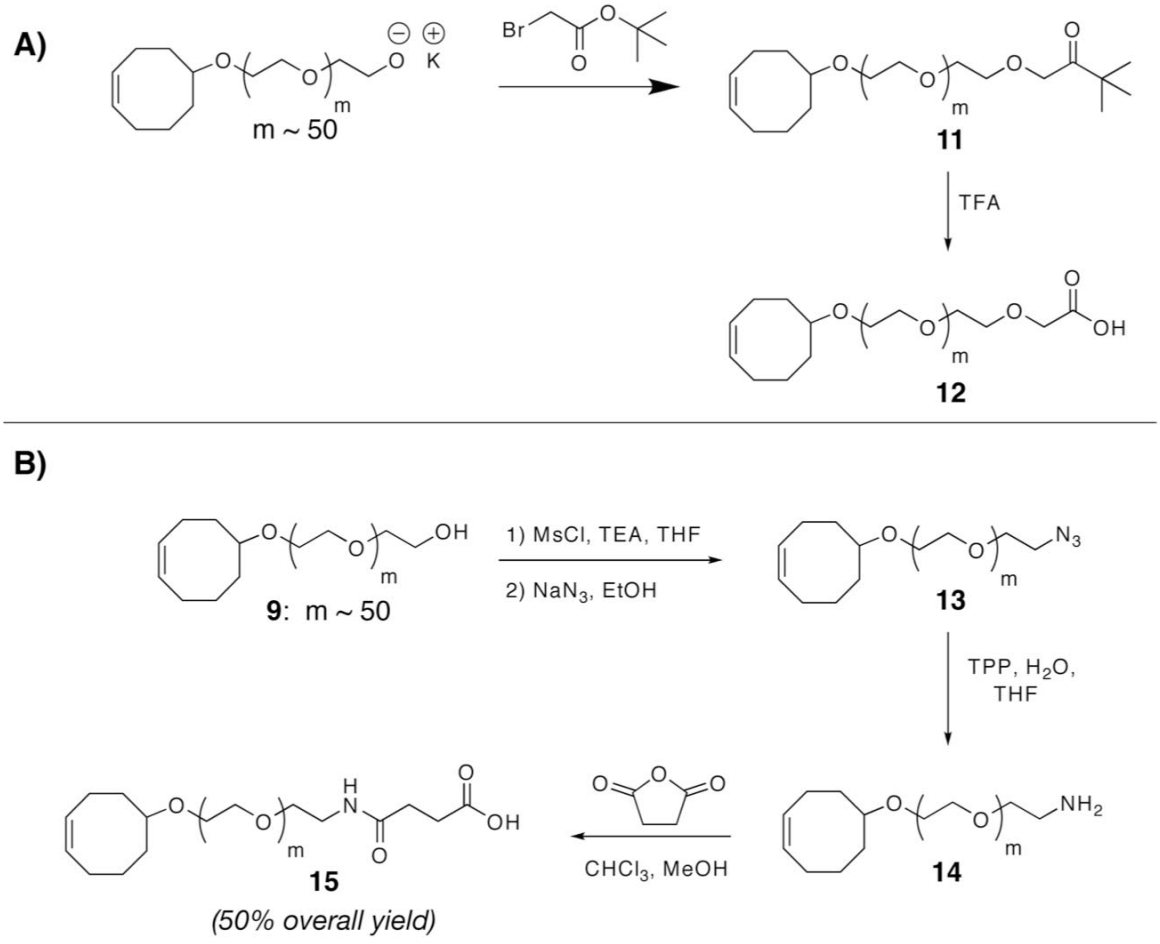

Scheme 2.4 Synthetic routes to carboxylic acid-functional PEG macromonomers 12 and 15

To circumvent this problem, a multi-step synthetic route to the carboxylic acid-functional macromonomer was pursued starting from hydroxyl-functional macromonomer **9** as shown in Scheme 2.4B. In the first step, the hydroxyl functionality of **9** was converted to the corresponding azide (**13**) through base-catalyzed reaction with methanesulfonyl chloride and subsequent substitution using sodium azide in refluxing ethanol. ^{1}H NMR spectroscopy of **13** in d_6-DMSO showed complete functionalization of the hydroxyl functionality as illustrated by the absence of resonances at δ 4.55 ppm and δ 3.00 ppm, corresponding to hydroxyl and mesylate protons, respectively. The presence of the terminal azide was confirmed by ATR-FTIR spectroscopy, which showed a significant absorbance at 2095 cm^{-1}. The azide of macromonomer **13** was subsequently converted to a primary amine (**14**) by Staudinger reduction with triphenylphosphine and water. Complete reduction of the azide was confirmed by the disappearance of the absorbance at 2095 cm^{-1} in the IR spectrum and appearance of a new resonance at δ 2.60 ppm in the ^{1}H NMR spectrum (d_6-DMSO), attributed to the methylene protons α to the terminal amine. In the final step, amine **14** was utilized in the ring-opening reaction of succinic anhydride to yield carboxylic acid-functionalized macromonomer **15**. ^{1}H NMR spectroscopy of **15** in d_6-DMSO showed unique resonances at δ 12.07 ppm and δ 2.50 ppm corresponding to the carboxylic acid and succinic acid linker, respectively. GPC analysis in THF showed a single peak with M_n of 2500 g/mol with a PDI of 1.12 (referenced against PEG standards). By employing this series of highly efficient reactions, macromonomer **15** was prepared with very high purity and with minimal purification required. The overall yield for this three step synthetic conversion was approximately 50%.

To synthesize the oligopeptide-functional macromonomer, a resin-bound GRGDS oligopeptide was prepared (by Rebecca Breitenkamp) using solid-phase peptide synthesis and standard Fmoc protection/deprotection chemistries. Each amino acid was coupled sequentially using 1-hydroxybenzotriazole (HOBt) and HBTU starting from a Ser(*t*-but)-loaded, 2-chlorotrityl resin. Following Fmoc removal from the N-terminal glycine residue with piperidine, a solution of macromonomer **15** in DMF was coupled to the oligopeptide using HBTU/HOBt as illustrated in Scheme 2.5. The coupling reaction with **15** was carried out twice for 3 hours in an effort to maximize coupling efficiency of this large macromolecule. After repeated washing of the resin with DMF and dichloromethane, the GRGDS-functional macromonomer was cleaved from the resin using trifluoroethanol. The 2-chlorotrityl resin permits the cleavage of **16** without removing the Pbf (arginine) and *t*-butyl protecting groups (glutamic acid and serine) of the oligopeptide. This is key since primary amine functionality on the arginine residue binds to ruthenium benzylidene catalysts, which would prevent ROMP of unprotected **16**.

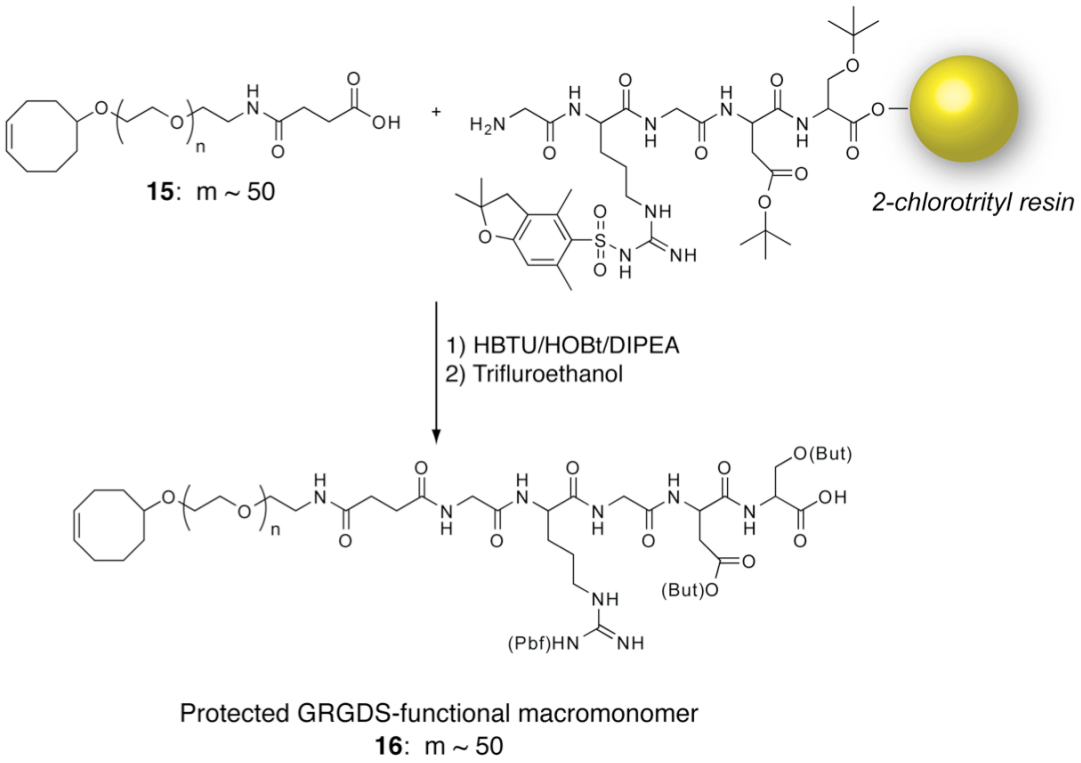

Scheme 2.5 Synthesis of GRGDS-functional macromonomer 16 by solid phase coupling chemistry

^{1}H NMR analysis of crude **16** shows the presence of PEG resonances at δ 3.50 ppm and oligopeptide resonances arising from amide protons ranging from δ 7.5 – 8.5 ppm. Resonances corresponding to protons of the *t*-butyl protecting groups of Ser and Glu and the amide backbone were also observed at δ 1.10 ppm and δ 7.80 – 8.30 ppm, respectively. However, GPC analysis of the crude product in THF showed multiple peaks with molecular weight values less than 1000 g/mol. This was attributed to the presence of free GRGDS oligopeptide that was not coupled to macromonomer **15**. The uncoupled oligopeptide, insoluble in water, was removed by filtration. GPC analysis of purified **16** in THF showed a single peak with M_p corresponding to 2500 g/mol with a PDI of 1.13 (referenced against PEG standards). Matrix-assisted laser

desorption/ionization (MALDI) mass spectrometry, shown in Figure 2.7, revealed a relatively narrow distribution of peaks centered at 3261 Da which corresponds to GRGDS-functionalized macromonomer **16** (calcd. 3259 Da) with a second distribution of peaks corresponding to the K^+ charged analogues.

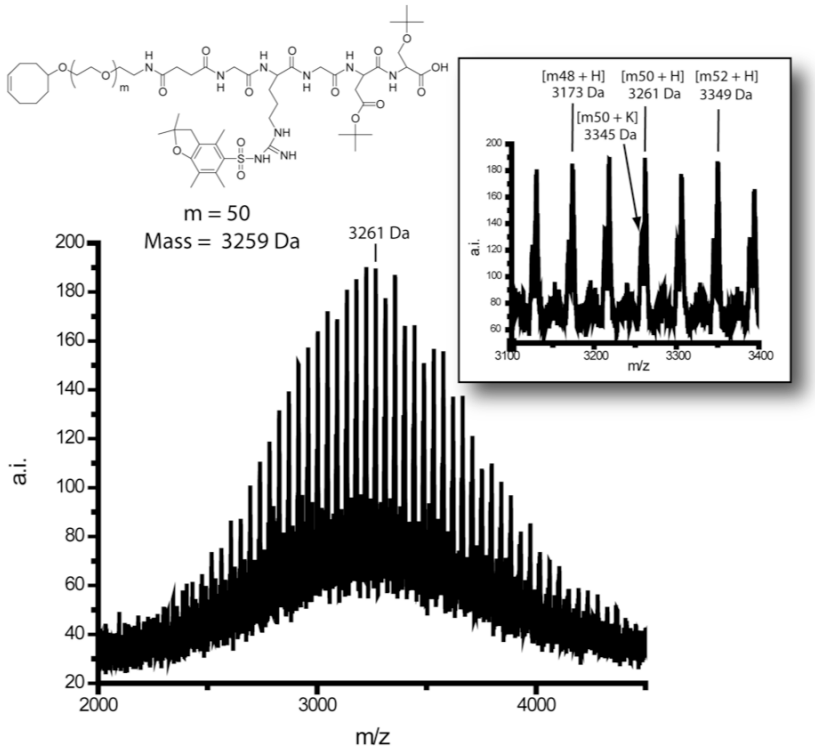

Figure 2.7 MALDI analysis of GRGDS-functional macromonomer 16

2.4 Synthesis of Polycyclooctene-*g*-PEG Copolymers

2.4.1 Copolymerization of Ester-linked Macromonomers 3 and 4

Macromonomers **3** and **4** were copolymerized with cyclooctene in the presence of bis(tricyclohexylphosphine)benzylidine ruthenium (IV) dichloride (catalyst **I**), or the mono-1,3-dimesitylimidazolidine-2-ylidene derivative (catalyst **II**), as illustrated in Scheme 2.6. Typical experiments employed about 0.42 mmol of macromonomer and 0.42 mmol to 3.80 mmol of cyclooctene. Catalysts were introduced to the

macromonomer/cyclooctene mixtures as solutions in dry dichloromethane and then removed after polymerization by termination with ethyl vinyl ether. The polymerizations were carried out under a variety of concentrations and temperatures that dictate the course of the reaction. Our initial polymerization attempts were conducted at room temperature using catalyst **I.** While these conditions achieved considerable molecular weights and conversion (>75 %) in about 16 hrs, the products possessed multi-modal molecular weight distributions. In contrast, when polymerizations were carried out at 45 ^{o}C and ca. 2.0 M, a noticeable change in reaction viscosity was observed within 15-30 minutes in the case of catalyst **I**, and in seconds using catalyst **II**.

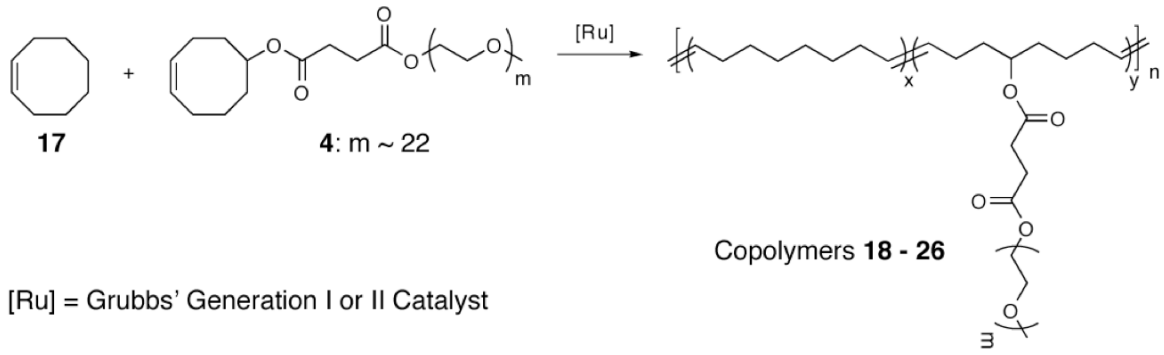

Scheme 2.6 Synthesis of PCOE-*g*-PEG by ROMP of macromonomer 4

Copolymers **18 - 23** in Table 2.3 represent copolymerizations of macromonomer **4** and cyclooctene (**17**) using catalyst **I**. The extent of macromonomer incorporation into the copolymer was determined by ^{1}H NMR spectroscopy by integration of olefinic protons of residual macromonomer (δ 5.65 ppm) against the methyne proton of the graft point (*i.e.*, RC<u>H</u>(OR')R). In all cases, approximately 60 - 70% of the starting macromonomer used became incorporated into the polymer product. Molecular weight estimation by GPC in DMF showed a decrease in M_n of the copolymers from approximately 330,000 g/mol (M_n) to 180,000 g/mol upon increasing cyclooctene ratios

from 0.5 to 0.9 (relative to macromonomer), respectively. The extent of low molecular weight by-products decreased as well. This suggests that while macromonomer conversion is relatively efficient, at higher macromonomer concentrations there is a barrier at the oligomeric stage, possibly due to cyclization.[58-60]

Monomer-to-catalyst ratios were investigated for these copolymerizations, as shown for copolymers **22** and **23** of Table 2.3. As expected, lower monomer-to-catalyst ratios gave lower molecular weight copolymers in a shorter period of time. For example, 50:50 copolymerizations using monomer-to-catalyst ratios of 500:1 (copolymer **18**) and 100:1 (copolymer **23**) gave products with M_n of 330 kDa and 140 kDa. Lower monomer-to-catalyst ratios also resulted in a decrease in low molecular weight oligomers, as observed by more nearly uni-modal GPC chromatograms. Similar syntheses using catalyst **II** are shown as copolymers **24** – **26** of Table 2.3, where nearly complete conversion of macromonomer **4** was observed. The increased activity of this catalyst is demonstrated by the excellent macromonomer incorporation achieved, even at lower concentrations (1.0 M). Figure 2.8 overlays chromatograms of copolymers **18** and **24**, prepared using catalysts **I** and **II**, respectively and otherwise identical reaction conditions (500:1 monomer-to-catalyst; 2.0 M in dichloromethane). In the case of copolymer **24**, where catalyst **II** was used, the presence of low molecular weight cyclized oligomers is reduced dramatically and reasonably narrow polydispersities are observed. Similar results were obtained when polymerizations were conducted at lower monomer concentrations (copolymers **25** and **26**).

Table 2.3 Characteristics of ester-linked PCOE-*g*-PEG copolymers 18 - 26 prepared using ruthenium benzylidene catalysts I and II

Copolymer[a]	[M]/[Cat I]	[M]/[Cat II]	[M]	f_{macro}[b]	F_{macro}[c]	10^{-3} M_n[d]	PDI
18	500	-	2.0	0.50	0.35	330	1.61
19	500		2.0	0.40	0.27	310	1.73
20	500		2.0	0.25	0.15	180	1.78
21	500		2.0	0.10	0.06	190	1.21
22	250	-	2.0	0.50	0.40	220	1.59
23	100	-	2.0	0.50	0.40	140	1.54
24	-	500	2.0	0.50	0.49	540	2.20
25	-	250	1.0	0.50	0.50	330	1.56
26	-	100	1.0	0.50	0.50	220	1.60

[a][M] = 2.0 mol/L, 40 °C in CH_2Cl_2, [b]f_{macro}= feed ratio of macromonomer relative to cyclooctene, [c]F_{macro} = fraction of macromonomer incorporated into polymer, determined by ^{1}H NMR, [d]Determined by GPC in DMF vs. polystyrene standards.

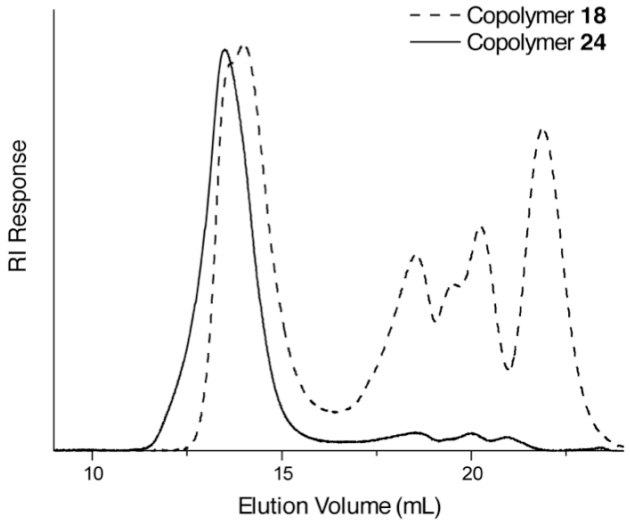

Figure 2.8 GPC chromatograms of copolymers 18 and 24 (in DMF) prepared using ruthenium benzylidene catalysts I and II, respectively

2.4.2 Copolymerization of Ether-linked Macromonomers 8 - 10

Copolymerizations of ether-linked macromonomers **8** - **10** showed similar physical characteristics to graft copolymers of **3** and **4** when polymerized with catalysts **I** and **II**. However, many applications for PCOE-*g*-PEG copolymers required the long-term hydrolytic stability imparted by the ether linkage. Thus, macromonomers **8** – **10** were extensively used in polymer capsule synthesis and membrane applications described in Chapters 3 and 4, respectively.

Recently, Grubbs and coworkers reported a third generation catalyst (catalyst **III**), which replaces tricyclohexylphosphine ligands of **II** with the more labile 3-bromopyridine ligands. This catalyst displays enhanced metathesis activity when compared to **I** and **II** and enables a faster, living polymerization of norbornene and oxanorbornene derivatives relative to **I**. Thus, catalyst **III** was utilized for the polymerization of macromonomers **8** – **10**. In this case, complete macromonomer conversion was obtained using much lower concentrations of this highly active catalyst. While monomer-to-catalyst ratios of 250:1 or 500:1 are typically employed for catalysts **I** and **II**, full macromonomer conversion was achieved with monomer-to-catalyst **III** ratios up to 10,000:1. 1-Hexene, an acyclic chain transfer agent, is added to these polymerizations to control the molecular weight.[61,62] By simply varying the monomer-to-chain transfer agent ratio, the molecular weight of the graft copolymer can be effectively tuned. The ability to utilize very high monomer-to-catalyst ratios is particularly important when preparing PCOE-*g*-PEG copolymers in multi-gram quantities since only small concentrations of these expensive catalysts are needed for effective polymerization.

As shown in Scheme 2.7, copolymers **27** – **29**, with ether-linked PEG grafts, were synthesized using catalyst **III** and a monomer-to-catalyst ratio of 250:1. 1-Hexene was employed at a monomer-to-chain transfer agent ratio of 150:1. These particular PCOE-*g*-PEG copolymers were synthesized to study the effect of graft length on the crystallization properties of hydrogenated PE-*g*-PEG copolymers. For this reason, the macromonomer content in the polymerization feed of copolymers **27** – **29** was held constant at 8 mol % and the macromonomer PEG length was varied from 25 to 100 repeat units. Polymerizations were carried out in a similar fashion as those described for copolymers

18 – 26 with the exception that the reactions were carried out at room temperature. The higher activity of catalyst **III** versus catalyst **II** permits the full conversion PEGylated macromonomers at lower temperatures in shorter time periods. ^{1}H NMR analysis of copolymers **27 – 29** performed in $CDCl_3$ showed an absence of cyclic olefin resonances at δ 5.65 ppm and new olefinic resonances of the PCOE backbone at δ 5.36 ppm, indicating complete conversion of the macromonomer. Integration of the methyne proton of the PEG graft point (RCH(OR')R, 3.25 ppm) versus olefinic proton resonances in the PCOE backbone (δ 5.36 ppm) provides an estimation of the number of grafts per polymer chain. Based on these ratios, it was calculated that approximately 8 PEG grafts were present per 100 cyclooctene repeat units for all three copolymers as shown in Table 2.4. GPC analysis of PCOE-*g*-PEG copolymers with low PEG contents, such as copolymers **27 – 29**, must be performed in $CHCl_3$ due to the limited solubility of PCOE backbone in common solvents for GPC, such as THF and DMF. Copolymers **27** and **28** with PEG graft lengths of 25 and 50 repeat units, respectively, possessed estimated molecular weight values of approximately 24,000 g/mol. Copolymer **29** showed significantly higher estimated molecular weights of 48 kDa, presumably due to the significantly longer PEG grafts (100 EO repeats). PDI values for the three polymers were approximately 2, as predicted when utilizing monofunctional chain transfer agents.[63]

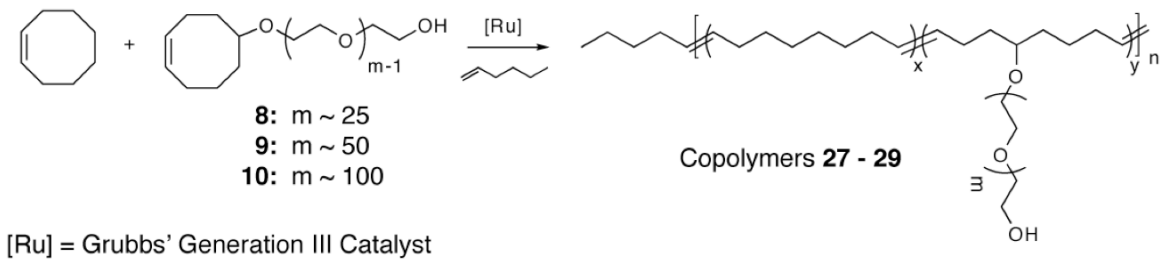

Scheme 2.7 Synthesis of PCOE-*g*-PEG copolymers 27 – 29 by ROMP of ether-linked macromonomers 8 – 10

Table 2.4 Characteristics of ether-linked PCOE-*g*-PEG copolymers 27-29

Copolymer[a]	Macromonomer	[M]/[Cat III]	[M]/[CTA]	[M]	f_{macro}[b]	F_{macro}[c]	10^{-3} M_n[d]	PDI
27	**8**	250	150	2.0	0.08	0.08	24.0	2.02
28	**9**	250	150	2.0	0.08	0.08	24.6	2.26
29	**10**	250	150	2.0	0.08	0.08	48.8	2.77

[a][M] = 1.5 mol/L, 25 ^{o}C in CH_2Cl_2, [b]f_{macro}= feed ratio of macromonomer relative to cyclooctene, [c]F_{macro} = fraction of macromonomer incorporated into polymer, determined by ^{1}H NMR, [d]Determined by GPC in $CHCl_3$ vs. polystyrene standards.

The PCOE-*g*-PEG copolymers described above are amphiphilic and soluble in a range of organic solvents (MeOH, acetone, CH_2Cl_2, $CHCl_3$, THF, DMF, and toluene) at all percentages of macromonomer incorporation. Polymers with PEG grafts of 2000 g/mol or longer (*i.e.* copolymers **28** and **29**) were precipitated into diethyl ether. Hexane proved suitable for precipitation of graft copolymers with shorter PEG lengths (*i.e.* copolymers **18** – **27**). With the exception of copolymer **21**, copolymers **18** – **26** all readily form aqueous solutions. These amphiphilic copolymers stabilize oil-in-water emulsions for hours to days, depending on macromonomer content. In general, the unsaturated PCOE-based copolymers have limited shelf life, due to their propensity to undergo oxidative cross-linking of the olefinic backbone. However, it was found that polycyclooctene copolymers containing high weight percentages of PEG (> 75 wt %) showed minimal cross-linking over several weeks, presumably due to the lower concentration of olefins present in these samples. For copolymers with low PEG content (< 50 wt %), the introduction of 1 wt % 2,6-di-*tert*-butyl-*p*-cresol (BHT) during precipitation and storage in the freezer (-20 ^{o}C) proved useful for prolonging the polymer shelf life.

2.4.3 Copolymerization of GRGDS-functional Macromonomer 16

To test the feasibility of incorporating oligopeptides into PCOE-*g*-PEG copolymers, GRGDS-substituted macromonomer **16** was copolymerized with

cyclooctene (**17**) and macromonomer **9** using catalyst **III** at room temperature. For this initial demonstration, 5 mol % of **16** was introduced into the monomer feed with 75 mol % of **17** and 20 mol % of **9** as shown in Scheme 2.8. This amount of **16** in the monomer feed was chosen based on numerous studies which indicate that only low incorporations of targeting ligands are needed to facilitate interactions with cellular receptors for drug delivery[64] or to stimulate cellular adhesion and proliferation.[65,66]

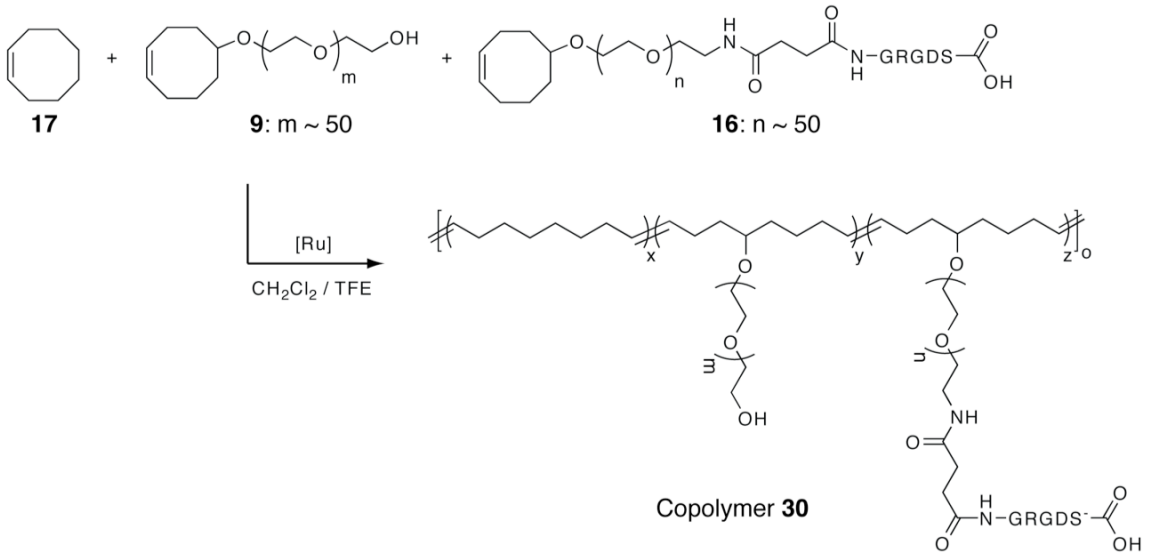

Scheme 2.8 Synthesis of GRGDS-containing PCOE-*g*-PEG copolymer 30 by ROMP of peptide-functional macromonomer 16

Due to the limited solubility of **16** in pure dichloromethane, a small amount of trifluoroethanol (0.1 mL) was added to give a homogeneous solution for the polymerization. ROMP in solvent mixtures containing trifluoroethanol has been reported previously by our group,[67] and others,[68] and was found in this case to permit the ROMP of **16** in yields greater than 90%. Following termination with ethyl vinyl ether and precipitation into diethyl ether, ^{1}H NMR spectroscopy of copolymer **30** in d_6-DMSO revealed an absence of cyclic olefin resonances at δ 5.65 ppm, indicating complete

conversion of macromonomers **16** and **9**. Unique resonances corresponding to the protected GRGDS oligopeptide at δ 7.90 – 8.10 ppm (-N<u>H</u>-C(O)- peptide backbone resonances), δ 4.20 ppm ((-C(O)-C<u>H</u>(R)-NH- peptide backbone resonances), and δ 1.10 ppm (Asp(*t*-but) and Ser(*t*-but) resonances) also verified incorporation of macromonomer **16**. The molecular weight of copolymer **30** was estimated to be 77,000 g/mol by GPC analysis in THF versus polystyrene standards with a PDI of 2.9. In addition, GPC analysis of **30** using UV detection showed a strong absorbance at 254 nm, indicative of the aromatic Pbf protecting group of the incorporated GRGDS oligopeptide. By comparison, PCOE-*g*-PEG copolymers without pendent oligopeptides (*e.g.* copolymers **18** – **29**) show minimal UV absorbance at this wavelength.

2.5 Hydrogenation of PCOE-*g*-PEG Copolymers to PE-*g*-PEG

The unsaturated polycyclooctene-*g*-PEG copolymers were hydrogenated using *p*-toluenesulfonhydrazide[54] to give the saturated analogs with PE backbones as shown in Scheme 2.9. This chemical transformation resulted in dramatic differences in solubility and crystallinity, with variations depending on macromonomer content. Hydrogenated products with low macromonomer content, such as copolymers **20a** and **21a**, were completely insoluble at room temperature, while copolymer **19a** was soluble in polar solvents. Copolymer **20a**, with the highest macromonomer content studied here, remained water-soluble after hydrogenation. Differential scanning calorimetry (DSC) analysis confirmed the increasing crystallinity of these copolymers with decreasing macromonomer incorporation. As shown in Figure 2.9, two endotherms at 8 ^{o}C and 115 ^{o}C for copolymer **21a** were observed and correspond to melting transitions of the PEG grafts and PE backbone, respectively. ^{1}H NMR spectroscopy and GPC analysis were

used to further confirm the structure of these hydrogenated products. The ^{1}H NMR spectrum of copolymer **19a** in $CDCl_3$, for example, showed no signals in the olefinic region and showed resonances that reflect the methyne proton of the graft point, the succinic anhydride linker, and the methyl ether end-group of the PEG graft, all in accord with the expected structure. GPC analysis (in trichlorobenzene at 135 °C) of copolymer **21a** showed only small changes in molecular weight (using multiple angle laser light scattering detection) from its unsaturated precursor.

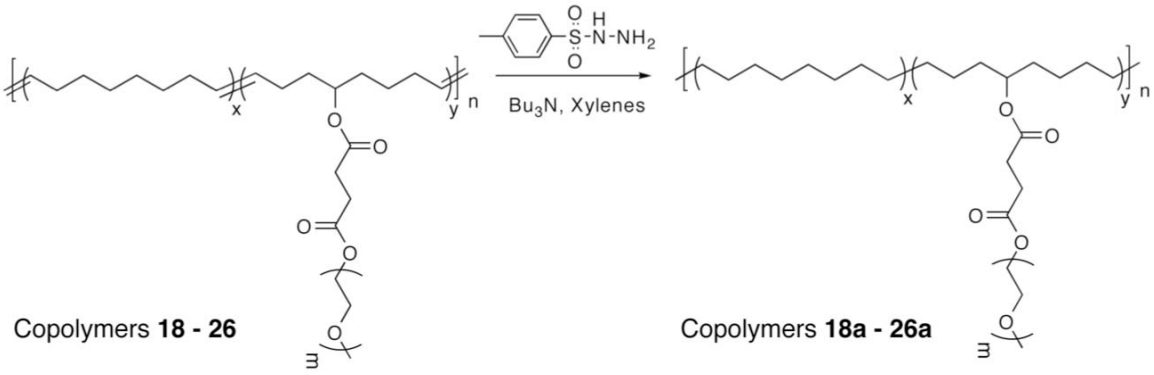

Scheme 2.9 Synthesis of PE-*g*-PEG by hydrogenation of PCOE-*g*-PEG

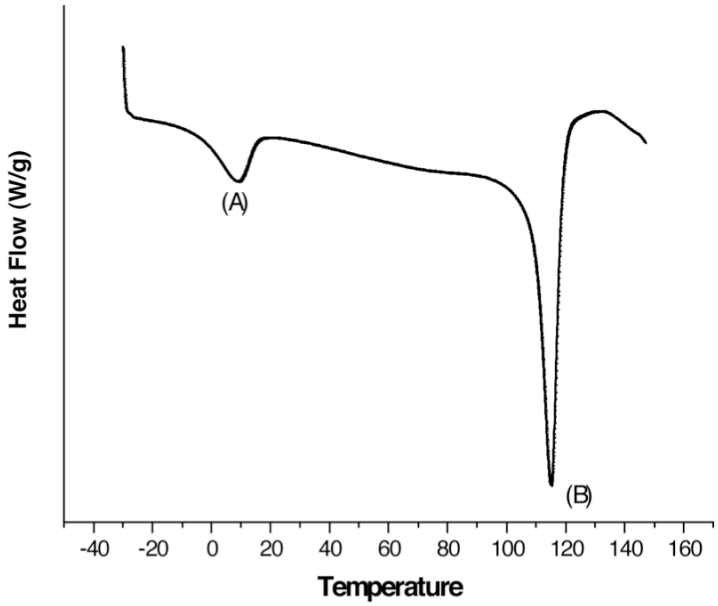

Figure 2.9 DSC chromatogram of copolymer 21a, A) PEG T_m= 8.7 ^{o}C, B) PE T_m=115.1 ^{o}C

Extensive thermal and X-ray scattering studies of ether-linked, hydrogenated PE-*g*-PEG copolymers **27a** – **29a** with varying PEG chain lengths were performed in collaborative efforts with Prof. Sanjeeva Murthy at Rutgers University. A detailed report of these experiments and their results has been published.[69]

2.6 Summary and Outlook

In summary, novel PEG-substituted cyclooctene macromonomers were synthesized and integrated into graft copolymers by ring-opening metathesis polymerization using ruthenium benzylidene catalysts **I**, **II** and **III**. Macromonomers **3** and **4** were prepared by coupling chemistry using commercially available mPEG derivatives. These monomers present a hydrolytically-degradable ester linkage between the PEG graft and PCOE backbone. Hydrolytically-stable PCOE-*g*-PEG copolymers were also prepared using ether-linked macromonomers **8** – **10**, made by ring-opening anionic polymerization of ethylene oxide using cyclooctene-based initiator **1**. The synthesis of macromonomers by direct polymerization of ethylene oxide presents a number of advantages including the ability to synthesize macromonomers with a wide range of PEG molecular weights and the potential for end-functionalization with oligopeptides, drugs, dyes, or other biological functionality.

These unique graft copolymers offer many tunable features based on extent of macromonomer incorporation, including a wide range of organic and aqueous solubility, crystallinity, and ability to function as macromolecular surfactants. The polymerization of cyclooctene-based macromonomers is also a viable method towards novel polyethylene-*g*-PEG copolymers through hydrogenation of the polycyclooctene backbone. These PEG-functional polyolefins are expected to present many possibilities

for the synthesis of novel macromolecules with controlled hydrophilicity and biofunctionality for potential applications in delivery, implant, and bio-medical coating applications.

2.7 References

(1) Ikkala, O.; ten Brinke, G. *Science* **2002**, *295*, 2407-2409.
(2) Chai, J.; Wang, D.; Fan, X. N.; Buriak, J. M. *Nature Nanotech.* **2007**, *2*, 500-506.
(3) Boudouris, B. W.; Frisbie, C. D.; Hillmyer, M. A. *Macromolecules* **2008**, *41*, 67-75.
(4) Zhang, S. *Biotechnol. Adv.* **2002**, *20*, 321-339.
(5) Duncan, R. *Nat. Rev. Drug Discov.* **2003**, *2*, 347-360.
(6) Ratner, B. D.; Bryant, S. J. *Annu. Rev. Biomed. Eng.* **2004**, *6*, 41-75.
(7) Langer, R. *Biopolymers* **2003**, *71*, 284-284.
(8) Lee, E. S.; Na, K.; Bae, Y. H. *J. Control. Release* **2005**, *103*, 405-418.
(9) Schacht, E.; Toncheva, V.; Vandertaelen, K.; Heller, *J. Control. Release* **2006**, *116*, 219-225.
(10) Lavasanifar, A.; Samuel, J.; Kwon, G. S. *Adv. Drug Deliver. Rev.* **2002**, *54*, 169-190.
(11) Adams, M. L.; Lavasanifar, A.; Kwon, G. S. *J. Pharm. Sci.* **2003**, *92*, 1343-1355.
(12) Metters, A. T.; Anseth, K. S.; Bowman, C. N. *Polymer* **2000**, *41*, 3993-4004.
(13) Vazquez-Dorbatt, V.; Maynard, H. D. *Biomacromolecules* **2006**, *7*, 2297-2302.
(14) Nagasaki, Y.; Yasugi, K.; Yamamoto, Y.; Harada, A.; Kataoka, K. *Biomacromolecules* **2001**, *2*, 1067-1070.
(15) Koo, L. Y.; Irvine, D. J.; Mayes, A. M.; Lauffenburger, D. A.; Griffith, L. G. *J. Cell. Sci.* **2002**, *115*, 1423-1433.
(16) Gacal, B.; Durmaz, H.; Tasdelen, M. A.; Hizal, G.; Tunca, U.; Yagci, Y.; Demirel, A. L. *Macromolecules* **2006**, *39*, 5330-5336.
(17) Parrish, B.; Breitenkamp, R. B.; Emrick, T. *J. Am. Chem. Soc.* **2005**, *127*, 7404-7410.
(18) George, M. H.; Majid, M. A.; Barrie, J. A.; Rezaian, I. *Polymer* **1987**, *28*, 1217-1220.
(19) Roy, D.; Guthrie, J. T.; Perrier, S. *Macromolecules* **2005**, *38*, 10363-10372.
(20) Kowalczuk, M.; Adamus, G.; Jedlinski, Z. *Macromolecules* **1994**, *27*, 572-575.
(21) Norton, R. L.; Mccarthy, T. J. *Macromolecules* **1989**, *22*, 1022-1025.
(22) Czelusniak, I.; Khosravi, E.; Kenwright, A. M.; Ansell, C. W. G. *Macromolecules* **2007**, *40*, 1444-1452.

(23) Heroguez, V.; Gnanou, Y.; Fontanille, M. *Macromol. Rapid. Comm.* **1996**, *17*, 137-142.
(24) Heroguez, V.; Gnanou, Y.; Fontanille, M. *Macromolecules* **1997**, *30*, 4791-4798.
(25) O'donnell, P. M.; Brzezinska, K.; Powell, D.; Wagener, K. B. *Macromolecules* **2001**, *34*, 6845-6849.
(26) Irvine, D. J.; Mayes, A. M.; Griffith, L. G. *Biomacromolecules* **2001**, *2*, 85-94.
(27) Chatterjee, A. K.; Morgan, J. P.; Scholl, M.; Grubbs, R. H. *J. Am. Chem. Soc.* **2000**, *122*, 3783-3784.
(28) Blackwell, H. E.; O'Leary, D. J.; Chatterjee, A. K.; Washenfelder, R. A.; Bussmann, D. A.; Grubbs, R. H. *J. Am. Chem. Soc.* **2000**, *122*, 58-71.
(29) Connon, S. J.; Blechert, S. *Angew. Chem. Int. Edit.* **2003**, *42*, 1900-1923.
(30) Bielawski, C. W.; Benitez, D.; Grubbs, R. H. *Science* **2002**, *297*, 2041-2044.
(31) Watson, K. J.; Anderson, D. R.; Nguyen, S. T. *Macromolecules* **2001**, *34*, 3507-3509.
(32) Ilker, M. F.; Schule, H.; Coughlin, E. B. *Macromolecules* **2004**, *37*, 694-700.
(33) Hopkins, T. E.; Wagener, K. B. *Macromolecules* **2004**, *37*, 1180-1189.
(34) Berda, E. B.; Lande, R. E.; Wagener, K. B. *Macromolecules* **2007**, *40*, 8547-8552.
(35) Rinehart, R. E.; Smith, H. P. *J. Polym. Sci. Pol. Lett.* **1965**, *3*, 1049.
(36) Novak, B. M.; Grubbs, R. H. *J. Am. Chem. Soc.* **1988**, *110*, 7542-7543.
(37) Herisson, J. L.; Chauvin, Y. *Makromolekul. Chem.* **1971**, *141*, 161.
(38) Schrock, R. R.; Murdzek, J. S.; Bazan, G. C.; Robbins, J.; Dimare, M.; Oregan, M. *J. Am. Chem. Soc.* **1990**, *112*, 3875-3886.
(39) Schwab, P.; Grubbs, R. H.; Ziller, J. W. *J. Am. Chem. Soc.* **1996**, *118*, 100-110.
(40) Scholl, M.; Ding, S.; Lee, C. W.; Grubbs, R. H. *Org. Lett.* **1999**, *1*, 953-956.
(41) Love, J. A.; Morgan, J. P.; Trnka, T. M.; Grubbs, R. H. *Angew. Chem. Int. Edit.* **2002**, *41*, 4035-4037.
(42) Heroguez, V.; Breunig, S.; Gnanou, Y.; Fontanille, M. *Macromolecules* **1996**, *29*, 4459-4464.
(43) Maynard, H. D.; Okada, S. Y.; Grubbs, R. H. *J. Am. Chem. Soc.* **2001**, *123*, 1275-1279.
(44) Strong, L. E.; Kiessling, L. L. *J. Am. Chem. Soc.* **1999**, *121*, 6193-6196.
(45) Schleyer, P. V.; Williams, J. E.; Blanchard, K. R. *J. Am. Chem. Soc.* **1970**, *92*, 2377-2386.
(46) Bazan, G. C.; Khosravi, E.; Schrock, R. R.; Feast, W. J.; Gibson, V. C.; Oregan, M. B.; Thomas, J. K.; Davis, W. M. *J. Am. Chem. Soc.* **1990**, *112*, 8378-8387.
(47) Choi, T. L.; Grubbs, R. H. *Angew. Chem. Int. Edit.* **2003**, *42*, 1743-1746.
(48) Allinger, N. L.; Sprague, J. T. *J. Am. Chem. Soc.* **1972**, *94*, 5734-5747.

(49) Trzaska, S. T.; Lee, L. B. W.; Register, R. A. *Macromolecules* **2000**, *33*, 9215-9221.
(50) Myers, S. B.; Register, R. A. *Polymer* **2008**, *49*, 877-882.
(51) Willert, H. G.; Buchhorn, G.; Eyerer, P. *Ultra-high molecular weight polyethylene as biomaterial in orthopedic surgery*; Hogrefe & Huber Publishers: Toronto ; Lewiston, NY, 1991.
(52) Bilyk, J. R.; Rubin, P. A.; Shore, J. W. *Int. Ophthalmol. Clin.* **1992**, *32*, 151-156.
(53) Heroguez, V.; Fontanille, M.; Gnanou, Y. *Macromol. Symp.* **2000**, *150*, 269-274.
(54) Hillmyer, M. A.; Laredo, W. R.; Grubbs, R. H. *Macromolecules* **1995**, *28*, 6311-6316.
(55) Cardoen, G.; Breitenkamp, K.; Emrick, T.; Coughlin, E. B. *Macromolecules* **2006**, *39*, 7170-7173.
(56) Ruoslahti, E. *Matrix Biol.* **2003**, *22*, 459-465.
(57) Kim, T. G.; Park, T. G. *Tissue Eng.* **2006**, *12*, 221-233.
(58) Thorn-Csanyi, E.; Ruhland, K. *Macromol. Chem. Phys.* **1999**, *200*, 2245-2249.
(59) Thorn-Csanyi, E.; Ruhland, K. *Macromol. Chem. Phys.* **1999**, *200*, 1662-1671.
(60) Thorn-Csanyi, E.; Hammer, J.; Pflug, K. P.; Zilles, J. U. *Macromol. Chem. Phys.* **1995**, *196*, 1043-1050.
(61) Schitter, R. M. E.; Jocham, D.; Stelzer, F.; Moszner, N.; Volkel, T. *J. Appl. Polym. Sci.* **2000**, *78*, 47-60.
(62) Preishuber-Pflugl, P.; Buchacher, P.; Eder, E.; Schitter, R. M.; Stelzer, F. *J. Mol. Catal. A-Chem.* **1998**, *133*, 151-158.
(63) Flory, P. J. *Principles of polymer chemistry*; Cornell University Press: Ithaca,, 1953.
(64) Gu, F.; Zhang, L.; Teply, B. A.; Mann, N.; Wang, A.; Radovic-Moreno, A. F.; Langer, R.; Farokhzad, O. C. *P. Natl. Acad. Sci. USA* **2008**, *105*, 2586-2591.
(65) Yang, F.; Williams, C. G.; Wang, D. A.; Lee, H.; Manson, P. N.; Elisseeff, J. *Biomaterials* **2005**, *26*, 5991-5998.
(66) Burdick, J. A.; Anseth, K. S. *Biomaterials* **2002**, *23*, 4315-4323.
(67) Breitenkamp, R. B.; Ou, Z.; Breitenkamp, K.; Muthukumar, M.; Emrick, T. *Macromolecules* **2007**, *40*, 7617-7624.
(68) Rankin, D. A.; P'Pool, S. J.; Schanz, H. J.; Lowe, A. B. *J. Polym. Sci. Pol. Chem.* **2007**, *45*, 2113-2128.
(69) Mark, P. R.; Murthy, N. S.; Weigand, S.; Breitenkamp, K.; Kade, M.; Emrick, T. *Polymer* **2008**, *49*, 3116-3124.

CHAPTER 3

PREPARATION OF POLYMER CAPSULES BY SELF-ASSEMBLY AND CROSS-LINKING OF POLYCYCLOOCTENE-*GRAFT*-PEG COPOLYMERS

3.1 Polymer Capsules for Encapsulation and Release Applications

Encapsulation and release strategies impact a wide range of technologies, particularly those which involve the controlled release of pharmaceuticals, flavors, fragrances, and agricultural agents.[1] Capsules and vesicles derived from polymer-based materials are well-suited for these applications because of their mechanical stability and tunable chemistries that can provide control over degradation rates, ionic charge, and cross-linking.[2] Such chemical strategies can be utilized to tailor the release rates of encapsulated agents over defined time periods, or in response to environmental changes.

Polymer capsules are distinguished by their hollow nature with a polymer-based shell that acts as a membrane to control diffusion of encapsulated species. This contrasts other solid, polymer microparticles prepared using degradable materials where drug release is controlled by diffusion and degradation of the polymer matrix. Polymer-based capsules have been prepared by a number of techniques. Classical methods of capsule preparation involve interfacial polycondensation utilizing complementary monomers (*e.g.* multifunctional carboxylic acid chlorides and amines) in a two-phase suspension system (*e.g.* chloroform and water) where each monomer is soluble in one of the two liquid phases.[3] To produce capsules, the resulting polymer formed at the fluid-fluid interface is insoluble in either phase and precipitates at the interface to form a membrane, ranging from nanometers (nm) to microns (μm) in thickness, which encapsulates the droplets. The encapsulated droplet can then be utilized as a reservoir for the controlled release of

active agents. Capsule production methods that utilize free-radical polymerization of vinyl monomers have been developed as well. For example, Stöver and coworkers demonstrated that the suspension copolymerization of methyl methacrylate (MMA) and poly(ethylene glycol) monomethacrylate (PEGMA) produces hollow capsules with micron-thick membranes when the feed ratio of PEGMA is sufficiently high (>15 mol %) and a cross-linker such as diethylene glycol dimethacrylate is added to the polymerization.[4] They hypothesized that the hydrophilicity imparted by PEGMA resulted in an amphiphilic copolymer which assembles and is subsequently cross-linked at the oil-water interface. Polymer capsules with diameters of approximately 100 nm and wall thicknesses ranging from 20 – 50 nm have been prepared by Landfester and coworkers using free-radical miniemulsion techniques.[5] In this case, the free-radical polymerization of methyl methacrylate or styrene was performed in an excess of a hexadecane using ultrasonication to produce the miniemulsion. Although the monomers are soluble in the hydrophobic phase, the polymer that is subsequently formed is immiscible and precipitates to form a shell around surrounding the hexadecane droplet.

In most cases, interfacial polymerization techniques produce polymer capsules with poor control of membrane thickness and inconsistencies in obtaining reproducible capsule morphologies. More recent strategies utilize the self-assembly of polymeric building blocks to produce capsules with well-defined diameters, wall thickness, and permeability.[6] For example, amphiphilic diblock copolymers with precisely controlled volume fractions (f) of hydrophobic and hydrophilic components can produce hollow capsules, termed polymersomes, when hydrated in water. In general, diblock copolymers with large hydrophilic block lengths (f >50%) produce spherical micelles in water with

diameters on the order of 20 - 200 nm. However, when the hydrophilic block constitutes a volume fraction of 25%>*f*>40%, polymersomes are formed upon electroformation[6] or hydration in water.[7] These hollow structures possess a polymeric bilayer shell that is analogues to phospholipid-based liposomes. The molecular weight and conformational freedom of the polymeric bilayer, however, make these vesicles inherently more mechanically robust and ten times less permeable to water than liposomes, and these unique attributes make polymersomes particularly promising in drug delivery. For example, Discher and coworkers have utilized polymersomes formed from poly(ethylene glycol)-*b*-poly(L-lactic acid) (PEG-*b*-PLA) and PEG-*b*-poly(ε-caprolactone) to encapsulate drugs such as doxorubicin and paclitaxel.[8] They demonstrated that a higher maximum tolerated dose (MTD) and increased tumor localization could be achieved in tumor-bearing mice with polymersome-encapsulated drugs when compared to the unencapsulated drugs.

Recently, Weitz and coworkers introduced a new method of preparing polymersomes from PEG-*b*-PLA copolymers by utilizing a microfluidic approach. Using block copolymer-stabilized double emulsion as templates, they showed that monodisperse polymersomes were produced upon evaporation of the organic solvent.[9] Using this approach, they encapsulated a hydrophilic fluorescent dye and demonstrated its triggered release by osmotic shock of the polymersomes. Using the double emulsion method, they also found that polymersomes could be formed from a wide range of diblock copolymer compositions. This represents a major advantage over the previously discussed polymersome production methods that utilize hydration or electroformation

since this technique does not require precise control over of the hydrophobic and hydrophilic copolymer components.

The structural integrity of polymersomes can be further enhanced through chemical cross-linking strategies, made possible by using reactive block copolymers. For example, Meier and coworkers cross-linked polymersomes prepared from poly(2-methyloxazoline)-*b*-poly(dimethylsiloxane)-*b*-poly(2-methyloxazoline) ABA copolymers which were functionalized with acrylate moieties on the polymer chain-ends.[10] UV-induced polymerization gave polymer capsules that were shape-persistent after drying. These vesicles were found suitable for the encapsulation of small-molecule dyes such as sulforhodamine B and proteins such as avidin.[11] Using a similar approach, Bates and coworkers produced elastic capsules by free-radical cross-linking of unsaturated polybutadiene-*b*-PEG copolymers.[12] They showed that the cross-linked capsules were stable in both water and chloroform and also demonstrated the effective encapsulation and retention of sucrose inside the polymer capsules, suggesting that defect-free capsules could be prepared by this method.

Weitz and coworkers have pioneered the fabrication of capsules by oil-water interfacial assembly of micron-sized colloidal particles. The particles assemble at the interface due to the substantially reduced particle-oil and particle-water surface energies compared to the oil-water surface energy.[13] Mechanically robust capsules are then formed by either sintering the assembled polymer particles or by co-assembly of cationic polyelectrolytes such as poly(L-lysine) (PLL). The use of excess PLL is advantageous since these capsules can be subsequently inflated or deflated by changes in osmotic pressure resulting from encapsulated polyelectrolyte.[14] Environmental stimuli that alter

the osmotic pressure of the capsule (*e.g.* salt concentration, pH, solvent) may offer an effective trigger for the release of encapsulated agents.

The layer-by-layer (LbL) assembly of polyelectrolytes onto a sacrificial colloidal core is another commonly utilized method to produce polymer capsules.[15] In this approach, oppositely charged polyelectrolytes (*e.g.* poly(vinylpyrrolidone) (PVP) and poly(methacrylic acid) (PMAA)) are adsorbed onto degradable templates in a stepwise fashion to generate layers of oppositely charged polymers. The templating core, which is typically composed of colloidal particles of silica, polystyrene, or melamine formaldehyde resin, is then subsequently removed by dissolution to form the hollow capsules. By varying the number of polyelectrolyte layers, the thickness of the capsule membrane can be tuned, with values typically ranging from 5 – 20 nanometers.[16] Due to the extremely thin nature of the capsule wall, capsule prepared by the LbL are generally permeable to small molecules but can retain macromolecules in the capsule core. For example, Möhwald and coworkers demonstrated the sustained release of fluorescein, a small molecule dye, from LbL capsules made from alternating layers of poly(styrene sulfonate) (PSS) and poly(allylamine hydrochloride) (PAH). In this study, the encapsulated dye was completely released from the capsules with a membrane thickness of 20 nm after only 10 minutes.[17] However, they showed that PSS with molecular weights greater than 4200 g/mol were not permeable and could be retained within the capsule interior.[18]

The ionic interactions that stabilize LbL capsules are inherently reversible by varying the ionic strength and pH of the capsule environment. Thus, poor capsule stability or dissolution is often observed at physiological conditions, a key limitation for

their use as a drug delivery system. Several groups have attempted to address this stability issue by covalent cross-linking of LbL capsules. In one approach, Advincula and coworkers incorporated benzophenone-functionalized PAH into LbL capsules. Following stepwise deposition and template dissolution, the layers were cross-linked by irradiation with UV light to covalently stabilize the capsule structure.[19] Using this approach, they showed that a hydrophilic dye, Rhodamine B, could be effectively loaded into the capsules prior to cross-linking and its release could be varied from approximately 10 to 20 minutes through variation in cross-link density. Caruso and coworkers prepared thiol-functionalized PMAA which was incorporated into LbL capsules with PVP and subsequently oxidized to form disulfide cross-links.[20] These capsules were stable to simulated physiological conditions and could be utilized for the encapsulation and triggered release of the protein, Transferrin. In this case, triggered capsule degradation and release of Transferrin was observed after treatment with dithiothreitol (DTT), a thiol-disulfide exchange agent.

Recently, there has been a considerable interest in producing polymer capsules with diameters less than 1 micron for nanotechnology applications such as targeted drug delivery and high-resolution electronic inks. Currently, LbL techniques cannot be easily extended to produce sub-micron capsules due to difficulties arising from aggregation of the colloidal particles at practical reaction concentrations. To overcome this limitation, nano-sized polymer capsules have been prepared by a number of methods using inorganic nanoparticles as templates.[21] Feldheim and coworkers were among the first to utilize such an approach by employing olefin metathesis chemistry to cross-link multi-functional, alkene-covered gold nanoparticles. Following metathesis cross-linking,

chemical etching of the nanoparticle template with a mixture of potassium cyanide (KCN) and $K_3[Fe(CN)_6]$ afforded polymer capsules with diameters of approximately 10 nm. In another approach, Möhwald and coworkers used atom transfer radical polymerization (ATRP) to radially polymerize 2-(dimethylamino)ethyl methacrylate (DMA) from gold nanoparticles with 2-bromo-2-methylpropionyloxy-functionalized thiol ligands.[22] Polymer capsules were then formed by cross-linking the polyDMA with 1,2-bis(2-iodoethoxy)ethane (BIE) and subsequent etching of the nanoparticle template with KCN. The nanocapsules were loaded with Rhodamine 6G but complete dye release was observed after only a few minutes, suggesting that small molecule diffusion is rapid across the thin polymer membrane (approx. 5 – 20 nm).

Recently, Caruso and workers demonstrated a new approach to produce sub-micron polymer capsules by adsorption and cross-linking of polyelectrolytes (*e.g.* PAH or poly(L-glutamic acid) (PGA)) in the mesoporous shells of solid core/mesoporous shell (SC/MS) templates.[23] SC/MS templates with diameters of approximately 280 - 400 nm were prepared and mixed with solutions of either PAH, PLL, or PGA to form polyelectrolyte-infiltrated templates. In the case of PAH and PLL-infiltrated SC/MS templates, polymer cross-linking was carried out using glutaraldehyde or 3,3′-dithiopropionimidate dihydrochloride. For PGA-infiltrated templates, cystamine was used for cross-linking. Following SC/MS template removal with hydrofluoric acid, hollow capsules with membrane thicknesses of approximately 15 - 45 nm were obtained, with thicknesses dependant on the molecular weight of the polyelectrolyte. The authors also demonstrated that this technique could be extended to the infiltration of doxorubicin-functional PGA conjugates (PGA-DOX), thereby creating chemotherapeutic-loaded

capsules for drug delivery applications. Under simulated conditions found in the bloodstream, they observed negligible release of DOX from the capsule but observed rapid release of the drug in a simulated lysosomal environment (pH 5.8 with 10 mM carboxypeptidase). In LIM1215 human colorectal tumor cells, PGA-DOX loaded capsules demonstrated similar cell toxicity when compared to free DOX suggesting its potential use in chemotherapeutic applications.

3.2 Polymer Capsules Prepared by Interfacial Assembly and Cross-linking of PCOE-*g*-PEG copolymers

While many of the previously described assembly techniques are effective in producing well-defined polymer capsules, a major drawback of these methods is the multiple processing steps that are required for their production. For example, LbL assembly and other templating techniques require a multi-step adsorption process followed by a dissolution step. The preparation of polymersomes is often very tedious, requiring time-consuming hydration steps and the use of block copolymer building blocks with precise ratios of hydrophobic and hydrophilic components. In contrast to these approaches, this chapter describes a novel method to produce micron-sized capsules using oil-water interfacial assembly and subsequent cross-linking of amphiphilic graft copolymers at the interface. In early experiments, the polycyclooctene-*g*-poly(ethylene glycol) (PCOE-*g*-PEG) copolymers described in Chapter 2 were observed to segregate to the toluene-water interface. We exploited this interfacial activity in conjunction with novel covalent cross-linking chemistries to develop a rapid route to produce robust, polymer capsules. In the first approach, we describe capsules that are cross-linked by a ring-opening cross-metathesis mechanism using a *bis*-cyclooctene PEG derivative in

combination with a ruthenium benzylidene catalyst. The second strategy involves the integration of phenyl azide or acyl hydrazine moieties into the polycyclooctene backbone which permits rapid UV cross-linking (in the case of phenyl azide) or glutaraldehyde cross-linking (in the acyl hydrazine case) at the oil-water interface. In all cases, cross-linking of the assemblies imparts mechanical integrity to the hollow capsules as confirmed by confocal laser scanning microscopy (CLSM), atomic force microscopy (AFM), and scanning electron microscopy (SEM). This relatively simple strategy requires only a few steps to produce hollow capsules, and oil-in-water assembly can be utilized for the encapsulation of hydrophobic molecules, such as neutral doxorubicin and Coumarin 153. These novel capsules may be well-suited for controlled release therapies, where the transport of drugs and/or drug conjugates can be regulated by factors such as the composition of capsule oil phase, capsule cross-link density, and encapsulant size and solubility. In addition, the choice of cross-linking chemistry (amide-linked phenyl azide, ester-linked phenyl azide, or hydrazone) should allow for tunable capsule degradation through pH-dependent hydrolysis.

3.2.1 Polymer Capsules Prepared by Ring-opening Cross-Metathesis at the Oil-water Interface

Amphiphilic polymers are particularly useful for mediating interfaces, as demonstrated by their history of applications as polymeric surfactants.[24] While amphiphilic block copolymers and polyelectrolytes have been well-studied, amphiphilic graft copolymers have received comparatively little attention. The novel PCOE-*g*-PEG copolymers described herein are inherently amphiphilic and dissolve in many organic solvents and water. These copolymers are also interfacially active, stabilizing oil-in-

water emulsions for hours to days or more, depending on macromonomer content, thus prompting further exploration into encapsulation and release applications. Like other surfactant stabilized emulsions, oil-in-water assemblies formed from PCOE-*g*-PEG copolymers were destroyed upon drying or introduction of a common solvent such as methanol, ethanol, or acetone. To enhance the structural stability for encapsulation applications, covalent cross-linking strategies that utilize polymer backbone functionality were developed. It was anticipated that capsule cross-linking would not only provide structural stability to the polymer capsules but also provide a polymer membrane that could be chemically tuned to control diffusion and release of encapsulated agents. For example, ester-containing cross-links hydrolyze in aqueous solution while amide-containing cross-links are stable in water. Thus, the extent of cross-linking combined with variation of the cross-linking chemistry, provides opportunities for controlling diffusion across the membrane.

Although a number of cross-linking chemistries are accessible through the polyolefin backbone, a ring-opening cross-metathesis approach using *bis*-cyclooctene PEG was initially chosen to generate the desired cross-linking. Ring-opening cross-metathesis is an extremely useful methodology in small molecule synthesis[25] and can be performed under mild conditions that do not disrupt the polymer assembly. To accomplish the cross-linking, a *bis*-cyclooctene PEG cross-linker **31** was prepared by reaction of two equivalents of carboxylic acid functionalized cyclooctene **2** and α,ω-PEG diol under carbodiimide coupling conditions as shown in Scheme 3.1. These *bis*-functionalized molecules are, like the graft copolymers, interfacially active. This is key

to the cross-linking strategy since only small quantities of the *bis*-cyclooctene are needed to achieve effective cross-linking of the polymer assembly.

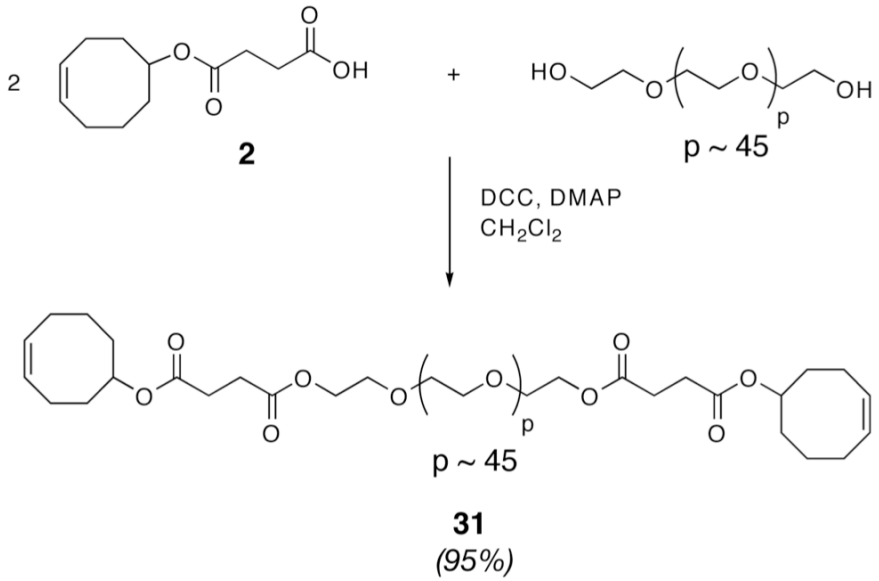

Scheme 3.1 Synthesis of *bis*-cyclooctene cross-linker 31 by carbodiimide coupling of 2 and PEG diol

Figure 3.1 depicts the segregation of PCOE-*g*-PEG copolymers to the oil-water interface and cross-linking with *bis*-cyclooctenyl PEG and a ruthenium benzylidene catalyst to generate capsules with cross-linked membranes. Experimentally, the hollow polymer capsules were prepared by combining graft copolymer **25** (0.25 wt %) with *bis*-cyclooctene cross-linker **31** (2 wt %) in toluene. Grubbs' Generation II catalyst (catalyst **II**) was then added to the solution, and the mixture is added to water. This heterogeneous mixture was shaken for 15 minutes to produce cross-linked capsules with sufficiently robust membranes. Catalysts **I** and **III** were also tested in interfacial metathesis cross-linking but reaction kinetics were found to be too slow in the case of catalyst **I** and too fast for catalyst **III** to cleanly form cross-linked capsules.

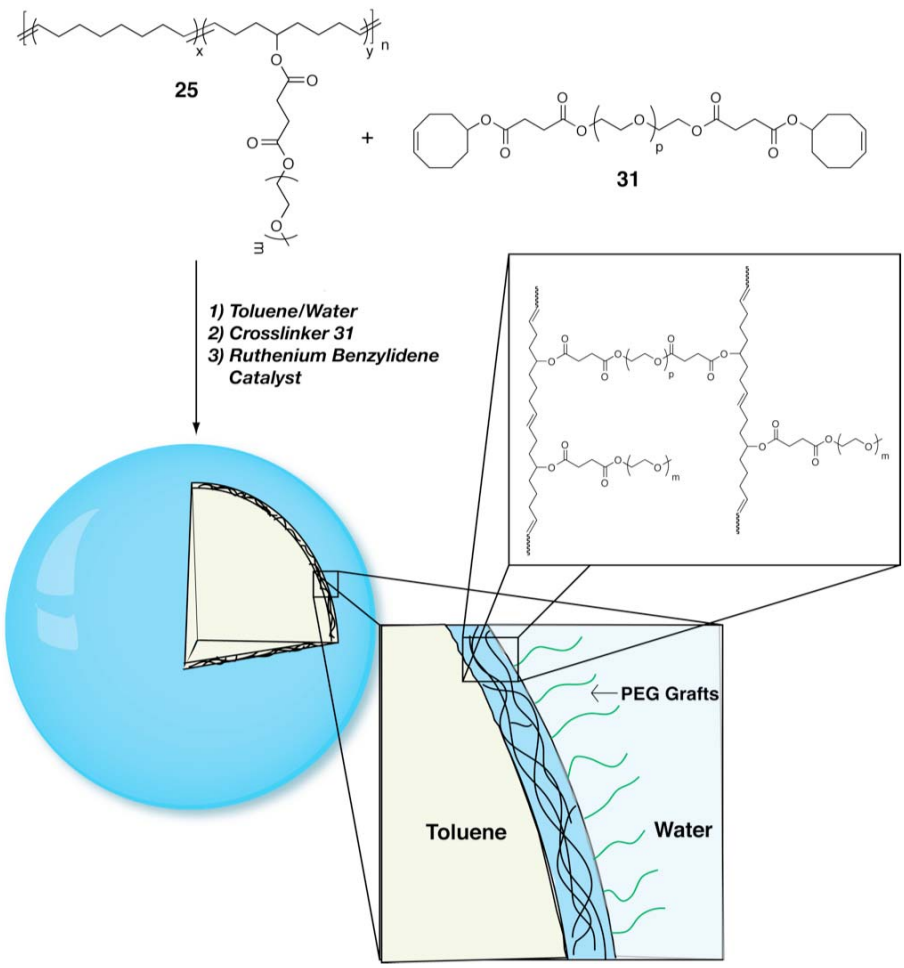

Figure 3.1 Schematic illustration of interfacial assembly of polycyclooctene-*g*-PEG and cross-linking by ring-opening cross-metathesis with *bis*-cyclooctene 31

The capsules possess diameters in the micron-size range and can easily be visualized by optical microscopy. However, the spatial distribution of polymer in the assembly (*i.e.* oil phase, aqueous phase, or interface) could not be determined by optical microscopy. The polymer was also not amenable to fluorescence microscopy due to the lack of fluorescence emission from the as-prepared copolymers. Thus, we prepared a fluorescent cyclooctene derivative **32** through esterification of 5-hydroxy-1-cyclooctene (**1**) with Rhodamine B as shown in Scheme 3.2, and integrated this new monomer into

the amphiphilic graft copolymer by copolymerization with cyclooctene and the PEG-functional cyclooctene macromonomer. The functional group tolerance of catalyst **II** was essential for the preparation of this fluorescent polyolefin.

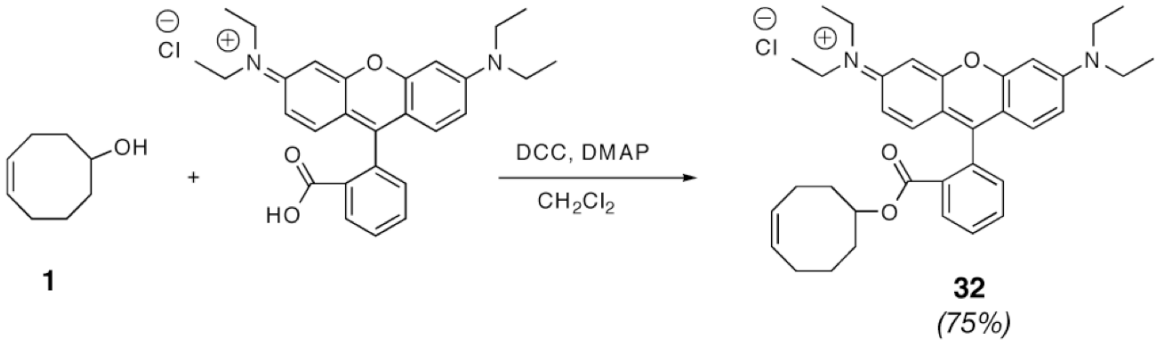

Scheme 3.2 Synthesis of fluorescent-labeled cyclooctene 32 by coupling of 1 and Rhodamine B

Confocal laser scanning microscopy (CLSM) images of the fluorescent amphiphilic graft copolymer in oil-in-water biphasic systems (shown in Figure 3.2A) reveals a strong preference of the graft copolymer for the interface, as indicated by the emission at 556 nm at the equator of an oil droplet in water while a very weak fluorescence was observed in both the toluene-filled droplet core and the aqueous phase. The integration of the fluorescent probe into the polyolefin backbone also permitted further investigation of the capsule morphology, mechanical integrity, and size distribution. Using confocal microscopy, a three-dimensional reconstruction of the capsules was assembled (Figure 3.2B) to illustrate their spherical nature and complete coverage by the polymer. Figure 3.2C demonstrates the robust nature of the interfacial cross-linking reaction. In this experiment, the two-phase oil/water mixture used to create the assembly is replaced with ethanol, a mutually good solvent for both phases. In this

case, the capsules do not dissolve away and the collapsed, cross-linked membrane can be isolated and visualized clearly.

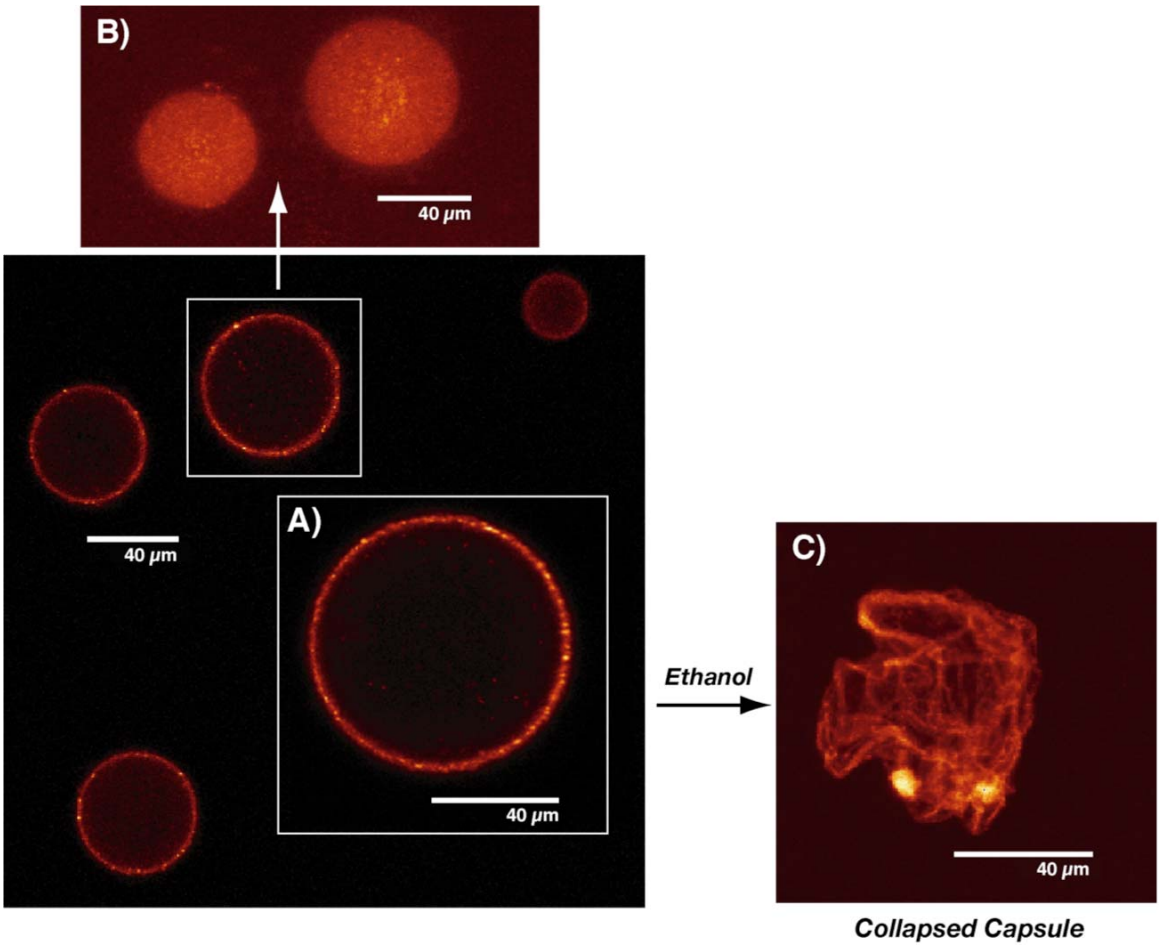

Figure 3.2 Confocal laser scanning microscopy of fluorescent-labeled graft copolymer capsules, A) cross-sectional slice, B) 3-D projection image of polymer-covered capsules, C) collapsed capsule after introduction of ethanol

Figure 3.3A illustrates a representative confocal micrograph showing cross-sectional slices of several fluorescent-labeled capsules following preparation by hand shaking the oil-water mixture. Capsules produced by this method typically possess diameters ranging from 20 – 50 μm with an average diameter of approximately 30 μm. AFM analysis was also performed on a dried capsule to qualitatively determine the thickness of the capsule membrane. A representative AFM micrograph, shown in Figure

3.3B, suggests the presence of a very thin polymer membrane (approx. 10 – 20 nm) on the droplet surface.

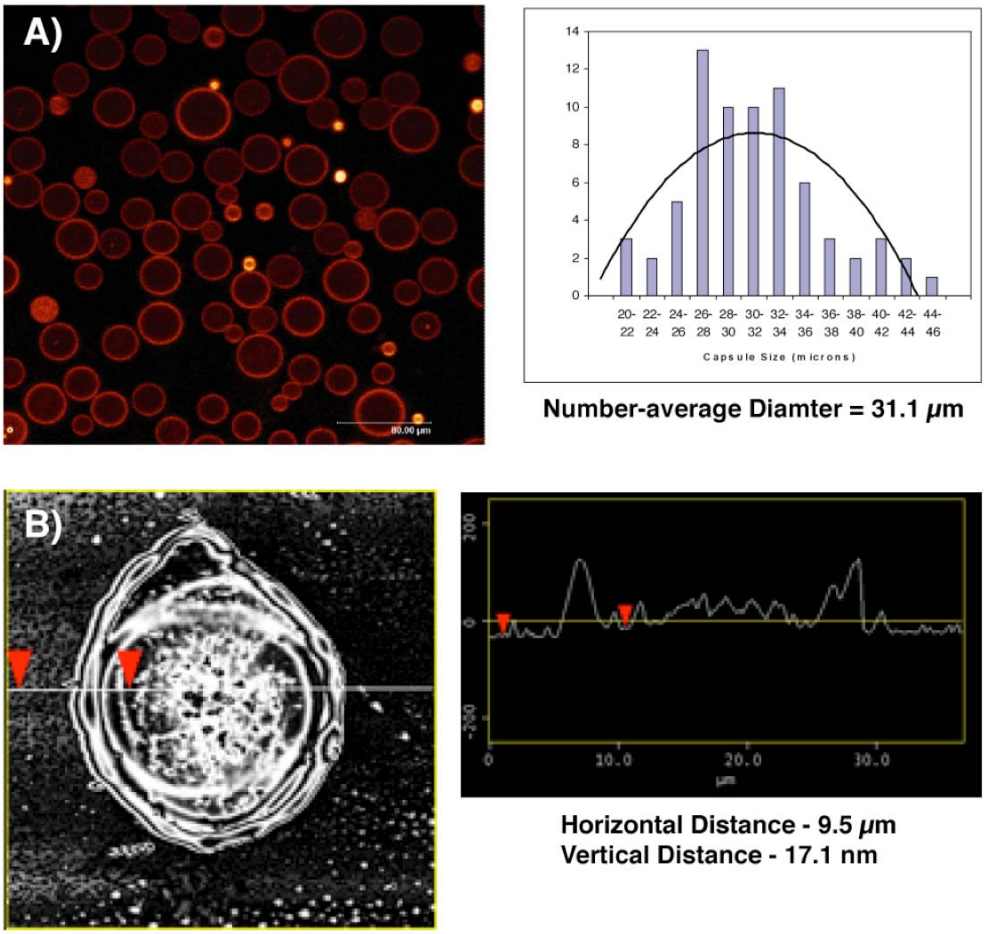

Figure 3.3 A) Confocal micrograph of cross-linked capsules and statistical analysis plotting capsule diameter versus capsule number, B) AFM height analysis of a dried capsule; the red arrows indicate where height measurements were made

The ease with which these oil-filled capsules can be prepared suggests a practicality for many types of encapsulation, where the encapsulant is either dissolved in an oil phase or is itself a hydrophobic liquid. In many cases, clinical use of attractive drug candidates has been impeded by their poor aqueous solubility. For the chemotherapy drug doxorubicin (DOX) (shown in Figure 3.4), water solubility is achieved by protonation of the primary amine. Drug modifications of this type can alter

pharmacokinetic profiles and in some cases increase renal clearance and thus shorten circulation lifetimes. Using the oil-in-water assembly method described above, DOX in its neutral form can be encapsulated in the oil phase of the capsule. The inherent fluorescence of DOX allows its visualization in the capsule by confocal microscopy. Figure 3.4 shows a three-dimensional projection image of these DOX-filled capsules (fluorescence at 580 nm).

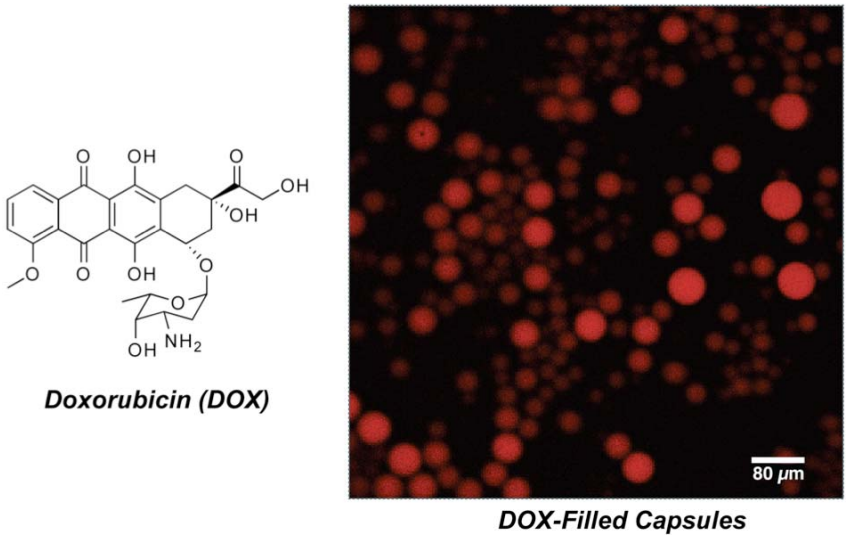

Figure 3.4 Confocal micrograph of DOX-filled, cross-linked capsules

Relative to lipid emulsions or polymer micelles, drug encapsulation using cross-linked, polymer capsules should allow for higher drug loadings and is limited only by the solubility of the drug in the oil medium. In addition, the use of PEG-grafted polyolefins in the oil-water interfacial assembly method presents PEG grafts and oligopeptide-functional PEG grafts (*e.g.* copolymer **30**) at the capsule surface. This unique feature should enhance capsule biocompatibility and may facilitate potential applications in targeted drug delivery.

3.2.2 Polymer Capsules Prepared from Reactive PCOE-*g*-PEG Copolymers at the Oil-water Interface

Ring-opening cross-metathesis cross-linking of interfacially segregated PEGylated polyolefins represents a rapid route to produce polymer capsules without the need for additional processing steps often encountered with other capsule preparation techniques (*e.g.* LbL assembly, nanoparticles templating). However, this method also presents a number of limitations when preparing capsules for application in drug delivery. First, PCOE-*g*-PEG copolymers, such as copolymer **25**, which are prepared by polymerization of ester-linked macromonomers **3** and **4** possess PEG grafts which are connected to the PCOE backbone through hydrolyzable ester linkages that may degrade upon storage in water and result in capsule instability. Second, the metathesis cross-linking technique utilizes a hydrophobic ruthenium benzylidene catalyst that remains encapsulated in the toluene droplet following cross-linking. Removal of the catalyst from the toluene phase was challenging and concerns existed over its potential reactivity towards other encapsulated species. Finally, attempts to control capsule size and dispersity using sizing techniques such as membrane extrusion were limited because metathesis cross-linking kinetics are difficult to control. In most cases, metathesis cross-linking using catalyst **II** was complete before membrane extrusion could be performed.

An ideal capsule preparation method would involve loading a hydrophobic solute in the oil-filled core of the polymer assembly, reducing the capsule diameter to 1 μm or smaller (*e.g.* by membrane extrusion, sonication, or other sizing techniques), and rapidly cross-linking the assembly to encapsulate the drug. We hypothesized that incorporating reactive, cross-linking functionality into the polymer backbone could address these issues by providing a means to control the kinetics and extent of cross-linking without the need

for additional hydrophobic additives. In addition, we sought to utilize cross-linking chemistries that are reversible in response to environmental stimuli (*e.g.* pH changes). By doing so, we envisioned the design of polymer capsules with triggered degradation and drug release based on the pH of the capsule environment.

In one example, we describe a new method of capsule cross-linking utilizing novel polyolefin-*graft*-PEG copolymers with pendent phenyl azides, prepared by ROMP of phenyl azide-functionalized cyclooctenes and PEGylated cyclooctene macromonomers. Ether-linked, PEG macromonomers **9** and **10** were used to synthesize graft copolymers in these studies and impart much greater hydrolytically-stable to the PEG grafts and the resulting capsules. The phenyl azide-functional amphiphilic copolymers segregate to the oil-water interface and undergo rapid cross-linking upon exposure to UV-light through highly reactive nitrenes generated upon photolysis of the phenyl azides. This method of capsule cross-linking simplifies the prior cross-metathesis technique, as precise amounts of cross-linking functionality can be incorporated directly into the polymer backbone by ROMP. Thus, variation of key properties such membrane thickness and cross-link density can be achieved without the need for additional additives (*e.g.* ruthenium catalysts and *bis*-cyclooctene cross-linkers) to the interfacial assembly.

Another approach utilizes hydrazine-functional PCOE-*g*-PEG copolymers that are prepared by ROMP of a novel N-butyloxycarbonyl (Boc)-protected, acyl hydrazine-functionalized cyclooctene. Upon deprotection of the Boc protecting group with trifluoroacetic acid (TFA) and oil-water interfacial assembly, the assembled polymer is cross-linked with glutaraldehyde to yield robust polymer capsules with pH-reversible hydrazone cross-links.

3.2.2.1 Polymer Capsules Prepared by Photolysis of Phenyl Azide-functional PCOE-*g*-PEG Copolymers at the Oil-water Interface

The incorporation of phenyl azide functionality into the graft copolymer backbone, for photo-induced cross-linking, was accomplished by the synthesis and copolymerization of both amide-linked and ester-linked phenyl azide-functionalized cyclooctenes. The choice of linker chemistry (between the cyclic olefin and azide) is an additional tunable parameter of the polymer capsule. As the phenyl azide serves as the cross-linking moiety during capsule formation, variation in the hydrolytic stability of the cyclooctene-phenyl azide linkage should control the degradation rates of the cross-linked capsules.

To prepare the hydrolytically-stable, amide-linked phenyl azide, amine-functionalized cyclooctene **35** was first prepared in two steps from 5-bromo-1-cyclooctene[26] as shown in Scheme 3.3. 5-bromo-1-cyclooctene (**33**) was converted to 5-azido-1-cyclooctene (**34**) by nucleophilic substitution with sodium azide in dimethylsulfoxide (DMSO). Next, the azide functionality was reduced with triphenylphosphine and water, and 5-amino-1-cyclooctene (**35**) was isolated by fractional distillation in 35% overall yield. To synthesize the phenyl azide-functional cyclooctene, 4-azidobenzonic acid[27,28] (**36**) was converted to 4-azidobenzoyl chloride (**37**) with thionyl chloride and excess triethylamine, and **35** was added to this solution by syringe in a one-pot reaction. Following work-up and purification by column chromatography, amide-linked, phenyl azide-functional cyclooctene **38** was isolated in 95% yield.

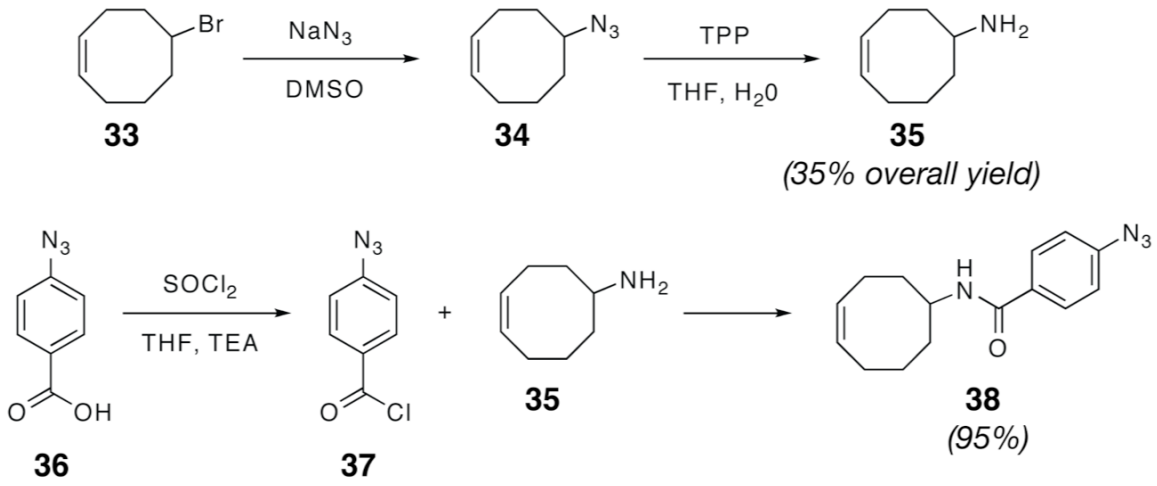

Scheme 3.3 Synthesis of amide-linked, phenyl azide-functionalized cyclooctene 38

The synthesis of hydrolytically-degradable, ester-linked cyclooctene phenyl azide was initially attempted by substituting 5-hydroxy-1-cyclooctene (**1**) for **35** in the reaction with 4-azidobenzoyl chloride as shown in Scheme 3.4A. In this case, however, yields of monomer **39** were less than 10% in all reaction attempts. We attributed low yields to the reduced reactivity and steric limitations of the secondary alcohol when compared to primary amine-functionalized **35**. In addition, monomer **39** is a liquid at room temperature, which reduces the storage stability of the highly reactive phenyl azide. It was hypothesized that both ester and amide linkages would be required to impart hydrolytic degradability and promote crystallization, as we found that isolating phenyl azide-functionalized molecules as crystalline solids dramatically improves their long-term storage stability. To accomplish this, a multi-step synthetic approach was undertaken as illustrated in Scheme 3.4B. In the first step, 5-hydroxy-1-cyclooctene (**1**) was reacted with N-Boc-protected glycine by carbodiimide coupling. The Boc-protecting group was subsequently removed with anhydrous hydrochloric acid (4.0 M HCl solution

in dioxane) to yield glycine-functionalized cyclooctene **40** as the hydrochloride salt. Finally, **40** was reacted with 4-azidobenzoyl chloride (**37)** in the presence of excess triethylamine to give phenyl azide-functional cyclooctene **41,** with both ester and amide linkages, in 85% yield. As expected, the incorporation of the amide linkage promoted crystallization of **41**, which dramatically improved its long-term stability. Monomers **38** and **41** remain chromatographically pure after over two years of storage at -80 ^{o}C in the dark.

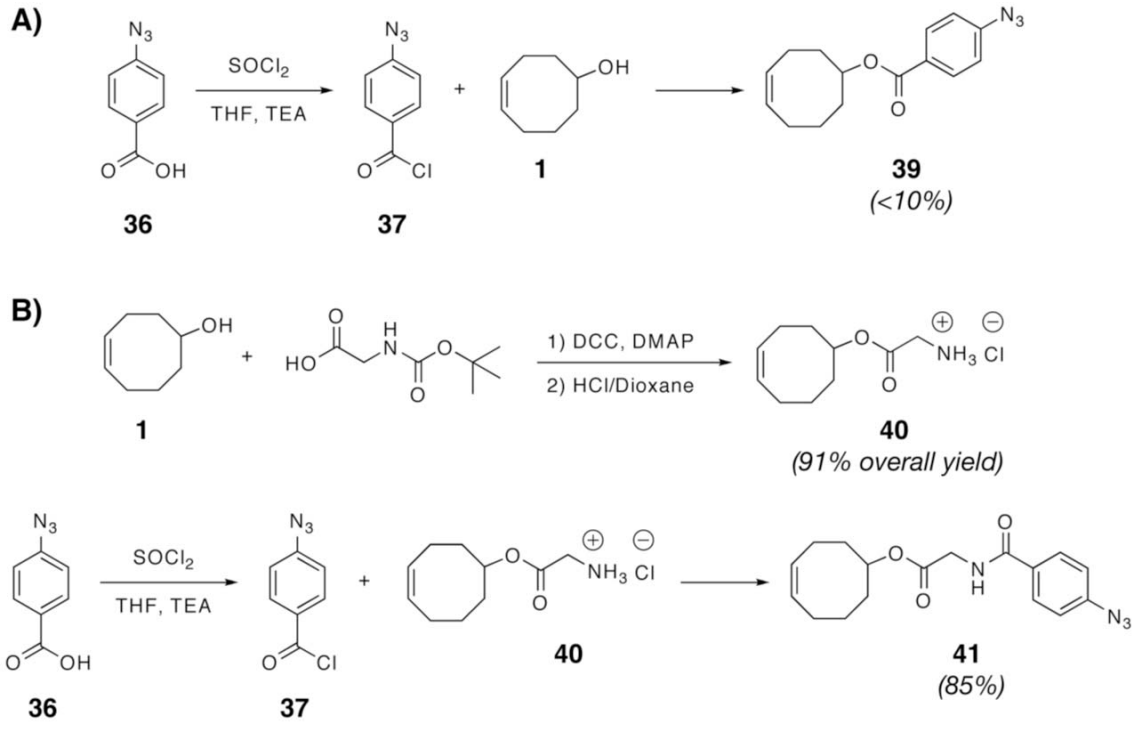

Scheme 3.4 Synthetic routes to hydrolytically-degradable, ester-linked phenyl azide-functionalized cyclooctenes

Amide-linked and ester-linked phenyl azide-functionalized cyclooctenes **38** and **41** were then copolymerized with ether-linked PEG macromonomers **9** and **10** and cyclooctene to prepare phenyl azide-functionalized graft copolymers. The incorporation of azide functionality into polymer materials has recently gained considerable attention,

mainly due to interest in post-polymerization functionalization reactions with alkyne-functional substrates using Sharpless type "click chemistry" (*i.e.* [3+2] cycloaddition).[29,30] However, reports of azide incorporation into polyolefins have been limited, presumably due to the incompatibility of azides and transition metal catalysts. For example, Noels and coworkers were unsuccessful in their attempts to ROMP an azide-functional cyclooctene which they attributed to deactivation of the Ru(II)-arene catalyst.[31] In more recent work, Binder and coworkers prepared poly(oxanorbornenes) with pendent azides, but these were synthesized by post-ROMP incorporation of azide functionality by reaction of sodium azide with bromide-functional polymers.[32] Indeed, in our initial attempts to polymerize phenyl azide-functional cyclooctenes **38** and **41** using catalyst **II**, we found that polymerizations required relatively long times (1-2 hours) to achieve high conversions. In addition, the polymers possessed very broad PDI values (>3.0) and multi-modal molecular weight distributions.

In contrast, we found that phenyl azide-functionalized amphiphilic graft copolymers could be prepared by in very short time periods and with relatively good control of both molecular weight and molecular weight distribution using catalyst **III**. For example, copolymers **42** and **43** (shown in Scheme 3.5) were prepared using 20 mol % of amide-linked, phenyl azide-functional cyclooctene **38** or ester-linked, phenyl azide-functional cyclooctene **41,** 50 mol % unsubstituted cyclooctene, and 30 mol % PEG-functionalized cyclooctene macromonomer **9** (PEG MW approx. 2200) in THF ([M] = 1.0 mol/L). Catalyst **III** was utilized at a monomer-to-catalyst ratio of 50:1. Polymerization was terminated with ethyl vinyl ether, and the polymer was isolated by precipitation into cold diethyl ether. In contrast to polymerizations using catalyst **II**,

GPC analysis of polymer **42**, prepared using catalyst **III**, showed a single Gaussian peak with number-average molecular weight of approximately 47,000 Da and a PDI of 2.6. ^{1}H NMR analysis of polymers **42** and **43** in $CDCl_3$ showed an absence of cyclic olefinic proton resonances at δ 5.70 ppm and new backbone olefin resonances at δ 5.35 ppm. Aromatic resonances from the phenyl azide at δ 7.04 and δ 8.00 ppm were also visible in the spectrum, and aromatic proton integration referenced against the olefinic backbone resonances suggested approximately 20 mol % of the azide-functional cyclooctene incorporated into the polymer. ATR-FTIR analysis of polymers **42** and **43** confirmed the incorporation of azides **38** and **41**, as indicated by the diagnostic azide stretch at 2190 cm^{-1} and carbonyl stretching vibrations at 1662 cm^{-1} (amide carbonyl stretch of polymers **42** and **43**) and 1747 cm^{-1} (ester carbonyl stretch, polymer **43**).

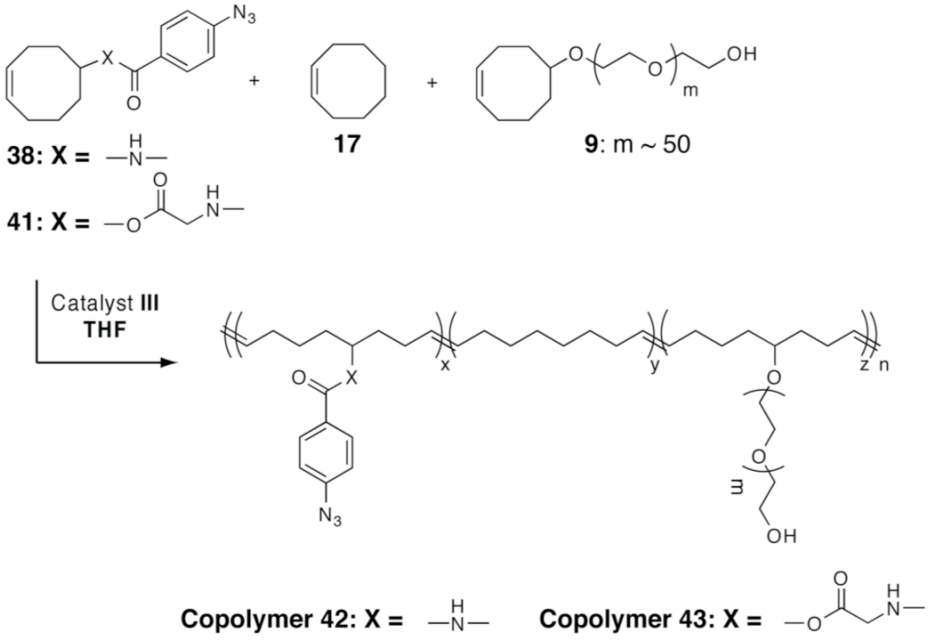

Scheme 3.5 Synthesis of phenyl azide-functionalized graft copolymers by copolymerization of 38 or 41 with 17 and macromonomer 9

Before utilizing phenyl azide-functionalized copolymers to prepare polymer capsules, cross-linking studies using solvent-cast films of **42** and **43** were performed to confirm the effectiveness of nitrene cross-linking. Solutions of these polymers were prepared in dichloromethane, cast onto glass slides, and dried in the dark. Next, both thin-film samples were analyzed by ATR-FTIR spectroscopy before and after placement in a UV-cross-linking apparatus (302 nm light source). As shown in Figure 3.5, after five minutes of exposure to 302 nm light, the diagnostic azide stretch at 2190 cm^{-1} disappears, suggesting a reaction of the incorporated phenyl azide. In addition, the films were no longer soluble in water or organic solvents. Attempts to re-dissolve the cast films in dichloromethane resulted in film swelling and delamination from the glass slide, but a homogeneous solution could not be obtained, suggesting effective cross-linking of the films. Cross-linked films of copolymer **43**, which contains a hydrolytically-degradable ester linkage between the phenyl azide functionality and the polymer backbone, could be hydrolyzed with an aqueous potassium hydroxide solution (0.1 M). After stirring overnight, homogeneous solutions of **43** were obtained, suggesting that polymer cross-linking occurs exclusively through reaction of the phenyl azide moiety. Copolymer **42**, which contains a hydrolytically-stable amide linkage, did not dissolve under similar conditions.

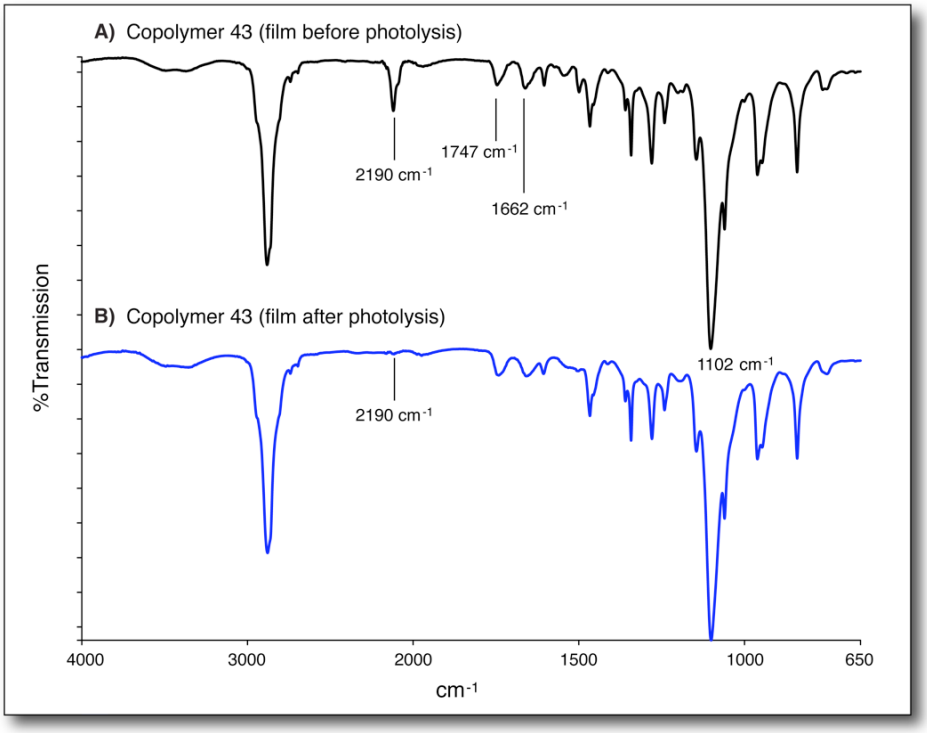

Figure 3.5 ATR-FTIR spectrum of a solvent-cast film of polymer 43 before and after UV cross-linking (5 min exposure)

Upon photolysis, phenyl azides are converted to highly reactive nitrenes, which can undergo a number of chemical reactions as illustrated in Figure 3.6B. For example, nitrenes are known to insert into C=C and C-H bonds to form aziridines and aryl amines, respectively,[33] and we hypothesized that nitrene insertion into the polyolefin backbone seemed most plausible in light of these known chemistries. However, based on the ATR-FTIR spectrum in Figure 3.5, there is insufficient spectral data to determine the exact chemistries involved in nitrene cross-linking of the graft copolymer films (*e.g.* aziridine formation, C-H bond insertion). ^{1}H NMR analysis of cross-linked copolymer **43** following hydrolysis and lyophilization also yielded few clues to the exact nature of the nitrene cross-linking reaction due to the complexity of the hydrolyzed polymer structure and the number of nitrene reactions that are possible.

To prepare polymer capsules using the nitrene cross-linking technique, polymer **42** or **43** was dissolved in toluene (0.2 wt % solution) and added to a glass vial containing deionized water (10 mL). The heterogeneous mixture was shaken gently for several seconds to form the polymer assembly as illustrated in Figure 3.6A. The vial was then placed in a UV cross-linking apparatus and exposed to 302 nm light for one minute. The vial was gently shaken to redisperse the capsules and re-exposed to 302 nm light for one minute. This process was repeated three more times for a total of 5 minutes of UV exposure.

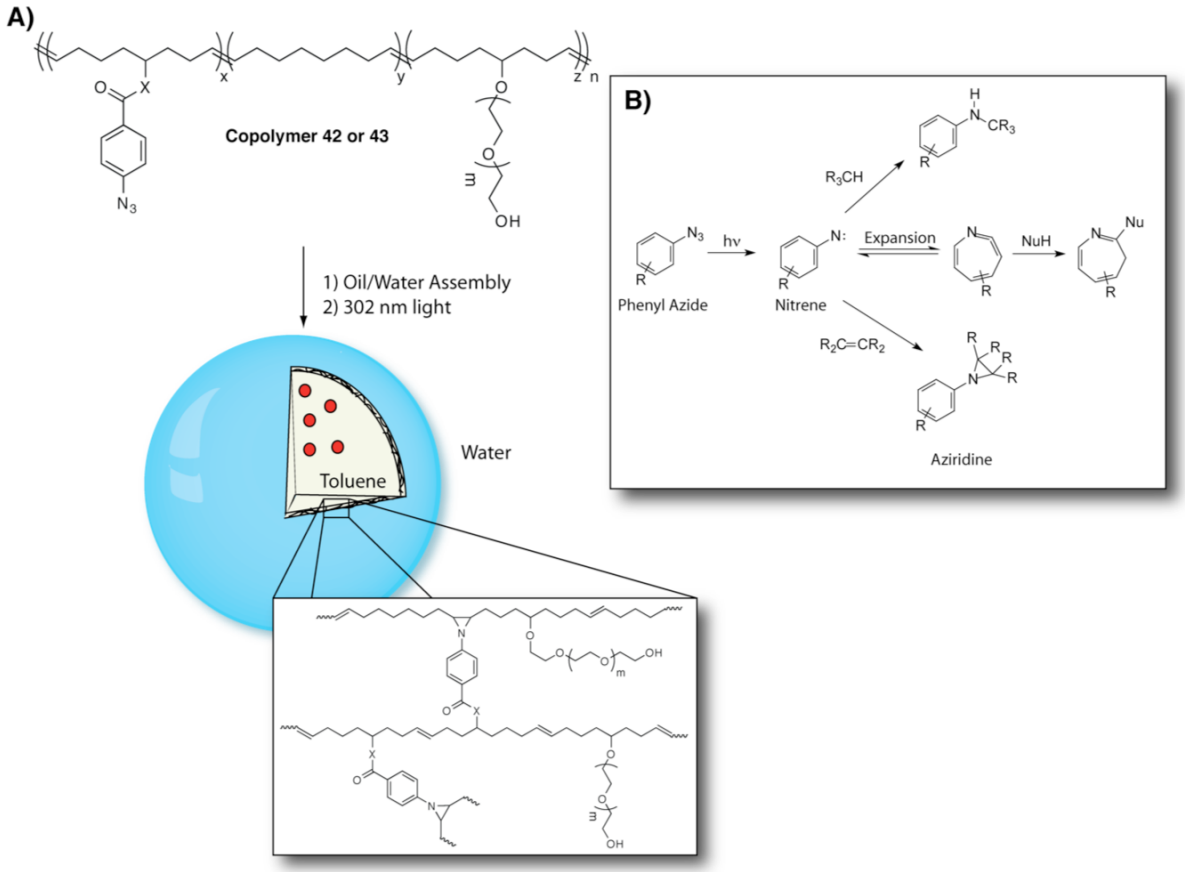

Figure 3.6 A) Illustrative representation of oil-water interfacial assembly and UV cross-linking of phenyl azide-functional copolymers, B) potential nitrene chemistries involved in interfacial cross-linking

Capsules prepared by this method using copolymer **42** are shown in Figure 3.7A. The contrast in this confocal scanning laser micrograph is provided by the encapsulation of a hydrophobic fluorescent dye, Coumarin 153 (excitation 423 nm, emission 530 nm) in the toluene phase of the assembly. Like the polymer assemblies created from copolymer **25**, the UV cross-linked capsules created with copolymer **42** are polydisperse in nature with diameters ranging from 10 – 40 microns. The capsules maintain their spherical shape and retain the dye in the oil-filled interior following the cross-linking reaction.

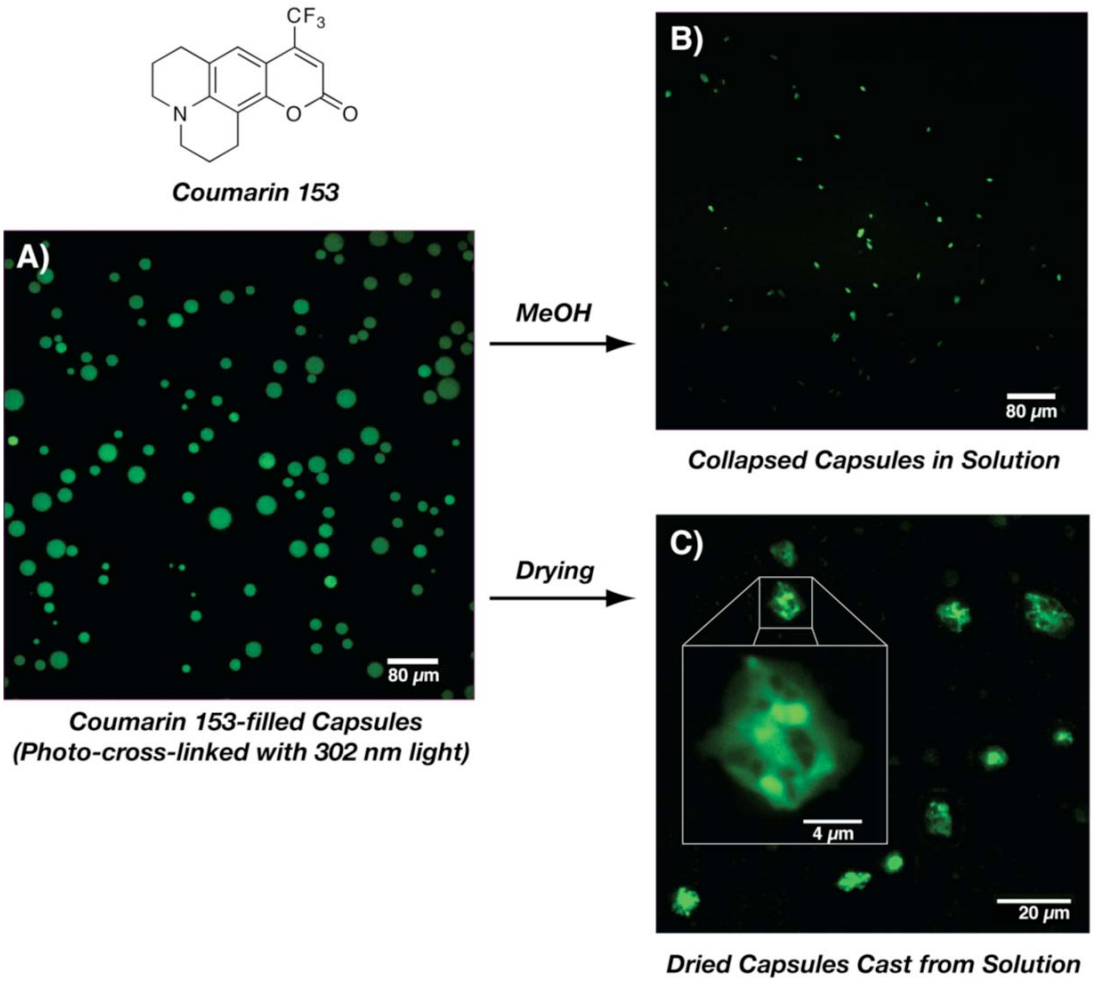

Figure 3.7 A) Confocal micrograph of Coumarin 153-filled, photo-cross-linked capsules prepared from copolymer 42, B) collapsed capsules in solution after interface removal with methanol, C) dried capsules drop-cast from solution

To demonstrate the effectiveness of nitrene cross-linking, the oil-water interface was removed by washing with methanol. Rather than dissolve away, the capsule membrane collapses and appears to retain some of the encapsulated dye as shown in Figure 3.7B. Fluorescence from released dye can also be seen in the background suggesting that the small molecules can permeate through the polymer membrane. UV cross-linked capsules were drop-cast onto glass slides and visualized in the dried state by confocal microscopy as shown in Figure 3.7C. In this experiment, the mechanical robustness of the capsule membrane is exemplified, as dried capsule membranes are observable with folds and ridges resulting from evaporation of the toluene phase and membrane collapse upon drying. In this micrograph, some released dye can be seen as a halo around the capsules further suggesting the permeability of small molecules across the membrane. To investigate the properties of the capsule membrane, UV cross-linked capsules prepared from copolymer **42** were drop cast from solution, coated with gold, and analyzed by SEM. Figure 3.8A shows an almost completely intact capsule membrane after drying while Figure 3.9B represents a dried capsule that has ruptured, presumably due to the reduced pressure (10^{-7} Torr) required for SEM analysis. Like the AFM data presented in Figure 3.3B, this micrograph further illustrates the extremely thin nature (less than 50 nm) of the polymer membrane produced from the interfacial assembly/cross-linking method.

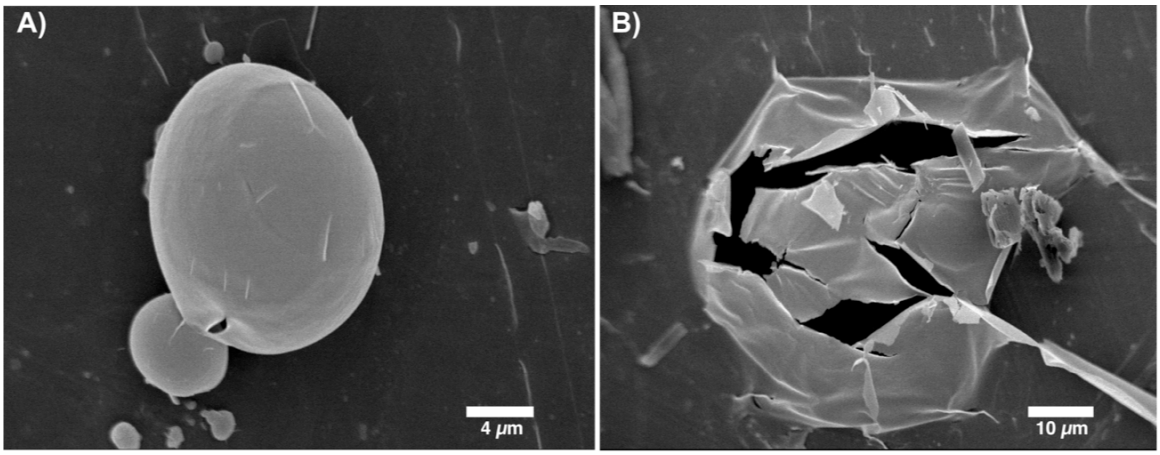

Figure 3.8 SEM micrographs of UV cross-linked capsules prepared from copolymer 42

3.2.2.2 Polymer Capsules Prepared from Acyl Hydrazine-containing PCOE-*g*-PEG Copolymers at the Oil-water Interface

The ability to trigger drug release from polymeric delivery systems in response to physiological stimuli (*e.g.* changes in pH, ionic strength, temperature) is a promising method to target drug delivery to a specific diseased site (*e.g.* solid tumors). Of these physiological stimuli, changes in environmental pH have been the most widely studied for triggered drug release.[34] This is due to pronounced pH gradients that exist in microenvironments of both healthy and diseased tissues in the body. For example, the pH in the stomach can be as low as 1.0 but rapidly increases to 6.0 – 6.5 in the small intestine. Within the cellular microenvironment, pH values range from 7.4 in the extracellular matrix to values of 6.0 – 4.5 in endosomal and lysosomal compartments, respectively. When targeting drugs to tumors, many groups have attempted to exploit the pH gradient between normal tissue and solid tumors, which possess values of approximately 7.4 and 6.0, respectively.[35,36] One approach has been to covalently attach drugs to polymeric delivery systems using pH-sensitive linkages that are reversible in

acidic pH environments. Thus, drug release can be isolated specifically in low pH environments encountered in solid tumors or inside diseased cells. Of these chemistries, the reaction between hydrazines and aldehyde or ketone-containing drugs to form hydrazone linkages (shown in Figure 3.9) has been widely used for pH-triggered drug delivery.[34] In neutral and basic pH environments, hydrazone hydrolysis is slow, but in acidic environments, hydrolysis becomes favored and results in triggered release of the conjugated drug from the delivery system. Thus, faster drug release rates are observed in environments with increasing acidity. Fréchet and coworkers utilized this chemistry to conjugate DOX, which contains ketone functionality, to hydrazine-functionalized polyester dendrimers and demonstrated dramatically accelerated DOX release in environments with a pH value of 5.5 or less.[37,38] Kataoka and coworkers used a similar approach to conjugate DOX to a hydrazine-functionalized, PEG-*b*-polyamino acid copolymer.[39] They also observed selective DOX release in the lysosomal compartments (*i.e.* pH 6.0 or less) of SBC-3 lung cancer cells using confocal microscopy.

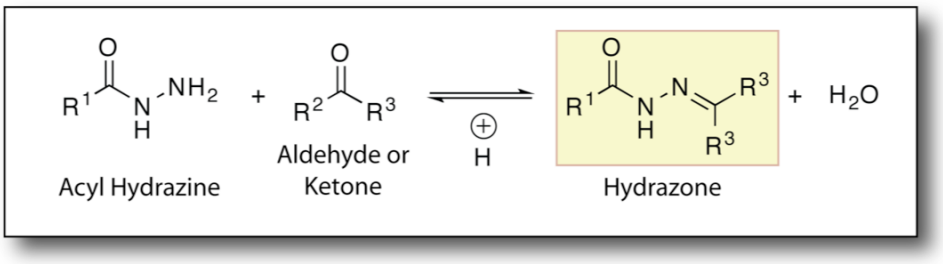

Figure 3.9 pH-reversible hydrazone formation by condensation of hydrazine and an aldehyde or ketone

We hypothesized that utilizing pH-sensitive reactions to cross-link amphiphilic polyolefins at the oil-water interface would produce stimuli-responsive polymer capsules, potentially capable of pH-triggered drug release. Our initial efforts focused on the

synthesis of photo-cross-linkable, phenyl azide-functional cyclooctenes that were linked by pH-sensitive hydrazone or acetal moieties, such as compounds **44** and **45**, in Figure 3.10. However, the synthesis and polymerization of these compounds proved challenging. Attempts to ROMP compound **44** were unsuccessful, possibly due to catalyst reactivity towards the hydrazone functionality, and compound **45** could not be isolated in sufficient purity for polymerization. Thus, a new pH-sensitive cross-linking strategy, which utilizes hydrazine-functionalized, amphiphilic graft copolymers in conjunction with *bis*-aldehyde cross-linking was devised to circumvent the use of phenyl azide-functional monomers **44** and **45**.

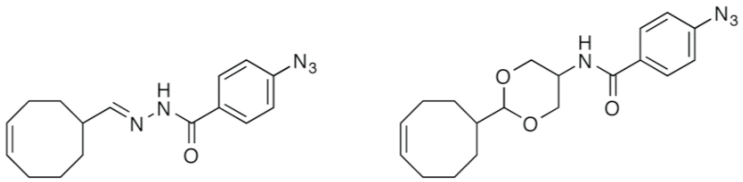

Figure 3.10 Examples of pH-reversible cyclooctene-phenyl azide derivatives

While a number of methodologies exist to introduce hydrazine functionality into amphiphilic polyolefins, we chose to synthesize a Boc-protected, hydrazine-functionalized cyclooctene since the introduction of this functional monomer provides much greater control over hydrazine content when compared to other post-polymerization functionalization strategies. To accomplish this, 5-cyano-1-cyclooctene (**46**) was first synthesized in two steps by monobromination of cyclooctadiene (COD) followed by nucleophilic substitution with sodium cyanide as reported by Grubbs and coworkers.[26] Nitrile-functionalized **46** was then oxidized to 5-carboxylic acid-1-cyclooctene (**47**) by alkaline hydrolysis with hydrogen peroxide in 62% yield.[40] In the final step, *tert*-butyl

carbazate was coupled to **47** by DMAP-catalyzed, carbodiimide coupling. Following purification by column chromatography and crystallization in hexanes, Boc-protected, acyl hydrazine-functionalized cyclooctene **48** was isolated as a solid in 63% yield.

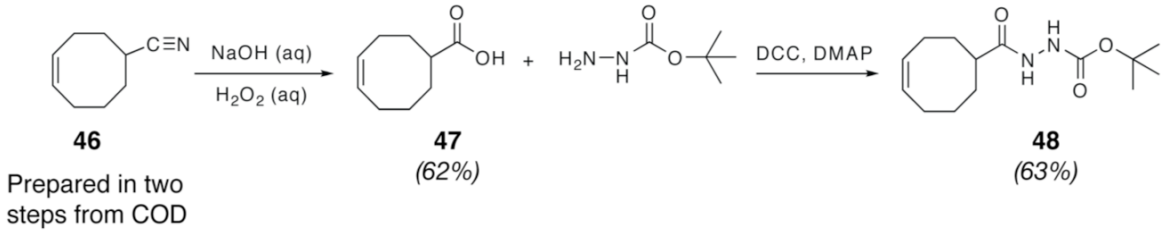

Scheme 3.6 Synthesis of Boc-protected, hydrazine-functionalized cyclooctene 48

Hydrazine-functional copolymer **49** was then prepared using 50 mol % Boc-protected, hydrazine-functionalized cyclooctene (**48**), 20 mol % unsubstituted cyclooctene, and 30 mol % PEG-functionalized cyclooctene macromonomer **9** (PEG MW approx. 2200) in DCM ([M] = 1.0 mol/L) using catalyst **II** as illustrated in Scheme 3.7. The molecular weight of the copolymer was controlled by the addition of the chain transfer agent, 1-hexene ([M]/[CTA] = 100). Boc-protection of the hydrazine-functionalized cyclooctene is needed for ROMP, as primary amines, and presumably hydrazines, coordinate to ruthenium benzylidene catalysts, such as catalysts **I**, **II**, and **III**, and render them unreactive for metathesis chemistry. In this case, Boc-protected **48** was found to successfully undergo ROMP when copolymerized with **17** and **9** in the presence of catalyst **II**. ^{1}H NMR analysis of copolymer **49** in d_6-DMSO revealed an absence of cyclic olefin resonances at δ 5.70 ppm and new olefin resonances at δ 5.35 corresponding the polyolefin backbone. Proton resonances at δ 1.39 ppm corresponding to the *tert*-butyl protons on the Boc protecting group and resonances at δ 9.47 ppm and δ 8.65 ppm, corresponding to the Boc-protected hydrazine, confirmed the incorporation of **48** into the

copolymer structure. However, unique resonances corresponding to the methyne proton adjacent to the acyl hydrazine at δ 1.95 ppm and *tert*-butyl protons of the Boc protecting group (δ 1.39 ppm) overlap with other polyolefin backbone resonances which precluded the quantification of **48** incorporated into copolymer **49**. ^{13}C NMR analysis provided further evidence of successful incorporation of hydrazine-functionalized **48** as carbonyl resonances of the Boc-protected hydrazine were observed at δ 155.0 ppm and δ 174.3 ppm. GPC analysis in THF approximated the molecular weight of copolymer **48** to be 97,800 g/mol with a PDI of 2.06.

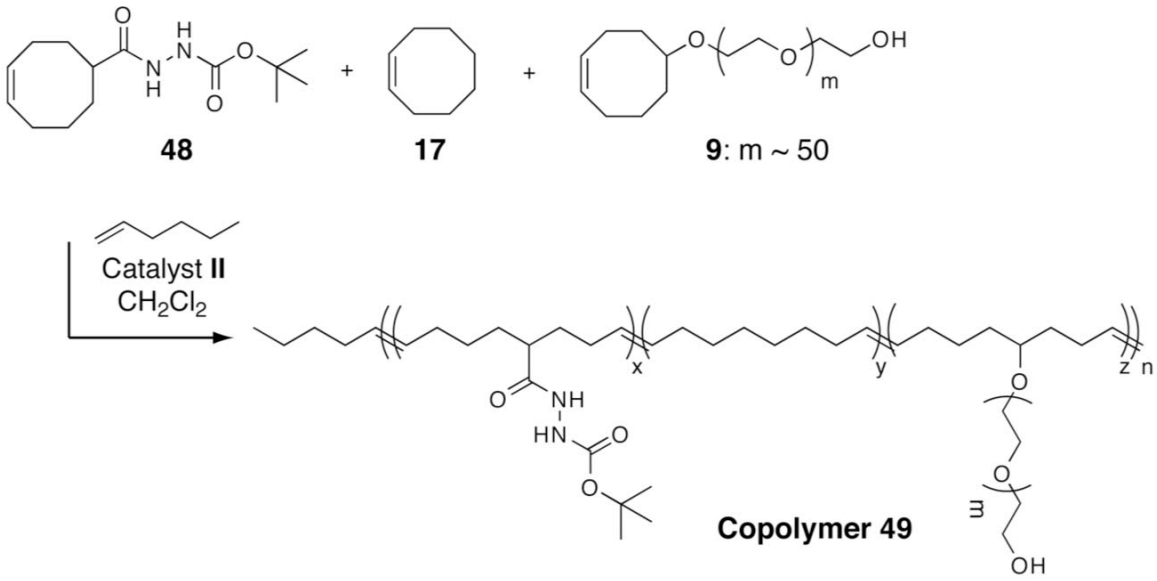

Scheme 3.7 Synthesis of hydrazine(Boc)-functional PCOE-*g*-PEG copolymer 49

Boc-protected copolymer **49** was deprotected with a 50% solution (v/v) of trifluoroacetic acid (TFA) in dichloromethane as illustrated in Scheme 3.8. Following precipitation into diethyl ether, hydrazine-functionalized graft copolymer **50** was isolated in near quantitative yield. ^{1}H NMR analysis of copolymer **50** revealed an absence of *tert*-butyl proton resonances at δ 1.39 ppm, confirming the deprotection of the Boc protecting

group. In this case, the copolymer is isolated as the trifluoracetate salt following deprotection as it was found that copolymer **50** can be utilized in the salt form for the preparation of polymer capsules by glutaraldehyde cross-linking. For long-term storage of the copolymer, the neutralization of the TFA salt with an organic base such as triethylamine proved to be advantageous to prevent polymer degradation.

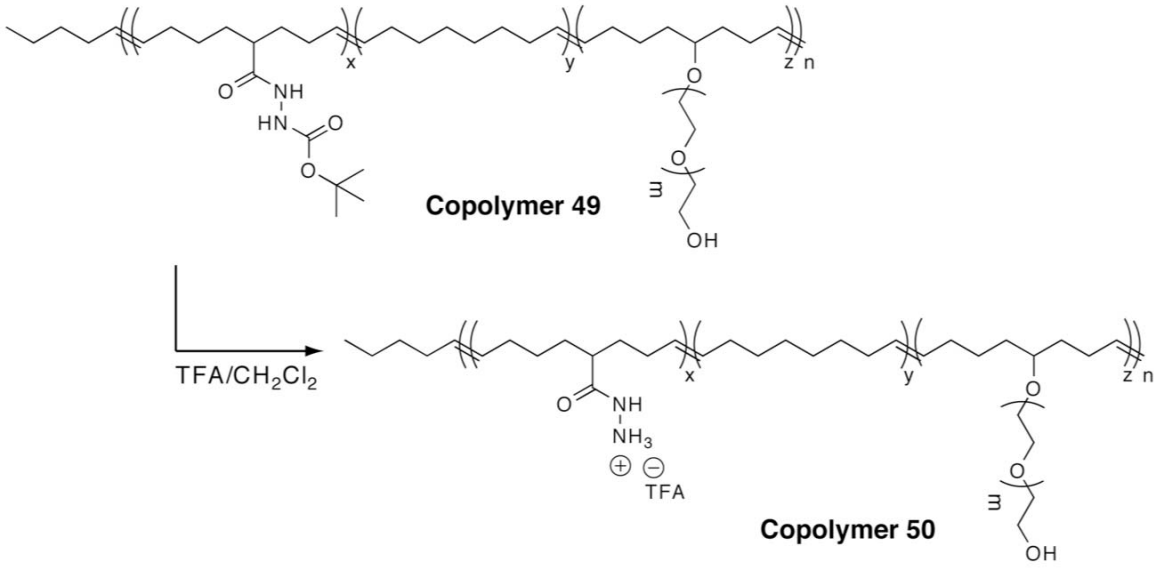

Scheme 3.8 Synthesis of hydrazine-functional PCOE-*g*-PEG copolymer 50

Polymer capsules were prepared by interfacial assembly of copolymer **50** and subsequent cross-linking by addition of glutaraldehyde as shown in Figure 3.11. Experimentally, copolymer **50** (15 mg) was dissolved in deionized water (10 mL) followed by addition of toluene (0.5 g). The mixture was shaken gently to form the polymer assembly, and 400 mg of a 50 wt % aqueous glutaraldehyde solution was added to create a 2 wt % solution of glutaraldehyde. The mixture was allowed to stand for at least 4 hours to produce the hydrazone cross-linked capsules. The toluene-filled capsules float to the top of the aqueous solution and excess water and glutaraldehyde were removed by pipette. Fresh DI water (adjusted to pH 8.0 by addition of NH_4OH) was

added to the capsule solution, and this washing process was repeated a total of four times. The use of water-soluble graft copolymers and cross-linkers, such as glutaraldehyde, is advantageous since repeated washing steps efficiently remove excess reagents. Dialysis of the capsules against basic water (pH 8.0) using a 250,000 molecular weight cutoff membrane was also found to be an effective method of removing excess polymer and glutaraldehyde.

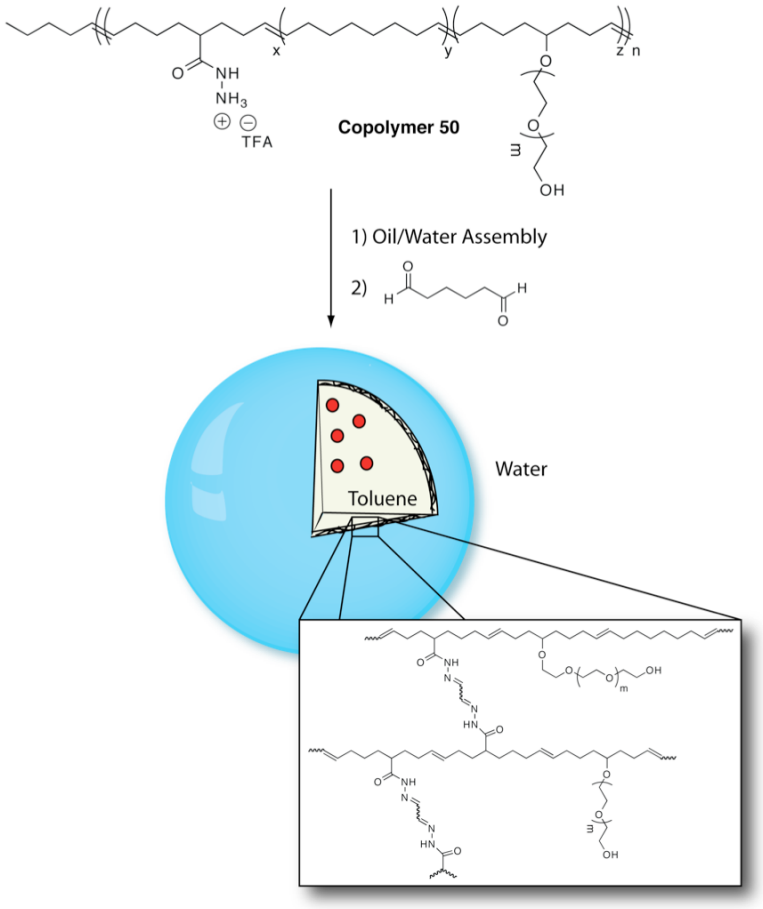

Figure 3.11 Illustration of oil-water interfacial assembly and cross-linking of hydrazine-functional copolymer 50 with glutaraldehyde

To test the effectiveness of hydrazone cross-linking, polymer capsules prepared using copolymer **50** were drop-cast onto glass slides and evaluated by optical microscopy. As seen in Figure 3.12, the capsules maintain the structural integrity due to cross-linking and the thin polymer membrane is observable at 20X magnification.

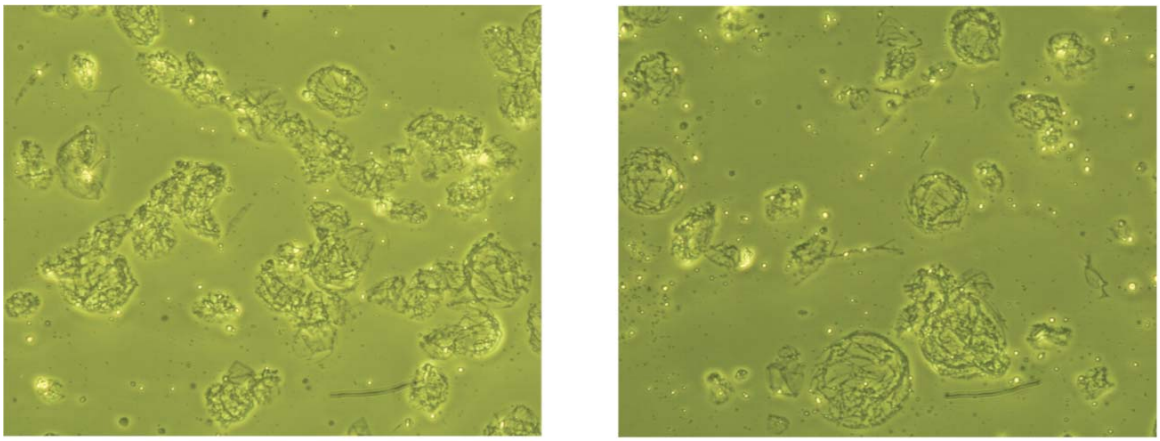

Dried Hydrazone Cross-linked Capsules Cast from Solution

Figure 3.12 Optical micrographs of hydrazone cross-linked polymer capsules prepared from copolymer 50 (20X magnification)

To further investigate the cross-linked capsules by confocal scanning laser microscopy, a fluorescent-labeled, hydrazine-functionalized graft copolymer was prepared in an analogous fashion to copolymer **50** but with the addition of 0.5 mol % Rhodamine B-labeled cyclooctene **32**. Following polymerization and deprotection with TFA, fluorescent-labeled copolymer **50** was utilized to prepare hydrazone cross-linked capsules as described above. As seen in Figure 3.13A, copolymer **50** shows a strong interfacial preference as the fluorescence signal is observed almost exclusively at the oil-water interface. Following introduction of methanol to the capsule suspension, the interface is removed, revealing collapsed capsules with cross-linked polymer membranes as illustrated in Figure 3.13B. The capsule membrane can also be visualized by simply

drop-casting the capsule suspension followed by solvent evaporation as seen in Figures 3.13C and 3.13D. These images further illustrate the very thin, mechanically robust polymeric shell that is produced using the hydrazone cross-linking technique.

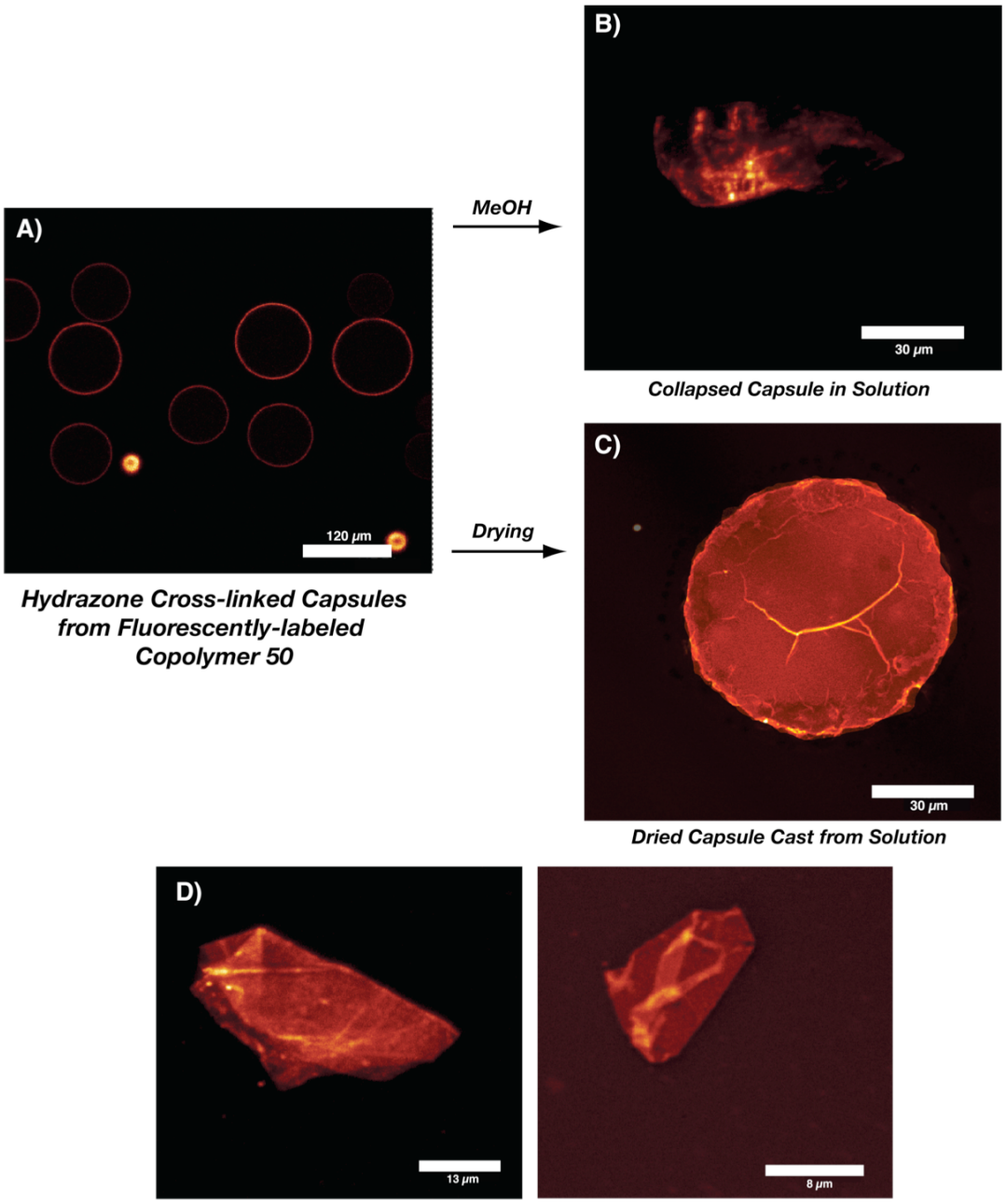

Figure 3.13 Confocal micrographs of hydrazone cross-linked polymer capsules prepared using fluorescent-labeled, copolymer 50; A) toluene-filled capsules, B) collapsed capsule following interface removal with methanol, C) and D) dried capsules that were cast from solution

To evaluate the degradation properties of hydrazone cross-linked polymer capsules, two fluorescent-labeled capsule samples were prepared from copolymer **50**, drop-cast from solution onto a glass slide, and then immersed in either acidic (HCl, pH 2.5) or neutral (PBS, pH 7.4) water. Sample degradation was monitored over time by confocal microscopy, as this allows for direct visualization of the degradation process. Figure 3.14 shows comparative images of capsules immersed in acidic water (Figure 3.14A) or neutral water (Figure 3.14B) after 0, 1, 2, 3, and 8 hours. Before immersion in water (0 hour), both capsules are flat with characteristic ridges created from the drying process. As seen in Figure 3.14A, after 1 hour of immersion in acidic water, the capsule appears to become porous with visible holes in the polymer membrane. This image suggests that capsule degradation occurs in acidic water, as expected from capsules cross-linked by hydrazone linkages. In comparison, Figure 3.14B shows time-lapse images of a capsule immersed in phosphate buffered saline (pH 7.4). In this case, the capsule does not degrade but appears to swell over time, a result of its hydrophilicity and cross-linking. Taken together, this data suggests that capsule degradation is a pH-dependant process with minimal degradation observed at neutral pH and slow degradation occurring due to hydrazone hydrolysis at pH 2.5.

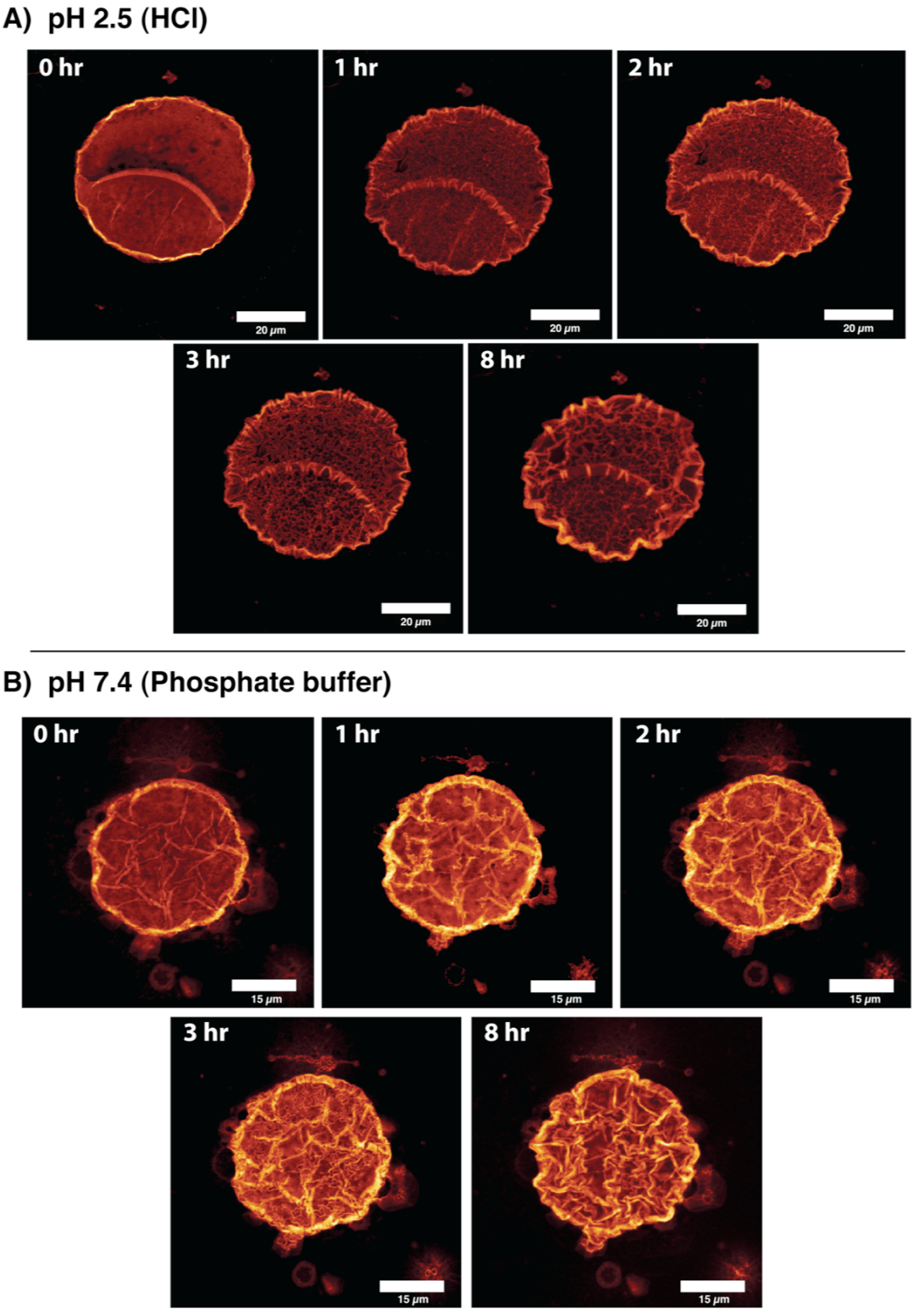

Figure 3.14 Time-lapse, confocal projection micrographs of hydrazone cross-linked polymer capsules prepared using fluorescent-labeled copolymer 50 after immersion in A) pH 2.5 water (HCl), B) pH 7.4 phosphate buffered saline

To compare the degradation and swelling of hydrazone-crosslinked capsules at pH 2.5 versus pH 7.4, cross-sectional image stacks of the two samples were used to produce three-dimensional height images using ImageJ software. In both cases, the capsules are not visible in height images compiled at 0 minutes and are barely visible in the images compiled after 30 minutes of immersion (Z place scale 0 – 18 μm) due to the extremely thin nature of the collapsed polymer membrane. Figure 3.15A compares the height image of a capsule following 30 minutes and 8 hours of immersion in pH 2.5 water. From these two images, it is clear that capsule swelling occurs at low pH as evidenced by the increase in height of the capsule, particularly at the capsule perimeter. However, when compared to similar images of the capsule immersed in PBS (Figure 3.15B), swelling in this environment is much more pronounced after 8 hours of immersion. Furthermore, comparison of the two images after 8 hours of immersion reveals some degradation in center of the capsule at pH 2.5, as evidenced by the decreased overall height of the polymer membrane when compared to the capsule immersed in PBS. In contrast, significant swelling of the entire capsule is observed for the sample immersed in PBS with little evidence of degradation. While this data suggests that hydrazone cross-linked capsule degradation is more pronounced at pH 2.5 versus 7.4, additional experiments will be needed to verify these observations. These experiments include the investigation of capsule degradation at neutral and acidic pH over longer time periods (several days to weeks) and GPC analysis of capsule degradation products at a range of pH values (e.g. 1.0 – 7.4) over time. This initial proof-of-concept along with additional experiments may prompt exploration of hydrazone cross-linked capsules for pH-triggered release of encapsulated solutes.

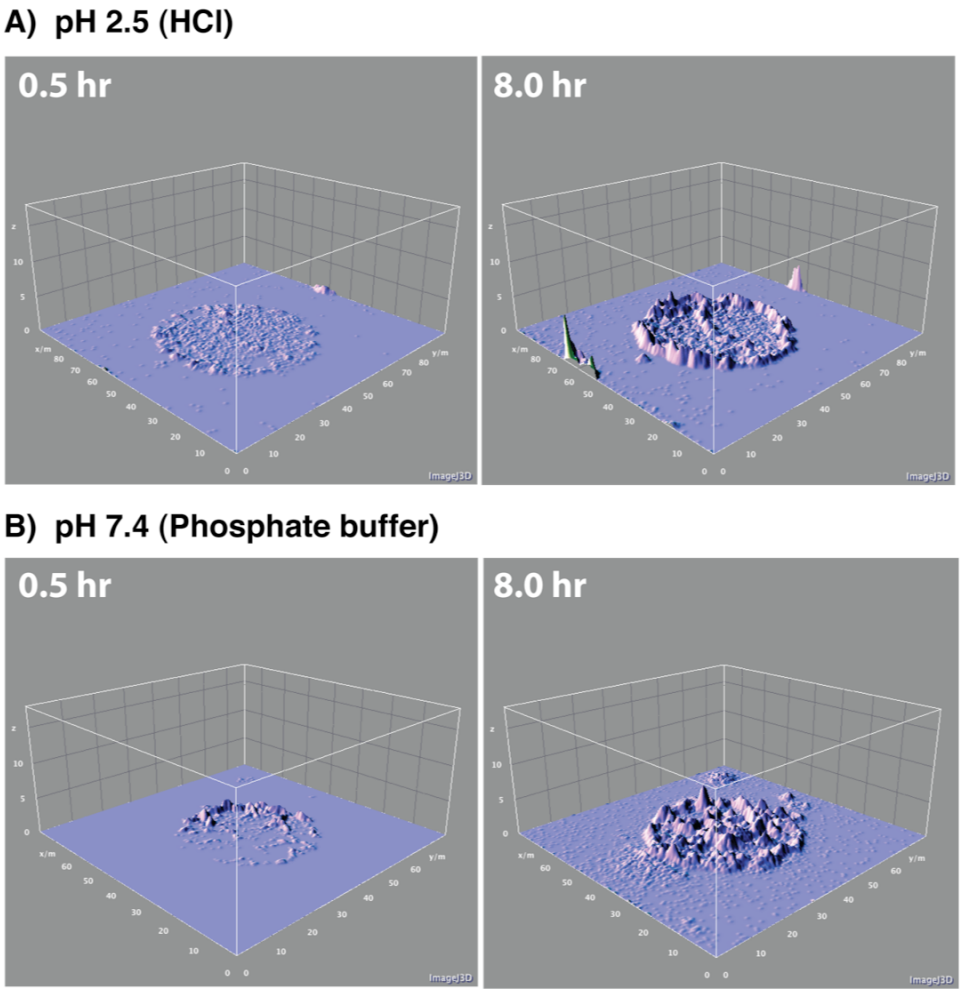

Figure 3.15 Three-dimensional height images constructed from confocal microscopy analysis of hydrazone cross-linked polymer capsules, A) pH 2.5 water (HCl), B) pH 7.4 phosphate buffered saline

3.2.3 Water-filled Polymer Capsules Prepared by Water-in-oil Assembly and Cross-linking of PCOE-*g*-PEG Copolymers

We have demonstrated that amphiphilic PEGylated polyolefins are well-suited for assembly and stabilization of oil-water interfaces. The majority of the experiments described in Chapter 3 of this thesis utilize oil-in-water dispersions for assembly and cross-linking, as this method is applicable for the encapsulation of hydrophobic drugs and other water-insoluble agents. However, for some applications, it is advantageous to produce polymer capsules from water-in-oil dispersions, thereby permitting the

encapsulation of water-soluble compounds. To demonstrate the versatility of PCOE-*g*-PEG copolymers in producing water-filled polymer capsules, these copolymers were also utilized to produce stable, water-in-toluene dispersions, which were subsequently UV cross-linked using a *bis*-phenyl azide cross-linking additive.

Initial attempts to prepare water-in-toluene dispersions were made using copolymer **42** which contains 20 mol % phenyl azide functionality and 30 mol % PEG 2200 macromonomer **9**. This level of PEG incorporation renders the copolymer very soluble in water, and we found that amphiphilic graft copolymers with such high PEG contents did not successfully form water-in-oil dispersions. Instead, PCOE-*g*-PEG copolymers such as copolymer **52** (shown in Figure 3.16), prepared in a similar fashion to copolymer **29** but with 5 mol % PEG 4400 grafts proved suitable for stabilizing water-in-toluene droplets. Copolymer **52** is not soluble in water but highly soluble in toluene, which proved to be a key feature for preparing water-in-oil capsules.

Initial efforts to cross-link water-in-toluene assemblies focused on the incorporation of phenyl azide functionality into the copolymer through copolymerization of **38**. Although these copolymers produced cross-linked capsules, we found that the use of a toluene-soluble, *bis*-phenyl azide was also effective for UV cross-linking of water-in-toluene dispersions. *bis*-Azide cross-linker **51** was prepared in one-step from commercially available, 4-aminophenyl sulfone as shown in Scheme 3.9. Utilizing this small molecule cross-linker obviates the need to synthesize and copolymerize **38**, and thus, copolymer **52** can be prepared using the commercially available catalyst **II**. These features are particularly attractive for making large batches of cross-linked capsules due to the reduced reagents costs and fewer synthetic steps needed.

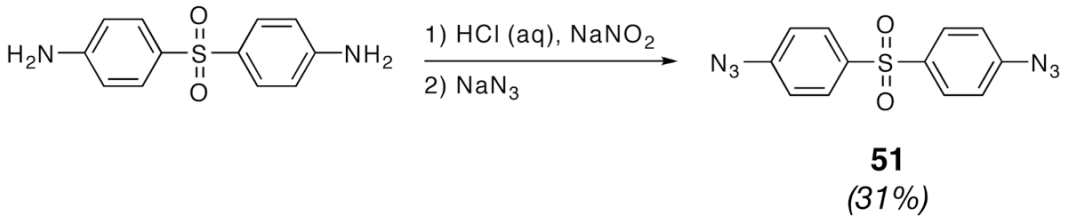

Scheme 3.9 Synthesis of *bis*-phenyl azide cross-linker 51

To prepare water-in-toluene capsules, copolymer **52** (12.5 mg) and *bis*-phenyl azide cross-linker **51** (5 mg) were dissolved in 10 mL of toluene followed by addition of 0.25 g of deionized water. The mixture was vigorously shaken to form the water-in-toluene assemblies which were subsequently UV cross-linked using a 302 nm light source as illustrated in Figure 3.16. The depiction of PEG grafts residing mainly in the aqueous phase of the dispersion is based on the known solubility preference of PEG 4400 in water compared to toluene. Although it is thought that PEG provides a stabilizing steric effect to oil-in-water dispersions prepared from PCOE-*g*-PEG copolymers, copolymer **52** clearly mediates the water/oil interface and produces dispersions which are stable for many hours, even without UV cross-linking. Water-filled capsules settle to the bottom of the toluene solution over time and repeated pipetting and washing with fresh toluene proved to be an effective method of purifying and concentrating the capsules.

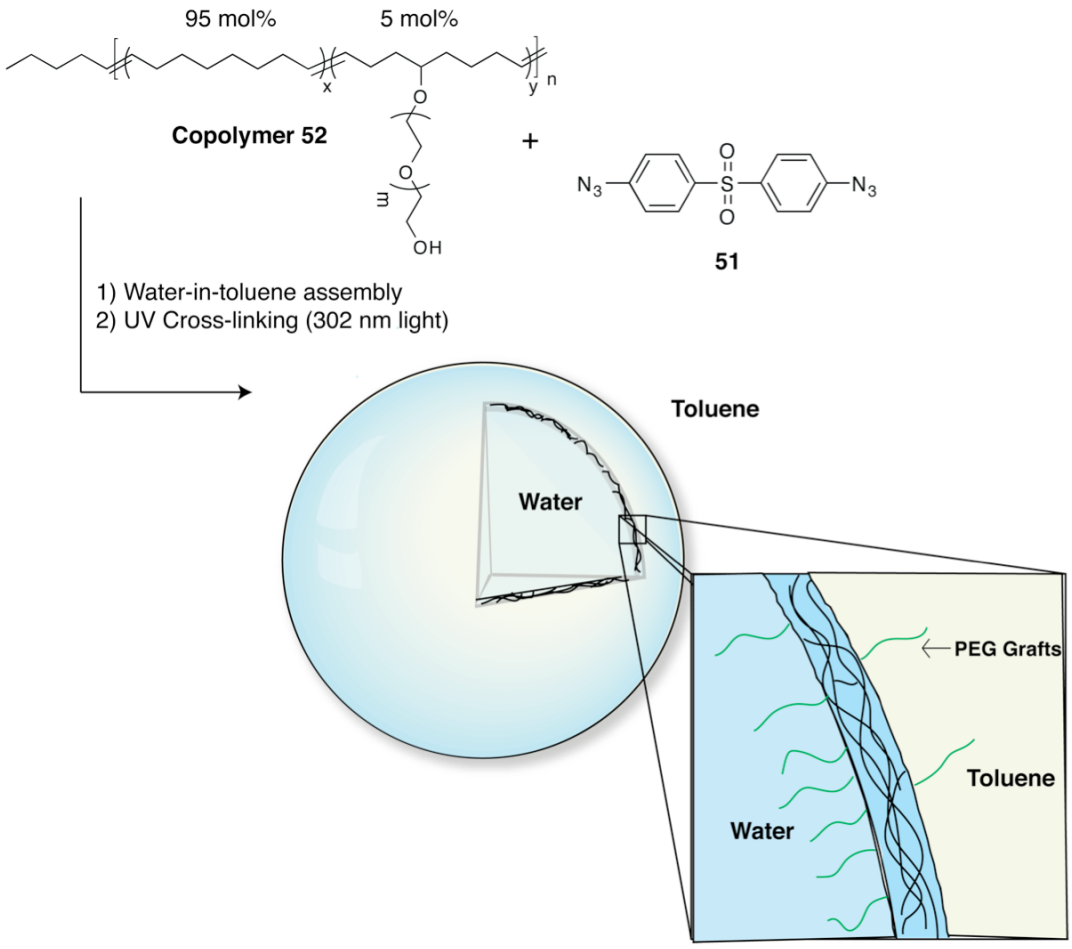

Figure 3.16 Illustrative depiction of polymer capsules prepared from the water-in-toluene assembly of copolymer 52 and UV cross-linking with *bis*-phenyl azide 51

To demonstrate the effectiveness of cross-linking using *bis*-phenyl azide **51**, water-in-toluene capsules were analyzed by optical microscopy. As illustrated in Figure 3.17A, spherical capsules are prepared by this method with mechanically robust membranes that are visible upon drying and highlighted by black boxes. This approach can also be utilized for encapsulating water-soluble reagents such as tetraethylene glycol and potassium hydroxide for accelerated sand core binder disintegration as shown in Figures 3.17B and 3.167, respectively. These capsules are currently being evaluated as part of an on-going collaboration with General Motors.

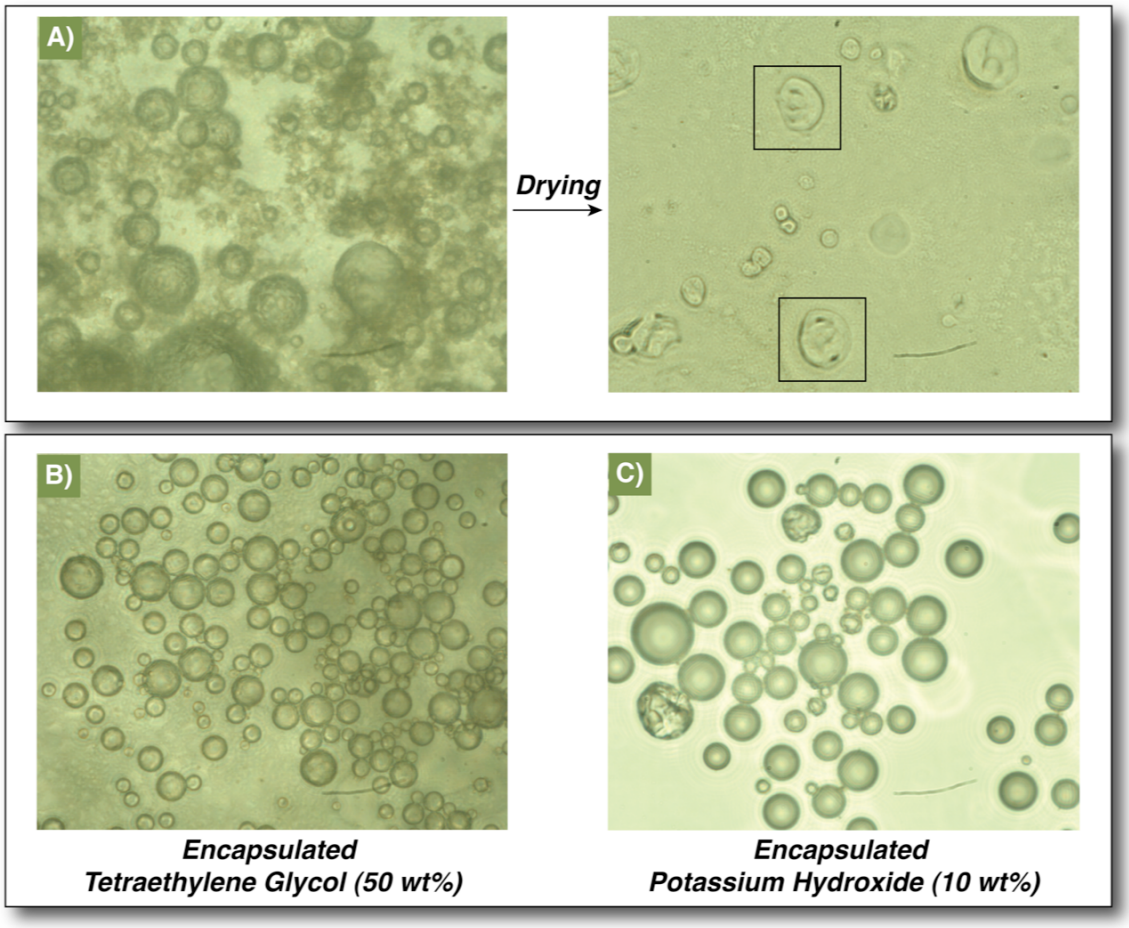

Figure 3.17 Optical micrographs of water-in-toluene capsules, A) cross-linked, water-filled capsules after drying, B) encapsulated tetraethylene glycol (50 wt % aqueous solution,) C) encapsulated potassium hydroxide (10 wt % aqueous solution)

3.3 Capsule Sizing by Membrane Extrusion and Ultrasonication

The size and size distribution of drug carriers are critical parameters that impact both their biodistribution[41] and drug release rate[42] in drug delivery applications. For example, an upper size limit of approximately 5 - 10 μm exists for injectable drug delivery systems due to the size of capillaries in which the carriers must traverse. Recently, there has been growing interest in producing delivery systems with particle sizes less than 200 nm because of their prolonged blood circulation lifetimes and reduced liver uptake compared to larger particles.[43] The interfacial assembly techniques

described in this chapter thus far utilize simple hand shaking of oil-water assemblies to produce polymer capsules with diameters in the range of tens of microns and which possess a relatively broad size distribution. In an effort to reduce the size and polydispersity of polymer capsules to a more applicable size range for drug delivery, we investigated two different methods of capsule sizing, membrane extrusion and ultrasonication.

Membrane extrusion involves the passage of a liquid suspension of vesicles or polymer assemblies through track-etch membranes with well-defined pore sizes in the micron to nanometer size range. The extrusion process causes the vesicles to rupture when their lysis tension is exceeded, forming smaller vesicles upon elution from the pore opening.[44,45] The technique has been widely used to reduce the size of multi-lamellar liposomes[46,47] and polymersomes[48] from tens of microns to 1μm or less . Recently, our group demonstrated that membrane extrusion could also be utilized to reduce the size of nanoparticles-covered droplets from 50 – 200 μm to 1 – 10 μm with a relatively narrow size distribution.[49] These reports inspired attempts to reduce the size of polymer assemblies made from amphiphilic graft copolymers using membrane extrusion techniques. Indeed, we found that membrane extrusion was suitable for sizing polymer capsules prepared by interfacial assembly. For example, Figure 3.18 illustrates a confocal micrograph of Coumarin 153-filled assemblies prepared from copolymer **42** before and after 10 passes through a membrane extruder equipped with a track-etch membrane having 1 μm pores. After extrusion, the capsule diameter was effectively reduced from 10 – 40 μm to approximately 1 μm with a relatively narrow size distribution. We observed that after several hours, the extruded, uncross-linked capsules

coalesce to form larger structures with a broadened size distribution. Photo-cross-linking of the phenyl azide-functional graft copolymer at the oil-water interface is particularly useful in this case since the capsules can be rapidly cross-linked following membrane extrusion to effectively "lock in" the desired size and distribution. In comparison, the size and distribution of UV cross-linked capsules were unchanged after several days of storage. Utilizing this membrane extrusion and rapid UV cross-linking technique to finely tune size features of polymer capsules may prove useful in tailoring polyolefin capsules for potential delivery applications.

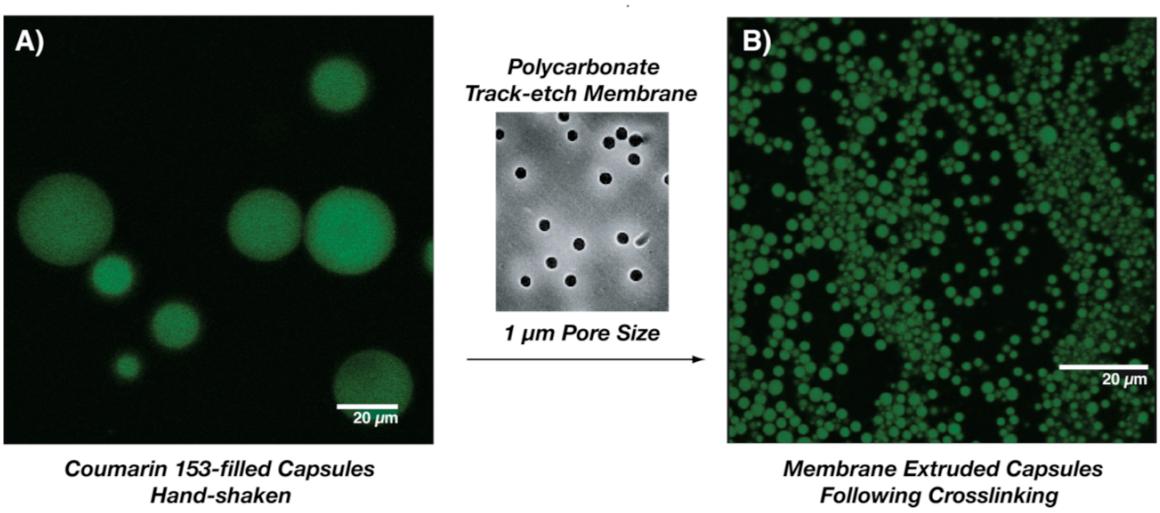

Figure 3.18 Confocal micrographs of Coumarin 153-filled, oil-in-water assemblies prepared from copolymer 42, A) hand-shaken assemblies, B) capsules obtained after 11 passes through a track-etch membrane (1 μm pore size) and subsequent UV cross-linking

Attempts to size capsules to the sub-micron size level were also conducted using the described membrane extrusion technique using track-etch membranes with 100 nm pores. In this case, extrusion through the smaller pores resulted in capsule instability, presumably due to increased pressure during the extrusion process. Thus, intact sub-micron capsules were difficult to prepare using this method and other methods of sizing

were explored. For example, ultrasonication has been used extensively to produce small, unilamellar liposomes from the larger, multilamellar vesicles that form from simple lipid hydration techniques.[50,51] In this case, the induced pressure of sonication can reduce liposomes to the nanometer size range (*e.g.* 50 – 100 nm), and it was found that this technique could be also utilized to form nanometer-sized capsules from larger, hand-shaken graft copolymer assemblies. In initial experiments, toluene-in-water assemblies produced using copolymer **42** were sonicated for several minutes to reduce the droplet size, but toluene evaporation proved problematic and resulted in either polymer precipitation or micelle formation in the aqueous phase. This issue was overcome by the use of a high-boiling hydrophobic liquid, glyceryl trioctanoate (*i.e.* trioctanoin), in place of toluene in the oil-in-water dispersion. To produce trioctanoin-filled capsules, polymer **42** (50 mg) was combined with trioctanoin (50 mg) and dissolved in 0.5 mL of dichloromethane. This solution was added to a flask containing deionized water (50 mL) and placed in a sonicating bath for 15 min. During the sonication process, dichloromethane evaporates from the dispersion, leaving a translucent solution of graft copolymer-stabilized trioctanoin droplets that were subsequently photo-cross-linked to yield sub-micron, polymer capsules as illustrated in Figure 3.19. The capsules produced by this technique could not be visualized by optical microscopy, suggesting a sub-micron size distribution. Dynamic light scattering (DLS) analysis of the cross-linked capsules at a 90^{o} angle (also shown in Figure 3.16) reveals an average capsule diameter of approximately 160 nm with a relatively narrow size distribution (standard deviation = 21 nm). The ability to produce oil-filled capsules in this size regime, combined with the

biocompatible PEG periphery, may permit their eventual use in a variety of systemic and targeted drug delivery applications.

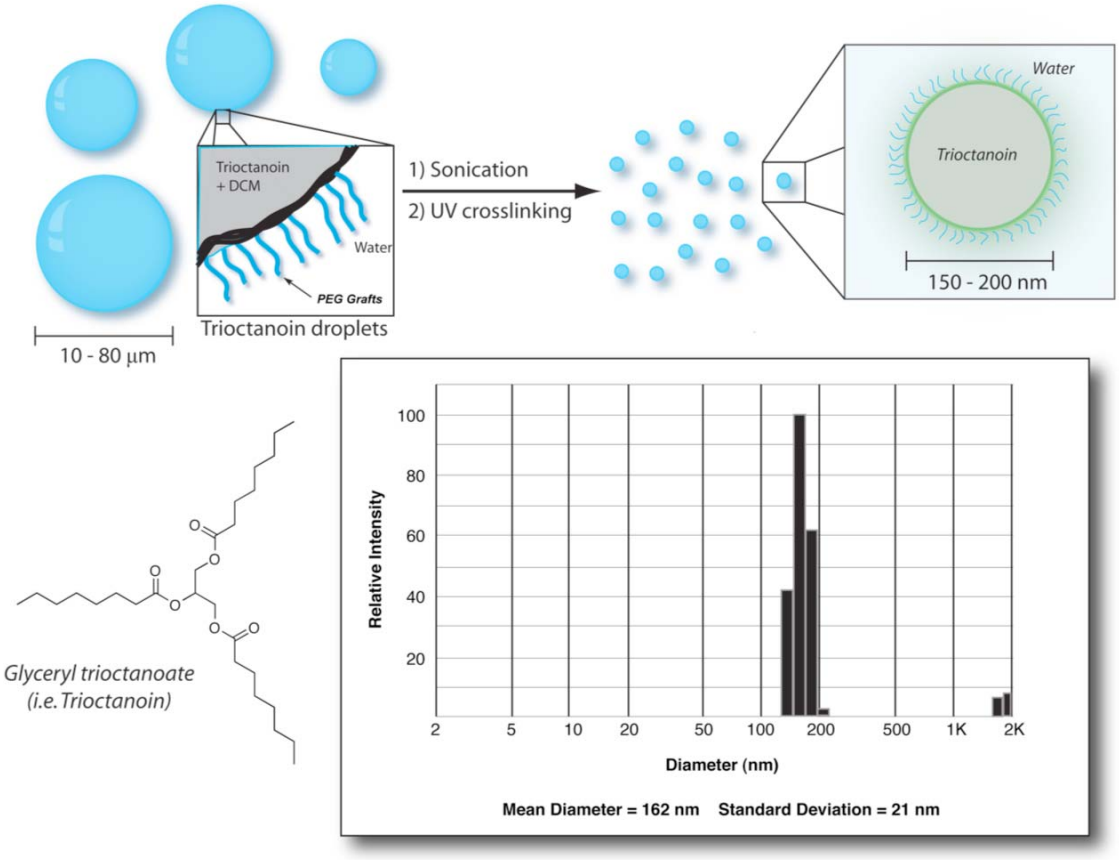

Figure 3.19 Illustrative depiction and DLS analysis (angle = 90^{o}) of sub-micron polymer capsules produced by sonication and UV cross-linking of copolymer 42-stabilized trioctanoin-in-water assemblies

3.4 Summary and Outlook

In summary, amphiphilic PCOE-*g*-PEG graft copolymers were utilized in oil-water interfacial assembly and cross-linked to form polymer capsules with thin, mechanically robust cross-linked membranes. In one method, a *bis*-cyclooctene PEG derivative was used in conjunction PCOE-*g*-PEG copolymer and cross-linked at the oil-water interface by ring-opening cross-metathesis with a ruthenium benzylidene catalyst. In a second approach, reactive functionality capable of cross-linking was incorporated

into the polymer backbone by copolymerization of phenyl azide and acyl hydrazine-functional cyclooctene derivatives. The reactive polymers were cross-linked by photo-generated nitrenes (in the phenyl azide case) or by addition of glutaraldehyde (in the acyl hydrazine case) to form capsules that possess tunable degradability (*i.e.* non-degradable or pH-dependent degradability). This interfacial assembly and cross-linking approach also permits the preparation of both water-in-oil capsules, enabling the encapsulation of hydrophilic agents such as tetraethylene glycol and potassium hydroxide. In addition, the assemblies can be sized from tens of microns to the 150 nm - 1 μm size range by either membrane extrusion or ultrasonication techniques. These techniques are complementary to the UV cross-linking approach as the assemblies can be sized and then rapidly cross-linked to "lock-in" the desired capsule size. Furthermore, these sizing techniques produce capsules that are of an applicable size range for many drug delivery applications. This data combined with preliminary encapsulation studies using a hydrophobic dye, Coumarin 153 and neutral doxorubicin suggest that the these capsules might be useful in the encapsulation and delivery of a variety hydrophobic agents.

3.5 References

(1) Ghosh, S. K. *Functional coatings: by polymer microencapsulation*; Wiley-VCH; John Wiley: Weinheim Chichester, 2006.

(2) Lensen, D.; Vriezema, D. M.; van Hest, J. C. *Macromol. Biosci.* **2008**, *8*, 991-1005.

(3) Arshady, R. *J. Microencapsulation* **1989**, *6*, 13-28.

(4) Ali, M. M.; Stover, H. D. H. *J. Polym. Sci. Pol. Chem.* **2006**, *44*, 156-171.

(5) Tiarks, F.; Landfester, K.; Antonietti, M. *Langmuir* **2001**, *17*, 908-918.

(6) Discher, B. M.; Won, Y. Y.; Ege, D. S.; Lee, J. C. M.; Bates, F. S.; Discher, D. E.; Hammer, D. A. *Science* **1999**, *284*, 1143-1146.

(7) Discher, B. M.; Hammer, D. A.; Bates, F. S.; Discher, D. E. *Curr. Opin. Colloid Interface Sci.* **2000**, *5*, 125-131.

(8) Ahmed, F.; Pakunlu, R. I.; Srinivas, G.; Brannan, A.; Bates, F.; Klein, M. L.; Minko, T.; Discher, D. E. *Mol. Pharm.* **2006**, *3*, 340-350.

(9) Shum, H. C.; Kim, J. W.; Weitz, D. A. *J. Am. Chem. Soc.* **2008**, *130*, 9543-9549.
(10) Nardin, C.; Hirt, T.; Leukel, J.; Meier, W. *Langmuir* **2000**, *16*, 1035-1041.
(11) Rigler, P.; Meier, W. *J. Am. Chem. Soc.* **2006**, *128*, 367-373.
(12) Discher, B. M.; Bermudez, H.; Hammer, D. A.; Discher, D. E.; Won, Y. Y.; Bates, F. S. *J. Phys. Chem. B* **2002**, *106*, 2848-2854.
(13) Dinsmore, A. D.; Hsu, M. F.; Nikolaides, M. G.; Marquez, M.; Bausch, A. R.; Weitz, D. A. *Science* **2002**, *298*, 1006-1009.
(14) Gordon, V. D.; Xi, C.; Hutchinson, J. W.; Bausch, A. R.; Marquez, M.; Weitz, D. A. *J. Am. Chem. Soc.* **2004**, *126*, 14117-14122.
(15) Sukhorukov, G. B.; Donath, E.; Davis, S.; Lichtenfeld, H.; Caruso, F.; Popov, V. I.; Mohwald, H. *Polym. Advan. Technol.* **1998**, *9*, 759-767.
(16) Dai, Z. F.; Voigt, A.; Leporatti, S.; Donath, E.; Dahne, L.; Mohwald, H. *Adv. Mater.* **2001**, *13*, 1339-1342.
(17) Antipov, A. A.; Sukhorukov, G. B.; Donath, E.; Mohwald, H. *J. Phys. Chem. B* **2001**, *105*, 2281-2284.
(18) Sukhorukov, G. B.; Antipov, A. A.; Voigt, A.; Donath, E.; Mohwald, H. *Macromol. Rapid Comm.* **2001**, *22*, 44-46.
(19) Park, M. K.; Deng, S. X.; Advincula, R. C. *Langmuir* **2005**, *21*, 5272-5277.
(20) Zelikin, A. N.; Quinn, J. F.; Caruso, F. *Biomacromolecules* **2006**, *7*, 27-30.
(21) Wu, M. L.; O'Neill, S. A.; Brousseau, L. C.; McConnell, W. P.; Shultz, D. A.; Linderman, R. J.; Feldheim, D. L. *Chem. Commun.* **2000**, 775-776.
(22) Duan, H. W.; Kuang, M.; Zhang, G.; Wang, D. Y.; Kurth, D. G.; Mohwald, H. *Langmuir* **2005**, *21*, 11495-11499.
(23) Wang, Y. J.; Bansal, V.; Zelikin, A. N.; Caruso, F. *Nano Lett.* **2008**, *8*, 1741-1745.
(24) Kwak, J. C. T. *Polymer-surfactant systems*; M. Dekker: New York, 1998.
(25) Randall, M. L.; Tallarico, J. A.; Snapper, M. L. *J. Am. Chem. Soc.* **1995**, *117*, 9610-9611.
(26) Hillmyer, M. A.; Laredo, W. R.; Grubbs, R. H. *Macromolecules* **1995**, *28*, 6311-6316.
(27) Ulbricht, M.; Hicke, H. G. *Angew. Makromol. Chem.* **1993**, *210*, 69-95.
(28) Ulbricht, M.; Hicke, H. G. *Angew. Makromol. Chem.* **1993**, *210*, 97-117.
(29) Kolb, H. C.; Finn, M. G.; Sharpless, K. B. *Angew. Chem. Int. Edit.* **2001**, *40*, 2004.
(30) Binder, W. H.; Sachsenhofer, R. *Macromol. Rapid Comm.* **2007**, *28*, 15-54.
(31) Delaude, L.; Jan, D.; Simal, F.; Demonceau, A.; Noels, A. F. *Macromol. Symp.* **2000**, *153*, 133-144.
(32) Binder, W. H.; Kluger, C. *Macromolecules* **2004**, *37*, 9321-9330.
(33) Brezlow, D. S. In *Azides and Nitrenes - Reactivity and Utility*; Scriven, E. V. S., Ed.; Academic Press: Orlando, FL, 1984, 491-517.
(34) Lee, E. S.; Gao, Z.; Bae, Y. H. *J. Control. Release* **2008**, *132*, 164-170.
(35) Engin, K.; Leeper, D. B.; Cater, J. R.; Thistlethwaite, A. J.; Tupchong, L.; McFarlane, J. D. *Int. J. Hyperthermia* **1995**, *11*, 211-6.

(36) Ojugo, A. S.; McSheehy, P. M.; McIntyre, D. J.; McCoy, C.; Stubbs, M.; Leach, M. O.; Judson, I. R.; Griffiths, J. R. *NMR Biomed.* **1999**, *12*, 495-504.
(37) De Jesus, O. L. P.; Ihre, H. R.; Gagne, L.; Fréchet, J. M. J.; Szoka, F. C. *Bioconjugate Chem.* **2002**, *13*, 453-461.
(38) Ihre, H. R.; De Jesus, O. L. P.; Szoka, F. C.; Fréchet, J. M. J. *Bioconjugate Chem.* **2002**, *13*, 443-452.
(39) Bae, Y.; Fukushima, S.; Harada, A.; Kataoka, K. *Angew. Chem. Int. Edit.* **2003**, *42*, 4640-4643.
(40) Hartley, D. *Journal of the Chemical Society* **1962**, 4722.
(41) Nagayasu, A.; Uchiyama, K.; Kiwada, H. *Adv. Drug Deliver. Rev* **1999**, *40*, 75-87.
(42) Siepmann, J.; Faisant, N.; Akiki, J.; Richard, J.; Benoit, J. P. *J. Control. Release* **2004**, *96*, 123-134.
(43) Li, S. D.; Huang, L. *Mol. Pharm.* **2008**, *5*, 496-504.
(44) Frisken, B. J.; Asman, C.; Patty, P. J. *Langmuir* **2000**, *16*, 928-933.
(45) Patty, P. J.; Frisken, B. J. *Biophys. J.* **2003**, *85*, 996-1004.
(46) Macdonald, R. C.; Macdonald, R. I.; Menco, B. P. M.; Takeshita, K.; Subbarao, N. K.; Hu, L. R. *Biochim. Biophys. Acta* **1991**, *1061*, 297-303.
(47) Nayar, R.; Hope, M. J.; Cullis, P. R. *Biochim. Biophys. Acta* **1989**, *986*, 200-206.
(48) Ahmed, F.; Discher, D. E. *J. Control. Release* **2004**, *96*, 37-53.
(49) Tangirala, R.; Revanur, R.; Russell, T. P.; Emrick, T. *Langmuir* **2007**, *23*, 965-969.
(50) Papahadj.D; Watkins, J. C. *Biochim. Biophys. Acta* **1967**, *135*, 639.
(51) Maulucci, G.; De Spirito, M.; Arcovito, G.; Boffi, F.; Castellano, A. C.; Briganti, G. *Biophys. J.* **2005**, *88*, 3545-3550.

CHAPTER 4

POLYOLEFIN-*GRAFT*-PEG COPOLYMERS AS COATINGS FOR WATER PURIFICATION MEMBRANES

4.1 PEGylation Strategies to Reduce Fouling of Water Purification Membranes

One example application deemed suitable for the polyolefin-*graft*-PEG copolymers described in Chapter 2 is in the area of water purification membranes. Fouling represents a critically important barrier against wider adoption of polymer membranes for many applications, including those intended for water purification.[1,2] Surface and inner-membrane fouling by solutes such as proteins, emulsified oil droplets, and various types of particles leads to considerable loss in flux and selectively over time.[3] While a number of commodity polymers have been fabricated into useful and commercially viable membranes, new synthetic polymers designed to improve existing membranes are needed to prevent fouling and/or improve separation efficiency, and advance the performance of existing commercial membranes beyond their current state.

The known anti-fouling and surface-active properties of polyethylene glycol (PEG), or polyethylene oxide (PEO), are appealing for integration into polymer membranes.[4,5] However, the water solubility and crystallinity of PEG make it unsuitable for fabrication into robust membranes for aqueous applications. Thus, covalent attachment of PEG to hydrophobic polymers provides a means by which PEG-based polymers can be integrated into membranes with anti-fouling character, yet maintain membrane integrity in an aqueous environment. PEG has been covalently attached to a variety of membrane materials, including cellulose,[6] poly(acrylonitrile),[7] poly(acrylonitrile-*co*-vinyl chloride),[8] polysulfone,[9,10] and polypropylene and cellulose

acetate.[11] Such PEGylated membranes typically show considerably different properties from the non-PEGylated versions, especially with regards to reduced fouling, and permeability/selectivity characteristics.[9,12-14] For polysulfone UF membranes, UV-induced reactions of PEG derivatives have been used for membrane surface modification.[9,10] In these examples, the ester linkage chosen to connect PEG to the underlying membrane is convenient synthetically, but ultimately not suitable for water purification applications due to the hydrolytic instability of esters. Composite membranes prepared from polymer blends, such as polyether sulfone/poly(vinylpyrrolidone),[15] and poly(vinylidene fluoride) (PVDF)/PVDF-PEGylated PMMA,[13,14] also provide examples of materials that exhibit reduced fouling relative to conventional commercial membranes.

4.2 Polycyclooctene-*graft*-PEG (PCOE-*g*-PEG) Copolymers as Coatings

Polyolefin-*graft*-PEG amphiphilic graft copolymers were prepared and used as anti-fouling coatings on commercial poly(vinylidene fluoride) ultrafiltration (PVDF-UF) membranes. These graft copolymers were fabricated into dense film membranes, and characterized in this form to evaluate their water uptake and ability to resist protein adsorption. Then, functionalized variants of the graft copolymers were prepared and applied as sub-micron thin-film coatings to PVDF-UF membrane supports. These composite membranes were subjected to oil-in-water emulsion feed streams under crossflow conditions at ~150 psi.

The presence of reactive functionality on the PEGylated polyolefin backbone proved critically important for the successful application of these coated composite UF membranes. Simple physical adsorption of the amphiphilic graft copolymer on the

underlying membrane proved ineffective as a coating method for these applications, due to delamination observed in the early stages of the crossflow experiment. However, cross-linking of the graft copolymers following the coating step proved effective for stabilization of the coating during crossflow, and provided a mechanism by which membrane fouling from oil-in-water emulsions was reduced markedly relative to the uncoated membranes. The presence of phenyl azide functional groups on the graft copolymer, and the UV-induced reactivity of these groups, provided a stabilization of the graft copolymer coating on the underlying PVDF-UF membranes, and prevented membrane fouling over time.

4.2.1 Synthesis of Amphiphilic PCOE-*g*-PEG Copolymers

Amphiphilic graft copolymers containing polycyclooctene backbones, and various length and density of PEG grafts, were prepared by ruthenium benzylidene-catalyzed ring-opening metathesis polymerization (ROMP) of cyclooctene with PEG-functional cyclooctene macromonomers as described in Chapter 2. Graft copolymers **53** – **57**, with both 1100 g/mol and 2200 g/mol PEG side chains, were prepared by polymerization of different ratios of cyclooctene (**17**) and PEGylated macromonomers **8** and **9**. These macromonomers were prepared by the 5-hydroxycyclooctene-initiated anionic polymerization of ethylene oxide (Scheme 2.3). This macromonomer synthesis enables the integration of PEG into the copolymer structure by ROMP, obviating the need for post-polymerization grafting chemistry. Moreover, this approach connects the PEG grafts to the polymer backbone by ether bonds, which carries the advantage of hydrolytic and chemical stability that is needed in long-term aqueous-based membrane applications.

As shown in Scheme 4.1, graft copolymers **53 - 57** were prepared by ROMP of the appropriate monomers/macromonomers in dichloromethane, using Grubbs' Generation II catalyst (catalyst **II**),[16] with a 250:1 monomer-to-catalyst ratio, and 1-hexene as the chain transfer agent (100:1 monomer-to-chain transfer agent ratio). The polymerization was terminated by addition of ethyl vinyl ether, and the polymer was isolated as a powder following precipitation into cold hexane containing 1 wt % of 2,6-di-*tert*-butyl-*p*-cresol (BHT). Gel permeation chromatography in $CHCl_3$ (against linear polystyrene standards) was used to estimate the molecular weights and polydispersities of the graft copolymers, as presented in Table 4.1. As expected for polymers prepared by ROMP using a monofunctional chain-transfer agent, the polydispersity of these samples was estimated by GPC to be in the range of ~ 2.0. Importantly, the copolymers obtained by this process, as characterized by NMR spectroscopy, show comonomer incorporation into the graft copolymer structure in accord with the feed ratio employed.

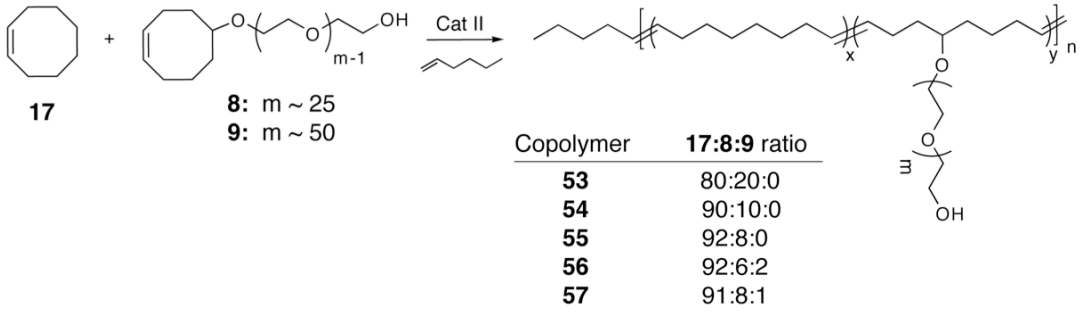

Scheme 4.1 Synthesis of PCOE-*g*-PEG with varying PEG length and graft density by ROMP of macromonomers 8 and 9

Table 4.1 Characteristics of PCOE-*g*-PEG copolymers 53 - 57

Copolymer[a]	Molar Ratio 17:8:9	PEG wt %	M_n (Da, GPC)	PDI	Water Uptake (wt %)
53	80:20:0	73	42,800	1.9	220 - 240
54	90:10:0	55	34,400	2.0	60 - 70
55	92:8:0	49	15,800	1.6	50 - 60
56	92:6:2	53	22,700	1.8	45 - 50
57	91:8:1	54	27,800	2.1	40 - 45

[a] [M]=2.0 mol/L, [M]/[Cat] = 500, [M]/[1-Hexene] = 100, 40 °C in CH_2Cl_2. [b] GPC in $CHCl_3$ versus polystyrene standards.

Phenyl azide-functionalized cyclooctene **38** was prepared as previously shown in Scheme 3.5, and used in ROMP copolymerizations with cyclooctene and PEG-functional macromonomer **10** (PEG MW 4,400 g/mol) in order to integrate this desirable reactive functionality into the graft copolymer structure. Monomer **38** was integrated into PCOE-*g*-PEG copolymers by metathesis copolymerization using Grubbs' Generation III catalyst (catalyst **III**)[17] to give graft copolymer **58** as shown in Scheme 4.2. For the membranes prepared in this work, graft copolymer **58** was prepared using 20 mol % cyclooctene azide **38**, 60 mol % cyclooctene (**17**), and 20 mol % PEG 4400 macromonomer **10**. This copolymer composition of amphiphilic graft copolymer **12** proved convenient for the PVDF-UF coating experiments for its solubility in ethanol, a suitable solvent for solution-based coating of PVDF-UF membranes (and in principle other commercial membranes), and also provided sufficient aryl azide functionality for effective cross-linking of the polymer coating. Typical preparations of graft copolymer **58** gave materials that by GPC in THF appeared as a single Gaussian peak; polymer with number-average molecular weights of ~35,000 g/mol, and PDI values of ~1.7, were obtained. ^{1}H NMR spectroscopy performed on $CDCl_3$ solutions of **58** showed the expected backbone olefin resonances at ~ δ 5.4 ppm and no signals for residual cyclic olefin monomers (~ δ 5.7 ppm). Aromatic resonances from the phenyl azide group were observed at δ 7.04 and δ 8.00 ppm, and integrated against protons of the polymer backbone to confirm the expected mole percent incorporation. FTIR spectroscopy of **58** showed a diagnostic azide stretch at ~2100 cm^{-1}. This synthetic strategy connects the reactive azide functionality to the polymer backbone through an amide bond which, like the ether connectivity of the PEG chains, is stable hydrolytically and thus well-suited for aqueous-

based membrane applications. We also prepared several combinations of polymers of type **58**, by fixing macromonomer **10** at 20 mol %, and varying **38** from 5-15 mol %, and **17** from 65-75 mol %. However, solubility proved problematic in these cases, as ethanol no longer dissolved the polymer, and good solvents such as chloroform and toluene swell or otherwise damage many underlying membrane supports. Thus, the composite membrane experiments described herein were performed with polymer **58** prepared with 20 mol % cyclooctene azide **38**, 60 mol % cyclooctene (**17**), and 20 mol % PEG 4400 macromonomer **10**.

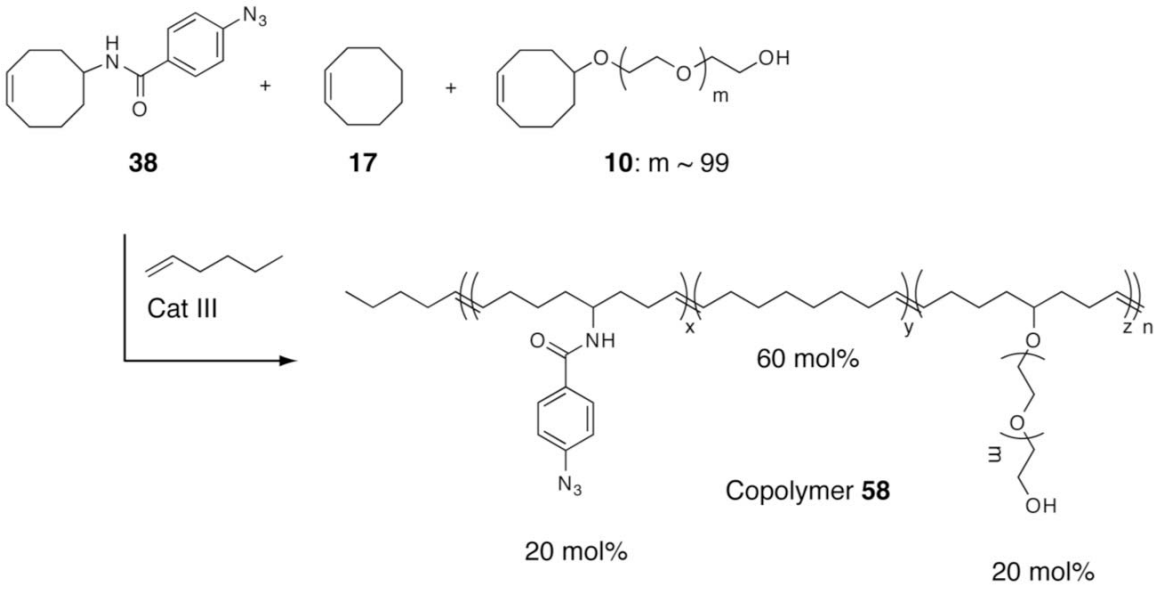

Scheme 4.2 Preparation of photo-reactive PCOE-*g*-PEG copolymer 58 by ROMP of phenyl azide-functional cyclooctene 38

4.2.2 Polycyclooctene-*graft*-PEG Copolymers: Membrane Preparation and Characterization

Before applying polyolefin-*graft*-PEG copolymers as coatings to PVDF-UF membranes, dense films of the copolymers were prepared and characterized for their pure water uptake and pure water flux under dead-end flow conditions. Such characterization is important for determining coating compositions that possess sufficient hydrophilicity

for water purification applications. Dense film membranes of PCOE-*g*-PEG copolymers **53** - **57** were prepared by Dr. Ravindra Revanur of the Emrick group by casting films from 20 wt % toluene solutions of the copolymers onto glass plates, then drawing the films to the desired thicknesses using a Gardco film applicator. Residual solvent was removed from the films by allowing them to stand at room temperature, then by their placement in a vacuum oven at reduced pressure (20 ºC, 12 hrs). For the preparation of cross-linked polymer films, ring-opening cross-metathesis using a *bis*-cyclooctene cross-linker was employed.[18] For these studies, *bis*-cyclooctene **60** with a tetraethylene glycol linker connected via hydrolytically-stable ether linkages was prepared by base-catalyzed, S_N2 chemistry with 5-hydroxycyclooctene (**1**) and tetraethylene glycol dimesylate (**59**) in DMF, as shown in Scheme 4.3. Films were then prepared from a toluene solution containing ~20 wt % of the graft copolymer and ~7 wt % of *bis*-cyclooctene **60**, to which was added a toluene solution of catalyst **II** (~3 mg) under constant agitation. As cross-linking occurs quickly using this method, the polymer/cross-linker/catalyst mixture was cast immediately on a glass slide to for the membrane as a cross-linked dense film of ~50 mm thickness. This cross-linking imparted the dense films with far more robust properties than obtained when attempting to prepare films without cross-linking. Moreover, the degree of cross-linking provides a means by which water uptake can be controlled. As shown in Table 4.1, PCOE-*g*-PEG membranes could be prepared with variable hydrophilicity, as indicated by the water uptake values. In copolymers containing lower PEG-grafting density (*i.e.,* from 1-8 mol % PEG 1,100 g/mol and/or PEG 2,200 g/mol), water uptake values in the 40-70% range were observed. Steady state water uptake values were obtained by dividing the difference in weight of the wet

(soaked in water) and dry membranes by that of the dry membrane. These membranes with lower PEG weight percentages qualitatively exhibited appreciable mechanical properties, such that they could be removed from the glass plate onto which they were cast, and handled without tearing.

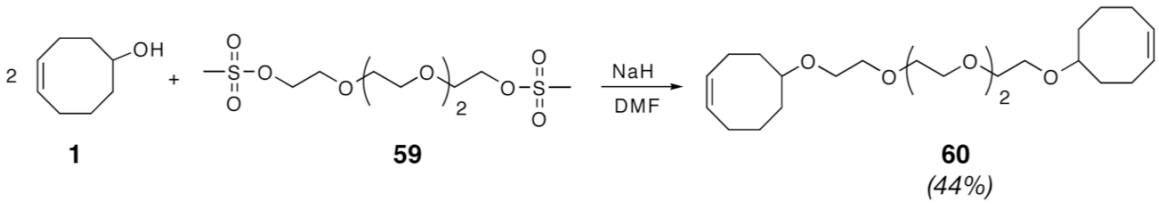

1 **59** **60** *(44%)*

Scheme 4.3 Preparation of hydrolytically-stable, *bis*-cyclooctene cross-linker 60

PCOE-*g*-PEG copolymer membranes with higher PEG densities, for example 20 mol % of PEG 1,100 g/mol, possessed very high water uptake values (200% or greater). However, copolymer films with such high PEG content were not mechanically robust, requiring cross-linking and/or an underlying substrate for effective application to water purification membranes. Increasing PEG density in the PCOE-*g*-PEG copolymer dense films was seen, as expected, to result in enhanced pure water flux, using an Amicon stirred cell in a dead-end flow setup. As shown in Table 4.1, films of polymers **54** and **57**, having similar weight percent PEG, were seen to have appreciable differences in water sorption and flux values. This may, however, not be an intrinsic property of the polymer composition, but rather due to variation in cross-linking efficiency from sample-to-sample. Nonetheless, it does appear that the integration of PEG 2,200 g/mol into the copolymer structures has a positive effect on both water sorption and flux.

Table 4.2 shows the effect of cross-linker concentration on both water sorption and permeance values. Membranes prepared from polymer **57** in the absence of cross-linking exhibit high water sorption and flux values. As seen in the table, water sorption

and flux drops to about 50% of the initial value with about 2 wt % cross-linker. This control over sorption and flux continues to about 7 wt % cross-linker, at which point a lower limit appears at about one-third the initial level. Additional experiments with these dense films were conducted to analyze the effect of cross-linker weight percent on water flux values obtained at various feed pressures in a dead-end flow setup. This is seen in Figure 4.1. From the dense membrane without any cross-linker, a measurable permeate was collected at a feed pressure of only 10 psi. The effect of percent cross-linker on feed pressure needed to obtain constant water flux shows that an appreciable level of control over flux can be obtained in these films, and that even upon cross-linking, sufficient water flux is observed such that application of these materials as coatings on commercial membranes is feasible.

Table 4.2 Effect of *bis*-cyclooctene cross-linker 60 concentration on percent of water sorption and water permeance through the membranes prepared from polymer 57; membrane thickness ~ 50 µm

Crosslinker (wt%)	Water Sorption (wt%)	Avg. Water Permeance (LMH)
0	108	11.0
2	65	6.2
5	50	3.7
7	42	3.0
12	40	2.8

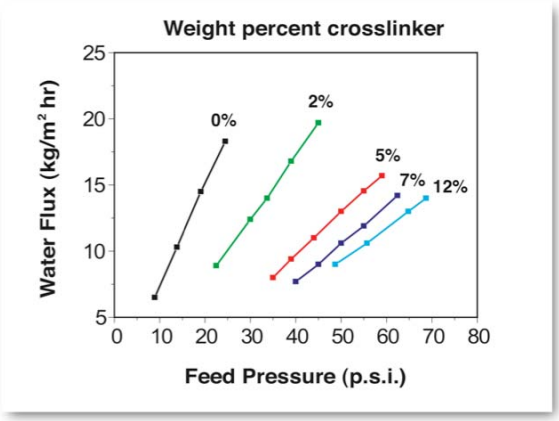

Figure 4.1 Effect of *bis*-cyclooctene cross-linker 60 concentration on water flux through the membranes prepared from copolymer 57

Protein adsorption on PCOE-*g*-PEG copolymer films were tested by immersion in bovine serum albumin (BSA) solutions and quantified using the Bradford titration method.[19] In these experiments, very low levels (~ 1 μg/cm^2) of protein adsorption were observed. In fact, the appreciable anti-fouling properties of these graft copolymer films made protein adsorption difficult to quantify by this method. This contrasts the situation for many commercial membranes, such as polysulfone and polyamide membranes, in which protein adsorption is appreciable and readily quantified. Fluorescence confocal laser scanning microscopy provides an alternative visual method to evaluate fouling[20] on both commercial and novel synthetic membranes. Figure 4.2 shows fluorescence confocal microscope images of several membranes following exposure to aqueous solutions of fluorescent BSA. These membranes were cut as ~2 cm^2 sections from polyamide reverse osmosis (RO) thin film composite membranes, cellulose acetate asymmetric RO membranes, polysulfone UF membranes, and PCOE-*g*-PEG dense films. The membranes were immersed in a phosphate buffered saline (PBS, pH 7.4) solution of fluorescein-conjugated BSA (0.02 mg/mL) for 24 hours, followed by rinsing with PBS. As shown in Figure 4.2, confocal fluorescence images of these membranes (excitation at 488 nm) reveal striking differences in protein adsorption on the commercial membranes relative to the PEGylated graft copolymer film. The PCOE-*g*-PEG membrane sample used these experiments contained 54 wt % PEG (polymer **57**), a modest level of PEGylation, yet clearly sufficient for resisting fouling. This data shows that the PEGylated graft copolymers are well-suited to prevent protein fouling, which is expected to translate to resisting fouling by oil particles in oil-in-water emulsions.

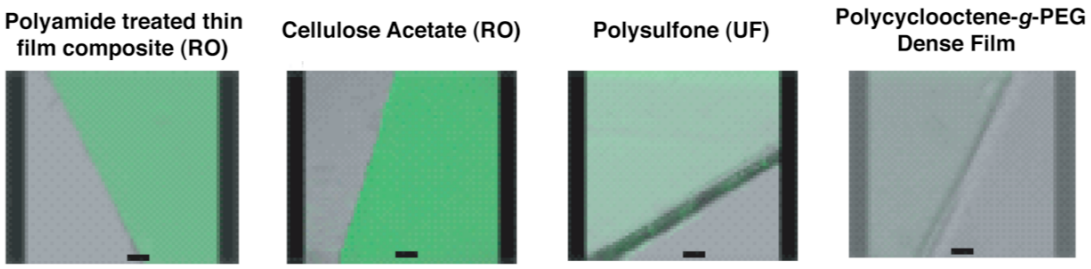

Figure 4.2 Fluorescence confocal microscopy images of protein adsorption (fluorescein-BSA in aqueous buffer solution at pH 7.4) on a dense film of PCOE-*g*-PEG (far right, copolymer 57) and on commercial samples of treated polyamide, cellulose acetate, and polysulfone; the black bar in each image is 50 microns

4.2.3 Phenyl Azide-functionalized Graft Copolymer Coatings on PVDF-UF Membranes

Initial studies targeted the preparation of PCOE-*g*-PEG coated PVDF-UF membranes, followed by evaluation of the coated membranes in a crossflow unit at 150 psi. However, in the early stages of the crossflow experiments, delamination of the graft copolymer coating from the membrane support was observed, due to the substantial hydrophilicity and swelling of the coating that overcomes its adhesion to the underlying PVDF support. Moreover, we found that cross-linking strategies using *bis*-cyclooctene **60** described above were not easily applied to cases involving underlying support membranes, due to the presence of defects within the coating that could not be avoided. Thus, a different method was sought to generate the desired composite membranes, in which the coating and cross-linking steps were conducted separately, by embedding UV-reactive phenyl azide groups into the copolymer structure. For this, graft copolymer **58** containing phenyl azide pendent groups was used, anticipating a nitrene-induced cross-linking upon exposure of the polymer-coated membrane to UV-irradiation.

The PVDF-UF membranes used in this study were purchased from Sterlitech, Inc. For the coating procedure, an ethanol solution of graft copolymer **58** (~ 50 mg/mL, M_n ~

35,000 Da, PDI 1.7) was applied by Dr. Ravindra Revanur by spin coating onto the membrane support to give a sub-micron graft copolymer coating. The coated membrane was then placed in a UV-light source (UVP, Inc.) and irradiated at 302 nm for 6 minutes. UV-irradiation converts the phenyl azide (Ph-N_3) groups into nitrenes (Ph-N:) by loss of nitrogen gas. The nitrenes generated in this process are highly reactive[21,22] and can insert into olefins in the polymer backbone to give aziridines, as well as C-H bonds in the polymer backbone and grafts, and possibly in the underlying PVDF-UF support, to give amines. This UV-induced cross-linking proved successful for stabilizing the graft copolymer coating on the PVDF-UF membrane surface, and eliminated problems associated with rapid delamination of the coating during crossflow. ATR-FTIR performed on the composite membrane following irradiation was used to confirm the complete disappearance of diagnostic azide stretch at ~ 2100 cm^{-1} in the graft copolymer structure. Whether any of the nitrenes generated during irradiation insert into the underlying substrate is a characterization challenge under investigation at this time.

4.3 Crossflow Experiments on Graft Copolymer-coated PVDF-UF Composite Membranes

Crossflow experiments were performed in Professor Benny Freeman's laboratory (University of Texas-Austin) on both uncoated and graft copolymer-coated PVDF-UF membranes were conducted at a feed pressure of 150 psi, and a crossflow velocity of 0.5 GPM. The feed solution consisted of a 1500 ppm oil-in-water emulsion (9:1 ratio of soybean oil: DC 193 surfactant obtained from The Dow Chemical Company), prepared by mixing the oil, water, and surfactant in a blender at 3000 rpm for ~3 minutes to give a homogeneous emulsion. Periodic evaluation of the oil concentration was carried out

using a total organic compounds (TOC) analyzer (Shimadzu TOC-5050A). It was immediately seen that the delamination problem observed for graft copolymers **53 - 57** during the crossflow operation did not occur in the irradiated coated membranes prepared from phenyl azide-functionalized graft copolymer **58**. The polymer coating remained intact despite the very high (>80 wt %) weight percent of PEG in the polymer coating. Control experiments confirmed the importance of phenyl azide incorporation. For example, a PVDF-UF membrane was coated with a graft copolymer containing an 4:1 molar ratio of cyclooctene and PEG-4400 cyclooctene macromonomer **10**, followed by an irradiation step identical to that used for the azide-containing coating. Crossflow experiments with oil-water emulsion feed solutions carried out with these uncross-linked copolymer coated membranes led to rapid membrane fouling, and thus minimal positive influence of the coating. This is shown in Figure 4.3, in which the uncoated (dashed line) and coated (solid line) PVDF supports follow the same membrane fouling trend reflected in decreased flux as a function of time. Water contact angle measurements taken on the membrane surface after crossflow (~ 60 - 65^{o}) were quite close to those of the uncoated membrane (64 - 67^{o}), confirming the loss of graft copolymer from the surface, and much higher than membranes with stable cross-linked graft copolymer coatings (shown in Figure 4.3). Thus, subsequent experiments exclusively used the azide-functionalized amphiphilic graft polymer as the coating material.

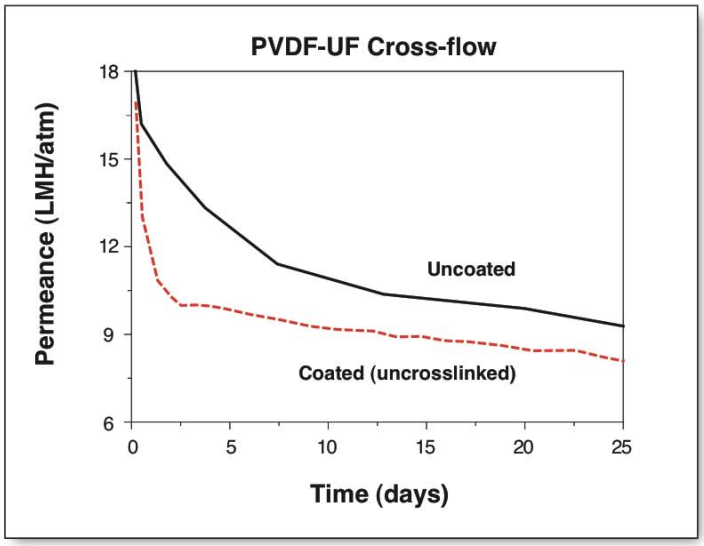

Figure 4.3 Crossflow experimental results with uncoated PVDF-UF membrane (black line) and graft copolymer 58 coated membrane (without phenyl azide, control)

Crossflow experiments were then performed to compare the uncoated PVDF-UF membranes to those coated with a cross-linked film of graft copolymer **58**, again using oil-in-water emulsions at 150 psi feed pressure and 0.5 GPM crossflow velocity. The ability of the graft copolymer coated membranes to resist fouling relative to the uncoated PVDF-UF membranes is seen in Figure 4.4. In Figure 4.4A, four different graft copolymer coated membranes are represented by the four dashed lines, in which each coating is of slightly different thickness. The performance of these coated membranes is compared to an uncoated PVDF-UF membrane over a period of three days. While the composite membranes exhibit an expected drop in initial flux as a consequence of the coating, all of the coated membranes maintain a relatively stable flux from about two hours through the end of the plotted timeframe. On the other hand, the uncoated PVDF

membrane shows a considerable decline in flux during the same period, from ~ 14 LMH/atm to ~ 6 - 7 LMH/atm.

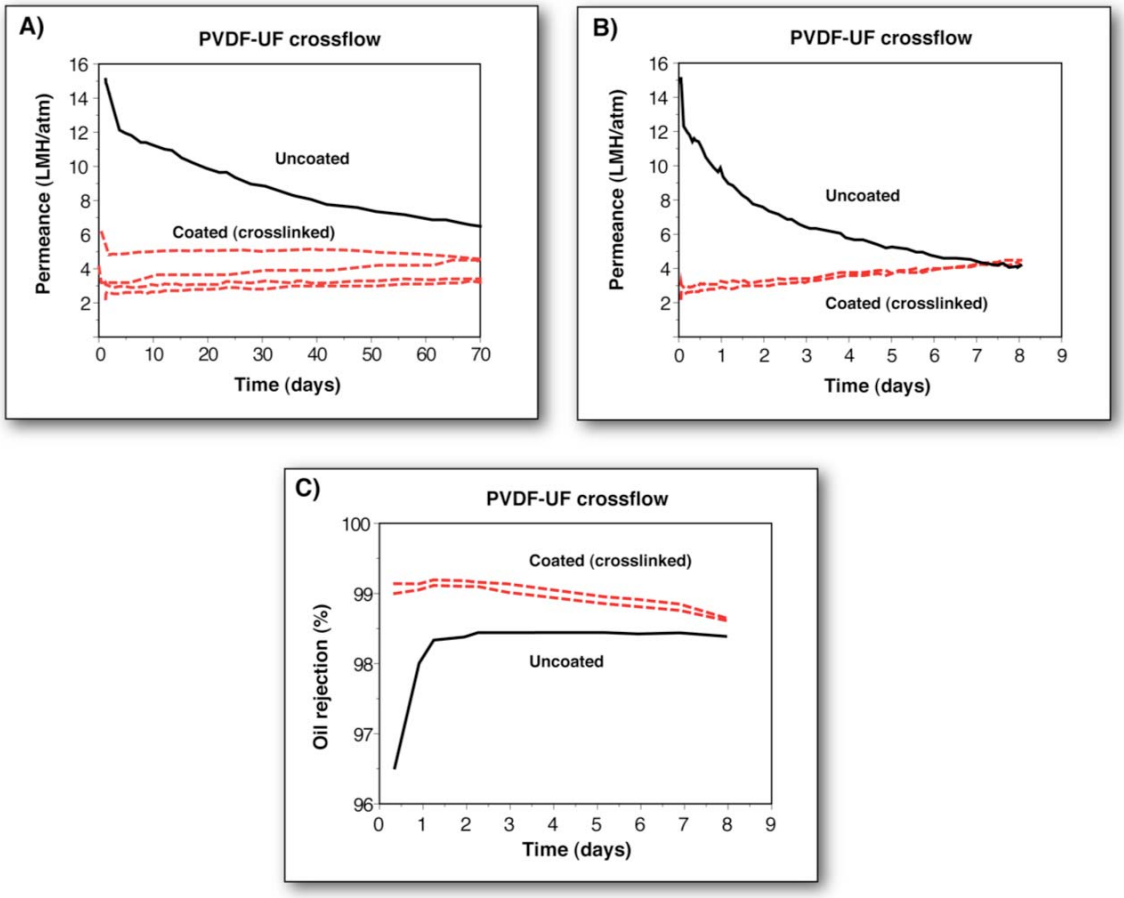

Figure 4.4 Crossflow experimental results with coated and uncoated PVDF-UF membranes; A) flux values obtained using membranes coated with a cross-linked coating of graft copolymer 58, B) continuation of crossflow experiment to eight days, C) oil rejection values

When this coated *vs.* uncoated membrane experiment is extended to longer time periods, as shown in Figure 4.4B, a cross-over is seen, such that water flux through the coated membrane equals and then exceeds that of the uncoated membrane. Ultimately, the uncoated membrane is expected to approach zero flux at some time period, due to complete fouling. This result carries considerable significance given the long usage

lifetime desired for membranes of this type, and the stability against oil droplet fouling provided by the graft copolymer coating. Interestingly, in some cases the observed flux of the graft copolymer coated membrane increases slightly over the measured period. This may be due to some loss of the graft copolymer in areas of the coated membrane where cross-linking was inefficient, either on the membrane surface, or perhaps more likely in areas where the polymer had penetrated the membrane pores. No matter the cause of this increased flux, it does not lead to rapid fouling.

Finally, as shown in Figure 4.4C, the graft copolymer coating was seen to improve the rejection of oil droplets, as determined by permeate analysis. The uncoated PVDF-UF membranes provide increasing oil droplet rejection as a consequence of fouling, while the graft copolymer coated membranes maintained 99-98.5% rejection during the course of the experiment.

Figure 4.5 shows SEM images of the top surface (Figure 4.5A) of both the uncoated and coated (Figure 4.5B) PVDF-UF membranes used in this study. SEM shows convincingly that the graft copolymer coating completely covers the membrane pore structure. Cross-sectional SEM images of the coated membrane confirm that pore penetration of the graft copolymer into the membrane does occur (Figures 4.5D and 4.5E). While the presence of the graft copolymer on the membrane surface, and in the inner-pore structure, is expected to lower the initial water flux, the substantial hydrophilicity of the graft copolymer used in the coating process leads to only a moderate initial flux decline that can eventually be overcome by the reduction in fouling over time relative to the uncoated membranes. An ideal coating process would minimize such pore penetration; efforts along these lines are in progress. Importantly, the graft copolymer

coating remains intact on the support throughout the crossflow experiments. This is confirmed in the SEM image of Figure 4.5C, taken on the composite membrane following removal from the crossflow unit. In addition, it seems that a smoother membrane surface in the coated composite is present following crossflow experiments. This may be associated with some loss of graft copolymer coating during crossflow operation, but is more likely a result of reorganization of the graft polymer during and after the crossflow experiment. Nevertheless, after crossflow operation, the water contact angle of the coated composite membrane (44 - 46^{o}) remains identical to that before the crossflow, and is considerably lower than that of the uncoated membrane (64 - 67^{o}). Finally, while fouling prevention can be attributed to the PEGylation, it should also be noted that the smoother surface of the coated membranes might augment the effect.

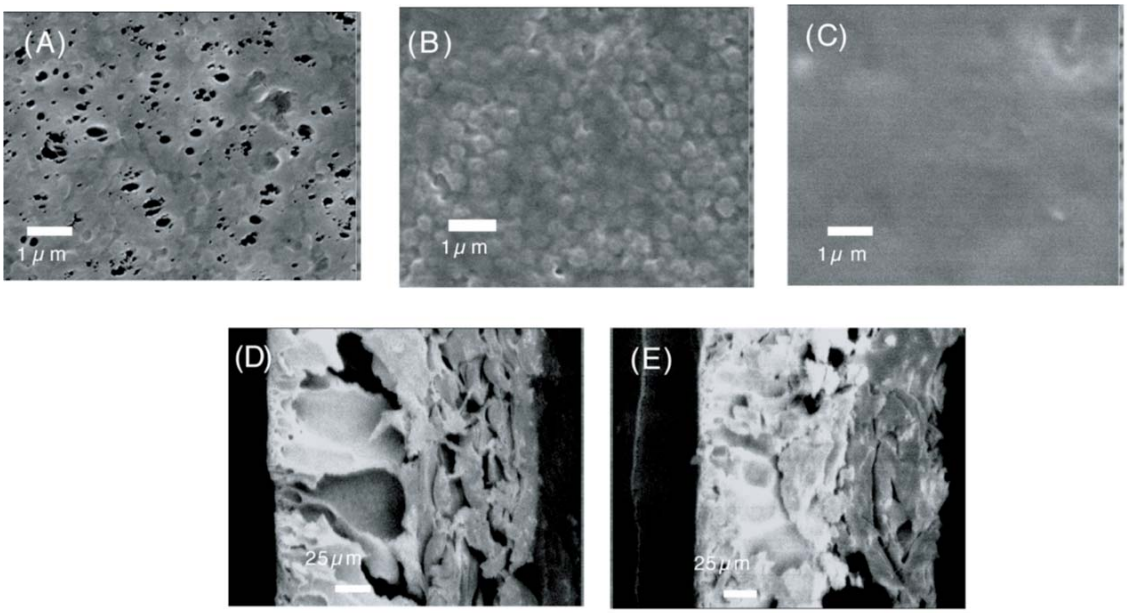

Figure 4.5 SEM images of PVDF-UF membranes, A) top view before coating, B) top view after coating and UV-irradiation with graft copolymer 58, C) top view after crossflow experiments, D) cross-section before coating with 58; E) cross-section after coating

4.4 Summary and Outlook

We have synthesized and applied polycyclooctene-*graft*-PEG copolymers as anti-fouling coatings for commercial PVDF-UF membranes. Problems associated with delamination of the graft copolymer from the underlying membrane were overcome using phenyl azide functionalized polymers for UV-irradiation and cross-linking on the PVDF-UF support. Crossflow experiments conducted with oil-in-water emulsions feed sources confirmed that the graft copolymer coating prevents fouling, and leads to an eventual crossover in flux with the uncoated commercial membranes. Future studies will include an optimization of both the graft copolymer as well as the coating process, taking advantage of the tunable nature of the graft copolymer itself, as well as the coating process. Moreover, the ability of these copolymer coatings to prevent fouling in other membranes, including those used in reverse osmosis for desalination will be studied.

4.5 References

(1) Belfort, G.; Davis, R. H.; Zydney, A. L. *J. Membrane Sci.* **1994**, *96*, 1-58.
(2) Zeman, L. J. Z., A. L. *Microfiltration and Ultrafiltration Principles and Applications*; Marcel Dekker: New York, 1996.
(3) Scott, K. *Handbook of Industrial Membranes*; 2nd ed.; Elsevier: Oxford, 2003.
(4) Lee, J. H.; Lee, H. B.; Andrade, J. D. *Prog. Polym. Sci.* **1995**, *20*, 1043-1079.
(5) Szleifer, I. *Curr. Opin. Solid St. M.* **1997**, *2*, 337-344.
(6) Akizawa, T. K., K.; Koshikawa, S.; Ikada, Y.; Kishida, A.; Yamashita, M.; Imamura, K. *T. Am. Soc. Art. Int. Org.* **1989**, *35*, 333.
(7) Ulbricht, M.; Matuschewski, H.; Oechel, A.; Hicke, H. G. *J. Membrane Sci.* **1996**, *115*, 31-47.
(8) Shoichet, M. S.; Winn, S. R.; Athavale, S.; Harris, J. M.; Gentile, F. T. *Biotechnol. Bioeng.* **1994**, *43*, 563-572.
(9) Harmer, M. A. *Langmuir* **1991**, *7*, 2010-2012.
(10) Thom, V.; Jankova, K.; Ulbricht, M.; Kops, J.; Jonsson, G. *Macromol. Chem. Physic.* **1998**, *199*, 2723-2729.
(11) Ma, H. M.; Davis, R. H.; Bowman, C. N. *Macromolecules* **2000**, *33*, 331-335.

(12) Iwata, H.; Ivanchenko, M. I.; Miyaki, Y. *J. Appl. Polym. Sci.* **1994**, *54*, 125-128.
(13) Hester, J. F.; Banerjee, P.; Won, Y. Y.; Akthakul, A.; Acar, M. H.; Mayes, A. M. *Macromolecules* **2002**, *35*, 7652-7661.
(14) Hester, J. F.; Mayes, A. M. *J. Membrane Sci.* **2002**, *202*, 119-135.
(15) Boom, R. M.; Wienk, I. M.; Vandenboomgaard, T.; Smolders, C. A. *J. Membrane Sci.* **1992**, *73*, 277-292.
(16) Scholl, M.; Ding, S.; Lee, C. W.; Grubbs, R. H. *Org. Lett.* **1999**, *1*, 953-956.
(17) Love, J. A.; Morgan, J. P.; Trnka, T. M.; Grubbs, R. H. *Angew. Chem. Int. Edit.* **2002**, *41*, 4035-4037.
(18) Breitenkamp, K.; Emrick, T. *J. Am. Chem. Soc.* **2003**, *125*, 12070-12071.
(19) Bradford, M. M. *Anal. Biochem.* **1976**, *72*, 248-254.
(20) Ferrando, M.; Rozek, A.; Zator, M.; Lopez, F.; Guell, C. *J. Membrane Sci.* **2005**, *250*, 283-293.
(21) Brezlow, D. S. In *Azides and Nitrenes - Reactivity and Utility*; Scriven, E. V. S., Ed.; Academic Press: Orlando, FL, 1984, 491-517.
(22) Brunner, J. *Annu. Rev. Biochem.* **1993**, *62*, 483-514.

CHAPTER 5

SYNTHESIS AND APPLICATION OF AN AMPHIPHILIC RUTHENIUM BENZYLIDENE CATALYST WITH PEG-SUBSTITUTED LIGANDS

5.1 Impact of Ligand Environment on the Properties of Ruthenium Benzylidene Metathesis Catalysts

The advent of well-defined ruthenium benzylidene catalysts has dramatically expanded the scope of metathesis reactions and polymerizations that can be performed in the presence of polar organic functionality and protic solvents. In general, catalyst properties are largely governed by the ligand environment surrounding the ruthenium center, which allows for tailoring of catalyst activity and solubility. For example, Grubbs' second generation ruthenium benzylidene catalyst **II** (Figure 5.1) utilizes an N-heterocyclic carbene ligand (4,5-dihydroimidazolylidene) that provides much greater metathesis activity than the first generation *bis*-tricyclohexylphosphine substituted ruthenium benzylidene catalyst **I**.[1] More recently, ruthenium catalysts have been prepared with pyridine, and derivatives of pyridine, as ligands in place of tricyclohexylphosphine.[2,3] For example, the 3-bromopyridine substituted ruthenium catalyst **III** has been shown to polymerize cyclic olefins by ring-opening metathesis polymerization (ROMP) at unprecedented rates, with very fast initiation that leads to characteristics of "living" polymerization when used in conjunction with certain norbornene and oxanorbornene monomers.[4] Efforts to improve the activity of ruthenium metathesis catalysts have been undertaken by a number of research groups over the past few decades.[5] However, improvement in the solubility and metathesis activity of ruthenium catalysts in polar solvents, particularly in water, is limited to only a few

reports. In light of this fact, nearly all metathesis reactions and polymerizations reported to date have been performed in organic solvents.

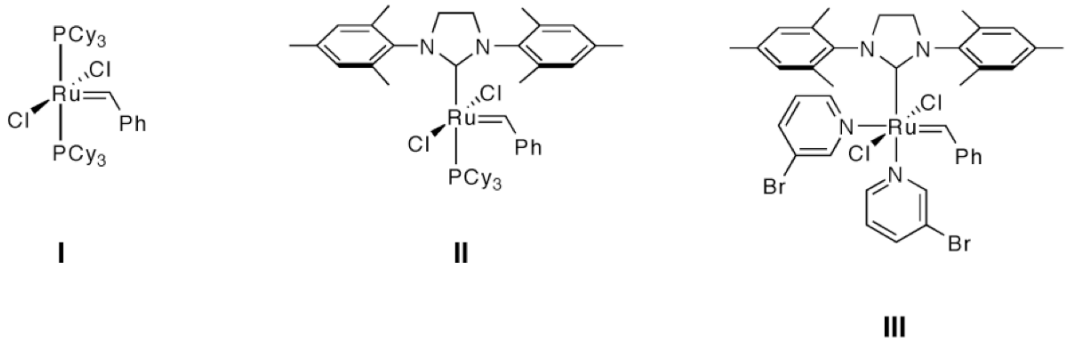

Figure 5.1 Chemical structures of Grubbs' Generation I, II, and III catalysts

5.2 Ring-Opening Metathesis Polymerization in Protic Solvents

ROMP in protic solvents and aqueous environments has been accomplished previously with non-benzylidene catalysts, such as ruthenium salts,[6] and more recently with ruthenium benzylidene catalysts containing tailored ligands, such as phosphines with ionic substituents in place of the more common tricyclohexylphosphine (Figure 5.2).[7-10] For example, catalysts **IV** and **V**, which bear cationically-functionalized phosphine ligands, are soluble and initiate ROMP in both methanol and water. However, the ruthenium alkylidene analogues of **IV** and **V** (*i.e.* propagating species) rapidly decompose in methanol and neutral water resulting in poor monomer conversion. In contrast, ROMP of norbornene and oxanorbornene derivatives, initiated by catalysts **IV** and **V**, was shown to be rapid and possess characteristics of a "living" polymerization in acidic water (HCl or DCl, from 0.3 to 1.0 equiv. relative to **IV** and **V**). It was hypothesized that the addition of Brønstead acids to the aqueous polymerization media neutralized hydroxide ions, which were shown to rapidly decompose catalysts **IV** and **V**.

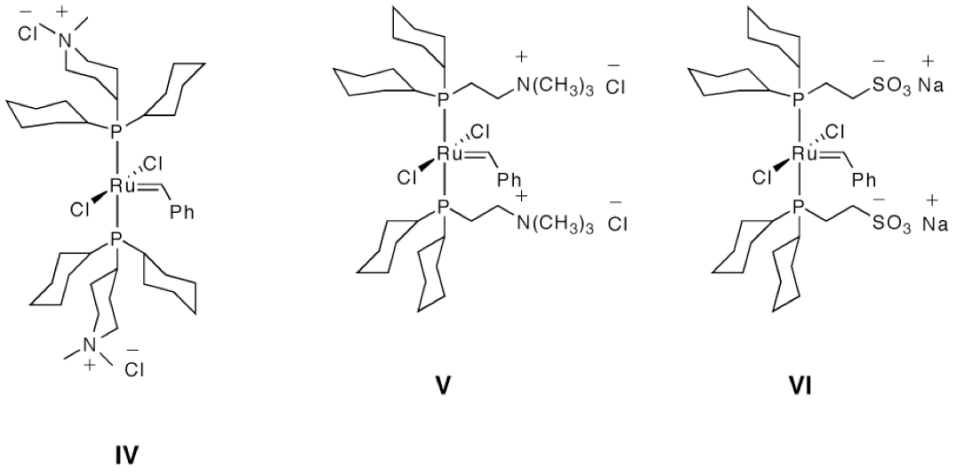

Figure 5.2 Examples of water-soluble ruthenium catalysts bearing ionic, phosphine ligands

This initial demonstration of metathesis activity using charged ruthenium benzylidene catalysts was an important step toward the synthesis of water-soluble polymers and substrates in purely aqueous media. However, several limitations of these catalysts have prompted new research. For example, catalysts **IV** - **VI** are soluble only in protic media and are therefore limited to polymerizations in water or methanol. A highly versatile metathesis catalyst would be soluble in aqueous and organic media and efficiently perform metathesis reactions in a variety of solvents. In addition, these catalysts lack the N-heterocyclic carbene (NHC) ligand which has been shown to dramatically improve the metathesis activity of ruthenium benzylidene catalysts.

The ruthenium benzylidene catalyst described in this chapter is made amphiphilic by incorporation of polyethylene glycol (PEG)-substituted pyridine ligands and effectively polymerizes cyclic olefins in both aqueous and organic media. In prior work by our group, PEGylated pyridine compounds were prepared for use as ligands to solubilize CdSe quantum dots in water.[11] Following reports on pyridine and 3-

bromopyridine substituted ruthenium benzylidene catalysts by Grubbs and coworkers,[2,3] and motivated by our interest in water-soluble polyolefins and interfacial chemistries,[12-14] these PEG-substituted pyridines were tested for their ability to solubilize Grubbs' second generation catalyst (catalyst **II**) by simple ligand exchange of the tricyclohexylphosphine ligands. This ligand exchange was found to provide access to a new metathesis catalyst that performs ROMP in both water and organic solvents. This work represents one the first reports of ROMP in a completely aqueous environment using the highly active NHC type ruthenium benzylidene catalyst. During the course of this project, PEGylated ruthenium catalysts **VII** and **VIII** (shown in Figure 5.3), which also possess the NHC ligand, were reported by Grubbs and coworkers.[15,16] PEGylation of these catalysts was accomplished through the synthesis of PEG-functionalized NHC ligands, and **VII** and **VIII** were observed to effectively perform ring-closing metathesis (RCM) and ROMP in both water and methanol. Attempts to perform similar metathesis reactions in organic media using **VII** and **VIII** were not reported. In contrast to catalysts **IV** – **VI**, catalyst **VIII**, a PEGylated analogue of Hoveyda-Grubbs catalyst, efficiently performs cross-metathesis, RCM, and ROMP in neutral water. Addition of HCl to aqueous metathesis reactions initiated by **VIII** did not improve catalytic activity. NMR spectroscopy of **VIII** in D_2O showed a lack of benzylidene resonances (δ 16.4 ppm in CD_2Cl_2) which was attributed the formation of micelles with the catalyst comprising the core and PEG (MW 2000 g/mol) forming the corona. No discussion was presented on how catalyst aggregation in water impacts metathesis activity.

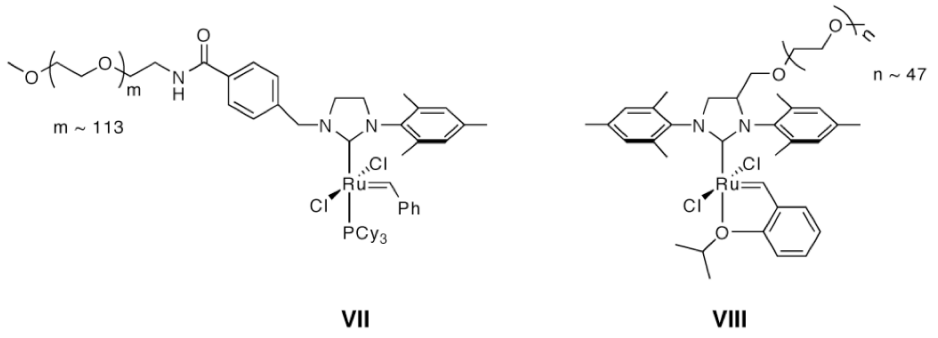

Figure 5.3 Chemical structures of PEGylated ruthenium catalysts prepared by Grubbs and coworkers

5.3 Synthesis of PEG-functional Pyridine Ligands and PEGylated Ruthenium Benzylidene Catalyst 63

The synthesis of PEG-substituted pyridines, such as *para*-substituted tetraethylene glycol **62**, was accomplished by Mitsunobu coupling of 4-hydroxypyridine (**61**) in the presence of excess tetraethylene glycol (TEG) (Scheme 5.1). The presence of the chain-end hydroxyl group of **62** is key, as this provides water solubility that is not observed in the methyl ether terminated TEG analogs. However, purification of **62** is difficult and the clean separation of **62** from excess TEG could not be achieved by column chromatography on silica or alumina. Similar polarities of the TEG and **62** give near identical behaviors on these separation media. Thus, purification of **62** was accomplished by removal of excess tetraethylene glycol by vacuum distillation followed by column chromatography on silica gel. This strategy proved effective for PEG-pyridines with up to four ethylene glycol repeat units. When PEGylated pyridine was made with hexa- or heptaethylene glycol, even distillation was unsuccessful in attempted purification of the ligand.

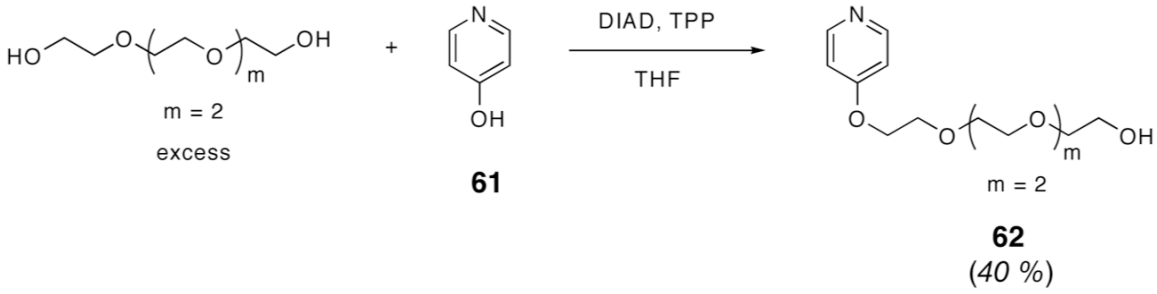

Scheme 5.1 Synthesis of PEG-substituted pyridine ligand 62 by Mitsunobu coupling of tetraethylene glycol and 4-hydroxypyridine (61)

Exchanging the tricyclohexylphosphine ligands of catalyst **II** for PEG-pyridine ligands was accomplished with a 10-fold excess of **62** (or related compounds with different ethylene glycol chain lengths) in minimal dichloromethane as shown in Scheme 5.2. Removal of dichloromethane *in vacuo* affords a mixture of **63** and **62** as a dark green oil. Dilution of this green oil in water causes precipitation of tricyclohexylphosphine, which is removed cleanly following centrifugation. Dark green homogeneous solutions of **63** and **62** can then be formed in many solvents, including water, methanol, toluene, and dichloromethane, all of which can be used for metathesis chemistry. Catalysts prepared in a similar fashion with 4-hydroxypyridine or PEG-pyridine ligands possessing one or more ethylene glycol repeats formed homogeneous solutions in methanol. PEG-pyridine ligands possessing 4 or more ethylene glycol repeat units formed homogeneous solutions in water. *meta*-Substituted PEG pyridine ligands have also been prepared and utilized in ligand exchange chemistry. These were found to require longer reaction time for successful ligand exchange with **II** but give comparable metathesis activity as **63**.

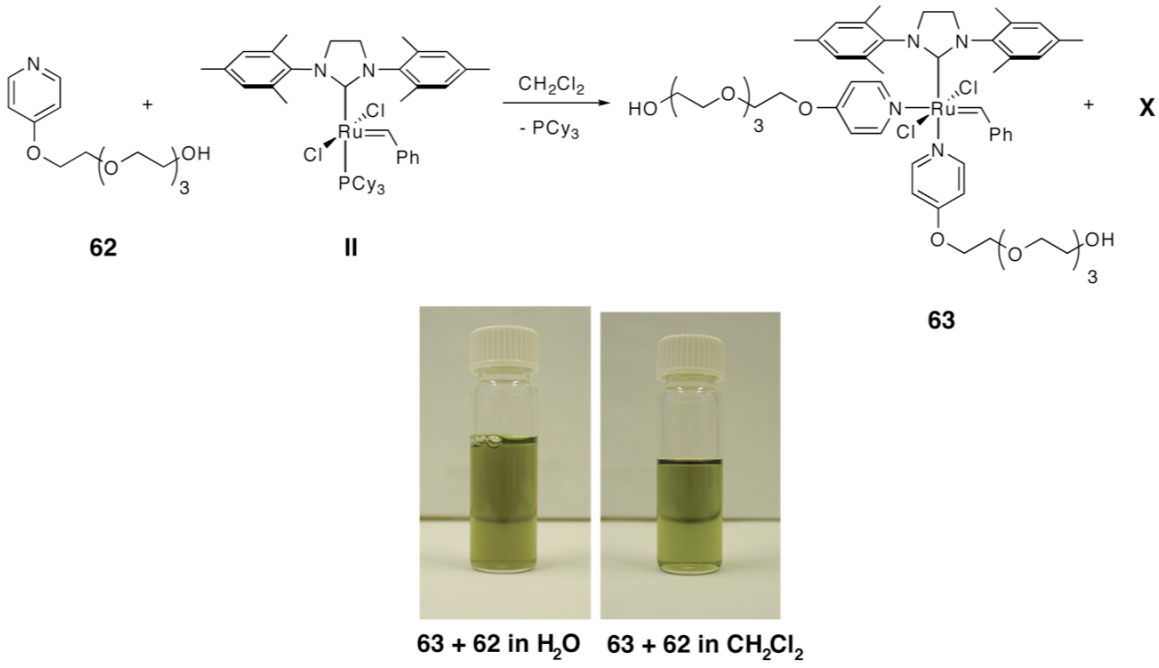

Scheme 5.2 Synthesis of amphiphilic ruthenium benzylidene catalyst 63 by ligand exchange of catalyst II with PEG-substituted pyridine 62

Nuclear magnetic resonance spectroscopy (^{1}H, ^{13}C, and ^{31}P) performed on the mixture of **63** and **62** in D_2O and $CDCl_3$ confirms the success of the ligand exchange. The ^{1}H NMR spectrum of the catalyst mixture taken in $CDCl_3$ shows resonances from δ 3.5-3.7 ppm, characteristic of the methylene protons of PEG. A singlet at δ 19.2 ppm corresponds to the benzylidene proton. As shown in Figure 5.4, this benzylidene proton is 0.11 ppm downfield from the benzylidene proton in the 3-bromopyridine substituted catalyst **III**, and 0.07 ppm downfield from the benzylidene proton of catalyst **II**. Unlike catalyst **III**, the PEG-pyridine substituted catalyst **63** described here is used in the presence of excess PEG-pyridine. Attempts to remove excess ligand using conventional flash chromatography resulted in catalyst decomposition of catalyst **63**, presumably due to the affinity of the PEG-pyridine ligands for silica gel. Thus, the graphical representation of catalyst **63**, with its two PEG-pyridine ligands coordinated to the

ruthenium center, is based on the known structure of catalyst **III**.[2] The lack of crystallinity of **63** prevents characterization by X-ray diffraction, and attempted mass spectrometric characterization was unsuccessful.

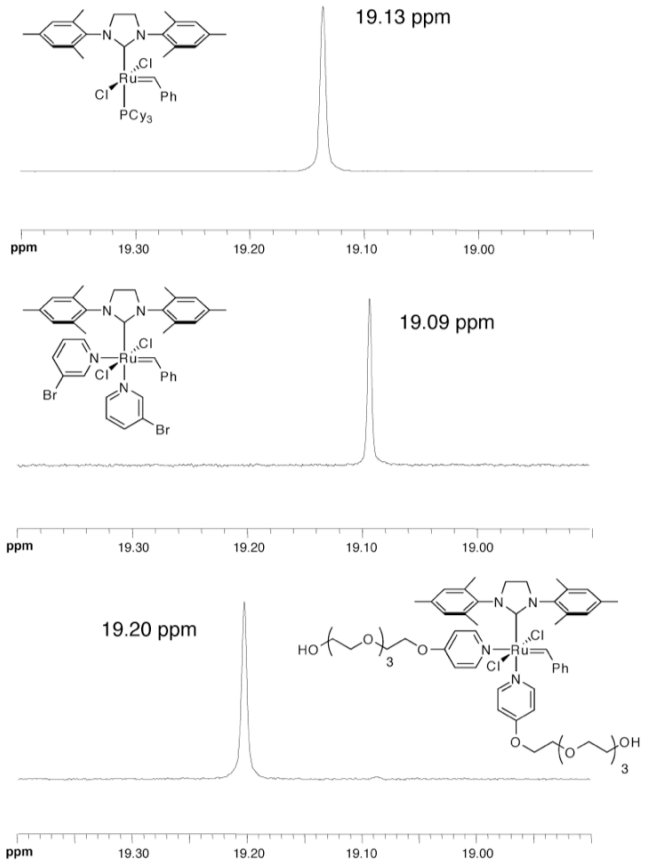

Figure 5.4 Comparison of benzylidene proton resonances for catalysts II, III, and 63 in $CDCl_3$

5.4 ROMP of Cyclic Olefins Initiated by 63

5.4.1 ROMP Initiated by Catalyst 63 in Organic Solvents

Catalyst **63** was tested for its ability to polymerize cyclic olefins in dichloromethane, and found to successfully polymerize cyclooctene and norbornene to full conversion at room temperature in seconds. The average molecular weights of the polymers produced could be controlled easily by adjustment of the monomer-to-catalyst

ratios. Figure 5.5 and Table 5.1 show GPC data for polymers **65 - 68** obtained from the polymerization of *exo*,*exo*-5,6-bis(methoxycarbonyl)-7-oxabicyclo[2.2.1] hept-2-ene (**64**) using catalyst **63** in dichloromethane at various monomer-to-catalyst ratios. In all ratios, polyolefins **65 - 68** were produced with low PDI values (<1.1) and good control over average molecular weight. Figure 5.5 shows a plot of molecular weight versus monomer-to-catalyst ratio, and a gel permeation chromatogram of polymer **67** prepared using a monomer-to-catalyst ratio of 200:1. The linear correlation of molecular weight and monomer-to-catalyst ratio, combined with the low PDI values of the resulting polymers, provide evidence for the "living" nature of this polymerization using this PEG-substituted ruthenium benzylidene catalyst. These results are in accord with those of Grubbs and coworkers on 3-bromopyridine substituted ruthenium catalysts, and contrast the polymerization of **63** with catalyst **II**, which produces polymers with PDI values greater than 1.5.

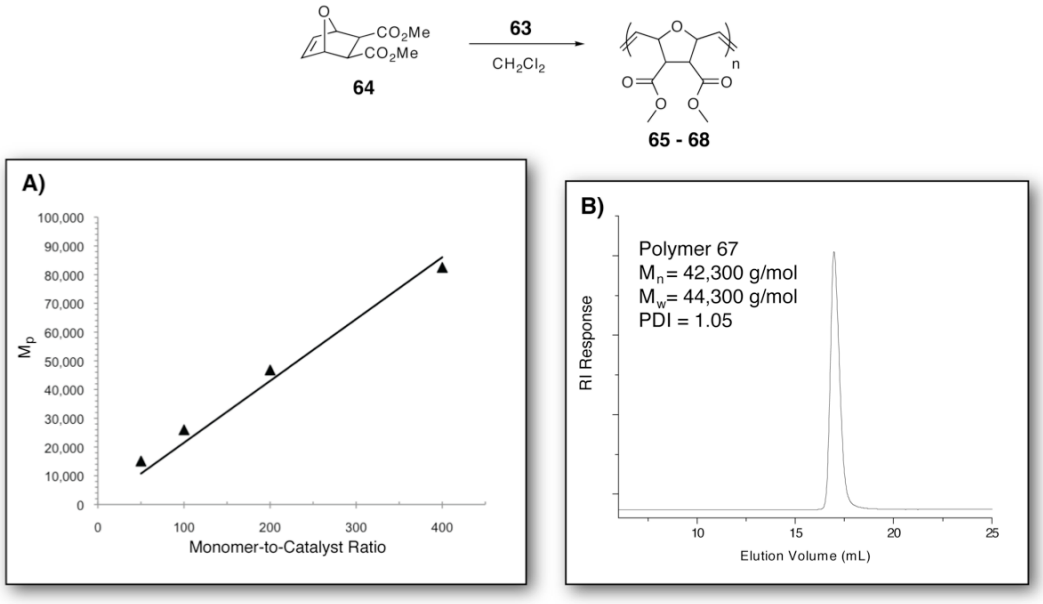

Figure 5.5 GPC analysis of polymers obtained by ROMP of 64 using catalyst 63 in DCM, A) plot of molecular weight versus monomer/catalyst ratio, B) GPC chromatogram of polymer 67

Table 5.1 Characteristics of polymers 65 – 68 prepared by ROMP of 64 using catalyst 63 in DCM

Polymer[a]	[M]/[Cat 63[b]]	M_p[c] (g/mol)	M_n[c] (g/mol)	M_w[c] (g/mol)	PDI
65	50	15,100	13,900	14,600	1.05
66	100	26,000	24,400	25,300	1.04
67	200	46,800	42,300	44,300	1.05
68	400	82,500	65,900	71,400	1.08

[a][M] = 0.2 M in CH_2Cl_2, [b]Used as a 0.03 M solution in DCM, [c]Determined by GPC in THF relative to PS standards

5.4.2 ROMP Initiated by Catalyst 63 in Water

The metathesis activity of catalyst **63** was tested in a completely aqueous environment on the water-soluble oxanorbornene **70**, synthesized by Mitsunobu coupling of *exo*-oxanorbornene imide (**69**) with tetraethylene glycol (Scheme 5.3). In neutral water, catalyst **63** failed to polymerize **70**. However, polymerization occurred in aqueous solution at low pH (2 or lower) as evidenced by a rapid increase in solution viscosity immediately after injection of **63** to a solution of **70** in acidified water. The pH-dependent metathesis activity is in accord with previously reported results for ionic, phosphine substituted ruthenium catalysts.[7-9] In this case, the presence of a Brønsted acid likely activates the catalyst by protonation of PEG-pyridine ligands, which diminishes their ligation capability and increases the reactivity of catalyst **63** towards cyclic olefins.

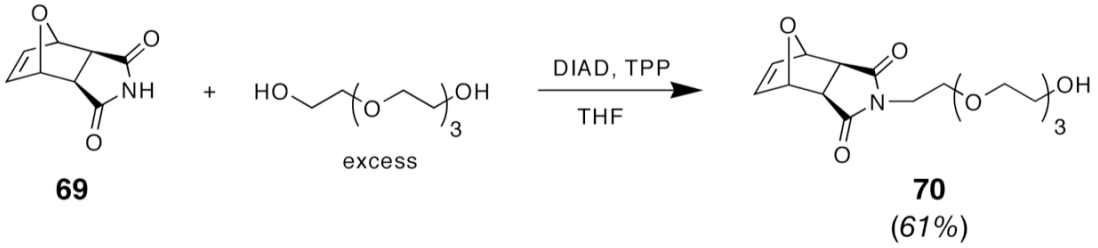

Scheme 5.3 Synthesis of tetraethylene glycol-substituted oxanorbornene 70 by Mitsunobu coupling of 69 and tetraethylene glycol

Figure 5.6 provides GPC-derived molecular weight data for polymers **71 - 73**, prepared by polymerizations that employed various ratios of monomer **70** to catalyst **63** in water at pH 1.5. The average molecular weight of polymers **71 - 73** could be adjusted to higher or lower values by variation of the monomer-to-catalyst ratio. However, the estimated molecular weights of the polymers obtained, using GPC in DMF, were not consistent with theoretical estimations. For example, in the polymerization of oxanorbornene **70** using monomer-to-catalyst ratios of 25:1 (polymer **71**) and 50:1 (polymer **72**), the polymers obtained had GPC-estimated M_n values of 67,000 and 116,000 g/mol, respectively. Full monomer conversion was confirmed by ^{1}H NMR spectroscopy recorded in $CDCl_3$, where resonances at δ 6.5 ppm for the cyclic olefin were not observed. Under ideal conditions of quantitative initiation and absence of termination reactions, M_n values of approximately 10,000 and 20,000 g/mol would have been obtained for polymers **71** and **72**, respectively. This rather significant discrepancy in theoretical *vs.* experimental molecular weight, along with the relatively broad PDI values (1.3 to 2.4), suggest that initiation by catalyst **63** under these conditions is incomplete or slow. In contrast, good agreement of theoretical versus experimentally estimated molecular weight (by GPC) was found for the polymerization of **64** in dichloromethane.

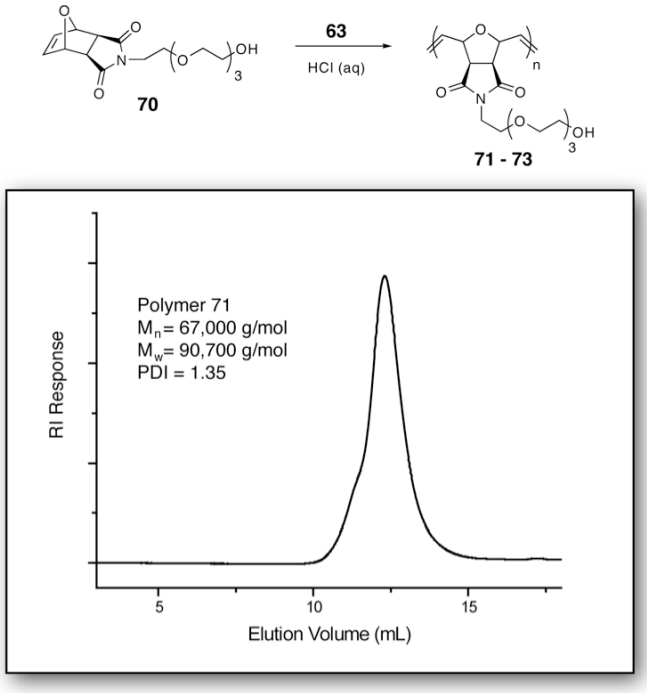

Figure 5.6 GPC analysis of polymer 71 obtained by ROMP of 70 using 63 in water

Table 5.2 Characteristics of polymers 71 – 73 prepared by ROMP of 70 using catalyst 63 in water

Polymer[a]	[M]/[Cat 63[b]]	M_p[c] (g/mol)	M_n[c] (g/mol)	M_w[c] (g/mol)	PDI
71	25	79,000	67,000	90,700	1.35
72	50	177,400	116,200	204,400	1.76
73	100	263,700	137,800	327,200	2.37

[a][M] = 0.15 M in acidified water (pH=1.5), 23 °C for 30 min, [b]Used as a 0.015 M solution in acidified water (HCl, pH=1.5), [c]Determined by GPC in DMF relative to PMMA standards

5.5 Summary and Future Studies

In summary, a new amphiphilic ruthenium benzylidene metathesis catalyst containing PEG-substituted pyridine ligands is reported. PEG-substituted catalyst **63** possesses the beneficial attributes of both the enhanced reactivity given by the N-heterocyclic carbene ligand and amphiphilicity imparted by PEGylation. Catalyst **63** is soluble in both organic and aqueous solvents and was shown to effectively polymerize cyclic olefins in both dichloromethane and water. In dichloromethane, polymers with

low polydispersity indices are obtained, suggesting a controlled or "living" polymerization similar to the 3-bromopyridine substituted catalyst **III**. The polymerization of cyclic olefins in water proceeds rapidly but without the molecular weight control observed in the case of dichloromethane.

Unlike PEGylated catalysts **VII** and **VIII**, which utilize polydisperse samples of relatively high molecular weight PEGs (MW >2000 g/mol), the use of PEG-pyridines with discrete ethylene glycol chain lengths can be utilized to produce a well-defined, amphiphilic catalyst with solubility in water and organic solvents. To accomplish this, future studies could focus on isolation of catalyst **63** in the absence of excess ligand. In this thesis work, the isolation of a pure catalyst has been limited because of difficulties in separating **63** from excess PEG-pyridine ligand. This problem may be overcome by utilizing PEG-pyridines in ligand exchange chemistry with catalyst **IX** as shown in Scheme 5.4. Catalyst **IX** possesses volatile pyridine ligands that can be removed under reduced pressure. If an exact stoichiometric amount of PEG-pyridine is exchanged for pyridine ligands, pure catalyst **63** might be made in this fashion. If successful, key questions regarding the chemical structure and aqueous solubility of pure **63** in the absence of excess ligand can be addressed. In addition, the polymerization kinetics associated with **63**, including the effect of solution pH and other parameters, can be further probed.

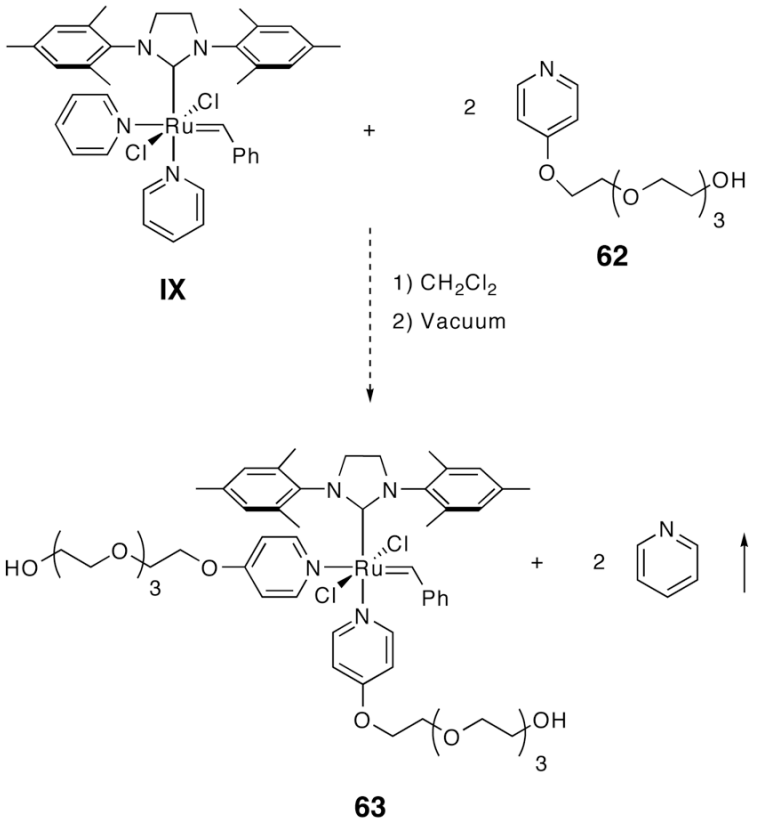

Scheme 5.4 Proposed synthesis of pure ruthenium benzylidene catalyst 63 by ligand exchange of catalyst IX with PEG-substituted pyridine 62

The synthetic route illustrated in Scheme 5.4 requires precise control over stoichiometry and very pure samples of PEG-pyridine ligand **62**. To date, the synthesis of appreciable quantities of pure **62** has been hindered due to previously described purification problems. Protection strategies may be utilized in the future to improve the yield and purity of PEG-pyridine **62**. For example, as shown in Scheme 5.5, tetraethylene glycol can be reacted with an appropriate silyl chloride (*e.g. tert*-butyldimethylsilyl chloride) to give monoprotected tetraethylene glycol **74**. Due to the large difference in polarity between the alcohol and TBDMS functionality, it is anticipated that the separation of **74** and excess tetraethylene glycol by column chromatography should become significantly less challenging. Mono-protected **74** will

then be reacted with a stoichiometric quantity of 4-hydroxypyridine under Mitsunobu coupling to give protected PEG-pyridine **75**. Acidic deprotection and subsequent neutralization should yield pure PEG-pyridine **62** with chain end hydroxyl functionality, which can be utilized in ligand exchange chemistry with catalyst **II**.

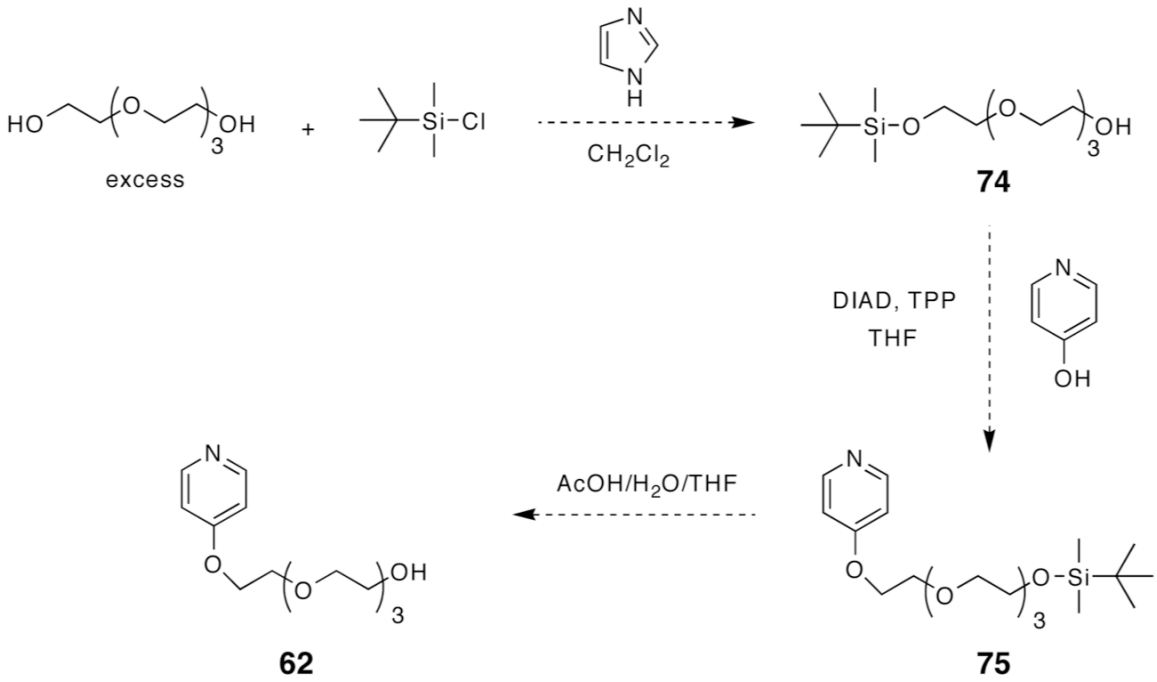

Scheme 5.5 Proposed synthesis of PEG-pyridine ligand 62 using silyl-protected tetraethylene glycol 73

5.6 References

(1) Scholl, M.; Ding, S.; Lee, C. W.; Grubbs, R. H. *Org. Lett.* **1999**, *1*, 953-956.

(2) Love, J. A.; Morgan, J. P.; Trnka, T. M.; Grubbs, R. H. *Angew. Chem. Int Edit.* **2002**, *41*, 4035-4037.

(3) Sanford, M. S.; Love, J. A.; Grubbs, R. H. *Organometallics* **2001**, *20*, 5314-5318.

(4) Choi, T. L.; Grubbs, R. H. *Angew. Chem. Int. Edit.* **2003**, *42*, 1743-1746.

(5) Trnka, T. M.; Grubbs, R. H. *Accounts Chem. Res.* **2001**, *34*, 18-29.

(6) Novak, B. M.; Grubbs, R. H. *J. Am. Chem. Soc.* **1988**, *110*, 7542-7543.

(7) Lynn, D. M.; Mohr, B.; Grubbs, R. H. *J. Am. Chem. Soc.* **1998**, *120*, 1627-1628.

(8) Lynn, D. M.; Mohr, B.; Grubbs, R. H.; Henling, L. M.; Day, M. W. *J. Am. Chem. Soc.* **2000**, *122*, 6601-6609.

(9) Mohr, B.; Lynn, D. M.; Grubbs, R. H. *Organometallics* **1996**, *15*, 4317-4325.
(10) Claverie, J. P.; Viala, S.; Maurel, V.; Novat, C. *Macromolecules* **2001**, *34*, 382-388.
(11) Skaff, H.; Emrick, T. *Chem. Commun.* **2003**, 52-53.
(12) Breitenkamp, K.; Emrick, T. *J. Am. Chem. Soc.* **2003**, *125*, 12070-12071.
(13) Breitenkamp, K.; Simeone, J.; Jin, E.; Emrick, T. *Macromolecules* **2002**, *35*, 9249-9252.
(14) Skaff, H.; Lin, Y.; Tangirala, R.; Breitenkamp, K.; Boker, A.; Russell, T. P.; Emrick, T. *Adv. Mater.* **2005**, *17*, 2082-2086.
(15) Gallivan, J. P.; Jordan, J. P.; Grubbs, R. H. *Tetrahedron Lett.* **2005**, *46*, 2577-2580.
(16) Hong, S. H.; Grubbs, R. H. *J. Am. Chem. Soc.* **2006**, *128*, 3508-3509.

CHAPTER 6

PROJECT OUTLOOK

6.1 Drug Release Studies using Polyolefin Capsules

During the course of this thesis work, significant efforts were made to tailor the properties of polymer capsules prepared from PCOE-*g*-PEG copolymers for encapsulation and release applications. Future efforts will continue in this direction as further exploration of capsule properties such as membrane degradability, permeability, and solute release are critical in this area. In initial encapsulation and release experiments using the anti-inflammatory drug Naproxen, significant drug release (>90%) was observed after only a few hours from polymer capsules prepared from assembly and UV cross-linking of phenyl azide-functional graft copolymers, such as copolymer **42**. This data is consistent with other drug release studies using polymer capsules prepared from polymersomes or by LbL techniques.[1-3] Thus, the encapsulation and sustained release of small molecules will be a major goal moving forward.

In an effort to create polymer capsules capable of either sustained or triggered release, several approaches have been contemplated. In one approach, a hydrophobic drug or other solute might be encapsulated in a non-volatile, hydrophobic oil such as soybean oil or trioctanoin. In this case, release would be slowed due to the preferential solubility of the solute in the hydrophobic oil, and parameters such as membrane thickness, cross-link density, and cross-linker chemistry could be varied to fine tune release properties. Figure 6.1 shows one proposed example where a hydrophobic drug, such as tetraethylene glycol-substituted camptothecin **76**, is solubilized in trioctanoin and encapsulated using PCOE-*g*-PEG copolymers. In this case, **76** has little therapeutic

activity due to the substitution at the 20-OH position of camptothecin, but upon ester hydrolysis in aqueous environments, the therapeutically-active drug is regenerated. Studies that focus on degradation and drug release from polymer capsules prepared with hydrolytically-stable cross-links (*e.g.* amide-linked phenyl azide cross-linked capsules) versus pH-sensitive cross-links (*e.g.* hydrazone cross-linked capsules) will be critical in achieving either sustained or triggered release from the capsule.

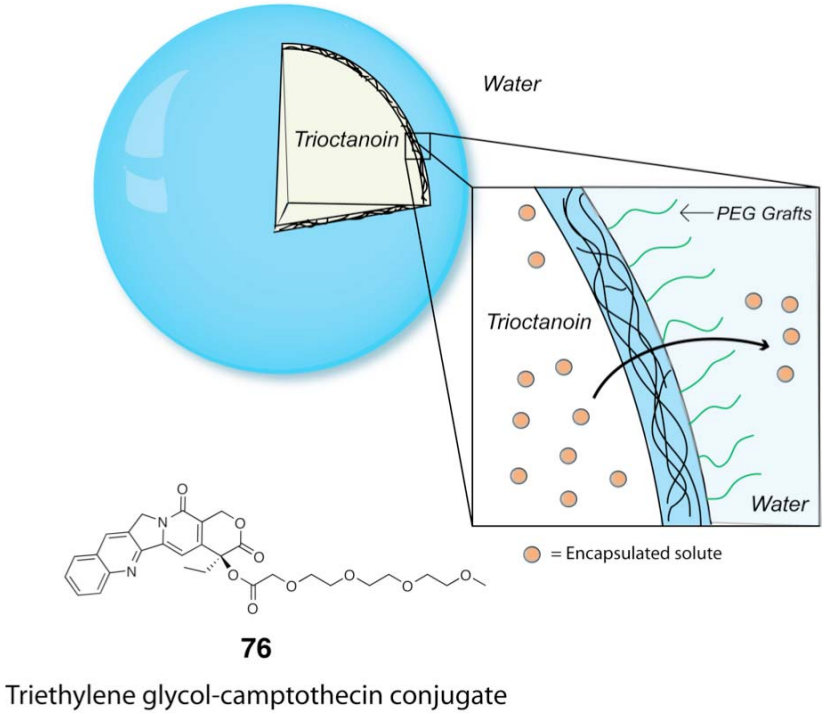

Figure 6.1 Illustration of solute encapsulation utilizing trioctanoin-filled polymer capsules prepared from PCOE-*g*-PEG copolymers

Based on release experiments performed with polymer capsules prepared by LbL techniques, it has been shown that large macromolecules can be encapsulated and retained in the core of these capsules. For example, Caruso and coworkers demonstrated the sustained encapsulation of the protein Transferrin in disulfide cross-linked capsules prepared by LbL assembly,[4] and Möhwald and coworkers showed that glutaraldehyde

cross-linked LbL capsules with a membrane thickness of ~ 20 nm were not permeable to high molecular weight dextran (460 - 2000 kDa).[5] Thus, a second strategy for controlled release of small molecules might involve the encapsulation of a polymer-drug conjugate of sufficient molecular weight as to limit the diffusion of the polymer but allow release of the small molecule once liberated from the backbone. For example, Figure 7.2 illustrates the encapsulation of a camptothecin-functionalized polyester previously reported by the Emrick group.[6] This novel polymer-drug conjugate was synthesized by copper-catalyzed "click coupling" of a propargyl-functionalized polyester and an azide-containing camptothecin derivative. In this case, the polyester-camptothecin conjugate should be retained in the capsule core based on its large size. However, upon significant hydrolysis of the polyester backbone or the ester linkage at the 20-OH position of the pendent camptothecin, drug diffusion across the membrane should be observed with release kinetics governed by the rate of ester hydrolysis. Studies to probe the molecular weight cut-off of the capsule membrane might also be performed using a range of polyester molecular weights (e.g. 5,000 – 50,000 g/mol). Variations in membrane properties such as cross-link density and chemistry may also be explored to fine-tune release properties.

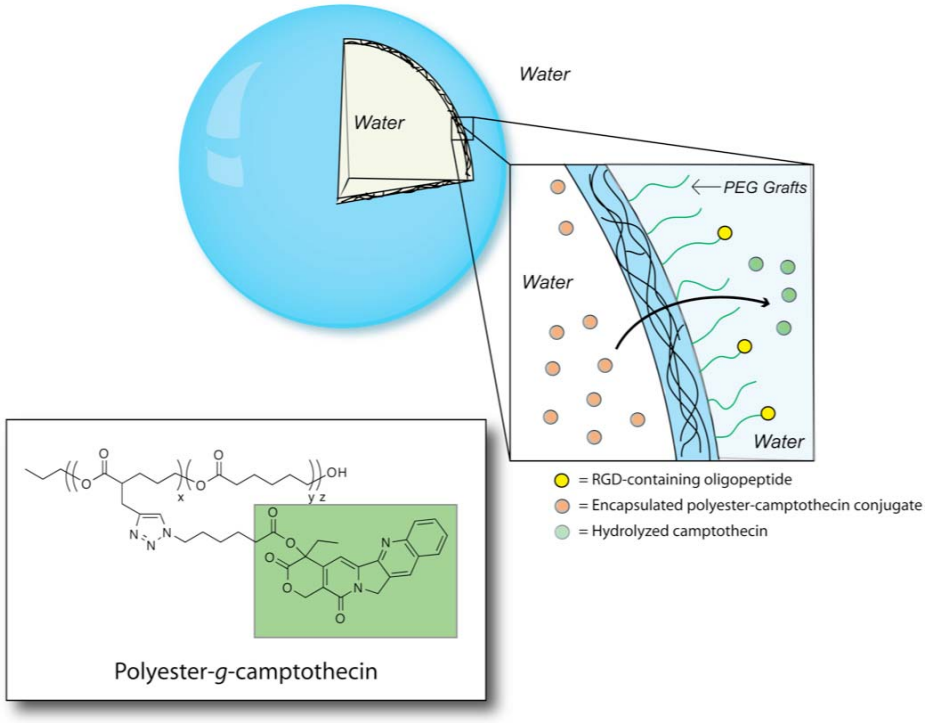

Figure 6.2 Illustration of polyester-camptothecin conjugate encapsulation and hydrolysis-controlled drug release from polymer capsules

Methods to vary the permeability of the capsule membrane might also be pursued using a novel copolymer illustrated in Scheme 6.1. In preliminary studies, ester-linked, α,ω-diene **77**, has been integrated into PCOE copolymers through a combination ROMP-ADMET polymerization mechanism using catalyst **II**. In this reaction, it is hypothesized that ROMP of cyclic olefins proceeds rapidly with **77** acting as a di-functional chain-transfer agent, producing oligomers containing terminal olefins. Over time, the molecular weight of copolymer **78** is increased through ADMET condensation of the terminal olefin end-groups. Utilizing this strategy, high molecular weight polyolefins could be prepared with a controllable number of hydrolytically-degradable ester linkages in the polymer backbone through variation of **77** in the polymerization feed. If copolymer **78** is utilized in interfacial assembly and UV cross-linking, polymer capsules

with hydrolytically-stable amide cross-links and a hydrolytically-degradable polymer backbone would be produced. Over time, the capsules should not dissolve away due to the stable cross-links, but the permeability of the capsule membrane should change based on ester hydrolysis of the polymer backbone. Variation of **77** in the copolymerization feed might produce capsules with selective permeability to macromolecules of various molecular weights which could prove useful for release applications, chemical transport/catalysis systems, and bioreactors.

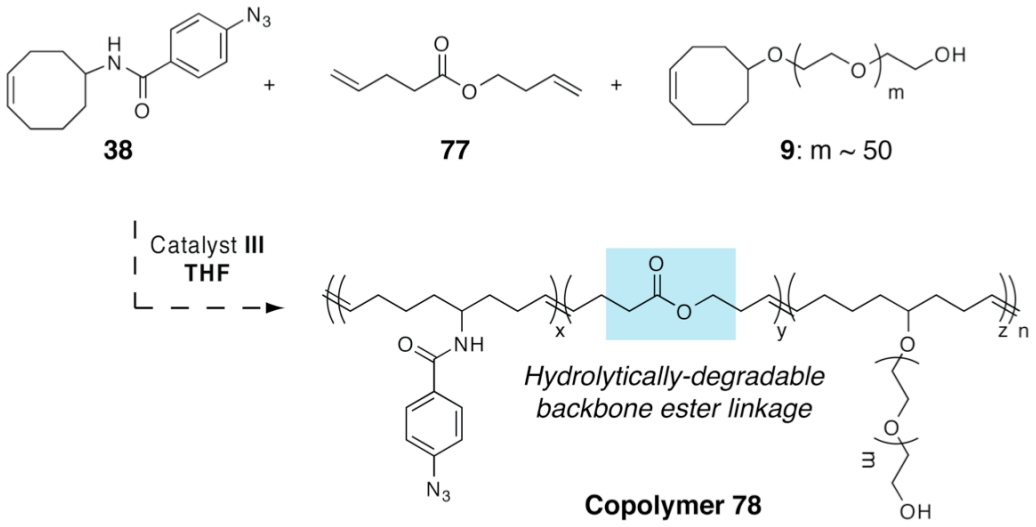

Scheme 6.1 Synthesis of hydrolytically-degradable PCOE-*g*-PEG copolymer 79 for the preparation of variable permeability polymer capsules

6.2 References

(1) Rigler, P.; Meier, W. *J. Am. Chem. Soc.* **2006**, *128*, 367-373.

(2) Antipov, A. A.; Sukhorukov, G. B.; Donath, E.; Mohwald, H. *J. Phys. Chem. B* **2001**, *105*, 2281-2284.

(3) Park, M. K.; Deng, S. X.; Advincula, R. C. *Langmuir* **2005**, *21*, 5272-5277.

(4) Zelikin, A. N.; Quinn, J. F.; Caruso, F. *Biomacromolecules* **2006**, *7*, 27-30.

(5) Tong, W.; Gao, C.; Mohwald, H. *Chem. Mater.* **2005**, *17*, 4610-4616.

(6) Parrish, B.; Emrick, T. *Bioconjugate Chem.* **2007**, *18*, 263-267.

CHAPTER 7

EXPERIMENTAL SECTION

7.1 Materials

cis-Cyclooctene, succinic anhydride (99%), lithium aluminum hydride (95%), and bis(tricyclohexylphosphine)benzylidine ruthenium (IV) dichloride (catalyst **I**) were purchased from Sigma-Aldrich or Alfa Aesar. Potassium hydroxide (technical grade), sodium hydroxide (97%), and hydrogen peroxide (34 - 37% aqueous solution) were purchased from Fisher Scientific and used as received. 1,5-Cyclooctadiene (99%) (COD), *m*-chloroperoxybenzoic acid (MCPBA) (77%), 4-dimethylaminopyridine (DMAP) (99%), 1,3-dicyclohexylcarbodiimide (DCC) (99%), N,N'-diisopropylcarbodiimide (DIC) (99%), 1-hexene (97%), ethyl vinyl ether (99%), ethylene oxide (EO) (99.5%), 3-bromopyridine (99%), sodium azide (99.5%), triphenylphosphine (99%), piperidine (99%), 2,2,2-trifluoroethanol (TFE) (99.5%), diisopropylethylamine (99.5%), polyethylene glycol (MW 2000 g/mol), Rhodamine B (90%), 3-bromopyridine (99%), sodium azide (99.5%), triphenylphosphine (99%), HCl (4.0 M in dioxane), diisopropyl azodicarboxylate (95%), maleic anhydride (99%), maleimide (99%), diethylene glycol vinyl ether (98%), dimethylsulfoxide (DMSO) (99.5%), thionyl chloride (99%), potassium chunks (98%), sodium cyanide (97%), *tert*-butyl carbazate (98%), sodium nitrite (97%), 4-aminobenzoic acid (99%), 4-aminophenyl sulfone (97%), triisopropylsilane (99%), *tert*-butyl bromoacetate (98%), potassium *tert*-butoxide (95%) and Grubbs' Generation II catalyst (catalyst **II**) were purchased from Sigma-Aldrich and used without further purification. Hydrobromic acid (HBr) (33% in acetic acid) was purchased from Fluka. Camptothecin (98%) was purchased from Acros and used as

received. Naphthalene (99%, Aldrich) was recrystallized from methanol and sublimed before use. 4-Hydroxypyridine (95%, Aldrich) was passed through a plug of neutral alumina (80/20 $CHCl_3$/MeOH eluent), precipitated into diethyl ether, filtered, and dried *in vacuo*. Furan (99%, Aldrich) was purified by vacuum distillation over calcium hydride. Triethylene glycol monomethyl ether (95%, Aldrich) was purified by fractional distillation over calcium hydride. Tetraethylene glycol (99%, Alfa-Aesar) was purified by fractional distillation over calcium hydride. Grubbs' Generation III catalyst (catalyst **III**) was prepared according to literature procedures.[1] Tetrahydrofuran (THF) was distilled from sodium benzophenone ketyl. Dichloromethane and triethylamine were distilled from calcium hydride before use. Polyethylene glycol monomethyl ether (mPEG) 750 was purchased from Polysciences, Inc and purified by column chromatography (in $CHCl_3$/Acetone/MeOH mixtures) before use. mPEG 1000 was purchased from Shearwater Polymer, Inc. and used without further purification. Fmoc-Gly-OH, Fmoc-Ser(But)-OH, Fmoc-Asp(OBut)-OH, Fmoc-Arg(Pbf)-OH, Boc-Gly-OH, trifluoroacetic acid, 1-hydroxybenzotriazole (HOBt) hydrate, O-(Benzotriazol-1-yl)-N,N,N',N'-tetramethyluronium hexafluorophosphate (HBTU), and 2-chlorotrityl chloride resin (1.4 mmol/g, 100-200 mesh) were purchased from Advanced ChemTech. PVDF-UF membrane with 30,000 molecular weight cutoff was purchased from Sterlitech Corporation, USA.

7.2 Methods and Instrumentation

Molecular weights and PDIs of macromonomers **3** and **4** were measured using gel permeation chromatography in THF (elution rate = 1.0 mL/min) and referenced against linear PEG standards. The system utilized three-columns (Polymer Laboratories Mixed-

D columns, 5 mm, 300 x 7.5 mm) and a refractive index detector (Waters R4010 or Knauer K-2301). Macromonomers **8**, **9**, **10**, **15** and **16** and copolymers **42**, **43**, **49** and **58** were analyzed in THF (1.0 mL/min) and referenced against linear polystyrene standards. The system utilizes three-columns (PL Mixed-D columns, 5 μm, 300 x 7.5 mm), a dual wavelength UV detector (Knauer K-2600**,** analysis at 260 nm), and a refractive index detector (Knauer K-2301). GPC analyses of copolymer **18** – **26** and *bis*-cyclooctene **31** were performed in dimethylformamide (DMF) (with 0.01 M LiCl, elution rate = 0.5 mL/min) and referenced against linear polystyrene standards. The system utilized three-columns (Polymer Laboratories Mixed-D columns, 5 mm, 300 x 7.5 mm) and a refractive index detector (Waters R4010). GPC analyses of polymers **71** – **73** were performed in DMF (1.0 mL/min) with LiBr (0.05 M) using a PL GPC 50 system at 50 °C equipped with two PL Resipore® columns (3 μm, 300 x 7.5 mm) and referenced against linear poly(methyl methacrylate) standards. GPC analyses of polymers **27** – **29** and copolymers **53** – **57** were performed in chloroform (elution rate = 1.0 mL/min) using a PL GPC 50 system at 25 °C equipped with two Polymer Laboratories (PL) Mixed D columns (5 μm, 300 x 7.5 mm) and referenced against linear polystyrene standards. High temperature GPC of hydrogenated polymers **18a** – **26a** was performed on a Polymer Laboratories PL-GPC 200 equipped with a Wyatt Minidawn multiple angle laser light scattering (MALLS) detector using trichlorobenzene (135 ^{o}C) at a flow rate of 1.0 mL/min.

NMR spectra were collected on either a Brüker DPX 300 spectrometer: ^{1}H at 300 MHz and ^{13}C at 75 MHz or on a Brüker Avance 400 spectrometer: ^{1}H at 400 MHz and ^{13}C at 100 MHz. Attenuated Total Reflectance Infrared Spectroscopy (ATR-FTIR) was performed on a Perkin-Elmer Spectrum One spectrometer equipped with a Universal

Diamond ATR sampling accessory. DSC experiments were performed on a TA instruments Q1000 at a heating rate of 10 ^{o}C/min. UV data was obtained using a Hitachi U-3010 spectrophotometer at a scan rate of 60 nm/mi. Confocal images were obtained using an inverted microscope with TCS SP2 confocal system (Leica). Atomic force microscopy (AFM) images were obtained using a Digital Instruments Dimension 3100 atomic force microscope. Electrospray Ionization (ESI) mass spectroscopy was performed on a Brüker Esquire liquid chromatography instrument. Matrix assisted laser desorption/ionization mass spectroscopy was performed on a Brüker Reflex III. A CL-1000 UV light source (UVP, Inc.) was utilized for UV cross-linking at 302 nm (intensity 3800 microwatts/cm^2). Scanning electron microscopy (SEM) images were obtained on a Jeol 6320FXV Field Emission SEM. Dynamic light scattering analysis was performed on a Particle Sizing Systems Nicomp 380 at a 90^{o} angle. A Rame-hart model 1000 goniometer system was used for contact angle measurements. Pure water flux through dense membrane made from polymers **53 – 57** was measured with Amicon 8200 stirred ultrafiltration cell. HPLC analysis was performed using a Waters Alliance 2695 multi-solvent delivery system equipped with a Waters 2996 photodiode array detector and a Waters XTerra® column (C8, 5 μm, 4.6 x 150 mm).

7.3 Synthetic Procedures

Synthesis of 5-hydroxy-1-cyclooctene (1)

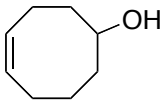

5-hydroxy-1-cyclooctene was prepared in two steps from commercially available 1,5-cyclooctadiene as described by Grubbs and coworkers.[2]

Succinic acid mono-cyclooct-4-enyl ester (2)

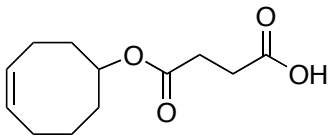

3.00 g (2.38 mmol) of 5-hydroxy-1-cyclooctene (**1**) 2.38 g (2.38 mmol) of succinic anhydride, and 50 mg (0.41 mmol) of N,N-dimethylaminopyridine (DMAP) were combined and stirred in refluxing toluene (20 mL) for 16 hours. The solution was cooled to room temperature, washed with 1 M HCl (aq), and concentrated to yield a white solid. The product was purified by crystallization in hexanes to afford 4.58 g (85 %) of **2**: m.p. 55-57 ^{o}C; ^{1}H NMR ($CDCl_3$) δ 10.75 (br s, 1H), 5.65 (m, 2H), 4.85 (m, 1H), 2.55-2.67 (m, 4H), 1.57-2.4 (m, 10H) ppm; ^{13}C NMR ($CDCl_3$) δ 178.9 (acid), 171.9 (ester), 130.2, 123.0, 76.7, 34.0, 33.9, 29.6, 29.4, 25.9, 22.2, 22.7 ppm; IR (KBr) 3018, 2938, 2866, 1728 (ester), 1704 (acid), 1447, 1408, 1355, 1255, 1236, 1213, 1171 cm^{-1}.

Representative synthesis of ester-linked PEG macromonomer (4)

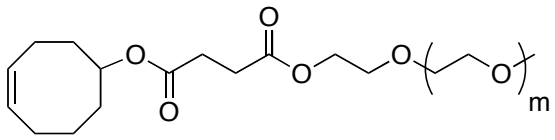

m ~ 22

2.0 g (8.8 mmol) of **2**, 8.8 g (8.8 mmol) of poly(ethylene glycol) monomethyl ether (MW 1000 g/mol), and 106 mg (0.88 mmol) DMAP were stirred in dry CH_2Cl_2 (15 mL) under N_2. Separately, 2.2 g (10.6 mmol) of DCC was dissolved in 1.4 g (17.6 mmol) of pyridine and DCM (15 mL); this solution was then added by syringe to the reaction mixture containing **2** and stirred for 12 hours at room temperature under N_2.

Upon completion, the mixture was washed with 1 M HCl (aq) and concentrated. The product was dissolved in a mixture of hexane and ethyl acetate and twice extracted with water. The aqueous phase was extracted with CH_2Cl_2, concentrated, and dissolved in toluene. This solution was washed twice with a sat. NaCl (aq) and dried using $MgSO_4$. Toluene was removed by evaporation, and the product was dissolved in a minimal amount of diethyl ether and precipitated into cold hexane. The product was collected and dried under vacuum overnight to yield 8.1 g (76 %) of **4** as a white solid: m.p. 42-43 ^oC; ^1H NMR ($CDCl_3$) δ 5.65 (m, 2H), 4.83 (m, 1H), 4.22 (t, 2H), 3.5-3.7 (complex, br m, ~90H), 3.38 (s, 3H), 2.55-2.67 (m, 4H), 1.57-2.4 (m, 10H) ppm; ^{13}C NMR ($CDCl_3$) δ 172.4 (ester), 171.6 (ester), 129.8, 129.6, 76.8, 72.0, 70.6, 69.1, 63.9, 59.1, 33.7, 33.6, 29.5, 29.2, 25.6, 24.9, 22.3 ppm.

Representative synthesis of ether-linked PEG macromonomer (9)

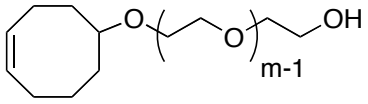

m ~ 50

In a flame dried air-free flask, 5-hydroxy-1-cyclooctene (**1**) (6.8 mL of 1.0 M solution in THF, 6.8 mmol) was added to dry THF (150 mL) while stirring under N_2. The solution was titrated with potassium napthalenide (0.2 M in THF) until a slight green end-point was observed (~ 35.0 mL). The cyclooctene alkoxide solution was stirred for an additional 30 minutes at room temperature before being cooled to 0 ^oC in an ice/water bath. Ethylene oxide (15.0 mL, 340.6 mmol) was condensed at -78 ^oC using a stainless steel gas transfer manifold, then slowly warmed to room temperature while transferring to the cooled cyclooctene alkoxide solution under static vacuum. The reaction mixture

was pressurized with argon, sealed, and stirred at room temperature for 16 hr. The solution was concentrated and the residue was purified by column chromatography on silica gel (93/7 → 90/10 $CHCl_3$/MeOH). The product recovered from the column was dissolved in a minimal amount of chloroform and precipitated into diethyl ether. A white powder was isolated by filtration and dried under vacuum to yield 11.3 g (75% yield) of macromonomer **9**. ^{1}H NMR ($CDCl_3$) δ 5.62 (m, 2H), 3.28-3.84 (complex, br m, 228 H), 2.54 (br s, 1H), 1.28-2.36 (complex br m, 11H); ^{13}C NMR ($CDCl_3$) δ 130.2, 129.6, 81.1, 72.7, 71.0, 70.7, 70.4, 67.8, 61.8, 34.2, 33.5, 25.9, 25.8, 22.8; ATR-FTIR 3491, 2882, 1467, 1359, 1341, 1280, 1242, 1100, 1060, 959, 841, 725 cm^{-1}; GPC (THF, relative to PEG standards) M_n 2300 Da, M_w 2350 Da, PDI 1.09.

Synthesis of cyclooctene-PEG azide (13)

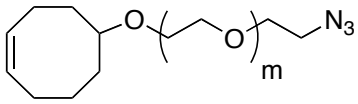

m ~ 49

Macromonomer **9 (**13.0 g, 5.7 mmol) was added to a dry round-bottom flask and dissolved in anhydrous THF (100 mL). The solution was cooled to 0 ^{o}C and methanesulfonyl chloride (0.6 mL, 7.1 mmol) was added by syringe. Triethylamine (1.2 mL, 8.5 mmol) was subsequently added by syringe over approximately 5 minutes. The reaction mixture was stirred for an additional 30 minutes at 0 ^{o}C, warmed to room temperature, and stirred for 16 hours. The mixture was concentrated, diluted with 95% ethanol (100 mL), and sodium azide (1.9 g, 28.5 mmol) was added. The mixture was heated to reflux and stirred for 16 hours. The reaction contents were allowed to cool to room temperature and concentrated by rotary evaporation. The residue was purified by

column chromatography on silica gel (93/7 → 90/10 $CHCl_3$/MeOH). The desired fractions were combined and concentrated, and the residue was dissolved in a minimal amount of chloroform and precipitated into diethyl ether. The white powder was isolated by filtration and dried under vacuum to yield the desired macromonomer (12.8 g, 98% yield). ^{1}H NMR (d_6-DMSO) δ 5.62 (m, 2H), 3.25-3.75 (complex, br m, 228 H), 2.54 (br s, 1H), 1.28-2.35 (complex br m, 11H); ^{13}C NMR (d_6-DMSO) δ 130.0, 129.1, 79.8, 70.3, 69.8, 69.4, 67.4, 50.3, 34.0, 33.5, 25.4, 25.3, 22.3; ATR-FTIR 2882, 2741, 2098, 1466, 1360, 1341, 1279, 1241, 1146, 1100, 1060, 959, 841 cm^{-1}; GPC (THF, relative to PEG standards) M_n 2360 Da, M_w 2550 Da, PDI 1.08.

Synthesis of cyclooctene-PEG amine (14)

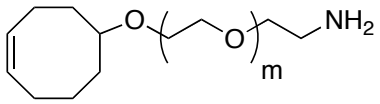

m ~ 49

COE-PEG azide **13** (12.8 g, 5.6 mmol) and triphenylphosphine (2.9 g, 11.1 mmol) were dissolved in THF (90 mL). The contents were stirred for 30 minutes with visible bubbling due to N_2 evolution. Water (10 mL) was subsequently added resulting in a heterogeneous solution. The reaction mixture was stirred an additional 16 hours at room temperature and eventually becoming a homogenous solution. Water was removed from the reaction by azeotropic distillation with benzene. The reaction mixture was then concentrated, dissolved in a minimal amount of chloroform, and precipitated into diethyl ether. The product was isolated by filtration, washed several times with diethyl ether, and dried *in vacuo* to afford 10.8 g (89% yield) of the desired macromonomer as a white powder. ^{1}H NMR (d_6-DMSO) δ 5.60 (m, 2H), 3.35-3.75 (complex, br m, 228 H), 2.64 (t,

2H), 1.28-2.35 (complex br m, 11H); ^{13}C NMR (d_6-DMSO) δ 129.1, 128.9, 79.9, 73.1, 70.3, 69.8, 69.6, 67.2, 34.0, 29.8, 25.3, 25.2, 22.3; GPC analysis of macromonomer **14** was not possible due to interactions with the GPC column media which artificially inflated molecular weight and PDI values.

Synthesis of cyclooctene-PEG-carboxylic acid (15)

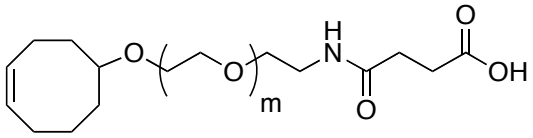

m ~ 49

COE-PEG amine **14** (13.7 g, 6.0 mmol) and succinic anhydride (1.5 g, 15.0 mmol) were dissolved in chloroform (60 mL). Methanol (10 mL) was added to improve solubility, and the reaction mixture was stirred for 16 hours at room temperature. The mixture was concentrated and purified by column chromatography on silica gel (93/7 → 90/10 $CHCl_3$/MeOH). The desired fractions were combined and concentrated, and the residue was dissolved in a minimal amount of chloroform and precipitated into diethyl ether. The white powder obtained was isolated by filtration and dried under vacuum to yield macromonomer **15** (13.1 g, 95% yield). ^{1}H NMR (d_6-DMSO) δ 12.07 (s, 1H), 7.88 (s, 1H), 5.60 (m, 2H), 3.25-3.75 (complex, br m, 228 H), 3.15 (m, 2H), 1.25-2.42 (complex br m, 11H); ^{13}C NMR (d_6-DMSO) δ 173.8, 171.0, 130.0, 129.1, 79.9, 70.2, 69.9, 69.2, 67.1, 33.9, 32.7, 29.9, 29.1, 25.2, 25.1, 22.2; ATR-FTIR 2881, 1733, 1467, 1359, 1342, 1279, 1241, 1147, 1099, 1060, 960, 841 cm^{-1}. GPC (THF, relative to PEG standards) M_n 2470 Da, M_w 2770 Da, PDI 1.12.

Synthesis of cyclooctene-PEG-GRGDS (16)

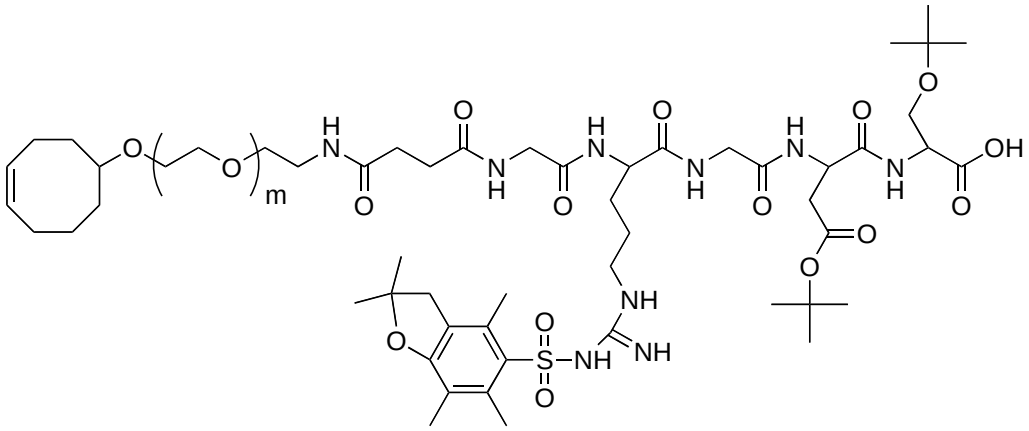

m ~ 49

RGD-functionalized PEG macromonomer **16** was synthesized via Fmoc-based solid phase peptide synthesis with the coupling agent HBTU using a 2-chlorotrityl chloride resin. 2-chlorotrityl chloride resin (2.89 g of resin with 1.40 mmol of functional groups per gram of resin, 4.05 mmol, 100-200 mesh) was weighed into an oven-dried, glass-fritted reaction tube and swollen with dry DCM (40 ml) for 5-10 minutes. The resin was filtered, and a solution of Fmoc-Ser(But)-OH (2.02 g, 5.26 mmol) in dry DIPEA (3.50 ml, 20.2 mmol),and dry DCM (30-40 ml) was added to the reaction tube. The tube was capped, vented, and agitated with nitrogen. After 30 minutes, the resin was filtered and rinsed with dry DMF three times. The remaining reactive groups on the resin were capped with a 80/15/5 dry DCM/methanol/DIPEA solution (40 ml, 2 x 10 min.) and then rinsed with reagent grade DMF. The Fmoc group was removed with a 25/75 piperidine/DMF cleavage solution (2 x 40 ml). The solution was added to the resin, and the resin was agitated for three minutes. Following filtration, fresh cleavage solution was added and agitated for 20 minutes. The resin was filtered and rinsed with DMF six times, DCM three times, isopropanol three times, and hexanes six times. The resin was dried by

filtration for 15 minutes, transferred to a vial, and dried under vacuum for 24-36 hours. The loading density was estimated by the mass differential between the unloaded and loaded resin.

After loading Fmoc-Ser(But)-OH, a portion of the dried resin (1.05 g, 0.447 mmol) was transferred to a dry, glass-fritted reaction tube and swollen with 20 ml of DCM for 5 minutes. Fmoc-Asp(But)-OH (0.920 g, 2.49 mmol), HOBt (0.382 g, 2.49 mmol), HBTU (0.831 g, 2.19 mmol), and DMF (15 mL, reagent grade) were combined in an oven-dried round bottom flask, and DIPEA (reagent grade, 0.80 mL, 4.47 mmol) was added to form a clear, yellow solution. The activated amino acid solution was then added to the resin, and the resin was agitated for one hour, filtered, and washed with DMF three times. The Fmoc protecting group was cleaved with 25/75 piperidine/DMF, after which the resin was washed with DMF six times. The amino acid addition procedure was repeated for Fmoc-Gly-OH, Fmoc-Arg(Pbf)-OH, and a second unit of Fmoc-Gly-OH.

Following the addition of the second glycine residue, the Fmoc protecting group was cleaved, and the resin was thoroughly washed with DMF. A solution of cyclooctene-PEG-carboxylic acid (**15**) (8.26 g, 3.42 mmol), HOBt (0.38 g, 2.49 mmol), HBTU (0.83 g, 2.19 mmol), DIPEA (1.00 mL, 5.60 mmol), and 25 ml of DMF was added to the resin and agitated from four hours. The resin was filtered and washed with DMF and DCM three times. A fresh solution of cyclooctene-PEG-carboxylic acid (**15**) (4.32 g, 1.79 mmol), HOBt (0.27 g, 1.76 mmol), HBTU (0.67 g, 1.77 mmol), DIPEA (1.00 mL, 5.60 mmol), and DMF (20 mL) prepared, added to the resin, and agitated for four hours. The resin was washed with DMF and DCM five times.

The macromonomer was then cleaved from the resin under mildly acidic conditions (4:1 DCM:TFE). After 90 minutes, the resin was filtered into a clean flask, and fresh solution was added. The resin was agitated for another 30 minutes, filtered, and washed with 4:1 DCM:TFE and then DCM three times. This resulting filtrate was concentrated on a rotary evaporator and then precipitated into diethyl ether. After sitting at 4°C for several hours, the product was isolated by filtration and then dried under vacuum. To remove uncoupled GRGDS oligopeptide, the crude product was dissolved in deionized water and filtered to remove the insoluble material. The filtrate was subsequently lyophilized and 610 mg (41% yield) of macromonomer **16** was isolated as a white product. ^{1}H NMR (d_6-DMSO) δ 8.82 (s), 7.80 - 8.18 (m), 5.58 (m), 4.69 (m), 4.30 (t), 4.22 (m), 3.25-3.75 (br m), 3.15 (m), 3.04 (br s), 2.96 (s), 2.65 (m), 2.47 (s), 2.35 (s), 2.24 (m), 1.93 – 2.14 (m), 1.80 – 1.90 (m), 1.50 – 1.76 (m), 1.38 (d), 1.10 (s); ^{13}C NMR (d_6-DMSO) δ 171.9, 171.6, 170.5, 169.5, 168.8, 159.0, 158.7, 158.3, 157.9, 130.2, 129.3, 119.5, 116.6, 113.7, 110.9, 80.5, 80.1, 73.1, 70.4, 70.0, 69.8, 69.3, 67.3, 61.6, 53.0, 49.2, 34.1, 32.9, 30.8, 30.7, 28.4, 27.8, 27.3, 25.4, 25.2, 22.4, 19.1, 17.7, 12.4; GPC (THF, relative to PEG standards) M_n 1880 Da, M_w 2130 Da, PDI 1.13. MALDI Peak MW m/z = 3261 g/mol.

Example Copolymerization using Macromonomer 4 (Copolymer 17)

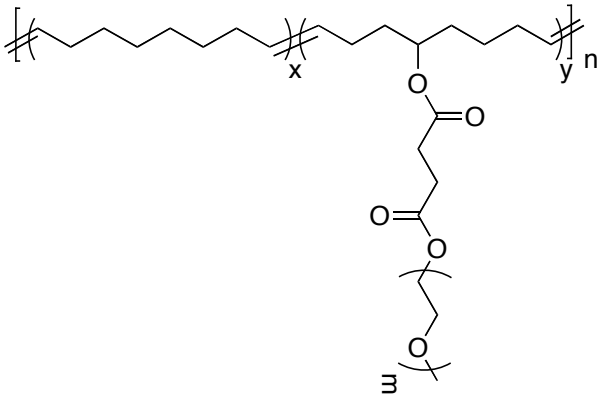

Macromonomer **4** (0.50 g, 0.52 mmol) was weighed into a reaction tube and degassed under vacuum while stirring at 45 ^{o}C. Cyclooctene (58 mg, 0.52 mmol) was injected into the vessel under N_2. Catalyst **II** (3.5 mg, 4.1 μmol) was weighed into a small vial, degassed, and dissolved in dry dichloromethane (1.0 mL) under N_2. The catalyst solution was introduced by syringe, and the mixture was stirred at 45 ^{o}C. Once stirring had ceased due to the increased solution viscosity, ethyl vinyl ether (1 mL) was added and a small amount of DCM (~1 mL) was added to improve stirring. The contents were precipitated into cold hexane, filtered, and dried under vacuum to yield copolymer **17** (0.42 g, 84%). ^{1}H NMR ($CDCl_3$) δ 5.34 (br, olefin 2H), 4.86 (br s, 1H), 4.22 (t, 2H), 3.5-3.7 (complex, br m), 3.36 (s, 3H), 2.61 (br m, 4H), 2.32 (br s), 1.94 (br s), 1.50 (br s), 1.26 ppm (br s); ^{13}C NMR ($CDCl_3$) δ 172.7 (ester), 172.3 (ester), 130.0, 130.8, 129.3, 74.7, 72.3, 70.9, 69.4, 64.2, 59.4, 34.4, 33.0, 30.0, 29.7, 29.5, 28.8, 25.6 ppm. IR (NaCl plate) 2922, 2867, 1733 (ester), 1456, 1349, 1300, 1250, 1111, 1040, 968, 860 cm^{-1}. GPC (DMF w/ 0.01% LiCl *vs.* linear polystyrene standards) M_n = 330,000 g/mol, M_w = 515,000 g/mol, PDI = 1.56.

Representative synthesis of PCOE-*g*-PEG copolymer (Copolymer 27)

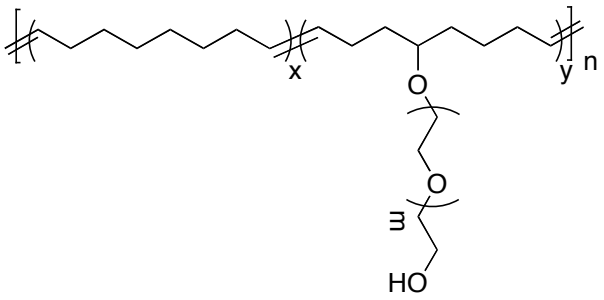

m ~ 24

PEG 1200 (m ~ 24) macromonomer (**8**) (0.16 g, 0.13 mmol) and cyclooctene (0.17 g, 1.54 mmol) were combined in a dry reaction tube. 0.2 mL of a 0.05 M 1-hexene solution in dichloromethane was added to the reaction under N_2 followed by 0.7 mL of dry dichloromethane. In a separate vial, catalyst **III** (5.9 mg, 6.7 μmol) was dissolved in 0.2 mL dry dichloromethane. Both the monomer mixture and catalyst solution were subjected to two freeze/pump/thaw cycles and subsequently warmed to 40 ^{o}C. The catalyst solution was then rapidly added to the monomer solution and stirred until vitrified (approx. 5 min). Ethyl vinyl ether (1 mL) was added to terminate the polymerization and dichloromethane was added to dilute the polymer solution. The product was precipitated into cold hexane containing 1 wt % BHT, isolated by filtration, and dried under vacuum to yield 0.30 g (90% yield) of copolymer **27** as an off-white solid. ^{1}H NMR ($CDCl_3$) δ 5.36 (m), 3.37-3.97 (br m), 3.24 (br s), 2.43 (br s), 1.94, (br m), 1.27-1.53 (br m); ^{13}C NMR ($CDCl_3$) δ 130.2, 72.6, 70.6, 70.3, 61.7, 32.6, 29.6, 29.1; ATR-FTIR 2921, 2852, 1468, 1344, 1281, 1242, 1104, 963, 842 cm^{-1}. GPC ($CHCl_3$, relative to PS standards) M_n 24,000 Da, M_w 48,500 Da, PDI 2.02.

Hydrogenation of PCOE-g-PEG graft copolymers (Copolymer 26a)

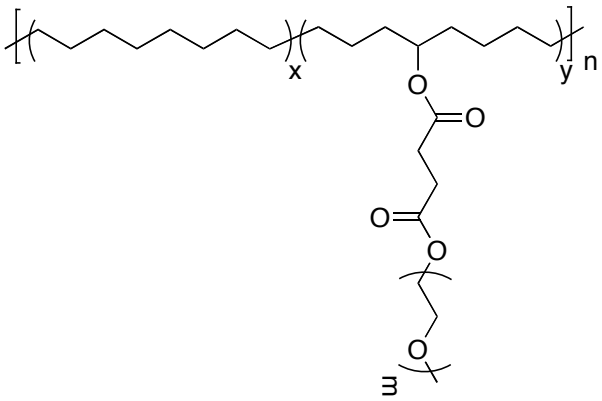

m ~ 16

Hydrogenated copolymers **18a** – **26a** were synthesized according to published procedures.[1] Precipitation of copolymers 18a - 25a were performed in cold hexane. Precipitation of **26a** was performed in cold methanol. Hydrogenated copolymer **26a**: ^{1}H NMR ($CDCl_3$) δ 4.86 (broad s, 1H), 4.24 (t, 2H), 3.5-3.7 (complex, br m), 3.38 (s, 3H), 2.61 (br m, 4H), 1.65 (br s), 1.50 (br s), 1.26 ppm (br s); ^{13}C NMR ($CDCl_3$) δ 172.7 (ester), 172.3 (ester), 75.2, 72.2, 70.8, 69.4, 64.0, 59.4, 30.0, 25.6 ppm. IR (NaCl plate) 2919, 2852, 1733 (ester), 1464, 1349, 1299, 1250, 1139, 1110, 1040, 957, 858 cm^{-1}.

Synthesis of *bis*-cyclooctene PEG 2000 (31)

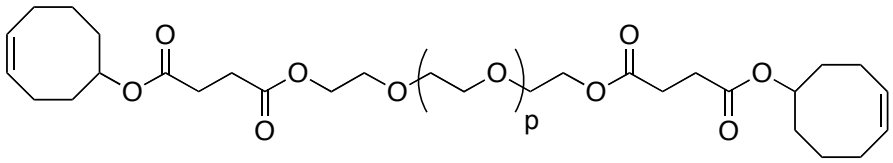

m ~ 45

Succinic acid mono-cyclooct-4-enyl ester (**2**) (2.55 g, 11.2 mmol), polyethylene glycol (MW 2000 g/mol) (9.00 g, 4.50 mmol), and N,N-dimethylaminopyridine (110 mg, 0.90 mmol) were stirred in dry CH_2Cl_2 (30 mL) under N_2. In a separate flask,

dicyclohexylcarbodiimide (1.96 g, 9.50 mmol) was dissolved with pyridine (1.18 g, 14.9 mmol) and CH_2Cl_2 (10 mL); this solution was added by syringe to the reaction mixture and stirred for 24 hours at room temperature under N_2. The mixture was washed with 1 M HCl (aq) and concentrated. The product was dissolved in water and extracted with hexane/ethyl acetate. The aqueous phase was extracted with CH_2Cl_2, dried over $MgSO_4$, concentrated, and dried under vacuum overnight to yield the *bis*-cyclooctene PEG product (10.3 g, 95 %) as a white, waxy solid; ^{1}H NMR ($CDCl_3$) δ 5.65 (m, 4H), 4.83 (m, 2H), 4.22 (t, 4H), 3.5-3.7 (complex, br m, ~180H), 2.55-2.67 (m, 8H), 1.57-2.4 (m, 20H) ppm; ^{13}C NMR ($CDCl_3$) δ 172.4 (ester), 171.6 (ester), 129.8, 129.6, 76.8, 72.0, 70.6, 69.1, 63.9, 59.1, 33.7, 33.6, 29.5, 29.2, 25.6, 24.9, 22.3 ppm; MALDI Peak MW m/z = 2393.7 g/mol.

Synthesis of Rhodamine B-functionalized cyclooctene (32)

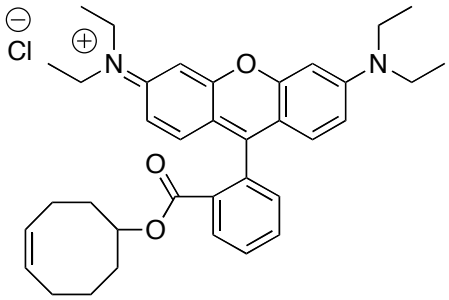

260 mg (2.09 mmol) of 5-hydroxy-1-cyclooctene (**1**), 500 mg (1.04 mmol) of Rhodamine B, and 1.5 mg (0.13 mmol) DMAP were stirred in dry CH_2Cl_2 (5 mL) under N_2. In a separate flask, 0.26 g (1.25 mmol) dicyclohexylcarbodiimide was dissolved with 0.20 g (2.5 mmol) pyridine and CH_2Cl_2 (5 mL); this solution was then added by syringe to the reaction mixture and stirred for 24 hours at reflux under N_2. The mixture was washed with 1 M HCl (aq) and concentrated. The product was purified by column chromatography to yield 460 mg (75 %) of **32**. ^{1}H NMR ($CDCl_3$) δ 8.22 (m, 1H), 7.70-

7.77 (m, 2H), 6.74-7.26 (m, 3H), 5.54 (m, 2H), 4.71 (m, 1H), 4.46 (m, 1H), 4.10 (m, 1H), 3.58-3.67 (m, 8H), 0.85-2.20 (br m, 22H) ppm; ^{13}C NMR ($CDCl_3$) δ 164.6 (ester), 159.03, 157.9, 155.65, 133.3, 133.0, 131.5, 131.4, 131.0, 130.5, 130.4, 130.3, 129.8, 129.5, 129.4, 114.4, 113.7, 96.5, 96.2, 78.9, 46.2, 35.3, 34.2, 33.3, 33.0, 30.8, 29.8, 26.1, 25.8, 25.5, 25.1, 25.0, 24.7, 23.1, 22.4, 12.8 ppm; ESI mass spec. m/z 551.0; UV-Vis λ_{max} = 556 nm.

Example Copolymerization using Rhodamine B-labeled cyclooctene (32)

PEGylated cyclooctene macromonomer **4** (0.50 g, 0.53 mmol) (MW ca. 950), cyclooctene (58 mg, 0.52 mmol), and Rhodamine B labeled **32** (3.1 mg, 5.3 μmol) were weighed into a small tube and dissolved in 0.2 mL dry CH_2Cl_2. The contents were subjected to two freeze/pump/thaw cycles and then stirred at 40 ^{o}C under N_2. Catalyst **II** (3.52 mg, 4.14 μmol) was weighed into a small vial, degassed, and dissolved in dry CH_2Cl_2 (0.35 mL) under N_2. The catalyst solution was introduced by syringe, and the mixture was stirred at 40 ^{o}C until stirring ceased due to increased viscosity (approx. 15 minutes). The reaction was terminated using dodecyl vinyl ether, and CH_2Cl_2 (~1 mL) was added to improve stirring. The contents were precipitated into cold hexane, filtered, and dried under vacuum to yield the fluorescent copolymer (0.46 g, 82%). ^{1}H NMR ($CDCl_3$) δ 5.34 (br, olefin 2H), 4.86 (br s, 1H), 4.22 (t, 2H), 3.5-3.7 (complex, br m), 3.36 (s, 3H), 2.61 (br m, 4H), 2.32 (br s), 1.94 (br s), 1.50 (br s), 1.26 ppm (br s); ^{13}C NMR ($CDCl_3$) δ 172.7 (ester), 172.3 (ester), 130.0, 130.8, 129.3, 74.7, 72.3, 70.9, 69.4, 64.2, 59.4, 34.4, 33.0, 30.0, 29.7, 29.5, 28.8, 25.6 ppm. IR (NaCl plate) 2922, 2867, 1733 (ester), 1456, 1349, 1300, 1250, 1111, 1040, 968, 860 cm^{-1}. GPC (DMF w/ 0.01% LiCl

vs. linear polystyrene standards) M_n = 235,000 g/mol, M_w = 313,000 g/mol, PDI = 1.33. UV-Vis λ_{max} = 556 nm.

Synthesis of 5-bromo-1-cyclooctene (33)

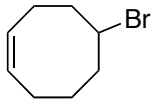

5-Bromo-1-cyclooctene was prepared in 80% yield from 1,5-cyclooctadiene as reported by Ashby and coworkers.[3]

Synthesis of 5-azido-1-cyclooctene (34)

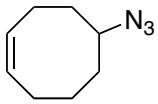

5-bromo-1-cyclooctene (**34**) (18.0 g, 95.2 mmol) and sodium azide (18.6 g, 285.5 mmol) were dissolved in dimethylsulfoxide (150 mL) and heated to 115 ºC for 4 hours. The mixture was cooled to room temperature, poured into water (400 mL), and extracted twice with diethyl ether. The organic fractions were combined, dried over $MgSO_4$, and concentrated to a dark brown oil. The product was purified, first, by column chromatography on silica gel eluting with hexanes, followed by distillation (b.p. 37 ºC, 85 mTorr) to yield 6.5 g (45% yield) of a colorless oil. ^{1}H NMR ($CDCl_3$) δ 5.64 (m, 2H), 3.47 (m, 1H), 2.37 (m, 1H), 2.17 (m, 3H), 1.39 - 1.96 (complex m, 6H) ppm; ^{13}C NMR ($CDCl_3$) δ 133.3, 130.0, 129.5, 125.8, 62.3, 33.9, 32.9, 31.2, 30.5, 28.6, 26.0, 23.2, 22.4 ppm; ATR-IR 3018, 2929, 2858, 2087, 1467, 1446, 1368, 1318, 1251, 1123, 1033, 991, 971, 926, 882, 726 cm^{-1}.

Synthesis of 5-amino-1-cyclooctene (35)

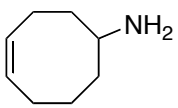

5-azido-1-cyclooctene (**34**) (5.9 g, 39.0 mmol) was diluted with THF (50 mL) and triphenylphosphine (14.3 g, 54.6 mmol) was added while stirring. The mixture was stirred for 30 minutes with visible gas evolution resulting from the loss of N_2. Deionized water (5 mL) was subsequently added, and the contents were stirred for 12 hours. The mixture was concentrated, dissolved in diethyl ether, and extracted three times with 1 M HCl (aq). The combined aqueous fractions were neutralized to pH 12 with a 30 wt % NaOH solution (aq) and extracted 3 times with diethyl ether. The combined organic fractions were dried over $MgSO_4$ and concentrated. The product was purified by distillation (b.p. 40 ºC, 40 mTorr) to yield 3.8 g (78% yield) of a colorless oil. ^{1}H NMR ($CDCl_3$) δ 5.62 (m, 2H), 2.85 (m, 1H), 2.02 – 2.27 (m, 3H), 1.22 – 1.72 (m, 6H) ppm; ^{13}C NMR ($CDCl_3$) δ 130.2, 129.6, 51.7, 39.0, 37.0, 26.2, 25.9, 24.0 ppm; ATR-IR 3354, 3281, 3014, 2917, 2852, 1661, 1595, 1466, 1448, 1370, 1241, 1068, 882, 756, 723 cm^{-1}.

Synthesis of 4-azidobenzoic acid (36)

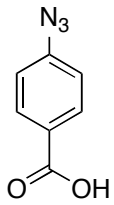

4-azidobenzoic acid was prepared in 70% yield from 4-aminobenzoic acid as described by Ulbricht and coworkers.[4,5]

Synthesis of amide-linked, phenyl azide-functional cyclooctene (38)

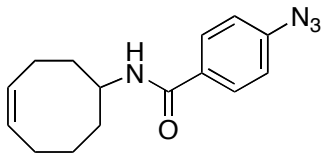

4-azidobenzoic acid (**36**) (2.0 g, 12.2 mmol) was added to a dry round-bottom flask and dissolved in anhydrous THF (100 mL) under N_2. The solution was cooled to 0^oC and thionyl chloride (0.9 mL, 12.8 mmol) was added by syringe over approx. 5 minutes. The reaction mixture was allowed to stir for 1 hr while warming to room temperature. The reaction was again cooled to 0 ^oC and triethylamine (4.2 mL, 24.4 mmol) was added by syringe. A white precipitate was immediately formed and the mixture was allowed to stir for an additional 15 minutes at 0 ^oC. A solution of 5-amino-1-cyclooctene (**35**) (1.7 g, 13.4 mmol) in anhydrous THF (10 mL) was then added by syringe and the reaction was warmed to room temperature and stirred for 16 hours. The reaction mixture was filtered over Celite to remove the salt by-products and the solution was concentrated to a light yellow solid. The crude product was dissolved in diethyl ether and washed once with DI water and once with 1 M HCl (aq). The organic layer was dried over $MgSO_4$ and concentrated. The resulting solid was purified by column chromatography on silica gel (90/10 → 70/30 hexanes/ethyl acetate) followed by crystallization from hexanes to afford 3.0 g (91% yield) of **38** as light yellow crystals. ^1H NMR ($CDCl_3$) δ 7.74 (m, 2H), 7.02 (m, 2H), 6.23 (br s, 1H), 5.72 (m, 2H), 4.16 (m, 1H), 2.14-2.40 (complex br m, 4H), 1.80-2.01 (complex br m, 2H), 1.50-1.76 (complex br m, 4H); ^{13}C NMR ($CDCl_3$) δ 165.1, 143.1, 131.5, 130.5, 129.8, 128.7, 128.6, 118.9, 49.9, 35.3, 34.4, 26.0, 25.9, 23.4; ATR-FTIR 3306, 3058, 3023, 2933, 2855, 2410, 2120, 1625, 1601, 1571, 1542, 1498, 1337, 1279, 1187, 1149, 1123, 847, 768, 725 cm^{-1}.

Synthesis of glycine(Boc)-functionalized cyclooctene

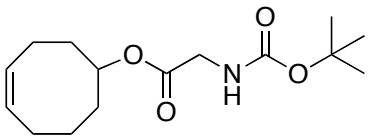

5-hydroxy-1-cyclooctene (**1**) (5.0 g, 39.6 mmol) and Boc-protected glycine (6.6 g, 37.6 mmol) were combined in a round-bottom flask and dissolved in anhydrous dichloromethane (80 mL) and anhydrous dimethylformamide (20 mL). In a separate flask, dicyclohexylcarbodiimide (DCC) (7.8 g, 38.0 mmol) and N,N-dimethylaminopyridine (DMAP) (0.50 g, 4.1 mmol) were combined and dissolved in dichloromethane (20 mL). The solution of DCC and DMAP were subsequently added to the solution of **1** and Boc-protected glycine while stirring with N,N'-dicyclohexylurea (DCU) precipitate observed almost immediately after addition. The mixture was stirred for 16 hours at room temperature under N_2. DCU was removed by filtration, and the contents were concentrated to yield a viscous oil. The crude product was then dissolved in diethyl ether and washed twice with water. The organic layer was dried over $MgSO_4$, concentrated, and purified by column chromatography on silica gel (90/10 → 80/20 hexanes/ethyl acetate) to yield 9.4 g (85% yield) of a colorless, viscous oil. ^{1}H NMR ($CDCl_3$) δ 5.60 (m, 2H), 5.05 (br s, 1H), 4.86 (m, 1H), 3.81 (d, 2H), 2.30 (m, 1H), 2.03-2.15 (m, 3H), 1.78-1.95 (m, 2H), 1.63-1.74 (m, 1H), 1.48-1.62 (m, 3H), 1.40 (s, 9H); ^{13}C NMR ($CDCl_3$) δ 170.0, 156.0, 130.1, 129.8, 80.1, 77.7, 43.0, 33.9, 33.8, 28.6, 25.8, 25.0, 22.5; ATR-FTIR 3370, 3015, 2976, 2933, 2861, 1700, 1511, 1467, 1452, 1390, 1365, 1282, 1249, 1198, 1161, 1054, 1030, 964, 918, 865, 778, 726 cm^{-1}.

Synthesis of glycine-functionalized cyclooctene (HCl salt) (40)

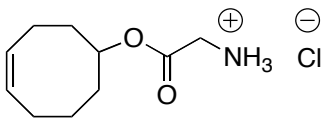

Glycine(Boc)-functionalized cyclooctene (3.0 g, 10.6 mmol) was weighed into a dry, round-bottom flask and dissolved in anhydrous THF (20 mL). HCl (20 mL, 4.0 M in

dioxane) was added to the stirring solution by syringe, and the contents were stirred for 12 hrs at room temperature under N_2. After stirring for some time, a white precipitate was observed. The mixture was concentrated, and the solid contents were suspended in hexane, filtered, and dried under reduced pressure to yield 2.2 g (94% yield) of a white powder. ^{1}H NMR (d_6-DMSO) δ 8.55 (br s, 3H), 5.66 (m, 2H), 4.81 (m, 1H), 3.69 (s, 2H), 2.35 (m, 1H), 2.03-2.19 (br m, 3H), 1.85 (m, 2H), 1.73 (m, 1H), 1.63 (m, 2H), 1.47 (m, 1H); ^{13}C NMR (d_6-DMSO) δ 166.8, 129.7, 129.5, 77.0, 49.9, 33.1, 33.0, 25.1, 24.5, 21.7; ATR-FTIR 3206, 3010, 2937, 2860, 1737, 1553, 1513, 1463, 1430, 1403, 1223, 1126, 1058, 1038, 971, 912, 885, 730 cm^{-1}.

Synthesis of ester-linked, phenyl azide-functional cyclooctene (41)

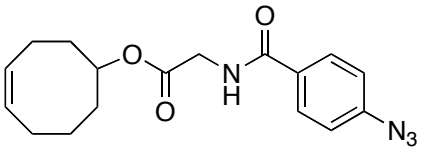

4-azidobenzoic acid (**36**) (1.00 g, 12.2 mmol) was added to a dry round-bottom flask and dissolved in anhydrous THF (50 mL) under N_2. The solution was cooled to 0 ^{o}C and thionyl chloride (0.47 mL, 6.4 mmol) was added by syringe. The mixture was stirred for 1 hr while warming to room temperature. The reaction was again cooled to 0 ^{o}C and triethylamine (6.30 mL, 36.6 mmol) was added over five minutes by syringe. A white precipitate was immediately formed and the contents were stirred for 15 minutes at 0 ^{o}C. In a separate flask, glycine-functionalized cyclooctene **40** (1.5 g, 6.7 mmol) was dissolved in anhydrous THF (10 mL) and added to the reaction by syringe. The reaction contents were then warmed to room temperature and stirred for 16 hours. The mixture was filtered over Celite to remove the salt by-products and concentrated to a light yellow solid. The solid was dissolved in diethyl ether and washed once with DI water and once

with 1 M HCl (aq). The organic layer was dried over $MgSO_4$ and concentrated. The product was purified by column chromatography on silica gel (80/20 → 70/30 hexanes/ethyl acetate) followed by crystallization in hexanes to afford 1.7 g (85% yield) of **41** as light yellow crystals. ^{1}H NMR ($CDCl_3$) δ 7.80 (m, 2H), 7.04 (m, 2H), 6.78 (br m, 1H), 5.67 (m, 2H), 4.94 (m, 1H), 4.15 (d, 2H), 2.35 (br m, 1H), 2.06-2.20 (br m, 3H), 1.91 (br m, 2H), 1.51-1.80 (complex br m, 4H); ^{13}C NMR ($CDCl_3$) δ 169.7, 166.5, 143.8, 130.4, 130.1, 129.6, 129.0, 119.2, 77.7, 42.3, 33.8, 25.7, 25.0, 22.3; ATR-FTIR 3366, 3020, 2933, 2858, 2114, 2089, 1734, 1640, 1603, 1548, 1498, 1364, 1302, 1285, 1203, 995, 847, 761 cm^{-1}.

Synthesis of phenyl azide (amide)-functionalized PCOE-*g*-PEG 2200 (Copolymer 42)

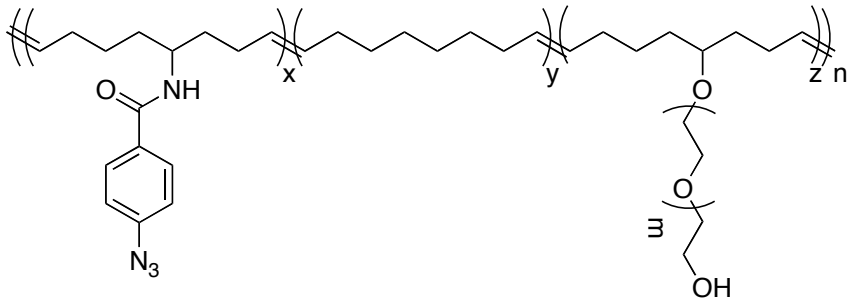

m ~ 49

PEG 2200 (m ~ 49) macromonomer (**9**) (0.62 g, 0.27 mmol), cyclooctene (0.05 g, 0.45 mmol), and phenyl azide-functional cyclooctene **38** (0.05 g, 0.19 mmol) were combined in a dry reaction tube. 0.7 mL of anhydrous THF was added to the reaction under N_2. In a separate vial, catalyst **III** (16.0 mg, 18.1 μmol) was dissolved in 0.2 mL dry THF. Both the monomer mixture and catalyst solution were subjected to two freeze/pump/thaw cycles and subsequently warmed to room temperature. The catalyst solution was rapidly added to the monomer mixture and stirred for 30 min. Ethyl vinyl

ether (1 mL) was added to terminate the polymerization and dichloromethane was added to dilute the polymer solution. The product was precipitated into diethyl ether, isolated by filtration, and dried under vacuum to yield 0.67 g (93% yield) of a light purple solid. ^{1}H NMR ($CDCl_3$) δ 7.74 (d), 7.02 (d), 5.35 (m), 4.30 (m), 4.12 (m), 3.37-3.80 (br m), 3.23 (br m), 2.30 (br s), 1.94, (br m), 1.27-1.53 (br m); ATR-FTIR 3477, 2882, 2121, 1634, 1467, 1360, 1342, 1279, 1241, 1147, 1102, 1061, 962, 842 cm^{-1}. GPC (THF, relative to PS standards) M_n 46,700 Da, M_w 123,300 Da, PDI 2.64.

Synthesis of phenyl azide (ester)-functionalized PCOE-*g*-PEG 2200 (Copolymer 43)

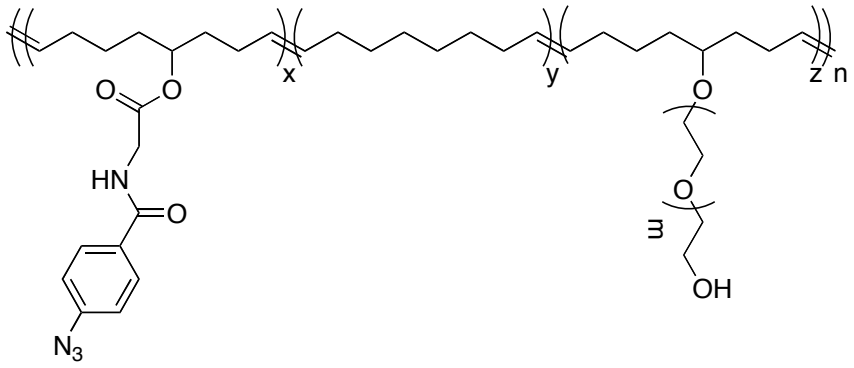

m ~ 49

PEG 2200 (m ~ 49) macromonomer (**9**) (0.63 g, 0.27 mmol), cyclooctene (0.05 g, 0.45 mmol), and phenyl azide-functional cyclooctene **41** (0.06 g, 0.18 mmol) were combined in a dry reaction tube. 0.7 mL of anhydrous THF was added under N_2. In a separate vial, catalyst **III** (16.1 mg, 10.4 μmol) was dissolved in 0.2 mL dry THF. Both the monomer mixture and catalyst solution were subjected to two freeze/pump/thaw cycles and subsequently warmed to room temperature. The catalyst solution was rapidly added to the monomer mixture and stirred for 30 min. Ethyl vinyl ether (1 mL) was added to terminate the polymerization and dichloromethane was added to dilute the polymer solution. The product was precipitated into diethyl ether, isolated by filtration,

and dried under vacuum to yield 0.63 g (85% yield) of a light purple solid. ^{1}H NMR ($CDCl_3$) δ 7.80 (br s), 7.03 (br s), 5.35 (m), 4.95 (s), 4.16 (s), 3.40-3.80 (br m), 3.22 (s), 2.49 (br s), 1.93, (br m), 1.27-1.53 (br m); ^{13}C NMR ($CDCl_3$) δ 170.0, 166.4, 143.7, 130.8, 130.4, 130.0, 129.5, 129.1, 128. 8, 119.1, 87.3, 79.5, 72.63, 71.1, 71.0, 70.7, 68.1, 61.9, 54.1, 42.1, 34.1, 33.7, 32.7, 33.5, 29.8, 29.2, 28.6, 27.3, 25.4, 23.3;

Synthesis of 5-cyano-1-cyclooctene (46)

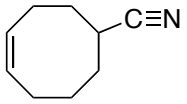

5-cyano-1-cyclooctene was prepared in 68% yield from 5-bromo-1-cyclooctene (**33**) as described by Grubbs and coworkers.[2]

Synthesis of 5-carboxylic acid-1-cyclooctene (47)

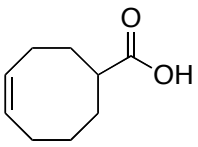

5-carboxylic acid-1-cyclooctene was prepared in 62% yield from 5-cyano-1-cyclooctene (**46**) as described by Hartley and coworkers.[6]

Synthesis of hydrazine (Boc)-functionalized cyclooctene (48)

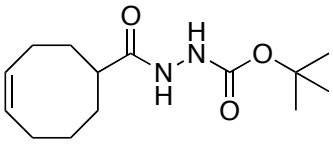

5-carboxylic acid-1-cyclooctene (**47**) (5.0 g, 32.4 mmol), *tert*-butyl carbazate (4.7 g, 35.7 mmol), and DMAP (0.5 g, 3.8 mmol) were weighed into an oven-dried round bottom flask and dissolved in 100 mL anhydrous dichloromethane under N_2. DCC (7.4 g, 35.7 mmol) was added to the solution as a solid with stirring, and a white precipitate was immediately observed. The reaction was stirred for 16 hrs at room temperature

under N_2. The reaction solution was filtered, and the product was concentrated to a viscous liquid. The contents were dissolved in diethyl ether and cooled to -20 ^{o}C for 6 hours to precipitate dissolved DCU. Following filtration, the filtrate was washed with 0.1 M HCl (aq) and then 0.1 M $NaHCO_3$ (aq). The organic phase was dried with $MgSO_4$ and concentrated to a viscous oil. The product was purified by column chromatography on silica gel (80/20 → 70/30 hexanes/ethyl acetate) followed by crystallization in hexanes to afford 5.5 g (63% yield) of white crystals. ^{1}H NMR ($CDCl_3$) δ 7.70 (br s, 1H), 6.73 (br s, 1H), 5.65 (m, 2H), 1.28 - 2.40 (complex br m, 20H); ^{13}C NMR ($CDCl_3$) δ 177.4, 155.9, 130.8, 129.8, 81.8, 43.1, 32.2, 30.1, 28.3, 28.1, 26.1, 24.2; ATR-FTIR 3236, 3016, 2928, 2855, 1734, 1710, 1662, 1631, 1540, 1450, 1367, 1255, 1161, 1009, 863, 719 cm^{-1}.

Synthesis of hydrazine (Boc)-functionalized PCOE-*g*-PEG 2200 (Copolymer 49)

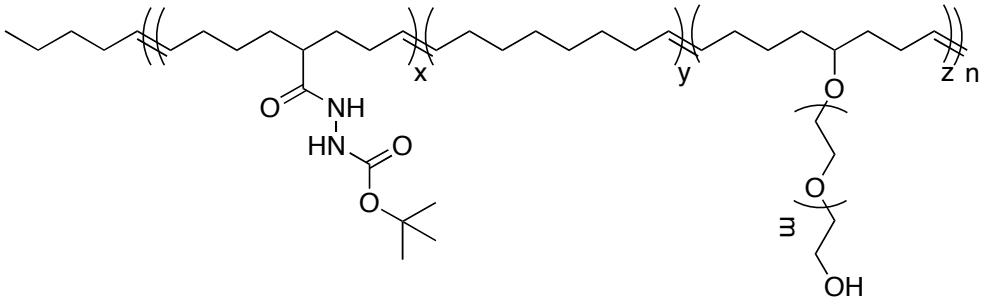

m ~ 49

PEG 2200 (m ~ 49) macromonomer (**9**) (1.25 g, 0.54 mmol), cyclooctene (0.04 g, 0.36 mmol), and hydrazine (Boc)-functional cyclooctene **48** (0.24 g, 0.89 mmol) were combined in a dry round-bottom flask. 0.35 mL of a 0.05 M 1-hexene solution in DCM was added to the reaction under N_2 followed by 1.2 mL dry DCM. In a separate vial, catalyst **II** (6.1 mg, 7.2 μmol) was dissolved in 0.2 mL dry DCM. The catalyst solution was rapidly added to the monomer mixture and stirred until the polymerization had vitrified (approx. 10 minutes). Ethyl vinyl ether (1 mL) was added to terminate the

polymerization and dichloromethane was added to dilute the polymer solution. The product was precipitated into diethyl ether, isolated by filtration, and dried under vacuum to yield 1.45 g (95% yield) of an off-white solid. ^{1}H NMR (d_6-DMSO) δ 9.47 (d), 8.65 (d), 5.35 (m), 3.30-3.75 (br m), 3.22 (br m), 1.75-2.20, (br m), 1.15-1.60 (br m); ^{13}C NMR (d_6-DMSO) δ 174.5, 154.9, 130.1, 129.8, 129.4, 129.1, 78.1, 77.5, 72.6, 71.1, 71.0, 70.7, 67.6, 60.0, 43.2, 33.2, 32.8, 32.2, 30.1, 29.1, 28.3, 28.1, 26.1, 24.8; ATR-FTIR 3291, 2882, 1726, 1466, 1359, 1342, 1279, 1241, 1103, 1060, 961, 841, 750 cm^{-1}, GPC (THF, relative to PS standards) M_n 97,800 Da, M_w 201,700 Da, PDI 2.06

Deprotection of hydrazine (Boc)-functionalized PCOE-*g*-PEG 2200 (Copolymer 50)

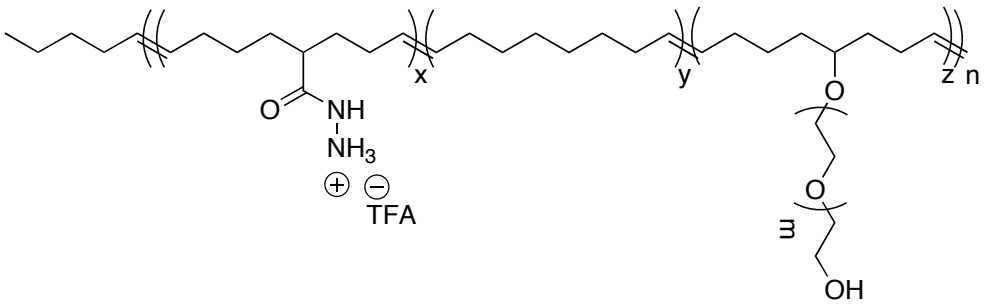

m ~ 49

Hydrazine (Boc)-functionalized PCOE-*g*-PEG 2200 (**49**) (550 mg) was dissolved in DCM (5 mL). Trifluoroacetic acid (5 mL) was added and gas evolution was immediately observed. The reaction contents were stirred for 1 hour, open to the atmosphere. The deprotected polymer was precipitated into cold diethyl ether and filtered. The polymer was dissolved in a dichloromethane/methanol mixture and precipitated again into cold diethyl ether. Copolymer **50** was isolated by filtration and dried *in vacuo* to yield 420 mg (95% yield) of a light yellow powder. ^{1}H NMR (d_6-DMSO) δ 10.47 (s), 5.34 (m), 4.50 (s), 3.30-3.75 (br m), 3.22 (s), 1.75-2.20, (br m), 1.15-1.60 (br m); ^{13}C NMR (d_6-DMSO) δ 174.1, 158.1, 130.0, 129.6, 129.2, 118.6, 115.7,

86.4, 78.1, 72.4, 71.1, 70.6, 70.2, 69.8, 67.6, 60.2, 53.3, 43.1, 40.1, 38.9, 33.4, 32.9, 32.0, 29.9, 29.1, 28.5, 27.9, 26.7, 24.7, 22.6; ATR-FTIR 2882, 1675, 1466, 1342, 1280, 1241, 1099, 961, 841, 721 cm^{-1}.

Synthesis of 4-azidophenyl sulfone (51)

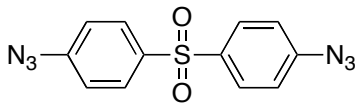

4-aminophenyl sulfone (6.2 g, 25.0 mmol) was dissolved in 50 mL of deionized water and cooled to 0°C. 15 mL of concentrated HCl was added and the solution was stirred for 5 minutes. In a separate flask, $NaNO_2$ (6.9 g, 100 mmol) was dissolved in 40 mL of DI water and cooled to 0°C. The $NaNO_2$ solution was added to the 4-aminophenyl sulfone solution over 15 minutes being careful to control of temperature at 0°C. The diazophenyl sulfone solution was then added to a solution of NaN_3 (9.8 g, 150 mmol) in 1 L of DI water which had been cooled to 0 °C. 4-azidophenyl sulfone precipitated immediately upon addition with N_2 evolution forming a foaming suspension. DI water (400 mL) was added over the course of the reaction to improve stirring. The reaction was stirred for 30 minutes and ethyl acetate was added to dissolve the product. The solution was transferred to a separatory funnel and extracted 3X with ethyl acetate. The organic fractions were combined, dried of $MgSO_4$, and concentrated to a yellow solid. The product was purified by column chromatography on silica gel (70/30 → 50/50 hexanes/ethyl acetate) followed by crystallization in hexanes to afford 2.3 g (31% yield) of yellow crystals. ^{1}H NMR (d_6-DMSO) δ 7.95 (d, 4H), 7.32 (d, 4H); ATR-FTIR 3085, 3054, 2095, 1582, 1489, 1412, 1281, 1158, 1098, 820, 729 cm^{-1}.

Representative synthesis of PCOE-*g*-PEG (Copolymer 56)

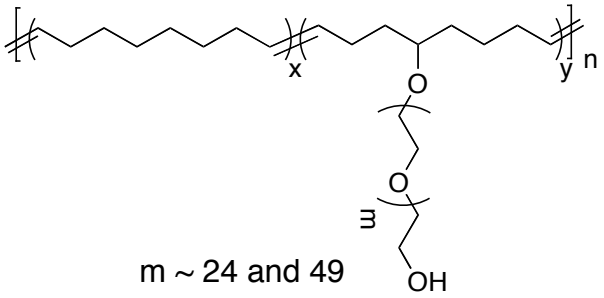

PEG 1200 (m ~ 24) macromonomer (**8**) (0.2 g, 0.2 mmol), PEG 2200 (m ~ 49) macromonomer (**9**) (0.1 g, 0.06 mmol), and cyclooctene (0.3 g, 2.7 mmol) were combined in a dry reaction tube. 0.6 mL of a 0.05 M 1-hexene solution in dichloromethane was added to the reaction under N_2 followed by 0.5 mL of dry dichloromethane. In a separate vial, catalyst **II** (4.9 mg, 5.7 μmol) was dissolved in 0.4 mL dry dichloromethane. Both the monomer mixture and catalyst solution were subjected to two freeze/pump/thaw cycles and subsequently warmed to 40 ^{o}C. The catalyst solution was then rapidly added to the monomer solution and stirred until vitrified (approx. 5 min). Ethyl vinyl ether (1 mL) was added to terminate the polymerization and dichloromethane was added to dilute the polymer solution. The product was precipitated into cold hexane containing 1 wt % BHT, isolated by filtration, and dried under vacuum to yield 0.58 g (93.5% yield) of an off-white solid. ^{1}H NMR ($CDCl_3$) δ 5.36 (m), 3.37-3.97 (br m), 3.24 (br s), 2.43 (br s), 1.94, (br m), 1.27-1.53 (br m); ^{13}C NMR ($CDCl_3$) δ 130.2, 72.6, 70.6, 70.3, 61.7, 32.6, 29.6, 29.1; ATR-FTIR 2921, 2852, 1468, 1344, 1281, 1242, 1104, 963, 842 cm^{-1}. GPC ($CHCl_3$, relative to PS standards) M_n 22,700 Da, M_w 39,800 Da, PDI 1.76.

Synthesis of PCOE-*g*-PEG 4400-*g*-Phenyl Azide copolymer (Copolymer 58)

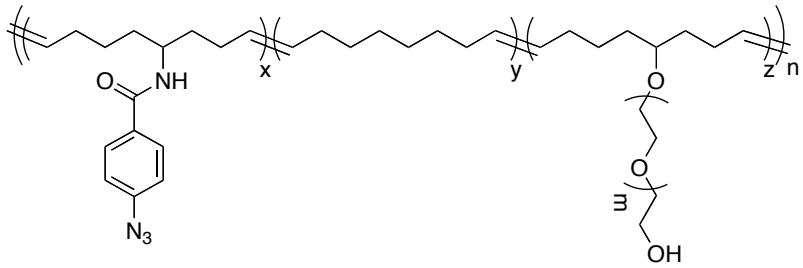

PEG 4400 (m ~ 99) macromonomer (**10**) (1.7 g, 0.4 mmol), cyclooctene (0.1 g, 1.1 mmol), and phenyl azide-functional cyclooctene **38** (0.1 g, 0.4 mmol) were combined in a dry reaction tube. 0.9 mL of a 0.05 M 1-hexene solution in dichloromethane was added to the reaction under N_2 followed by 0.7 mL dry THF. In a separate vial, catalyst **III** (9.2 mg, 10.4 μmol) was dissolved in 0.2 mL dry THF. Both the monomer mixture and catalyst solution were subjected to two freeze/pump/thaw cycles and subsequently warmed to room temperature. The catalyst solution was rapidly added to the monomer mixture and stirred for 30 min. Ethyl vinyl ether (1 mL) was added to terminate the polymerization and dichloromethane was added to dilute the polymer solution. The product was precipitated into diethyl ether, isolated by filtration, and dried under vacuum to yield 1.75 g (92% yield) of a light purple solid. ^{1}H NMR ($CDCl_3$) δ 7.74 (d), 7.02 (d), 5.35 (m), 4.30 (m), 4.12 (m), 3.37-3.80 (br m), 3.23 (br m), 2.30 (br s), 1.94, (br m), 1.27-1.53 (br m); ATR-FTIR 3477, 2882, 2121, 1634, 1467, 1360, 1342, 1279, 1241, 1147, 1102, 1061, 962, 842 cm^{-1}. GPC (THF, relative to PS standards) M_n 27,600 Da, M_w 54,000 Da, PDI 1.96.

Synthesis of tetraethylene glycol dimesylate (59)

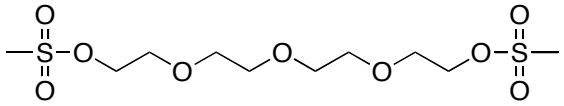

10.0 g (51.0 mmol) of tetraethylene glycol was diluted with 200 mL of anhydrous THF under N_2 and cooled to 0 ^oC. Methanesulfonyl chloride (8.8 mL, 114.7 mmol) was added by syringe, and triethylamine (17.8 mL, 127.5 mmol) was then added as a solution in 50 mL anhydrous THF via addition funnel over approximately 30 minutes. The reaction was allowed to warm to room temperature and stirred for an additional 2 hours. The reaction mixture was diluted with $NaHCO_3$ (aq), and the product was extracted 2X with chloroform. The product was concentrated, stirred over $NaHCO_3$ (aq) for approx. 30 minutes, and extracted 2X with chloroform. The organic fractions were combined, washed with1 M HCl (aq), and stirred over carbon black and magnesium sulfate. The solution was filtered and concentrated to yield 17.4 g (88 % yield) of a colorless oil. ^1H NMR ($CDCl_3$) δ 4.32 (m, 4H), 3.72 (m, 4 H), 3.62 (s, 8H), 3.03 (s, 6H); ^{13}C NMR ($CDCl_3$) δ 70.6, 69.3, 69.0, 37.7.

Synthesis of *bis*-cyclooctene tetraethylene glycol (60)

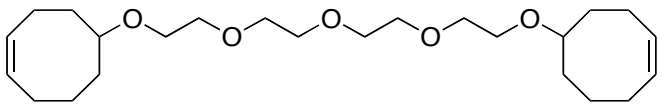

Sodium hydride (3.5 g, 145.2 mmol) was weighed into an oven dried RB flask and suspended in 300 mL of anhydrous DMF. A solution of 5-hydroxy-1-cyclootene (**1**) (16.7 g, 132.0 mmol) in 50 mL of anhydrous THF was added to the sodium hydride suspension and stirred for 1.5 hr. Tetraethylene glycol dimesylate (**59**) (18.5 g, 52.8 mmol) was then added as a solution in 50 mL anhydrous DMF and stirred overnight at room temperature. A small quantity of water was added slowly to the reaction mixture to quench the unreacted sodium hydride and subsequently diluted with a larger volume of water. The product was extracted 3X with diethyl ether, dried over magnesium sulfate,

and concentrated. The crude product was purified by column chromatography (silica, 85/15 hexane/ethyl acetate → 70/30 hexane/ethyl acetate) to afford 9.5 g (44 % yield) of product as a colorless oil. ^{1}H NMR ($CDCl_3$) δ 5.58 (m, 4H), 3.45-3.64 (complex m, 16H), 3.32 (m, 2H), 2.27 (m, 2H), 1.28-2.18 (complex br m, 20H); ^{13}C NMR ($CDCl_3$) δ 130.2, 129.7, 81.1, 71.1, 70.9, 70.8, 67.9, 34.3, 33.5, 25.9, 25.8, 22.8; ATR-FTIR 3014, 2925, 2858, 1729, 1467, 1450, 1345, 1298, 1243, 1092, 1044, 988, 949, 880, 754, 725 cm^{-1}.

Synthesis of tetraethylene glycol substituted pyridine (62)

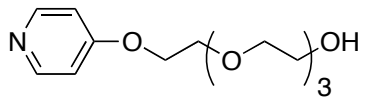

To a dry, round-bottom flask was added 4-hydroxypyridine (3.00 g, 31.6 mmol), triphenylphosphine (9.10 g, 34.7 mmol), tetraethylene glycol (36.8 g, 189 mmol), and dry THF (125 mL). The mixture was stirred under $N_{2(g)}$ at 0 °C (ice-water bath), and diisopropyl azodicarboxylate (6.80 mL, 34.7 mmol) was added by syringe over a 10 minute period. The mixture was stirred for 30 minutes, the ice bath was removed, and the reaction was allowed to stir under nitrogen for 12 hours at room temperature. The reaction mixture was then concentrated, dissolved in chloroform, and extracted three times with 1 M HCl (aq). The combined aqueous fractions were treated with a 30 weight percent NaOH solution until a pH of 12 was reached. The product was extracted three times with chloroform, and the combined organic fractions were dried over $MgSO_4$ and concentrated. Excess tetraethylene glycol was removed by vacuum distillation, and the residue was purified by column chromatography over silica gel to yield 3.4 g of a colorless oil (40% yield): ^{1}H NMR ($CDCl_3$) δ 8.38 (d, 2H), 6.80 (d, 2H), 4.14 (t, 2H), 3.83 (t, 2H), 3.55-3.70 (br m, 12H), 3.08 (br s, 1H); ^{13}C NMR ($CDCl_3$) δ 164.8, 150.6,

110.3, 72.6, 70.7, 70.2, 69.2, 69.1, 67.1, 61.2; ATR-FTIR 3246, 3036, 2870, 1639, 1591, 1568, 1502, 1454, 1422, 1352, 1284, 1211, 1119, 1051, 1000, 991, 929, 887, 817, 730, 699 cm^{-1}; HPLC (7:3 H_2O:acetonitrile (0.1% trifluoroacetic acid)) retention time, 1.62 min.

Synthesis of tetraethylene glycol substituted ruthenium benzylidene catalyst (63)

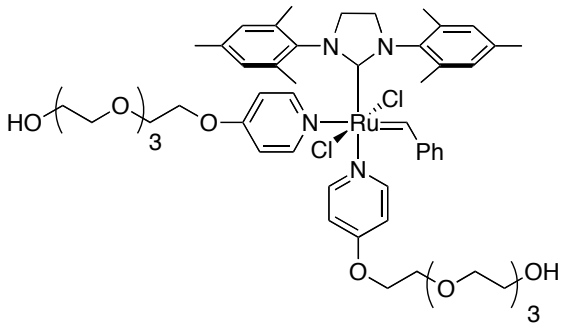

A solution of Grubbs' Generation II catalyst (catalyst **II**) (50.0 mg, 58.9 mmol) and PEG-pyridine ligand **62** (0.16 g, 0.59 mmol) in dry dichloromethane (0.3 mL) was stirred under nitrogen for 1 hour. Dichloromethane was removed *in vacuo*, and the remaining green oil was diluted with water to precipitate tricyclohexylphosphine. This aqueous solution was subjected to centrifugation for five minutes, to give a clear, dark green, aqueous solution that was removed by pipette. The green aqueous catalyst solutions was concentrated under vacuum (Kügelrohr) to afford a viscous green oil composed of a mixture of **62** and **63**. This oil could be diluted in either organic solvents or water for use in ring-opening metathesis polymerization. ^{1}H NMR ($CDCl_3$) δ 19.20 (s, catalyst, benzylidene), 8.38 (d, PEG-pyridine ligand), 7.83 (d, catalyst), 7.71 (br s, catalyst), 7.65 (d, catalyst), 7.45 (m, catalyst), 7.33 (m, catalyst), 7.20 (m, catalyst), 7.05 (m, catalyst), 6.94 (t, catalyst), 6.93 (s, catalyst), 6.80 (d, PEG-pyridine ligand), 6.76 (m, catalyst), 6.21 (br s, catalyst), 4.14 (t, PEG-pyridine ligand), 3.83 (t, PEG-pyridine

ligand), 3.55-3.70 (br m, PEG-pyridine ligand), 3.18 (m, catalyst), 2.93 (m, catalyst), 2.57, (s, catalyst), 2.15-2.4 (br m, catalyst); ^{31}P – no signals, indicative of absence of tricyclohexylphosphine.

Synthesis of *exo,exo*-5,6-bis(methoxycarbonyl)-7-oxabicyclo[2.2.1] hept-2-ene (64)

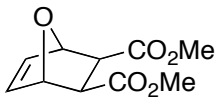

exo,exo-5,6-bis(methoxycarbonyl)-7-oxabicyclo[2.2.1] hept-2-ene was prepared as described by France and coworkers.[7]

Representative polymerization of 64 in dichloromethane (Polymer 68)

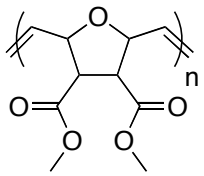

Exo,exo-5,6-bis(methoxycarbonyl)-7-oxabicyclo[2.2.1] hept-2-ene (**64**) (0.2 g, 0.9 mmol) was stirred in dry dichloromethane (1.9 mL) at room temperature under $N_{2(g)}$. 0.64 mL of a 0.03 M solution of **63** in dichloromethane was added rapidly by syringe. The mixture was stirred for 30 minutes, and ethyl vinyl ether (0.5 mL) was added. Precipitation into cold methanol gave a white solid that was filtered and dried *in vacuo* to afford 0.17 g (85% yield) of polymer **68**. ^{1}H NMR ($CDCl_3$) δ 5.89 (m, 1H), 5.62 (m, 2H), 5.05 (br m, 2H), 4.71 (br m, 1H), 3.68 (br m, 6H), 3.08 (m, 2H); GPC (in THF *vs.* linear polystyrene standards) M_n = 65,900 g/mol, M_w = 71,400 g/mol, PDI = 1.08.

Synthesis of 10-oxa-4-aza-tricyclo[5.2.1.0^{2,6}]dec-8-ene-3,5-dione (69)

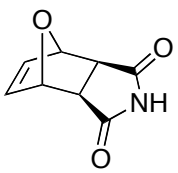

10-oxa-4-aza-tricyclo[5.2.1.$0^{2,6}$]dec-8-ene-3,5-dione was prepared as described by Kwart and coworkers.[8]

Synthesis of tetraethylene glycol substituted oxanorbornene (70)

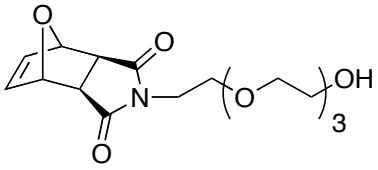

To a dry round-bottom flask was added the oxanorbornene imide, 10-oxa-4-aza-tricyclo[5.2.1.$0^{2,6}$]dec-8-ene-3,5-dione (**69**) (3.00 g, 18.2 mmol), triphenylphosphine (5.50 g, 20.9 mmol), tetraethylene glycol (17.6 g, 90.8 mmol), and dry THF (150 mL). The mixture was stirred under N_2 at 0 °C (ice-water bath), and diisopropyl azodicarboxylate (4.10 mL, 20.9 mmol) was added by syringe over a 10 minute period. The mixture was stirred for 30 minutes. The ice bath was then removed, and the mixture stirred for 12 hours at room temperature. The mixture was then concentrated, dissolved in ether, and extracted three times with water. The aqueous fractions were combined, and the product was then extracted from the aqueous phase with chloroform. The chloroform solution was dried over $MgSO_4$ and concentrated, and the product was purified by column chromatography on silica gel using hexane/ethyl acetate mixtures to yield 3.8 g (61% yield) of a viscous, colorless oil. ^{1}H NMR ($CDCl_3$) δ 6.48 (s, 2H), 5.23 (s, 2H), 3.55-3.70 (br m, 18H), 2.84 (s, 2H); ^{13}C NMR ($CDCl_3$) δ 176.4, 136.7, 81.0, 72.6, 70.7, 70.6, 70.5, 70.2, 67.3, 61.8, 47.6, 38.3; ATR-FTIR 3458, 2896, 1772, 1694, 1429, 1398, 1336, 1287, 1193, 1096, 1067, 1020, 916, 877, 853, 825, 813, 721, 710 cm^{-1}; HPLC (7:3 H_2O:acetonitrile, 0.1% trifluoroacetic acid) retention time, 1.99 min.

Representative polymerization of 70 in water (Polymer 71)

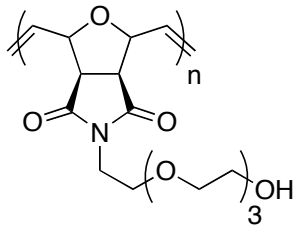

1.6 mL of a 0.015 M solution of **63** in acidified water (HCl, pH 1.5) was added to 1.3 mL acidified water (HCl, pH 1.5) in a reaction tube, and the mixture was stirred at room temperature under nitrogen. 1.0 mL of a 0.60 M stock solution of tetraethylene glycol substituted oxanorbornene **70** in acidified water (HCl, pH=1.0) was injected rapidly into the catalyst solution, and the mixture was allowed to stir for 30 minutes. Diethylene glycol vinyl ether was added, and the mixture was then concentrated, dissolved in a minimal amount of $CHCl_3$, and precipitated into cold hexane. The hexane was decanted and the polymer residue dried under vacuum to afford 0.16 g (80% yield) of polymer **71** as a tacky solid: ^{1}H NMR ($CDCl_3$) δ 6.08 (br s, 1H), 5.78 (br m, 1H), 5.05 (br m, 1H), 4.49 (br m, 1H), 3.55-3.70 (br m, 18H), 2.84 (br s, 2H); GPC (DMF with LiBr (0.05 M) *vs.* linear poly(methyl methacrylate) standards) M_n = 67,000 g/mol, M_w = 90,700 g/mol, PDI = 1.35.

7.4 References

(1) Love, J. A.; Morgan, J. P.; Trnka, T. M.; Grubbs, R. H. *Angew. Chem. Int. Edit.* **2002**, *41*, 4035-4037.
(2) Hillmyer, M. A.; Laredo, W. R.; Grubbs, R. H. *Macromolecules* **1995**, *28*, 6311-6316.
(3) Ashby, E. C.; Coleman, D. *J. Org. Chem.* **1987**, *52*, 4554-4565.
(4) Ulbricht, M.; Hicke, H. G. *Angew. Makromol. Chem.* **1993**, *210*, 69-95.
(5) Ulbricht, M.; Hicke, H. G. *Angewandte Makromol. Chem.* **1993**, *210*, 97-117.

(6) Hartley, D. *J. Chem. Soc.* **1962**, 4722.
(7) France, M. B.; Alty, L. T.; Earl, T. M. *J. Chem. Educ.* **1999**, *76*, 659-660.
(8) Kwart, H.; Burchuk, I. *J. Am. Chem. Soc.* **1952**, *74*, 3094-3097.

BIBLIOGRAPHY

Abuchowski, A. and F. F. Davis (1979). "Preparation and Properties of Polyethylene Glycol Trypsin Adducts." *Biochimica Et Biophysica Acta* 578(1): 41-46.

Abuchowski, A., G. M. Kazo, et al. (1984). "Cancer-Therapy with Chemically Modified Enzymes .1. Antitumor Properties of Polyethylene Glycol-Asparaginase Conjugates." *Cancer Biochemistry Biophysics* 7(2): 175-186.

Abuchowski, A., J. R. Mccoy, et al. (1977). "Effect of Covalent Attachment of Polyethylene-Glycol on Immunogenicity and Circulating Life of Bovine Liver Catalase." *Journal of Biological Chemistry* 252(11): 3582-3586.

Abuchowski, A., T. Vanes, et al. (1977). "Alteration of Immunological Properties of Bovine Serum-Albumin by Covalent Attachment of Polyethylene-Glycol." *Journal of Biological Chemistry* 252(11): 3578-3581.

Adams, M. L., A. Lavasanifar, et al. (2003). "Amphiphilic block copolymers for drug delivery." *Journal of Pharmaceutical Sciences* 92(7): 1343-1355.

Ahmed, F. and D. E. Discher (2004). "Self-porating polymersomes of PEG-PLA and PEG-PCL: hydrolysis-triggered controlled release vesicles." *Journal of Controlled Release* 96(1): 37-53.

Ahmed, F., R. I. Pakunlu, et al. (2006). "Shrinkage of a rapidly growing tumor by drug-loaded polymersomes: pH-triggered release through copolymer degradation." *Molecular Pharmaceutics* 3(3): 340-350.

Akizawa, T. K., K.; Koshikawa, S.; Ikada, Y.; Kishida, A.; Yamashita, M.; Imamura, K. (1989). *Transactions American Society for Artificial Internal Organs* 35: 333.

Ali, M. M. and H. D. H. Stover (2006). "Interfacial living radical copolymerization of oil- and water-soluble comonomers to form composite polymer capsules." *Journal of Polymer Science Part A-Polymer Chemistry* 44(1): 156-171.

Allen, C., D. Maysinger, et al. (1999). "Nano-engineering block copolymer aggregates for drug delivery." *Colloids and Surfaces B-Biointerfaces* 16(1-4): 3-27.

Allinger, N. L. and J. T. Sprague (1972). "Conformational-Analysis .84. Study of Structures and Energies of Some Alkenes and Cycloalkenes by Force Field Method." *Journal of the American Chemical Society* 94(16): 5734-&.

Antipov, A. A., G. B. Sukhorukov, et al. (2001). "Sustained release properties of polyelectrolyte multilayer capsules." *Journal of Physical Chemistry B* 105(12): 2281-2284.

Arshady, R. (1989). "Preparation of Microspheres and Microcapsules by Interfacial Polycondensation Techniques." Journal of Microencapsulation 6(1): 13-28.

Ashby, E. C. and D. Coleman (1987). "Evidence for Single Electron-Transfer in the Reactions of Lithium Dimethylcuprate with Alkyl-Halides." *Journal of Organic Chemistry* 52(20): 4554-4565.

Badaru, A., D. M. Wilson, et al. (2006). "Sequential comparisons of one-month and three-month depot leuprolide regimens in central precocious puberty." *Journal of Clinical Endocrinology and Metabolism* 91(5): 1862-1867.

Bae, Y., S. Fukushima, et al. (2003). "Design of environment-sensitive supramolecular assemblies for intracellular drug delivery: Polymeric micelles that are responsive

to intracellular pH change." *Angewandte Chemie-International Edition* 42(38): 4640-4643.

Bala, I., S. Hariharan, et al. (2004). "PLGA nanoparticles in drug delivery: The state of the art." *Critical Reviews in Therapeutic Drug Carrier Systems* 21(5): 387-422.

Bazan, G. C., E. Khosravi, et al. (1990). "Living Ring-Opening Metathesis Polymerization of 2,3-Difunctionalized Norbornadienes by Mo(Ch-Tert-Bu)(N-2,6-C6h3-Iso-Pr2)(O-Tert-Bu)2." *Journal of the American Chemical Society* 112(23): 8378-8387.

Belfort, G., R. H. Davis, et al. (1994). "The Behavior of Suspensions and Macromolecular Solutions in Cross-Flow Microfiltration." *Journal of Membrane Science* 96(1-2): 1-58.

Bell, C. L. and N. A. Peppas (1996). "Modulation of drug permeation through interpolymer complexed hydrogels for drug delivery applications." *Journal of Controlled Release* 39(2-3): 201-207.

Bell, C. L. and N. A. Peppas (1996). "Water, solute and protein diffusion in physiologically responsive hydrogels of poly(methacrylic acid-g-ethylene glycol)." *Biomaterials* 17(12): 1203-1218.

Berda, E. B., R. E. Lande, et al. (2007). "Precisely defined amphiphilic graft copolymers." *Macromolecules* 40(24): 8547-8552.

Bielawski, C. W., D. Benitez, et al. (2002). "An "endless" route to cyclic polymers." *Science* 297(5589): 2041-2044.

Bilyk, J. R., P. A. Rubin, et al. (1992). "Correction of enophthalmos with porous polyethylene implants." *International Ophthalmology Clinics* 32(3): 151-6.

Binder, W. H. and C. Kluger (2004). "Combining ring-opening metathesis polymerization (ROMP) with sharpless-type "click" reactions: An easy method for the preparation of side chain functionalized poly(oxynorbornenes)." *Macromolecules* 37(25): 9321-9330.

Binder, W. H. and R. Sachsenhofer (2007). "'Click' chemistry in polymer and materials science." *Macromolecular Rapid Communications* 28(1): 15-54.

Blackwell, H. E., D. J. O'Leary, et al. (2000). "New approaches to olefin cross-metathesis." *Journal of the American Chemical Society* 122(1): 58-71.

Boom, R. M., I. M. Wienk, et al. (1992). "Microstructures in Phase Inversion Membranes .2. The Role of a Polymeric Additive." *Journal of Membrane Science* 73(2-3): 277-292.

Boudouris, B. W., C. D. Frisbie, et al. (2008). "Nanoporous poly(3-alkylthiophene) thin films generated from block copolymer templates." *Macromolecules* 41(1): 67-75.

Bradford, M. M. (1976). "Rapid and Sensitive Method for Quantitation of Microgram Quantities of Protein Utilizing Principle of Protein-Dye Binding." *Analytical Biochemistry* 72(1-2): 248-254.

Breitenkamp, K. and T. Emrick (2003). "Novel polymer capsules from amphiphilic graft copolymers and cross-metathesis." *Journal of the American Chemical Society* 125(40): 12070-12071.

Breitenkamp, K., J. Simeone, et al. (2002). "Novel amphiphilic graft copolymers prepared by ring-opening metathesis polymerization of poly(ethylene glycol)-substituted cyclooctene macromonomers." *Macromolecules* 35(25): 9249-9252.

Breitenkamp, R. B., Z. Ou, et al. (2007). "Synthesis and characterization of polyolefin-graft-oligopeptide polyelectrolytes." *Macromolecules* 40(21): 7617-7624.

Brezlow, D. S. (1984). Azides and Nitrenes - Reactivity and Utility. E. V. S. Scriven. Orlando, FL, Academic Press: 491-517.

Brocchini, S. D., R (1999). Encyclopedia of Controlled Drug Delivery. E. Mathiowitz. New York, Wiley: 786-816.

Brunner, J. (1993). "New Photolabeling and Cross-Linking Methods." *Annual Review of Biochemistry* 62: 483-514.

Burdick, J. A. and K. S. Anseth (2002). "Photoencapsulation of osteoblasts in injectable RGD-modified PEG hydrogels for bone tissue engineering." *Biomaterials* 23(22): 4315-4323.

Cardoen, G., K. Breitenkamp, et al. (2006). "Manifold assembly for the convenient polymerization of ethylene oxide and butadiene." *Macromolecules* 39(20): 7170-7173.

Chai, J., D. Wang, et al. (2007). "Assembly of aligned linear metallic patterns on silicon." *Nature Nanotechnology* 2(8): 500-506.

Chatterjee, A. K., J. P. Morgan, et al. (2000). "Synthesis of functionalized olefins by cross and ring-closing metatheses." *Journal of the American Chemical Society* 122(15): 3783-3784.

Choi, T. L. and R. H. Grubbs (2003). "Controlled living ring-opening-metathesis polymerization by a fast-initiating ruthenium catalyst." *Angewandte Chemie-International Edition* 42(15): 1743-1746.

Claverie, J. P., S. Viala, et al. (2001). "Ring-opening metathesis polymerization in emulsion." *Macromolecules* 34(3): 382-388.

Connon, S. J. and S. Blechert (2003). "Recent developments in olefin cross-metathesis." *Angewandte Chemie-International Edition* 42(17): 1900-1923.

Conti, B., F. Pavanetto, et al. (1992). "Use of Polylactic Acid for the Preparation of Microparticulate Drug Delivery Systems." *Journal of Microencapsulation* 9(2): 153-166.

Couvreur, P., M. J. BlancoPrieto, et al. (1997). "Multiple emulsion technology for the design of microspheres containing peptides and oligopeptides." *Advanced Drug Delivery Reviews* 28(1): 85-96.

Czelusniak, I., E. Khosravi, et al. (2007). "Synthesis, characterization, and hydrolytic degradation of polylactide-functionalized polyoxanorbornenes." *Macromolecules* 40(5): 1444-1452.

Dai, Z. F., A. Voigt, et al. (2001). "Layer-by-layer self-assembly of polyelectrolyte and low molecular weight species into capsules." *Advanced Materials* 13(17): 1339-1342.

De Jesus, O. L. P., H. R. Ihre, et al. (2002). "Polyester dendritic systems for drug delivery applications: In vitro and in vivo evaluation." *Bioconjugate Chemistry* 13(3): 453-461.

Delaude, L., D. Jan, et al. (2000). "Ruthenium-based catalysts for the ring-opening metathesis polymerization (ROMP) of functionalized cyclic olefins." *Macromolecular Symposia* 153: 133-144.

Dinsmore, A. D., M. F. Hsu, et al. (2002). "Colloidosomes: Selectively permeable capsules composed of colloidal particles." *Science* 298(5595): 1006-1009.

Discher, B. M., H. Bermudez, et al. (2002). "Cross-linked polymersome membranes: Vesicles with broadly adjustable properties." *Journal of Physical Chemistry B* 106(11): 2848-2854.

Discher, B. M., D. A. Hammer, et al. (2000). "Polymer vesicles in various media." *Current Opinion in Colloid & Interface Science* 5(1-2): 125-131.

Discher, B. M., Y. Y. Won, et al. (1999). "Polymersomes: Tough vesicles made from diblock copolymers." *Science* 284(5417): 1143-1146.

Discher, D. E., V. Ortiz, et al. (2007). "Emerging applications of polymersomes in delivery: From molecular dynamics to shrinkage of tumors." *Progress in Polymer Science* 32(8-9): 838-857.

Duan, H. W., M. Kuang, et al. (2005). "pH-Responsive capsules derived from nanocrystal templating." *Langmuir* 21(24): 11495-11499.

Duncan, R. (2003). "The dawning era of polymer therapeutics." *Nature Reviews Drug Discovery* 2(5): 347-360.

Engin, K., D. B. Leeper, et al. (1995). "Extracellular pH distribution in human tumours." *International Journal of Hyperthermia* 11(2): 211-6.

Ferrando, M., A. Rozek, et al. (2005). "An approach to membrane fouling characterization by confocal scanning laser microscopy." *Journal of Membrane Science* 250(1-2): 283-293.

Flory, P. J. (1953). Principles of polymer chemistry. Ithaca,, Cornell University Press.

France, M. B., L. T. Alty, et al. (1999). "Synthesis of a 7-oxanorbornene derivative: A two-step sequence preparation for the organic laboratory." *Journal of Chemical Education* 76(5): 659-660.

Fréchet, J. M. J., C. J. Hawker, et al. (1996). "Dendrimers and hyperbranched polymers: Two families of three-dimensional macromolecules with similar but clearly distinct properties." *Journal of Macromolecular Science-Pure and Applied Chemistry* A33(10): 1399-1425.

Frisken, B. J., C. Asman, et al. (2000). "Studies of vesicle extrusion." *Langmuir* 16(3): 928-933.

Gacal, B., H. Durmaz, et al. (2006). "Anthracene-maleimide-based Diels-Alder "click chemistry" as a novel route to graft copolymers." *Macromolecules* 39(16): 5330-5336.

Gallivan, J. P., J. P. Jordan, et al. (2005). "A neutral, water-soluble olefin metathesis catalyst based on an N-heterocyclic carbene ligand." *Tetrahedron Letters* 46(15): 2577-2580.

Gaponik, N., I. L. Radtchenko, et al. (2003). "Labeling of biocompatible polymer microcapsules with near-infrared emitting nanocrystals." *Nano Letters* 3(3): 369-372.

George, M. H., M. A. Majid, et al. (1987). "The Anionic Synthesis and Characterization of Poly(Styrene-G-Ethylene Oxide) Copolymers." Polymer 28(7): 1217-1220.

Ghosh, S. K. (2006). Functional coatings: by polymer microencapsulation. Weinheim Chichester, Wiley-VCH; John Wiley [distributor].

Gillies, E. R. and J. M. J. Fréchet (2005). "Dendrimers and dendritic polymers in drug delivery." *Drug Discovery Today* 10(1): 35-43.

Gillies, E. R. and J. M. J. Fréchet (2005). "pH-responsive copolymer assemblies for controlled release of doxorubicin." *Bioconjugate Chemistry* 16(2): 361-368.

Gordon, V. D., C. Xi, et al. (2004). "Self-assembled polymer membrane capsules inflated by osmotic pressure." *Journal of the American Chemical Society* 126(43): 14117-14122.

Greenwald, R. B., Y. H. Choe, et al. (2003). "Effective drug delivery by PEGylated drug conjugates." *Advanced Drug Delivery Reviews* 55(2): 217-250.

Grigoriev, D. O., T. Bukreeva, et al. (2008). "New method for fabrication of loaded micro- and nanocontainers: Emulsion encapsulation by polyelectrolyte layer-by-layer deposition on the liquid core." *Langmuir* 24(3): 999-1004.

Gros, L., H. Ringsdorf, et al. (1981). "Polymeric Anti-Tumor Agents on a Molecular and on a Cellular-Level." *Angewandte Chemie-International Edition* 20(4): 305-325.

Gu, F., L. Zhang, et al. (2008). "Precise engineering of targeted nanoparticles by using self-assembled biointegrated block copolymers." *Proceedings of the National Academy of Sciences of the United States of America* 105(7): 2586-2591.

Harmer, M. A. (1991). "Photomodification of Surfaces Using Heterocyclic Azides." *Langmuir* 7(10): 2010-2012.

Hartley, D. (1962). "Preparation of Delta-Oxoazelaic Acid." *Journal of the Chemical Society* (Nov): 4722.

Hawker, C. J. and J. M. J. Fréchet (1996). "Comparison of linear, hyperbranched, and dendritic macromolecules." *Step-Growth Polymers for High-Performance Materials* 624: 132-144.

Heller, J., J. Barr, et al. (2002). "Poly(ortho esters): synthesis, characterization, properties and uses." *Advanced Drug Delivery Reviews* 54(7): 1015-1039.

Herisson, J. L. and Y. Chauvin (1971). "Transformation Catalysis of Olefins by Tungsten Complexes .2. Telomerization of Cyclic Olefins in Presence of Acyclic Olefins." *Makromolekulare Chemie* 141: 16.

Heroguez, V., S. Breunig, et al. (1996). "Synthesis of alpha-norbornenylpoly(ethylene oxide) macromonomers and their ring-opening metathesis polymerization." *Macromolecules* 29(13): 4459-4464.

Heroguez, V., M. Fontanille, et al. (2000). "Synthesis of latex particles by ring-opening metathesis polymerization in dispersed medium." *Macromolecular Symposia* 150: 269-274.

Heroguez, V., Y. Gnanou, et al. (1996). "Synthesis of alpha-norbornenyl polystyrene macromonomers and their ring-opening metathesis polymerization." *Macromolecular Rapid Communications* 17(2): 137-142.

Heroguez, V., Y. Gnanou, et al. (1997). "Novel amphiphilic architectures by ring-opening metathesis polymerization of macromonomers." *Macromolecules* 30(17): 4791-4798.

Hester, J. F., P. Banerjee, et al. (2002). "ATRP of amphiphilic graft copolymers based on PVDF and their use as membrane additives." Macromolecules 35(20): 7652-7661.

Hester, J. F. and A. M. Mayes (2002). "Design and performance of foul-resistant poly(vinylidene fluoride) membranes prepared in a single-step by surface segregation." *Journal of Membrane Science* 202(1-2): 119-135.

Hillmyer, M. A., W. R. Laredo, et al. (1995). "Ring-Opening Metathesis Polymerization of Functionalized Cyclooctenes by a Ruthenium-Based Metathesis Catalyst." *Macromolecules* 28(18): 6311-6316.

Hoffman, A. (1998). *Journal of Controlled Release* 132: 153-163.

Hoffman, A. S., P. S. Stayton, et al. (2007). "Design of "Smart" nano-scale delivery systems for Biomolecular therapeutics." *Journal of Biomedical Nanotechnology* 3(3): 213-217.

Hoffman, A. S., P. S. Stayton, et al. (2002). "Design of "smart" polymers that can direct intracellular drug delivery." *Polymers for Advanced Technologies* 13(10-12): 992-999.

Hong, S. H. and R. H. Grubbs (2006). "Highly active water-soluble olefin metathesis catalyst." *Journal of the American Chemical Society* 128(11): 3508-3509.

Hopkins, T. E. and K. B. Wagener (2004). "ADMET synthesis of polyolefins targeted for biological applications." *Macromolecules* 37(4): 1180-1189.

Ihre, H., O. L. P. De Jesus, et al. (2001). "Fast and convenient divergent synthesis of aliphatic ester dendrimers by anhydride coupling." *Journal of the American Chemical Society* 123(25): 5908-5917.

Ihre, H. R., O. L. P. De Jesus, et al. (2002). "Polyester dendritic systems for drug delivery applications: Design, synthesis, and characterization." *Bioconjugate Chemistry* 13(3): 443-452.

Ikkala, O. and G. ten Brinke (2002). "Functional materials based on self-assembly of polymeric supramolecules." *Science* 295(5564): 2407-2409.

Ilker, M. F., H. Schule, et al. (2004). "Modular norbornene derivatives for the preparation of well-defined amphiphilic polymers: Study of the lipid membrane disruption activities." *Macromolecules* 37(3): 694-700.

Irvine, D. J., A. M. Mayes, et al. (2001). "Nanoscale clustering of RGD peptides at surfaces using comb polymers. 1. Synthesis and characterization of comb thin films." *Biomacromolecules* 2(1): 85-94.

Iwata, H., M. I. Ivanchenko, et al. (1994). "Preparation of Anti-Oil Stained Membrane by Grafting Polyethylene-Glycol Macromer onto Polysulfone Membrane." *Journal of Applied Polymer Science* 54(1): 125-128.

Kabanov, A. V., E. V. Batrakova, et al. (2002). "Pluronic (R) block copolymers as novel polymer therapeutics for drug and gene delivery." *Journal of Controlled Release* 82(2-3): 189-212.

Kabanov, A. V., E. V. Batrakova, et al. (2002). "Pluronic((R)) block copolymers for overcoming drug resistance in cancer." *Advanced Drug Delivery Reviews* 54(5): 759-779.

Kabanov, A. V., E. V. Batrakova, et al. (2005). "Polymer genomics: shifting the gene and drug delivery paradigms." *Journal of Controlled Release* 101(1-3): 259-271.

Kataoka, K., A. Harada, et al. (2001). "Block copolymer micelles for drug delivery: design, characterization and biological significance." *Advanced Drug Delivery Reviews* 47(1): 113-131.

Kim, B. and N. A. Peppas (2003). "In vitro release behavior and stability of insulin in complexation hydrogels as oral drug delivery carriers." *International Journal of Pharmaceutics* 266(1-2): 29-37.

Kim, B. and N. A. Peppas (2003). "Poly(ethylene glycol)-containing hydrogels for oral protein delivery applications." *Biomedical Microdevices* 5(4): 333-341.

Kim, S. Y., Y. M. Lee, et al. (2001). "Indomethacin-loaded methoxy poly(ethylene glycol)/poly(epsilon-caprolactone) diblock copolymeric nanosphere:

pharmacokinetic characteristics of indomethacin in the normal Sprague-Dawley rats." *Biomaterials* 22(14): 2049-2056.
Kim, T. G. and T. G. Park (2006). "Biomimicking extracellular matrix: cell adhesive RGD peptide modified electrospun poly(D,L-lactic-co-glycolic acid) nanofiber mesh." *Tissue Engineering* 12(2): 221-33.
Kolb, H. C., M. G. Finn, et al. (2001). "Click chemistry: Diverse chemical function from a few good reactions." *Angewandte Chemie-International Edition* 40(11): 2004-2021.
Koo, L. Y., D. J. Irvine, et al. (2002). "Co-regulation of cell adhesion by nanoscale RGD organization and mechanical stimulus." *Journal of Cell Science* 115(7): 1423-33.
Kopecek, J., P. Kopeckova, et al. (2000). "HPMA copolymer-anticancer drug conjugates: design, activity, and mechanism of action." *European Journal of Pharmaceutics and Biopharmaceutics* 50(1): 61-81.
Kost, J. and R. Langer (2001). "Responsive polymeric delivery systems." *Advanced Drug Delivery Reviews* 46(1-3): 125-148.
Kowalczuk, M., G. Adamus, et al. (1994). "Synthesis of New Graft Polymers Via Anionic Grafting of Beta-Butyrolactone on Poly(Methyl Methacrylate)." *Macromolecules* 27(2): 572-575.
Kwak, J. C. T. (1998). Polymer-surfactant systems. New York, M. Dekker.
Kwart, H. and I. Burchuk (1952). "Isomerism and Adduct Stability in the Diels Alder Reaction .1. The Adducts of Furan and Maleimide." *Journal of the American Chemical Society* 74(12): 3094-3097.
Langer, R. (1998). "Drug delivery and targeting." *Nature* 392(6679): 5-10.
Langer, R. (2003). "Controlled release (of peptides and proteins) and tissue engineering." *Biopolymers* 71(3): 284-284.
Lavasanifar, A., J. Samuel, et al. (2002). "Poly(ethylene oxide)-block-poly(L-amino acid) micelles for drug delivery." *Advanced Drug Delivery Reviews* 54(2): 169-190.
Lee, E. S., Z. Gao, et al. (2008). "Recent progress in tumor pH targeting nanotechnology." *Journal of Controlled Release* 132(3): 164-170.
Lee, E. S., K. Na, et al. (2005). "Doxorubicin loaded pH-sensitive polymeric micelles for reversal of resistant MCF-7 tumor." *Journal of Controlled Release* 103(2): 405-418.
Lee, J. H., H. B. Lee, et al. (1995). "Blood Compatibility of Polyethylene Oxide Surfaces." *Progress in Polymer Science* 20(6): 1043-1079.
Lensen, D., D. M. Vriezema, et al. (2008). "Polymeric microcapsules for synthetic applications." *Macromolecular Bioscience* 8(11): 991-1005.
Li, C. and S. Wallace (2008). "Polymer-drug conjugates: Recent development in clinical oncology." *Advanced Drug Delivery Reviews* 60(8): 886-898.
Li, S. D. and L. Huang (2008). "Pharmacokinetics and biodistribution of nanoparticles." *Molecular Pharmaceutics* 5(4): 496-504.
Love, J. A., J. P. Morgan, et al. (2002). "A practical and highly active ruthenium-based catalyst that effects the cross metathesis of acrylonitrile." *Angewandte Chemie-International Edition* 41(21): 4035-4037.
Lynn, D. M., B. Mohr, et al. (1998). "Living ring-opening metathesis polymerization in water." *Journal of the American Chemical Society* 120(7): 1627-1628.

Lynn, D. M., B. Mohr, et al. (2000). "Water-soluble ruthenium alkylidenes: Synthesis, characterization, and application to olefin metathesis in protic solvents." *Journal of the American Chemical Society* 122(28): 6601-6609.

Ma, H. M., R. H. Davis, et al. (2000). "A novel sequential photoinduced living graft polymerization." *Macromolecules* 33(2): 331-335.

Macdonald, R. C., R. I. Macdonald, et al. (1991). "Small-Volume Extrusion Apparatus for Preparation of Large, Unilamellar Vesicles." *Biochimica Et Biophysica Acta* 1061(2): 297-303.

Maeda, H., J. Wu, et al. (2000). "Tumor vascular permeability and the EPR effect in macromolecular therapeutics: a review." Journal of Controlled Release 65(1-2): 271-284.

Mark, P. R., N. S. Murthy, et al. (2008). "Microphase separated structures in the solid and molten states of double-crystal graft copolymers of polyethylene and poly(ethylene oxide)." *Polymer* 49(13-14): 3116-3124.

Matsumura, Y. and H. Maeda (1986). "A New Concept for Macromolecular Therapeutics in Cancer-Chemotherapy - Mechanism of Tumoritropic Accumulation of Proteins and the Antitumor Agent Smancs." *Cancer Research* 46(12): 6387-6392.

Maulucci, G., M. De Spirito, et al. (2005). "Particle size distribution in DMPC vesicles solutions undergoing different sonication times." *Biophysical Journal* 88(5): 3545-3550.

Maynard, H. D., S. Y. Okada, et al. (2001). "Inhibition of cell adhesion to fibronectin by oligopeptide-substituted polynorbornenes." *Journal of the American Chemical Society* 123(7): 1275-1279.

Metters, A. T., K. S. Anseth, et al. (2000). "Fundamental studies of a novel, biodegradable PEG-b-PLA hydrogel." *Polymer* 41(11): 3993-4004.

Mohr, B., D. M. Lynn, et al. (1996). "Synthesis of water-soluble, aliphatic phosphines and their application to well-defined ruthenium olefin metathesis catalysts." *Organometallics* 15(20): 4317-4325.

Mross, K., B. Niemann, et al. (2004). "Pharmacokinetics of liposomal doxorubicin (TLC-D99 ; Myocet) in patients with solid tumors: an open-label, single-dose study." *Cancer Chemotherapy and Pharmacology* 54(6): 514-524.

Myers, S. B. and R. A. Register (2008). "Synthesis of narrow-distribution polycyclopentene using a ruthenium ring-opening metathesis initiator." *Polymer* 49(4): 877-882.

Nagasaki, Y., K. Yasugi, et al. (2001). "Sugar-installed block copolymer micelles: Their preparation and specific interaction with lectin molecules." *Biomacromolecules* 2(4): 1067-1070.

Nagayasu, A., K. Uchiyama, et al. (1999). "The size of liposomes: a factor which affects their targeting efficiency to tumors and therapeutic activity of liposomal antitumor drugs." *Advanced Drug Delivery Reviews* 40(1-2): 75-87.

Nardin, C., T. Hirt, et al. (2000). "Polymerized ABA triblock copolymer vesicles." *Langmuir* 16(3): 1035-1041.

Nayar, R., M. J. Hope, et al. (1989). "Generation of Large Unilamellar Vesicles from Long-Chain Saturated Phosphatidylcholines by Extrusion Technique." *Biochimica Et Biophysica Acta* 986(2): 200-206.

Norton, R. L. and T. J. Mccarthy (1989). "Omega-Norbornenyl Polystyrene - an Olefin Metathesis Polymerizable Macromonomer." Macromolecules 22(3): 1022-1025.

Novak, B. M. and R. H. Grubbs (1988). "Catalytic Organometallic Chemistry in Water - the Aqueous Ring-Opening Metathesis Polymerization of 7-Oxanorbornene Derivatives." *Journal of the American Chemical Society* 110(22): 7542-7543.

O'donnell, P. M., K. Brzezinska, et al. (2001). ""Perfect comb" ADMET graft copolymers." *Macromolecules* 34(20): 6845-6849.

Ojugo, A. S., P. M. McSheehy, et al. (1999). "Measurement of the extracellular pH of solid tumours in mice by magnetic resonance spectroscopy: a comparison of exogenous (19)F and (31)P probes." *NMR in Biomedicine* 12(8): 495-504.

Papahadjopoulos, D. and J. C. Watkins (1967). "Phospholipid Model Membranes .2. Permeability Properties of Hydrated Liquid Crystals." *Biochimica Et Biophysica Acta* 135(4): 639-652.

Park, K. (1997). Controlled drug delivery : challenges and strategies. Washington, DC, American Chemical Society.

Park, M. K., S. X. Deng, et al. (2005). "Sustained release control via photo-cross-linking of polyelectrolyte layer-by-layer hollow capsules." *Langmuir* 21(12): 5272-5277.

Parrish, B., R. B. Breitenkamp, et al. (2005). "PEG- and peptide-grafted aliphatic polyesters by click chemistry." *Journal of the American Chemical Society* 127(20): 7404-7410.

Parrish, B. and T. Emrick (2007). "Soluble camptothecin derivatives prepared by click cycloaddition chemistry on functional aliphatic polyesters." *Bioconjugate Chemistry* 18(1): 263-7.

Patty, P. J. and B. J. Frisken (2003). "The pressure-dependence of the size of extruded vesicles." *Biophysical Journal* 85(2): 996-1004.

Pavanetto, F., I. Genta, et al. (1993). "Evaluation of Spray-Drying as a Method for Polylactide and Polylactide-Co-Glycolide Microsphere Preparation." *Journal of Microencapsulation* 10(4): 487-497.

Peppas, N. A. (1991). "Physiologically Responsive Hydrogels." *Journal of Bioactive and Compatible Polymers* 6(3): 241-246.

Peppas, N. A. and J. Klier (1991). "Controlled Release by Using Poly (Methacrylic Acid-G-Ethylene Glycol) Hydrogels." Journal of Controlled Release 16(1-2): 203-214.

Preishuber-Pflugl, P., P. Buchacher, et al. (1998). "New features of ROMP by heterogenization of molybdenum carbene complexes." *Journal of Molecular Catalysis A-Chemical* 133(1-2): 151-158.

Quattrin, T. (2006). "Inhaled insulin: a novel and non-invasive way for insulin administration?" *Current Drug Safety* 1(2): 151-8.

Randall, M. L., J. A. Tallarico, et al. (1995). "Selective Ring-Opening Cross-Metathesis - Short Syntheses of Multifidene and Viridiene." *Journal of the American Chemical Society* 117(37): 9610-9611.

Rankin, D. A., S. J. P'Pool, et al. (2007). "The controlled homogeneous organic solution polymerization of new hydrophilic cationic exo-7-oxa-norbornenes via ROMP with RuCl2(PCY3)(2)CHPh in a novel 2,2,2-trifluoroethanol/methylene chloride solvent mixture." *Journal of Polymer Science Part A-Polymer Chemistry* 45(11): 2113-2128.

Ratner, B. D. and S. J. Bryant (2004). "Biomaterials: Where we have been and where we are going." *Annual Review of Biomedical Engineering* 6: 41-75.

Rigler, P. and W. Meier (2006). "Encapsulation of fluorescent molecules by functionalized polymeric nanocontainers: Investigation by confocal fluorescence Imaging and fluorescence correlation Spectroscopy." *Journal of the American Chemical Society* 128(1): 367-373.

Rinehart, R. E. and H. P. Smith (1965). "Emulsion Polymerization of Norbornene Ring System Catalyzed by Noble Metal Compounds." *Journal of Polymer Science Part B-Polymer Letters* 3(12): 1049.

Ringsdorf, H. (1975). "Structure and Properties of Pharmacologically Active Polymers." J*ournal of Polymer Science Part C-Polymer Symposium* (51): 135-153.

Roy, D., J. T. Guthrie, et al. (2005). "Graft polymerization: Grafting poly(styrene) from cellulose via reversible addition-fragmentation chain transfer (RAFT) polymerization." *Macromolecules* 38(25): 10363-10372.

Ruoslahti, E. (2003). "The RGD story: a personal account." *Matrix Biology* 22(6): 459-65.

Safra, T., F. Muggia, et al. (2000). "Pegylated liposomal doxorubicin (doxil): Reduced clinical cardiotoxicity in patients reaching or exceeding cumulative doses of 500 mg/m(2)." *Annals of Oncology* 11(8): 1029-1033.

Sanford, M. S., J. A. Love, et al. (2001). "A versatile precursor for the synthesis of new ruthenium olefin metathesis catalysts." *Organometallics* 20(25): 5314-5318.

Sat, Y. N., M. Bibby, et al. (1999). "Effect of tumour size and tumour type on passive tumour accumulation of polymeric anticancer agents." *British Journal of Cancer* 81(4): 583-583.

Savic, R., L. B. Luo, et al. (2003). "Micellar nanocontainers distribute to defined cytoplasmic organelles." *Science* 300(5619): 615-618.

Schacht, E., V. Toncheva, et al. (2006). "Polyacetal and poly(ortho ester)-poly(ethylene glycol) graft copolymer thermogels: Preparation, hydrolysis and FITC-BSA release studies." *Journal of Controlled Release* 116(2): 219-225.

Schitter, R. M. E., D. Jocham, et al. (2000). "Novel routes to polyelectrolytes and reactive polymers via ROMP." *Journal of Applied Polymer Science* 78(1): 47-60.

Schleyer, P. V., J. E. Williams, et al. (1970). "Evaluation of Strain in Hydrocarbons - Strain in Adamantane and Its Origin." *Journal of the American Chemical Society* 92(8): 2377-2386.

Scholl, M., S. Ding, et al. (1999). "Synthesis and activity of a new generation of ruthenium-based olefin metathesis catalysts coordinated with 1,3-dimesityl-4,5-dihydroimidazol-2-ylidene ligands." *Organic Letters* 1(6): 953-956.

Schrock, R. R., J. S. Murdzek, et al. (1990). "Synthesis of Molybdenum Imido Alkylidene Complexes and Some Reactions Involving Acyclic Olefins." J*ournal of the American Chemical Society* 112(10): 3875-3886.

Schwab, P., R. H. Grubbs, et al. (1996). "Synthesis and applications of RuCl2(=CHR')(PR(3))(2): The influence of the alkylidene moiety on metathesis activity." *Journal of the American Chemical Society* 118(1): 100-110.

Scott, K. (2003). Handbook of Industrial Membranes. Oxford, Elsevier.

Shoichet, M. S., S. R. Winn, et al. (1994). "Poly(Ethylene Oxide) Grafted Thermoplastic Membranes for Use as Cellular Hybrid Bioartificial Organs in the Central-Nervous-System." *Biotechnology and Bioengineering* 43(7): 563-572.

Shuai, X. T., H. Ai, et al. (2004). "Micellar carriers based on block copolymers of poly(e-caprolactone) and poly(ethylene glycol) for doxorubicin delivery." *Journal of Controlled Release* 98(3): 415-426.

Shum, H. C., J. W. Kim, et al. (2008). "Microfluidic fabrication of monodisperse biocompatible and biodegradable polymersomes with controlled permeability." *Journal of the American Chemical Society* 130(29): 9543-9549.

Siepmann, J., N. Faisant, et al. (2004). "Effect of the size of biodegradable microparticles on drug release: experiment and theory." *Journal of Controlled Release* 96(1): 123-134.

Skaff, H. and T. Emrick (2003). "The use of 4-substituted pyridines to afford amphiphilic, pegylated cadmium selenide nanoparticles." *Chemical Communications* (1): 52-53.

Skaff, H., Y. Lin, et al. (2005). "Crosslinked capsules of quantum dots by interfacial assembly and ligand crosslinking." Advanced Materials 17(17): 2082-+.

Strong, L. E. and L. L. Kiessling (1999). "A general synthetic route to defined, biologically active multivalent arrays." *Journal of the American Chemical Society* 121(26): 6193-6196.

Sukhorukov, G. B., A. A. Antipov, et al. (2001). "pH-controlled macromolecule encapsulation in and release from polyelectrolyte multilayer nanocapsules." *Macromolecular Rapid Communications* 22(1): 44-46.

Sukhorukov, G. B., E. Donath, et al. (1998). "Stepwise polyelectrolyte assembly on particle surfaces: a novel approach to colloid design." *Polymers for Advanced Technologies* 9(10-11): 759-767.

Szleifer, I. (1997). "Polymers and proteins: Interactions at interfaces." *Current Opinion in Solid State & Materials Science* 2(3): 337-344.

Tangirala, R., R. Revanur, et al. (2007). "Sizing nanoparticle-covered droplets by extrusion through track-etch membranes." *Langmuir* 23(3): 965-969.

Thom, V., K. Jankova, et al. (1998). "Synthesis of photoreactive alpha-4-azidobenzoyl-omega-methoxypoly(ethyleneglycol)s and their end-on photo-grafting onto polysulfone ultrafiltration membranes." *Macromolecular Chemistry and Physics* 199(12): 2723-2729.

Thomas, P. A., T. Padmaja, et al. (1997). "Polyanhydride blend microspheres: Novel carriers for the controlled release of macromolecular drugs." *Journal of Controlled Release* 43(2-3): 273-281.

Thorn-Csanyi, E. and K. Ruhland (1999). "Quantitative description of the metathesis polymerization depolymerization equilibrium in the 1,4-polybutadiene system, 1 - Influence of feed concentration and temperature." Macromolecular Chemistry and Physics 200(7): 1662-1671.

Thorn-Csanyi, E. and K. Ruhland (1999). "Quantitative description of the metathesis polymerization/depolymerization equilibrium in the 1,4-polybutadiene system, 2 - Unusual behaviour at lower temperature." *Macromolecular Chemistry and Physics* 200(10): 2245-2249.

Thorn-Csanyi, E., J. Hammer, et al. (1995). "Formation and Degradation of 1,4-Polybutadiene Via Metathesis - New Results Concerning Cyclic Oligomers." *Macromolecular Chemistry and Physics* 196(4): 1043-1050.

Tian, Y., L. Bromberg, et al. (2007). "Complexation and release of doxorubicin from its complexes with pluronic P85-b-poly(acrylic acid) block copolymers." J*ournal of Controlled Release* 121(3): 137-145.

Tiarks, F., K. Landfester, et al. (2001). "Preparation of polymeric nanocapsules by miniemulsion polymerization." *Langmuir* 17(3): 908-918.

Tomalia, D. A., H. Baker, et al. (1985). "A New Class of Polymers - Starburst-Dendritic Macromolecules." *Polymer Journal* 17(1): 117-132.

Tong, W., C. Gao, et al. (2005). "Manipulating the Properties of Polyelectrolyte Microcapsules by Glutaraldehyde Cross-Linking." *Chemistry of Materials* 17(18): 4610-4616.

Trnka, T. M. and R. H. Grubbs (2001). "The development of L2X2Ru = CHR olefin metathesis catalysts: An organometallic success story." *Accounts of Chemical Research* 34(1): 18-29.

Trzaska, S. T., L. B. W. Lee, et al. (2000). "Synthesis of narrow-distribution "perfect" polyethylene and its block copolymers by polymerization of cyclopentene." *Macromolecules* 33(25): 9215-9221.

Ulbricht, M. and H. G. Hicke (1993). "Photomodification of Ultrafiltration Membranes .1. Photochemical Modification of Polyacrylonitrile Ultrafiltration Membranes with Aryl Azides." *Angewandte Makromolekulare Chemie* 210: 69-95.

Ulbricht, M. and H. G. Hicke (1993). "Photomodification of Ultrafiltration Membranes .2. Ultrafiltration Properties of Polyacrylonitrile Membranes Photochemically Modified with Aryl Azides." *Angewandte Makromolekulare Chemie* 210: 97-117.

Ulbricht, M., H. Matuschewski, et al. (1996). "Photo-induced graft polymerization surface modifications for the preparation of hydrophilic and low-protein-adsorbing ultrafiltration membranes." *Journal of Membrane Science* 115(1): 31-47.

Vasey, P. A., S. B. Kaye, et al. (1999). "Phase I clinical and pharmacokinetic study of PK1 [N-(2-hydroxypropyl)methacrylamide copolymer doxorubicin]: First member of a new class of chemotherapeutic agents - Drug-polymer conjugates." *Clinical Cancer Research* 5(1): 83-94.

Vazquez-Dorbatt, V. and H. D. Maynard (2006). "Biotinylated glycopolymers synthesized by atom transfer radical polymerization." *Biomacromolecules* 7(8): 2297-302.

Wang, Y. J., V. Bansal, et al. (2008). "Templated synthesis of single-component polymer capsules and their application in drug delivery." Nano Letters 8(6): 1741-1745.

Watson, K. J., D. R. Anderson, et al. (2001). "Toward polymeric anticancer drug cocktails from ring-opening metathesis polymerization." *Macromolecules* 34(11): 3507-3509.

Willert, H. G., G. Buchhorn, et al. (1991). Ultra-high molecular weight polyethylene as biomaterial in orthopedic surgery. Toronto ; Lewiston, NY, Hogrefe & Huber Publishers.

Wu, M. L., S. A. O'Neill, et al. (2000). "Synthesis of nanometer-sized hollow polymer capsules from alkanethiol-coated gold particles." *Chemical Communications* (9): 775-776.

Yang, F., C. G. Williams, et al. (2005). "The effect of incorporating RGD adhesive peptide in polyethylene glycol diacrylate hydrogel on osteogenesis of bone marrow stromal cells." *Biomaterials* 26(30): 5991-5998.

Zelikin, A. N., J. F. Quinn, et al. (2006). "Disulfide cross-linked polymer capsules: En route to biodeconstructible systems." *Biomacromolecules* 7(1): 27-30.

Zeman, L. J., Zydney, A. L. (1996). Microfiltration and Ultrafiltration Principles and Applications. New York, Marcel Dekker.

Zhang, Q., E. E. Remsen, et al. (2000). "Shell cross-linked nanoparticles containing hydrolytically degradable, crystalline core domains." *Journal of the American Chemical Society* 122(15): 3642-3651.

Zhang, S. (2002). "Emerging biological materials through molecular self-assembly." *Biotechnology Advances* 20(5-6): 321-39.